論文 / 著書情報
Article / Book Information

題目(和文)	フォトレドックス触媒作用による窒素及び酸素含有反応性ラジカル種の発生とその合成化学的利用
Title(English)	Generation of reactive nitrogen- and oxygen-containing radical species by photoredox catalysis and their synthetic applications
著者(和文)	宮澤和己
Author(English)	Kazuki Miyazawa
出典(和文)	学位:博士(工学), 学位授与機関:東京工業大学, 報告番号:甲第10531号, 授与年月日:2017年3月26日, 学位の種別:課程博士, 審査員:穐田 宗隆,吉沢 道人,小坂田 耕太郎,中村 浩之,稲木 信介
Citation(English)	Degree:Doctor (Engineering), Conferring organization: Tokyo Institute of Technology, Report number:甲第10531号, Conferred date:2017/3/26, Degree Type:Course doctor, Examiner:,,,,
学位種別(和文)	博士論文
Type(English)	Doctoral Thesis

Generation of reactive nitrogen- and oxygen- containing radical species by photoredox catalysis and their synthetic applications

（フォトレドックス触媒作用による窒素及び酸素含有
反応性ラジカル種の発生とその合成化学的利用）

Kazuki Miyazawa

Department of Environmental Chemistry and Engineering
Interdisciplinary Graduate School of Science and Engineering

TOKYO INSTITUTE OF TECHNOLOGY

2017

Contents

Chapter 1

General introduction

Radical reactions have been regarded as a unique methodology in organic synthesis because reactivities of radical species are different from those of ionic species.[1] For example, most of carbon-centered radicals are tolerated with a variety of functional groups such as alcohol, ester, carbonyl and amine in contrast to ionic species. Furthermore, radical addition to alkenes shows characteristic regioselectivity as typically exemplified by the reaction of hydrogen bromide with alkene (Scheme 1.1 (a)). Addition of the Br radical gives *anti*-Markovnikov-type product **1** via the stabilized radical intermediate. In contrast, the reaction through protonation of alkenes by HBr affords the adduct **2** in the Markovnikov manner. The different regioselectivity results from the atomic group initially interacting with alkene, $Br^{\bullet}$ vs H^{+}. On the basis of selective radical addition to alkenes, radical polymerization of alkenes, *e.g.* synthesis of polymethyl methacrylate (**3**) (Scheme 1.1 (b)), has been well-developed. The practical methodology has been applied to industry. Furthermore, radical reaction has played important roles in the total synthesis of natural products by taking advantage of the functional group tolerance (Scheme 1.1 (c)).[2] Radical cyclization of 2-alkenylthioanilide **4**, which has various functional groups, by tributyltin hydride afforded the indole **5** in a chemoselective manner. The methodology for synthesis of indole skeleton is useful for synthesis of various indole alkaloids, for example (+)-vinblastine.[2d]

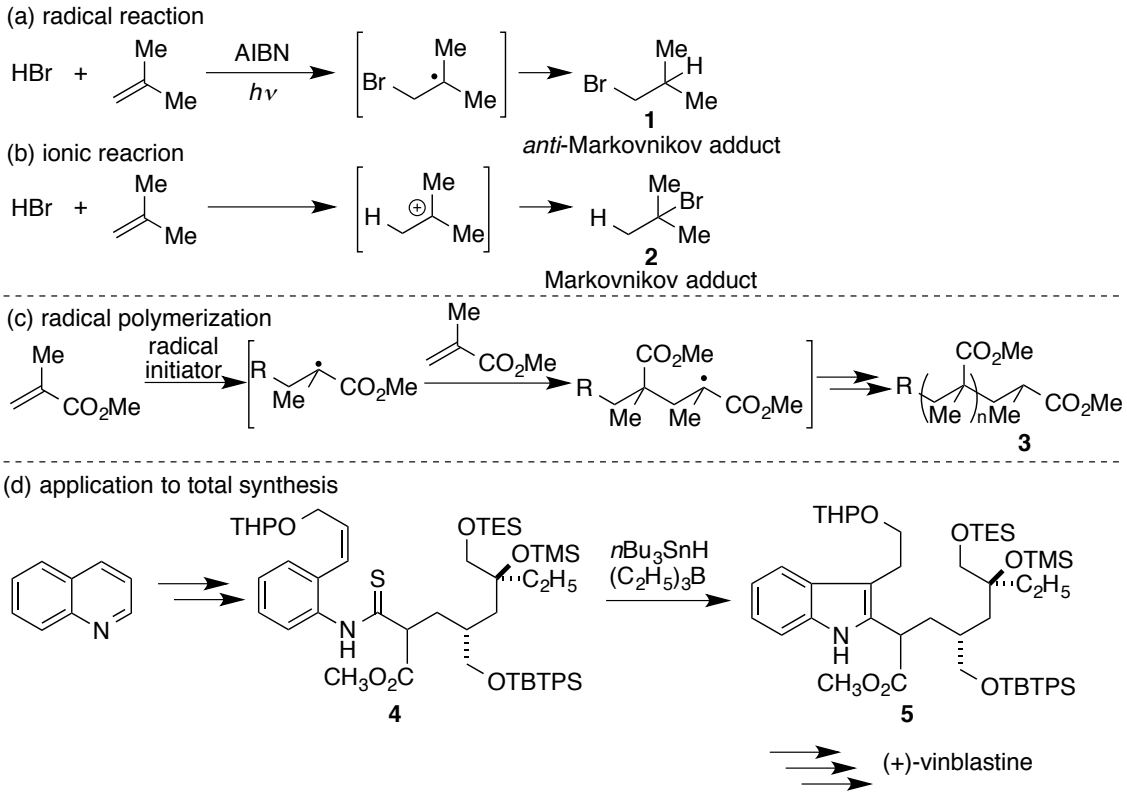

Scheme 1.1 Applications of radical reactions.

In radical reactions, choice of initiating systemes is important. Radical species have been usually generated by thermolysis, photolysis, or redox process of precursors having weak bonds such as peroxides with O-O bonds. Recently, visible light-promoted photoredox catalysis has attracted as a powerful synthetic tool in the field of organic synthesis, because photoredox catalysis is a green chemical process thanks to many favorable aspects as exemplified by visible light (sunlight) driven, atom-economic and redox neutral reactions.[3] The single electron transfer processes involved therein can be applied to generation of radicals via the redox process, as revealed by the studies by many scientists including our group. This process has advantages over the conventional radical systems that frequently use an excess amount of redox reagents. For the use of photoredox catalysis as a green radical generating method it is essential to design

appropriate precursors. In the present study, the author has developed new radical precursors containing heteroatoms and used them for selective reactions.

In the present thesis, the author has summarized the results of the studies aiming at incorporation of *N*- and *O*-functional groups via radical species generated by the action of photoredox catalysis.

1.1 Basic concepts on radical reactions[1]

1.1.1 Elementary process of radical reaction[1d]

Elementary processes of radical reactions are classified with the following six reactions (Scheme 1.2): (i) homolysis, (ii) coupling, (iii) disproportionation, (iv) addition, (v) β-scission and (vi) substitution including hydrogen abstraction.

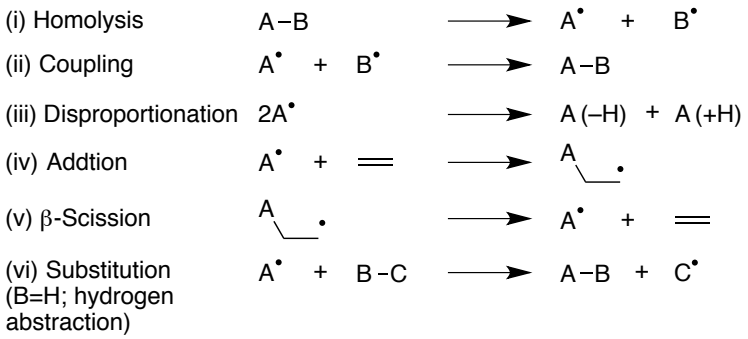

Scheme 1.2 Elementary processes.

(i) Homolysis is a basic process for generation of radicals via homolytic scission of the single bond (Scheme 1.2 (i)). Weak bonds can be homolytically cleaved by heating and irradiation. For further details see the section 1.4.

(ii) Coupling reaction is a reverse process of the homolysis (Scheme 1.2 (ii)). The reaction is exoergic, prompt and with low activation energy.

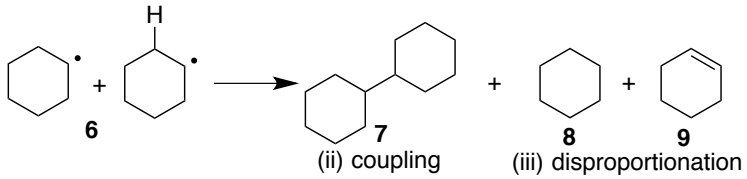

Scheme 1.3 Coupling and diproportionation with cyclohexyl radicals.

(iii) Disproportionation is dependent on the steric environment of the radical center to cause H-exchange processes. For example, reaction of cyclohexyl radical (**6**) affords the coupling product **7** together with cyclohexane (**8**)/cyclohexene (**9**) (Scheme 1.3).

(iv) Radical species add to many types of π bonds to generate new radical intermediate. The driving force for the process is formation of a strong σ-bond with the expense of a weak π bond. In case of addition of HX to alkenes, the regioselectivity follows *anti*-Markovnikov manner (Scheme 1.1 (a)). Details of the reactivity are described in section 1.3.

(v) β-Scission is the reverse process of addition. Examples of β-scission are shown in Scheme 1.4. Three-membered ring compounds (**10**) such as cyclopropane, epoxide and aziridine afford the ring-opening products (**11**) to release the distortion (Scheme 1.4 (a)). Carboxy radical (**12**) affords the phenyl radical (**13**) and carbon dioxide through the β-scission.

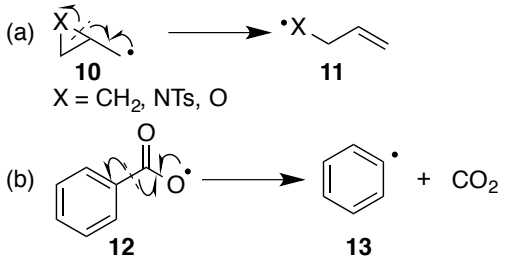

Scheme 1.4 Examples of β-scission.

(vi) Substitution involves abstraction of an atom by a radical species. An example of substitution is shown in Scheme 1.5. Tributylstannyl radical (**14**) abstracts the halogen (Cl, Br or I) of haloalkane **15** to generate *n*BuSnX (**16**) and the alkyl radical (**17**). This process is important as an initiating step of radical chain reactions.

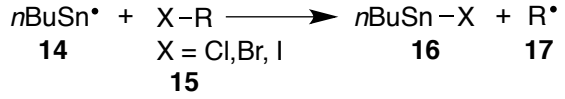

Scheme 1.5 Example of an abstraction of halogens.

1.1.2 Radical chain reaction[1d]

The mechanism of radical chain reaction (scheme 1.6 (a)) is composed of three stages: *initiation step*, which involves activation of the initiator by heating or irradiation to generate the radicals (i), *propagation cycle,* which involves the conversion of precursor into the production by consecutive radical reactions such as addition, β-scission and substitution (iv, v, vi), and *termination*, which is the end of reaction process by radical-radical coupling (ii). These radical reactions can be explained by combination of the *elementary processes*. The selected example of radical chain reaction is Kharasch reaction reported in 1940s (Scheme 1.6).[4] This chain reaction of *n*-octene (**18**) with trichloromethane (**19**) affords the product (**20**) having the C-Cl and C-CCl_3 bonds. Diacetyl peroxide (**21**) serves as a radical initiator and undergoes *homolysis* to give the acyloxy radicals (**22)**, which undergo *β-scission* rapidly to form the methyl radical (**23**) together with CO_2. The reactive intermediate abstracts a chlorine atom from CCl_4 to give chloromethane (**24**) and $^{\bullet}CCl_3$ (**25**). These successive processes are involved in the initiation phase of the reaction. The propagation cycle involves *addition* of $^{\bullet}CCl_3$ (**25**) to less substituted end of the π bond of alkene to generate the

more stable, more substituted radical intermediate **26**. The intermediate **26** undergoes the intermolecular *abstraction* of the chlorine from CCl_4 to give the final product (**20**) together with $^{\bullet}CCl_3$, which undergoes the propagation (**18** + **25** → **26**).

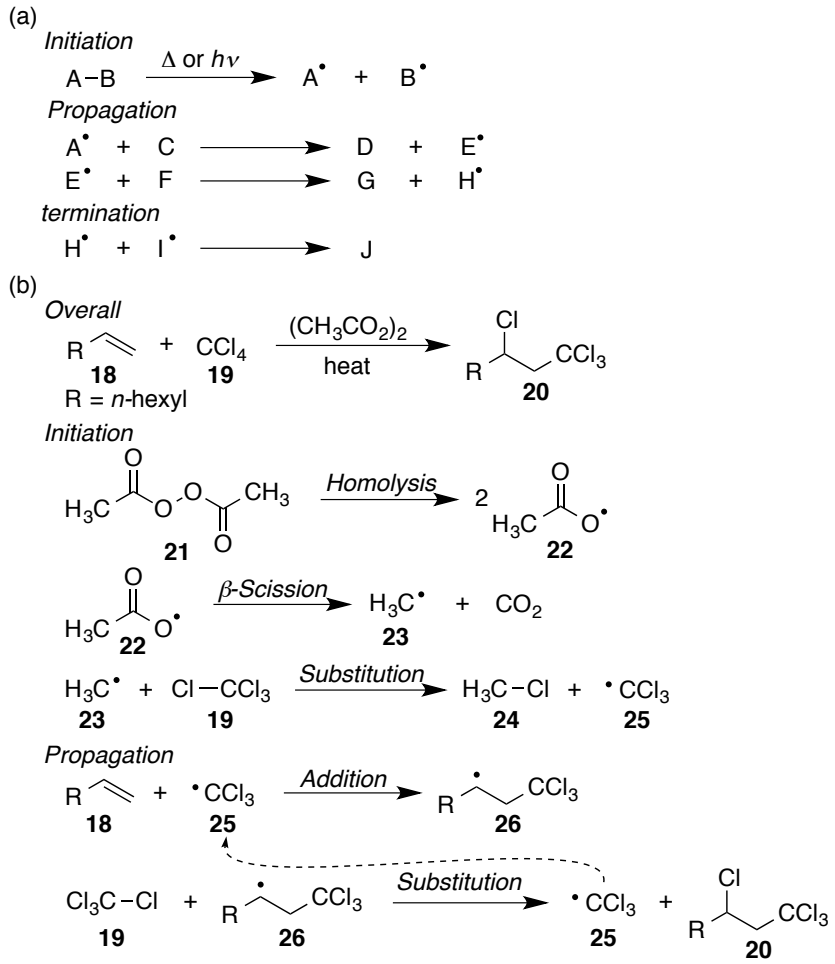

Scheme 1.6 (a) A generalized radical chain reaction. (b) The mechanism of Kharasch reaction.

1.2 Stability of radicals

1.2.1 Kinetic and thermodynamic aspects

Radical species are usually regarded as reactive and unstable species because of their electron-deficient nature due to violation of the octet rule. This statement is true when compared to closed shell species but the stability varies in a wide range and depends on

many factors such as the central atom where the radical resides, electronic and steric features of the substituents, and the electronic systems (σ/π systems). Kinetic and thermodynamic aspects contribute to the stability of radicals. Steric effect is representative kinetic aspect. Examples of persistent radicals are shown in Figure 1.1. While phenoxy radical is an unstable species, 2,4,6-tri-*tert*-butylphenoxy radical **27** is stable enough to be isolated presumably due to the bulky substituent preventing it from dimerization. Other radicals such as triphenylmethyl radical **28**, 2,2,6,6-tetramethylpiperidine-1-oxyl radical **29**, and 2,5,8-tri-*tert*-butylphenalenyl radical **30** are also stabilized enough to be isolated due to the steric and electric effects.

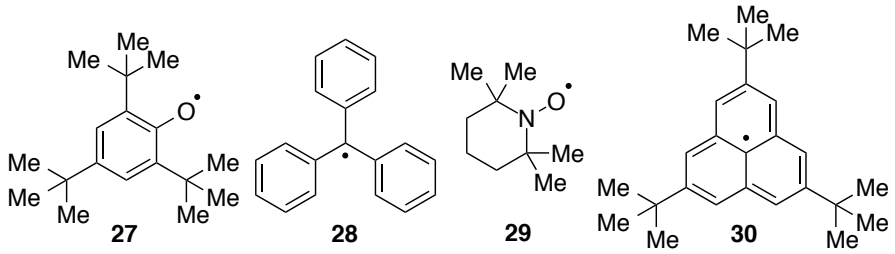

Figure 1.1 Examples of persistent radicals

Electric effect is also important for stability of the radicals because the radical species have an unpaired electron. In this section, thermodynamical stability of carbon-, nitrogen- and oxygen-centered radicals are described.

1.2.2 Stability of carbon-, oxygen- and nitrogen-centered radicals[1a]

Stability of C-centered radicals

Carbon-centered radicals are stabilized by the following three substituent effects: (i) resonance effects of conjugated C-C π bonds, *e.g.* allyl radical (**31**) and benzyl radical (**32**), (ii) lone-pair donation, *e.g.* carbon centered radical adjacent to a heteroatom (**33**), and (iii) hyperconjugative effects, *e.g.* ethyl radical (**34**) (Figure 1.2). BDE (bond

dissociation energy) is an index for considering a radical stability. As BDE is shown in Figure 1.2, carbon-hydrogen bond dissociation energies are in the order of ethene (368.6 kJ/mol) < toluene (370.3) < trimethylamine (380.7) < dimethyl ether (402.1) < ethane (420.5), indicating that resonance effect of conjugated C-C π bonds is influential.

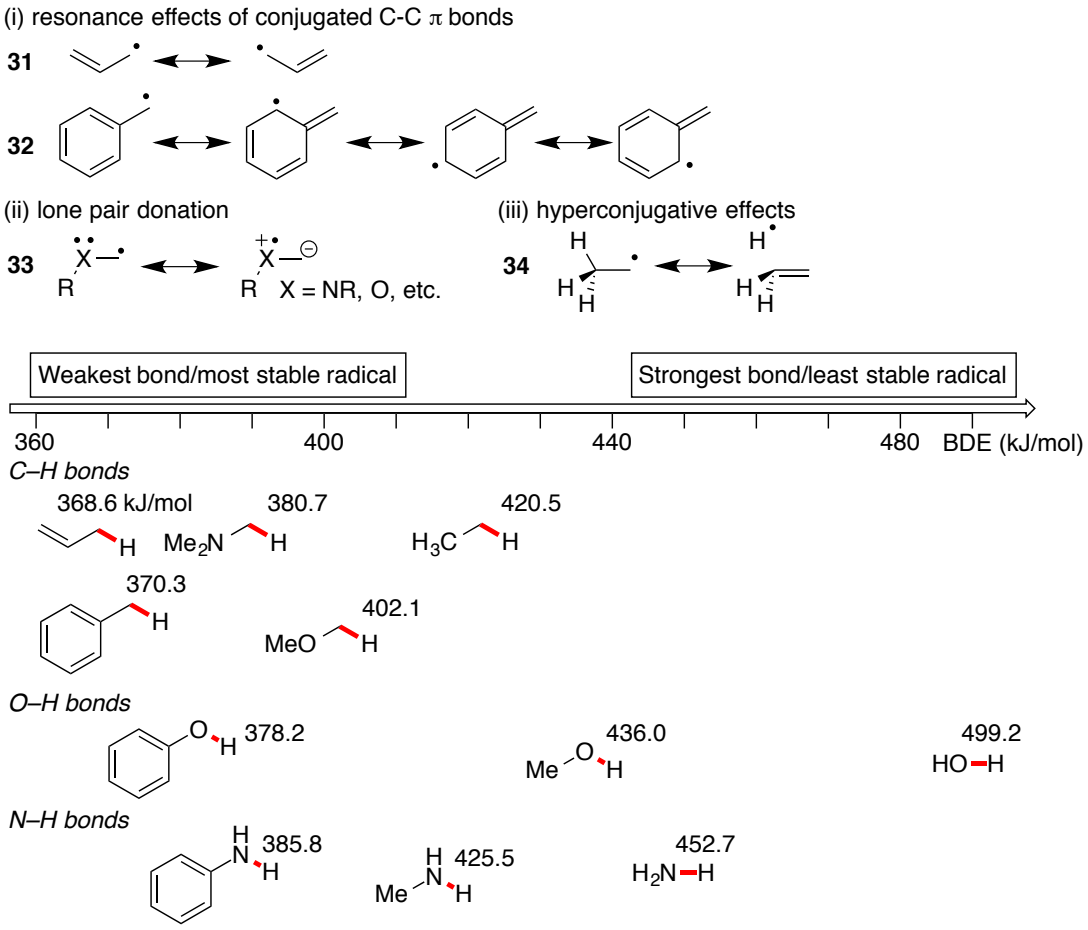

Figure 1.2 Stabilization of carbon-, oxygen- and nitrogen-centered radicals and the relationship with bond dissociation energies (BDE).

Stability of N, O-centered radicals

Substituent effects for stabilizing nitrogen- and oxygen-centered radicals are similar to those observed for the carbon-centered radical (Figure 1.2). The effects of oxygen-centered radical are stronger than carbon-centered radical analogues. The O-H

bond dissociation energy of methanol is 436.0 kJ/mol and that of phenol is 378.2 kJ/mol. Alkyl and aryl substituent greatly reduce the energy but even so N-H and O-H bonds are generally stronger than C-H bonds, resulting in that oxygen- and nitrogen-centered radicals easily abstract a hydrogen from C-H bond.

1.3. Intermolecular radical addition to alkene

Although all radical elementary reactions are important for comprehension of radical reaction, in this thesis, the author focuses on radical addition to olefins and describes it in detail.

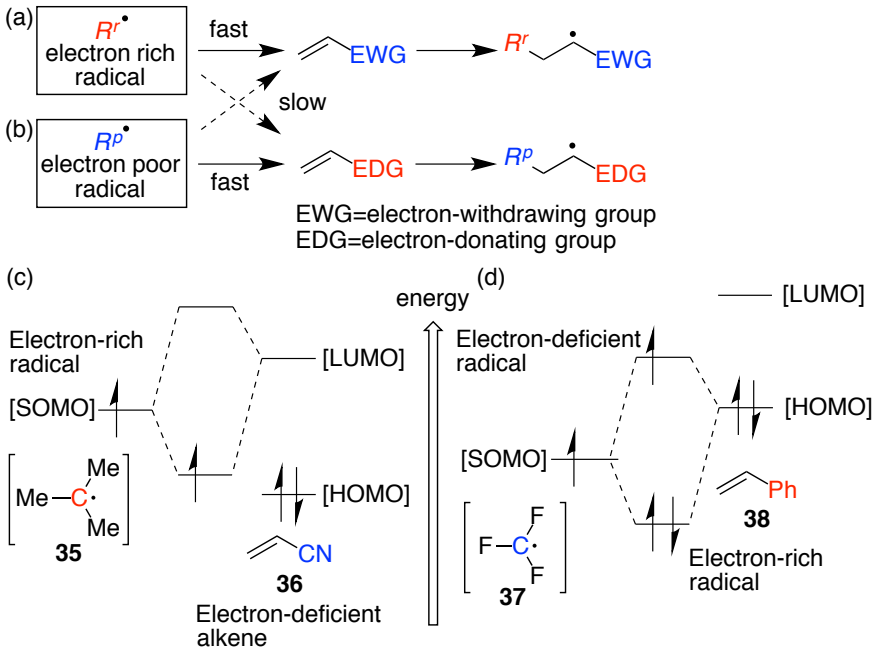

Figure 1.3 Reactivity and frontier molecular orbital interaction in radical addition

The reactivity of radicals depends on the relation of the electronic states of radicals and multiple bonds (Figure 1.3 (a) and (b)). It can be explained in terms of proximity in energy of the frontier molecular orbitals (Figure 1.3 (c) and (d)). An electron-rich radical with a higher SOMO, *e.g.* *tert*-butyl radical (**35**), smoothly reacts with

electron-deficient alkenes with a lower LUMO such as acrylonitrile (**36**) (Figure 1.3 (a) and (c)). On the other hand, electron-deficient radicals with SOMO, *e.g*. trifluoromethyl radical (**37**), smoothly react with electron-rich alkenes with a high HOMO such as styrene (**38**) (Figure 1.3 (b) and (d)).

1.4 Generation of radicals

The methods for generation of radicals are essential for achieving effective radical reactions. The generation of radical is triggered by stimulus such as heating (thermolysis) and light irradiation (photolysis). Various methods have been developed so far.[1] First, typical methodologies are briefly discussed.

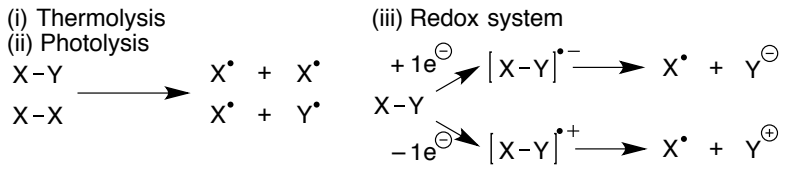

Scheme 1.7 Typical methodologies for generation of radical species.

Typical generation of radical is classified into three methods: (i) thermolysis, (ii) photolysis and (iii) redox system (Scheme 1.7). Thermolysis and photolysis cause the homolysis of a weak bond in the molecule. Bond dissociation energy (BDE) of typical single bonds are summarized in Table 1.1. As can be seen from the large BDEs shown in Table 1.1, carbon-carbon, carbon-hydrogen and carbon-fluorine bonds are too strong to undergo homolytic cleavage under ordinary conditions. In contrast, due to the smaller BDEs for carbon-heteroatom bonds and, in particular, heteroatom-heteroatom bonds they may be susceptible to homolysis to serve as radical precursors.

Table 1.1 Bond dissociation energy of typical single bonds.[5]

	single bonds	BDE (kJ/mol)
strong bonds	H_3C-F	460.2
	H_3C-H	439.3
	H_3C-CH_3	377.4
	PhH_2C-H	370.3
weak bonds	H_3C-Cl	350.2
	H_3C-Br	294.1
	H_3C-I	238.9
	$H_3CH_2C-NNC_2H_5$	209.2
	*t*BuO−NO	171.1
	$(H_3C)_2N-NO_2$	165.7
	*t*BuO−O*t*Bu	159.8
	$H_3CC(O)O-O(O)CH_3$	127.2

1.4.1 Generation of radicals by thermolysis

Covalent bonds that can be cleaved under 150 ºC are limited. Peroxides and AIBN (**39**) are one of representative radical precursors (Scheme 1.8). Thermolysis of AIBN affords the 2-cyano-2-propyl radicals (**40**) accompanying generation of nitrogen molecules to drive the decomposition process.

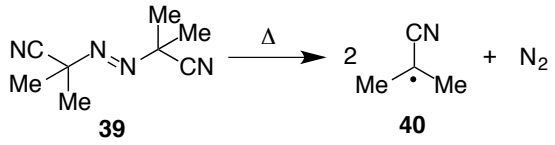

39 **40**

Scheme 1.8 Generation of radicals from AIBN.

1.4.2 Generation of radicals by photolysis

Irradiation of a molecule causes excitation of an electron in HOMO to LUMO, which has anti-bonding character to weaken the bond. As a result, such a photochemical electronic transition frequently leads to σ bond homolysis. For example, in the case of benzoyl peroxide (**41**), n-σ* excitation smoothly induces O-O bond homolysis, which is

followed by decarboxylation (Scheme 1.9 (a)). The resultant phenyl radical (**42**) has been utilized as an initiator of radical polymerization of styrenes and acrylates.

Carbonyl compounds (**43**) with C=O bonds undergoes photochemical n-π* transition to generate biradicals (**44**) with the radical centers on the C and O atoms, which may abstract a hydrogen atom from another substrate to initiate radical transformations (Scheme 1.9 (b)).

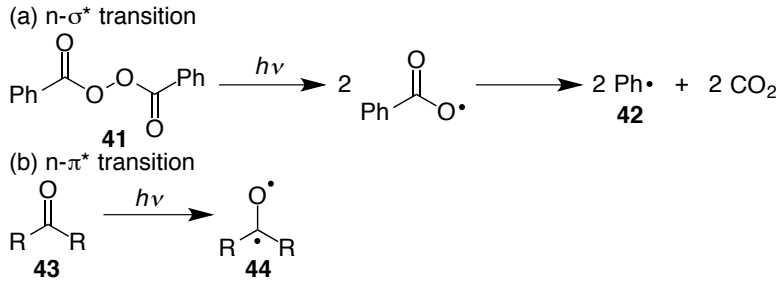

Scheme 1.9 Photochemical generation of radicals.

1.4.3 Generation of radicals by redox system

Radicals can be generated either by reduction or oxidation process through an intermolecular single electron transfer (SET) process (Scheme 1.10).[1d]

1-e reduction process

2-iodopropane (**45**) is reduced by zinc to afford isopropyl radical (**48**) and iodo-anion species (Scheme 1.10 (a)).[6] The radical **48** reacts with acrylonitrile to give the radical intermediate **49**. Second 1e-reduction of **49** and protonation of **50** give the product **47**.

1-e oxidation process

The enol **51'** is oxidized by Mn^{III} to give radical cation and Mn^{II} species. The radical **54** adds to 1-hexene (**52**) to yield **55**, which is oxidized by Mn^{III} to afford carbocation **56**. Nucleophilic attack to the carbocation **56** gives the product **53**. In general, a stoichiometric amount of redox reagents are required to generate one radical species,

resulting in generation of stoichiometric waste derived from redox reagents. Photoredox system is a typical solution for this problem as will be described in Chapter 2-4.

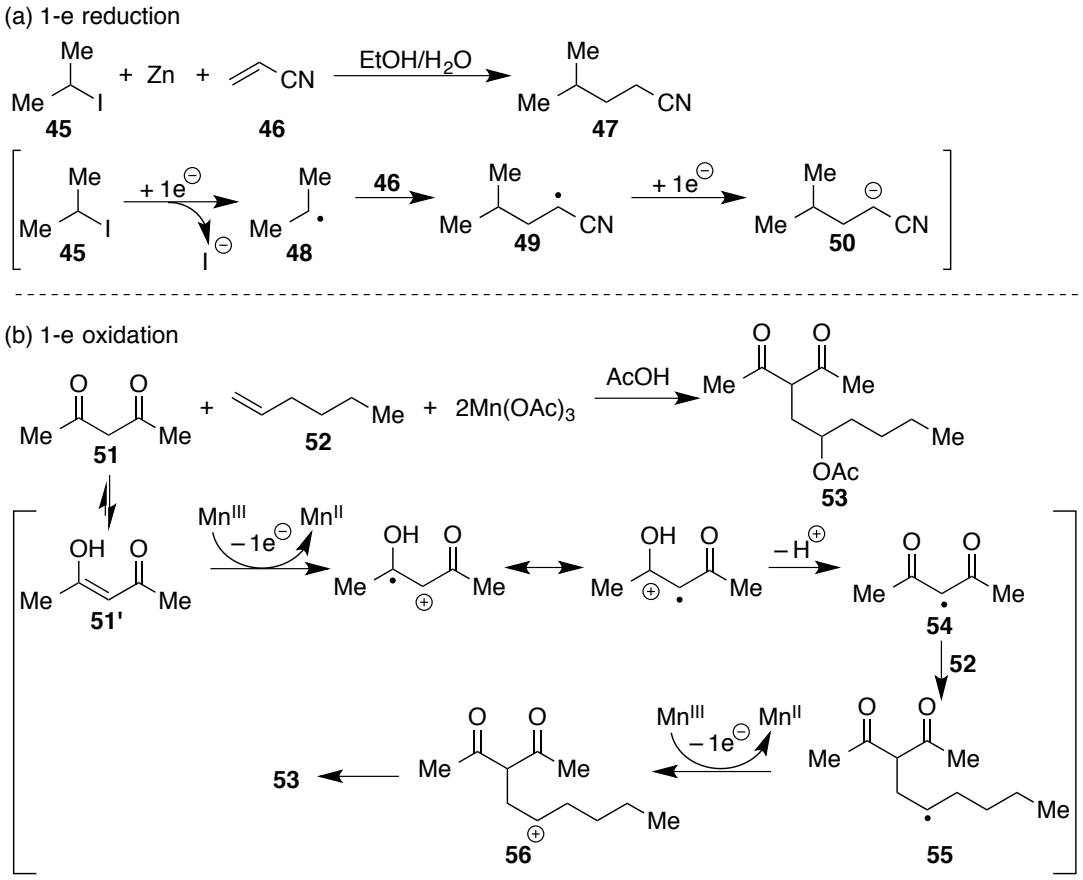

Scheme 1.10 Radical addition promoted by (i) zinc metal and (ii) manganese (III) salt.

1.5 Generation and reaction of organyl and heteroatom-centered radicals

In the previous section, the author showed basic concepts for generation and reactivity of radicals. The key methods for generation of carbon-, nitrogen- and oxygen-centered radicals will be described in this section.

1.5.1 Generation and reaction of carbon-centered radical from organoborates

As various examples of generation of radicals are shown above, there are many methods for generation of carbon-centered radicals. As shown in section 1.1, tributyltin plays important roles in synthesis of natural compounds due to a wide range of functional group tolerance. Organotin compounds, however, have a fatal drawback *i.e.* the high toxicity. Recently, organoboron reagents have been regarded as much less toxic radical precursors. These are autoxidized in the presence of a trace amount of oxygen even at –78 ºC to generate the corresponding carbon-centered radical species (Scheme 1.11). This radical system can be conducted under various reaction conditions (temperature and solvent).[1b, 6]

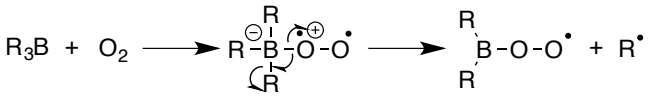

Scheme 1.11 Generation of carbon-centered radical from organoboranes

Conjugate addition reaction of organoboranes with α,β-unsaturated carbonyl compounds was reported by Brown (Scheme 1.12).[7] Oxidation of tricyclopentyl borane (**57**) generated the cyclopentyl radial (**60**), which added to 2-cyclopenten-1-one (**58**) to give the radical intermediate **61**. A propagation of **61** with **57** affords **60** and **62**. Hydrolysis of **62** gives the 1,4-addition product **59**.

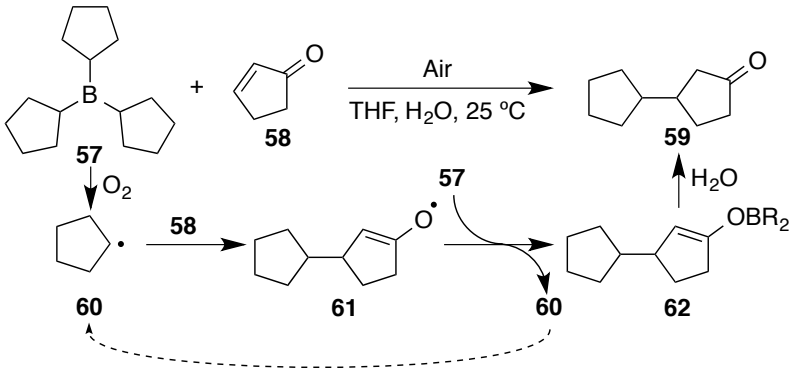

Scheme 1.12 1.4-Addition reaction of tricyclopentyl borane with 2-cyclopenten-1-one.

Highly reactive alkylboranes, however, are hard to be handled due to their pyrophoric nature and synthesis of trialkylboranes bearing functional groups is not always easy. Recently, organoboronic acid and their derivatives, which are stable under ambient conditions, play important roles as carbon-centered radical precursors[8] as well as Suzuki-Miyaura coupling reagents. For example, Baran's group reported C-H functionalization of quinones with boronic acid (**63**) (Scheme 1.13(a))[8m] and Chemler's group reported on the oxidative Heck reaction with alkyltirfluoroborates (**64**) (Scheme 1.13(b)).[8p] These methods require excess amounts of oxidants.

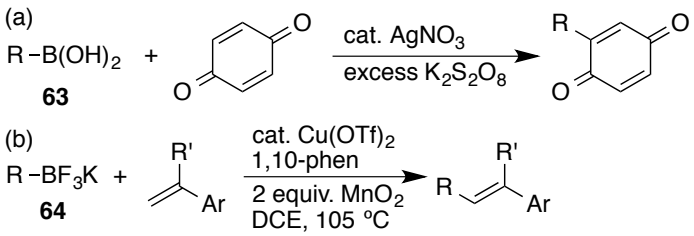

Scheme 1.13 Minisci and Heck type reactions with organo-boronic acid and borate.

1.5.2 Generation and reaction of nitrogen-centered radicals

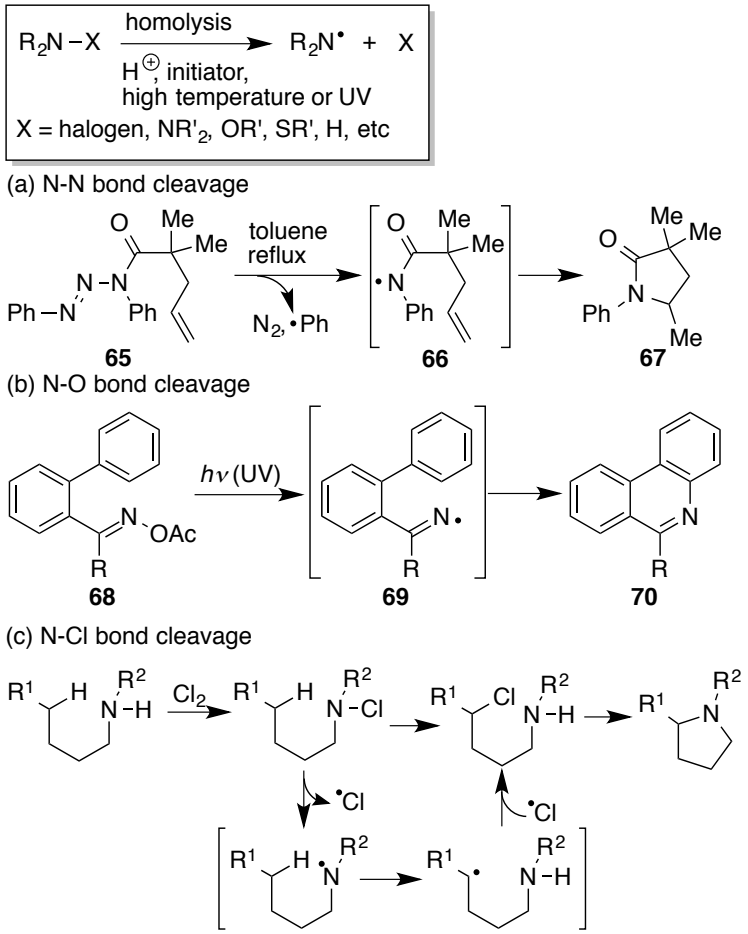

Scheme 1.14 Example of intramolecular reactions of nitrogen-centered radicals.

In general, nitrogen-centered radicals are generated by homolysis of weak N-X bonds (X = electronegative atoms such as halogen, nitrogen, oxygen and sulfur groups) under harsh conditions, *e.g.* the use of strong acid or a hazardous radical initiator, high temperature or UV irradiation.[1b,9] Examples of intramolecular cycloaddition with nitrogen-centered radical are shown in Scheme 1.14.

(a) *Cleavage of N-N bonds*

Several amine compounds serve as nitrogen-centered radicals such as hydrazine, hydrazone, azide and triazene derivatives. For example, *N*-acyltriazenes such as

65 is decomposed by thermolysis to generate the *N*-centered radical **66**. Cleavage of the weak N-N bond and loss of molecular nitrogen are the driving force for generation of the nitrogen-centered radical. The ring closure reaction proceeds to afford the product **67** (Scheme 1.14(a)).[10a]

(b) *Cleavage of N-O bonds*

N-O bonds are generally weaker than N-N bonds. Various derivatives of oximes and hydroxyamic acids have been exploited. For example, imidyl radical (**68**) is also generated from oxime acetates **69** under UV light irradiation to afford aza-phenanthrenes **70** (Scheme 1.14 (b)). [10b]

(c) *Cleavage of N-halogen bond*

Hoffmann-Löffler-Freytag (HLF) reaction has been known as a representative intramolecular ring closure reaction via a nitrogen-centered radical generated from *N*-chloroamine under photolysis or thermolysis (Scheme 1.14 (c)).[11] *N*-Chloro derivatives are most commonly used due to ease of preparation and stable when compared with *N*-bromo and *N*-iodo dericatives.

Nitrogen-centered radicals are mostly limited to intramolecular cyclization. Furthermore, nucleophilicity of aminyl radical ($R_2N^{\bullet}$), which is derived from amine, can be controlled by acid, metal or Lewis acid as well as substituent on the nitrogen atom. The reaction rate of 5-exo cyclization with an ordinary aminyl radical is slow (2×10^4 s^{-1}). In contrast, the reaction with a protonated aminyl radical becomes faster (1×10^8 s^{-1}) (Scheme 1.15 (a)).[9a] Brønsted acid inactivates the lone-pair on nitrogen to increase the electrophilicity of aminyl radicals. On the other hand, an amidyl radical ($R(R'CO)N^{\bullet}$) adjacent to a carbonyl group, which is derived from amide, causes an increase of the reaction rate (2×10^9 s^{-1}) without an addition of acid.

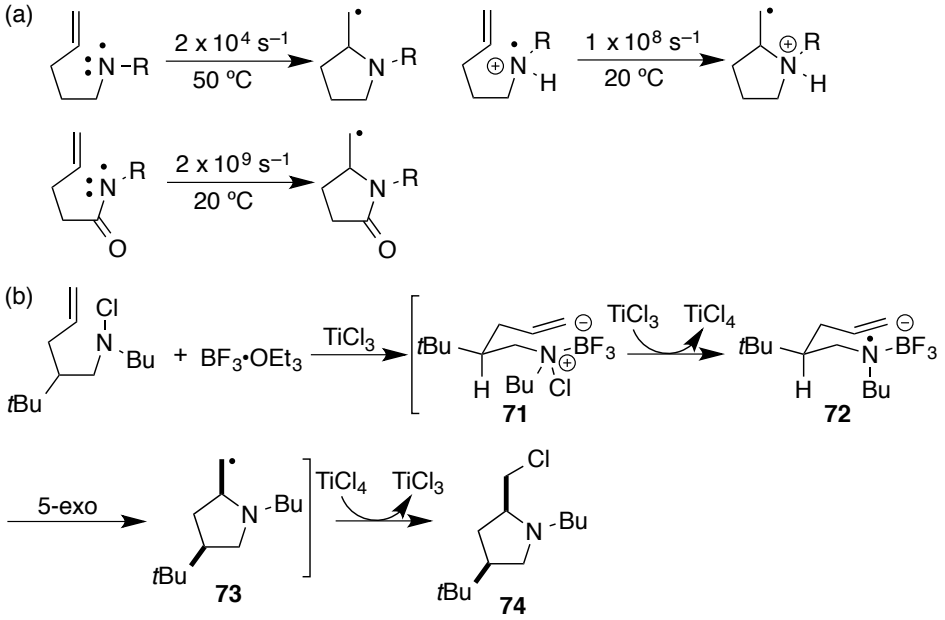

Scheme 1.15 5-*exo* Cycloaddition with *N*-centered radicals.

Lewis acid also promotes the rate of cycloaddtion.[11,12] Scheme 1.15 (b) is shown that titanium chloride (III) catalyzed cycloaddition with the aminyl radical.[11] Trifluoroborane serves as Lewis acid to give the adduct **71**, which is reduced by $TiCl_3$ to produce the aminyl radical **72**. The radical **72**, the electrophilicity of which is increased by Lewis acid, undergoes cyclization to afford the radical intermediate **73** and then the product **74**.

Although HLF reaction was developed in 1878, development of nitrogen-centered radical reactions has advanced slowly in contrast to carbon-centered radical reactions. Intermolecular radical amination is difficult due to the propensity of nitrogen-centered radicals to undergo hydrogen-abstraction and to engage in other degradation processes.[9] The synthetic utilities of nitrogen-centered radical remain unexplored because of lack of effective radical precursors and reaction systems.

1.5.3 Generation and reaction of oxygen-centered radicals

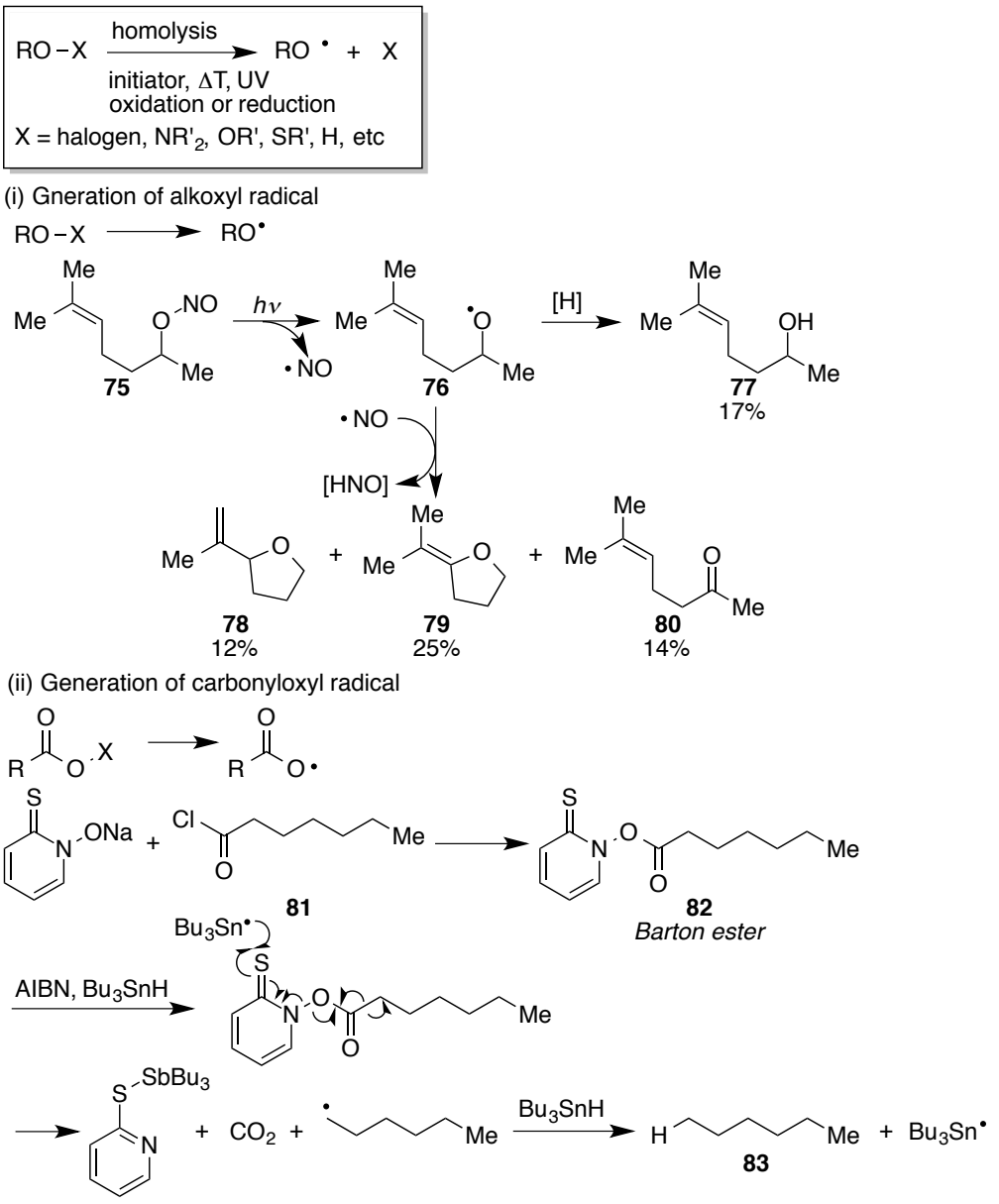

Scheme 1.16 Reactions with oxygen-centered radicals.

Oxygen-centered radicals are also generated via cleavage of weak O-X bond by heating, UV irradiation or redox condition.[13] In this section, reaction of alkoxy radical and carbonyloxy radical are described because carbonyloxy radicals are important in this thesis. Alkoxy radical in early investigations (i) and carbonyloxy radical with

Barton ester (ii) are shown in Scheme 1.16.

(i) Alkoxy radicals are short-lived reactive intermediates and moderately electrophilic.[12] An example of alkoxy radical reaction is shown in Scheme 1.16 (i). The alkoxy radical **76** is generated by the alkenyl nitrite **75** under UV irradiation. The radical **76** adds intramolecularly to the olefin to produce cyclic ether **78** and **79** but in low yields. Byproducts of **77** and **80** result from H-abstraction processes rather than the addition processes. Thus oxygen-centered radicals are too difficult to be controlled. Therefore, some reaction design is essential.

(ii) Barton ester (**82**)[14a] produces the carbonyloxy radical by visible light irradiation, heating or addition of addition of a radical initiator to generate alkyl radical via decarboxylation. By using this system, the acid chloride **81** afforded aliphatic product **83**.[14b]

It should be noted, as already pointed out for the *N*-centered radicals, it is difficult to control the reactivity of *O*-centered radicals.

A large number of organyl and heteroatom-centered radical reactions have been developed for many years. However, most of radical reaction systems require high temperature, UV irradiation conditions or an extra amount of metal oxidant or reductant. These points lower the synthetic utilities of radical reactions. Thus, the author thinks that the methodology for catalytic radical reaction under mild conditions is required to open a new field of synthetic radical chemistry.

1.6 Photoredox catalyzed reaction[3]

1.6.1 Photoredox catalysis

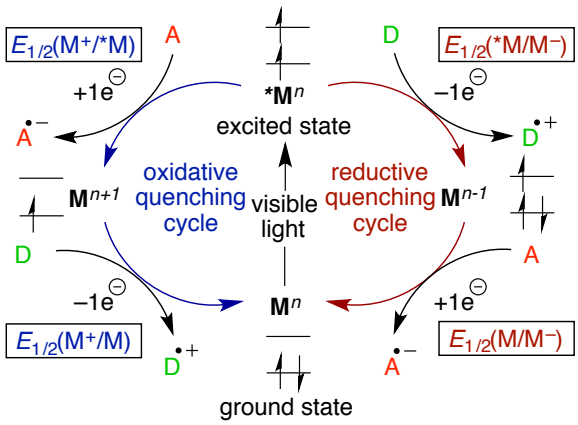

Scheme 1.17 Photoredox catalysis.

Mechanisms accepted for photoredox catalysis by metal complexes are summarized in Scheme 1.17, where the catalyst is denoted as $\mathbf{M}^n$. Visible light irradiation of $\mathbf{M}^n$ causes excitation via MLCT transition to form the singlet excited state, which is spontaneously converted to the more stable triplet excited state $^*\mathbf{M}^n$ via intersystem crossing. The excited state with a singly occupied higher SOMO and a hole in the lower SOMO can serve either as a 1e-reductant or as a 1e-oxidant following so-called oxidative quenching cycle and reductive quenching cycle, respectively.

Oxidative quenching cycle: The initial SET process from the higher SOMO to an external substrate **A** forms the anionic radical species $\mathbf{A}^{\cdot-}$ together with the oxidized metal species $\mathbf{M}^{n+1}$, which subsequently receives an electron from an external donor **D** to generate the cationic radical species $\mathbf{D}^{+\cdot}$ and the ground state catalyst **M**. Thus during the catalytic cycle a set of 1e-reduction and 1e-oxidation processes is accomplished.

Reductive quenching cycle: A catalytic cycle can be also initiated by accepting an electron to the hole in the lower SOMO as shown in Scheme 1.17.

Although the order of the redox processes involved in the two quenching cycles is reversed, they can undergo a set of 1e-reduction and 1e-oxidation processes with external substrates. If these processes are combined with chemical reactions which require these redox features, they can be driven by simple irradiation of visible light.

Research groups over the world including our group have developed a series of chemical transformations. As a result, the photoredox catalysis turns out to be fruitful and now many scientists are entering the field. After description on photoredox catalysts in the next section, organic reactions promoted by photoredox catalysis will be summarized in latter sections.

1.6.2 Photoredox catalyst[3d]

Table 1.2 Photoredox catalysts.

(a) Photoredox catalysts

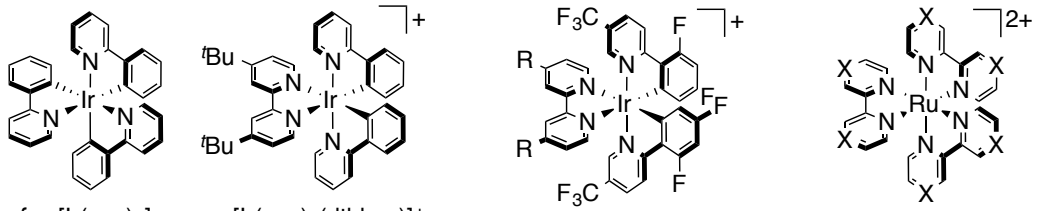

(b) Redox potential and photophysical properties

entry	photocatalyst	$E_{1/2}$ ($M^+/^*M$)	$E_{1/2}$ (M^+/M)	$E_{1/2}$ ($^*M/M^-$)	$E_{1/2}$ (M/M^-)	excited-state lifetime τ (ns)	excitation λ_{max} (nm)	emission λ_{max} (nm)
1	**Ir-1**	–2.14	+0.36	–0.10	–2.60	1900	375	494
2	**Ir-2**	–1.37	+0.80	+0.25	–1.92	557		581
3	**Ir-3**	–1.41	+1.28	+0.91	–1.78	2280	412	483
4	**Ir-4**	–1.30	+1.28	+0.80	–1.78	2300	380	470
5	**Ru-1**	–1.24	+0.88	+0.43	–1.74	1100	452	615
6	**Ru-2**	–0.67	+1.45	+1.04	–1.21	740	443	591

There are many kinds of photoredox catalysts ranging from the metal catalysts shown in Table 1.3 to organic dyes. Mechanisms for organic dyes are essentially the same as that for metal complexes discussed above and the singlet excited state of organic dyes works as the reactive redox species because of the slow intersystem crossing.

Key features of photoredox catalysts will be discussed from the viewpoints of (i) redox properties, (ii) lifetime of the photo-excited species, and (iii) absorption.

(i) redox properties: The most important feature of photoredox catalysts is the redox potentials of the photoexcited species ***M**, which are totally different from those of the ground state species. In Table 1.3 summarized are the oxidation potentials ($E_{1/2}(M^+/*M)$) and the reduction potentials ($E_{1/2}(*M/M^-)$), which are regarded as the indicators of reduction and oxidation power of the photoexcited species ***M** in the initial SET processes, respectively. In Table 1.3, the catalysts are arranged in the ascending order of the oxidation potentials of the photo-excited species ($E_{1/2}(M^+/*M)$). The order is roughly parallel to the ascending order of the reduction potentials ($E_{1/2}(M/M^-)$).

The redox potentials for the ground state is relevant to the second SET processes of the photoredox catalysis as shown in Scheme 1.17.

(ii) lifetime of the photo-excited species: It has been believed that a catalyst with a longer lifetime of the photo-excited state should work more efficiently. As summarized in Table 1.2, the lifetimes are μs order, which are long enough for most of organic reactions of ns order.

Because, however, organic dyes via singlet excited species with very short lifetime of ns-ps order turn out to be effective, lifetime may not be always a key issue.

(iii) absorption: For visible light photoredox catalysts it is, of course, essential to absorb visible light. Metal complexes are usually colored due to transitions associated with metal d electrons. For organic molecules, an extended π-system is essential for visible

light absorption. Compared to organic dyes, the absorption ranges of the metal catalysts are rather limited (i.e. in the shorter wavelength region) but absorption of the shorter wavelength light may be enough, because the shorter wavelength light is associated with higher energy and the longer wavelength light contains much of infrared rays (thermal energy).

In general, for reduction processes it is better to use a catalyst with a lower oxidation potential of the photoexcited species (e.g. **Ir-1**), and a catalyst with a higher reduction potential of the photoexcited species is better for oxidation processes.

1.6.3 Reaction patterns

Radical species can be connected to cationic and anionic species through SET processes as shown in Scheme 1.18, *i.e.* radical species can be generated either by 1e-reduction of a cation or by 1e-oxidation of an anion. The author's group recognized that photoredox catalysis may be used for these redox processes.

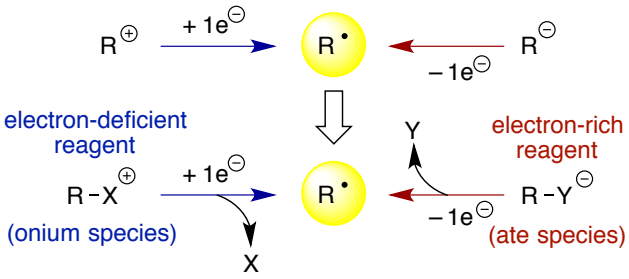

Scheme 1.18 Redox reaction by photoredox catalysis.

The free ionic species, however, are usually unstable. Then the author's group has employed the corresponding onium and ate species, which are regarded as stabilized forms of cation and anion, respectively. Relevant electron-deficient and electron-rich compounds may be also used as the precursors, as exemplified by hypervalent iodine

species as described below. But the key for success is selection of the leaving groups X and Y, which is one of the main subjects of the present thesis.

Selected examples of photoredox catalysis will be summarized below according to the precursors, which is also associated with the quenching cycles.

1.6.4 Radical generation from ate species via reductive quenching cycle

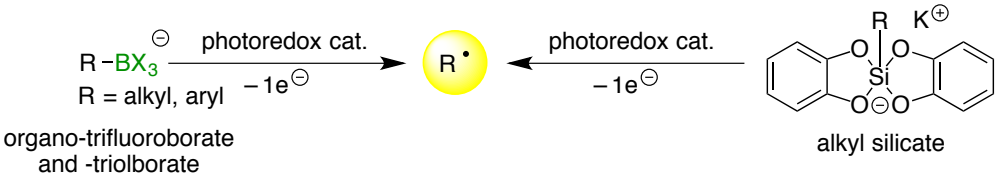

Scheme 1.19 Generation of carbon-centered radicals from ate species.

As shown Scheme 1.19, ate species such as organoborate and silicate reagents have been exploited as radical precursors by the action of 1e-oxidatoin process induced by photoredox catalysis. Organoborates have been regarded as radical precursors (Scheme 1.13).[15,16] The author's group reported that alkyl- and aryl-organotrifluoroborates/triolborates serve as carbon-centered radical precursors by photoredox catalysis under visible-light irradiation (Scheme 1.20).[15a] Recently, Fensterbank's group found that alkylsilicates (hypervalent biscatecholato silicon species) serve as radical precursors. These ate species are electron-rich enough to be oxidized.

C-C and C-O bond formation with organoborates by photoredox catalysis.[15a]

The reaction mixture of organoborate **84**, an electron-deficient olefin **85** and 2 mol% of **Ir-3** in an acetone–methanol mixture under visible light irradiation (425 ± 15 nm, blue LEDs) afforded the C-C coupling products **86**. Carbon-centered radical **87** which

was generated from organoborates **84** by 1e-oxidation mediated by photoredox catalysis reacts with olefin **85** to give the radical intermediate **88**. The radical **88** was reduced by the highly reducing Ir species ($\boldsymbol{Ir^{II}}$). Subsequent protonation with MeOH produces the hydoalkylated or hydroarylated product. This reaction following the reductive quenching cycle is called Giese-type reaction. In the presence of TEMPO (2,2,6,6-tetramethylpiperidin-1-yloxyl) instead of olefin **85**, the radical **87** was trapped by TEMPO to give the C-O coupling product **90**.

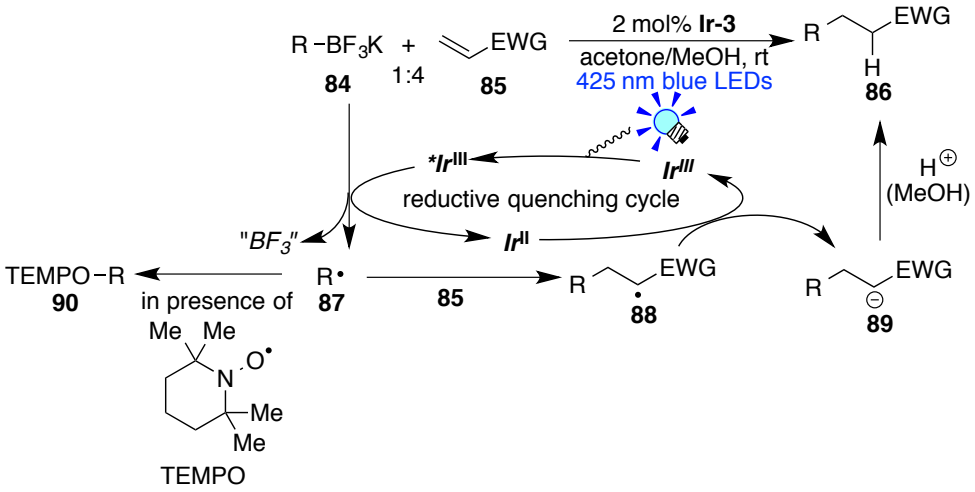

Scheme 1.20 Photocatalytic C-C and C-O bond formations.

1.6.5 Radical generation from onium species via oxidative quenching cycle

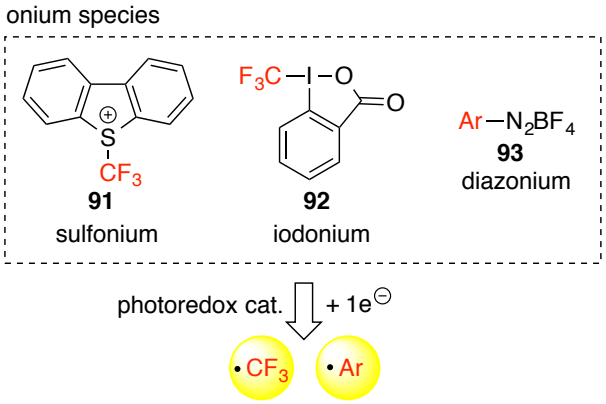

Figure 1.4 Generation of trifluoromethyl radical with onium species.

Onium salts such as Umemoto (**91**) and Togni (**92**) reagents and aryl diazonium salts (**93**), which are bench-stable and easy-to-use, have been regarded as trifluoromethyl and aryl radical precursors, respectively, by the action of photoredox catalysis (Figure 1.4). A great number of photoredox catalyzed trifluoromethylation and arylation were reported and the author describes the example of oxytrifluoromethylation in this section because it is a good example to understand oxidative quenching cycles.

Oxitrifluoromethylation of olefins with Umemoto's reagent by photoredox catalysis[18]

As shown in Scheme 1.21, Umemoto's reagent (**94**) serves as a CF_3 radical precursor upon 1e-reduction via oxidative quenching cycle. CF_3 radical **97** reacts with olefin **95** to afford radical intermediate **98**. The radical intermediate **98** is oxidized by highly oxidizing photocatalyst ($\mathbf{Ir^{IV}}$) to afford the carbocation species **99**, which is a key intermediate for synthesis of difunctionalized product. Nucleophilic attack of water or alcohol to **99** produces oxytrifluoromethyled products **96**.

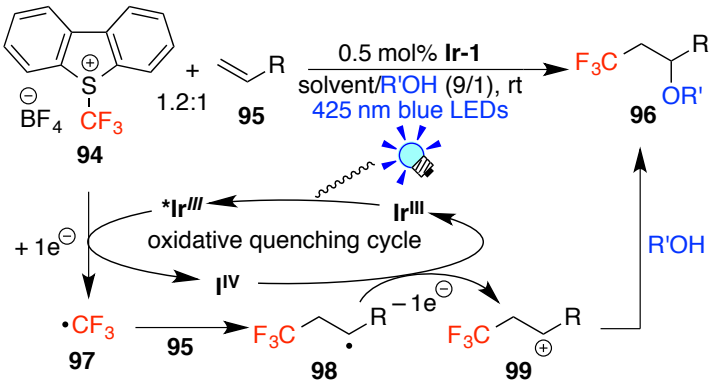

Scheme 1.21 Photoredox catalyzed oxytrifluoromethylation olefins.

1.7 Survey of the present thesis

A variety of studies on radical chemistry concerning structure, physical properties and reactivity have flourished. Recently, photoredox catalysis has been regarded as

attractive radical systems from the viewpoints of solar chemistry, green chemistry and clean chemical production processes. The laboratory, to which the author belongs, has developed a series of visible light promoted organic transformations by the action of photoredox catalysis. Many efforts have been devoted to construction of carbon skeletons via C-C coupling processes but, in sharp contrast, there remains much room for introduction of heteroatom-functional groups. Taking into account this situation, the author considered that heteroatom-functional groups can be introduced to organic skeletons by means of radical species generated by the action of photoredox catalysis.

In chapters 2, the author describes the results of hydro-alkoxymethylation and hydro-aminomethylation of olefins (**101**) with the corresponding organoborates (**100**) by the action of photoredox catalysis (Scheme 1.23). The key intermediates of the transformations are the alkoxymethyl and aminomethyl radicals and herein the heteroatom-functional groups are introduced via C-C coupling of heteroatom-substituted carbon radicals, which are regarded as *indirect* introduction of heteroatom-functional groups.

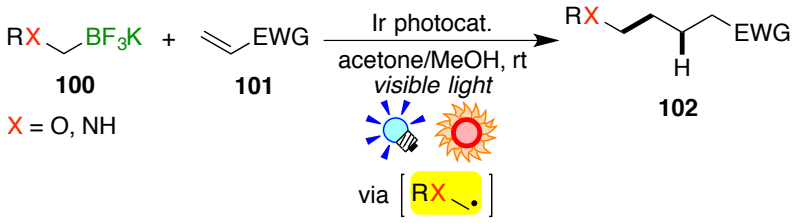

Scheme 1.22 Alkoxy- and amionmethylation of electron-deficient olefins

By contrast, chapters 3 and 4 deal with *direct* introduction of heteroatom functional group via coupling with heteroatom-centered radicals (Scheme 1.24). For these processes it is essential to develop efficient precursors, and the author prepared the unique precursors with pyridine leaving groups (**103-105**), which turned out to be

efficient for radical generation by the photochemical SET processes. In the presence of water the generated nitrogen radicals undergo regiospecific aminohydroxylation of olefins, whereas the *O*-centered aroyloxyl radicals with electron-withdrawing substituents react with electron-rich aromatic compounds to afford aryl arene-carboxylates.

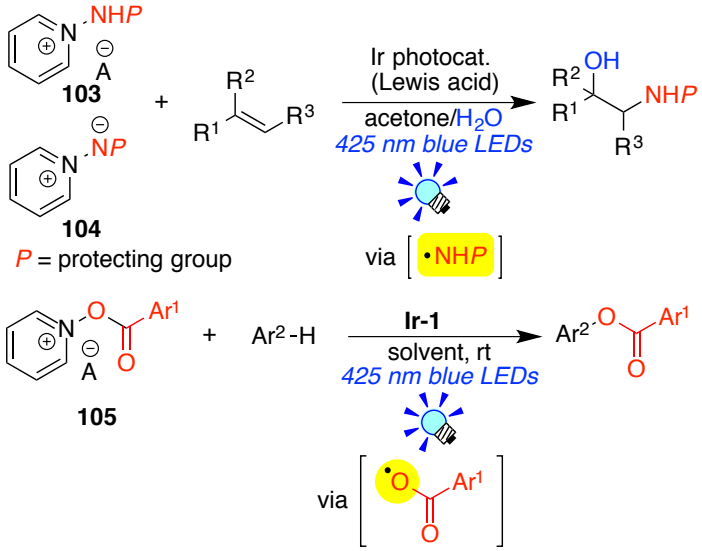

Scheme 1.23 Regioselective aminohydroxylation of olefins and aroyloxylation of arenes by photoredox catalysis.

1.8 References

1 (a) *Encyclopedia of Radicals in Chemistry, Biology and Materials,* Vol. 1-4 (Eds: C. Chatgilialoglu, A. Studer), John Wiley & Sons Ltd, Chichester, **2012**. (b) *Radicals in Organic Synthesis,* Vol. 1-4 (Eds: P. Renaud, M. P. Sibi), John Wiley-VCH: Weinheim, Germany, **2001**. (c) H. Togo, "*Free Radical Reaction for Organic synthesis*", MARUZEN, **2015**. (d) I. Ryu, "*Foundation of Organic Radical Reaction*", MARUZEN, **2015**. (e) M. Yan, J. C. Lo, J. T. Edwards, P. S. Baran, *J. Am. Chem. Soc.* **2016**, *138,* 12692-12714.

2 (a) H. Tokuyama, T. Yamashita, M. T. Reading, Y. Kaburagi, *J. Am. Chem. Soc.*

1999, *121,* 3791-3792; (b) M. T. Reding, T. Fukuyama, *Org. Lett.* **1999**, *1,* 973-976; (c) M. T. Reding, Y. Kaburagi, H. Tokuyama, T. Fukuyama, *Heterocycles*, **2002**, *56*, 313-330; (d) S. Yokoshima, T. Ueda, S. Kobayashi, A. Sato, T. Kuboyama, H. Tokuyama, T. Fukuyama, *J. Am. Chem. Soc.* **2002**, *124,* 2137-2139; (e) Y. Kaburagi, H. Tokuyama, T. Fukuyama, *J. Am. Chem. Soc.* **2004**, *126,* 10246-10247.

3 For reviews on the field of photoredox catalysis, see: (a) J. M. R. Narayanam, C. R. J. Stephenson, *Chem. Soc. Rev.* **2011**, *40,* 102-113. (b) J. Xuan, W.-J. Xiao, *Angew. Chem. Int. Ed.* **2012**, *51,* 6828-6838. (c) M. Reckenthäler, A. G. Griesbeck, *Adv. Synth. Catal.* **2013**, *355,* 2727-2744. (d) C. K. Prier, D. A. Rankic, D. W. C. MacMillan, *Chem. Rev.* **2013**, *113,* 5322-5363. (e) D. M. Schultz, T. P. Yoon, *Science* **2014**, *343,* 1239176-1-1239176-8. (f) K. L. Skubi, T. R. Blum, T. P. Yoon, *Chem. Rev.* **2016**, *116,* 10035-10074. (g) N. A. Romero, D. A. Nicewicz, *Chem. Rev.* **2016**, *116,* 10075-10166.

4 (a) M. S. Kharasch, F. R. Mayo, *J. Am. Chem. Soc.* **1933**, *55,* 2468-2496. (b) M. S. Kharasch, H. Engelmann, F. R. Mayo, *J. Org. Chem.* **1937**, *02,* 288-302. (c) M. S. Kharasch, E. V. Jensen, W. H. Urrry, *Science* **1945**, *102*, 128.

5 Y. R. Luo, *Handbook of bond dissociation energies in organic compounds*, CRCPress, Boca Rantonm, FL, 2003.

6 V. Darmency, P. Renaud, *Top. Cur. Chem.* **2006**, *263*, 71-106.

7 H. C. Brown, G. W. Kabalka, *J. Am. Chem. Soc.* **1970**, *92,* 714-716.

8 (a) G. B. Schuster, *Pure Appl. Chem*. **1990**, *62*, 1565-1572. (b) C. Ollivier, R. Chuard, P. Renaud, *Synlett* **1999**, 807-809. (c) C. Cadot, P. I. Dalko, J. Cossy, *J. Org. Chem.* **2002**, *67,* 7193-7202. (d) A. S. Demir, Ö. Reis, M. Emrullahoglu, *J. Org. Chem.* **2003**, *68,* 578-580. (e) L. A. Shundrin, V. V. Bardin, H.-J. Frohn, Z.

Arorg, *Allg. Chem*. **2004**, *630*, 1253-1257. (f) Y. Nishigaichi, T. Orimi, A. Takuwa, *J. Organomet. Chem.* **2009**, *694,* 3837-3839. (g) M. Pouliot, P. Renaud, K. Schenk, A. Studer, T. Vogler, *Angew. Chem. Int. Ed.* **2009**, *48,* 6037-6040. (h) C. Cazorla, E. Métay, B. Andrioletti, M. Lemaire, *Tetrahedron Lett.* **2009**, *50,* 6855-6857. (i) A. Dickschat, A. Studer, *Org. Lett.* **2010**, *12,* 3972-3974. (j) G. Sorin, R. M. Mallorquin, Y. Contie, A. Baralle, M. Malacria, J.-P. Ggoddard, L. Fensterbank, *Angew. Chem. Int. Ed.* **2010**, *49,* 8721-8723. (k) I. B. Seiple, S. Su, R. A. Rodriguez, R. Gianatassio, Y. Fujiwara, A. L. Sobel, P. S. Baran, *J. Am. Chem. Soc.* **2010**, *132,* 13194-13196. (l) G. A. Molander, V. Colombel, V. A. Braz, *Org. Lett.* **2011**, *13,* 1852-1855. (m) Y. Fujiwara, V. Domingo, I. B. Seiple, R. Gianatassio, M. D. Bel, P. S. Baran, *J. Am. Chem. Soc.* **2011**, *133,* 3292-3295. (n) J. W. Lockner, D. D. Dixon, R. Risgaard, P. S. Baran, *Org. Lett.* **2011**, *13,* 5628-5631. (o) S. R. Neufeldt, C. K. Seigerman, M. S. Sanford, *Org. Lett.* **2013**, *15,* 2302-2305. (p) T. W. Liwosz, S. R. Chemler, *Org. Lett.* **2013**, *15,* 3034-3037. (q) M. Presset, N. Fleury-Brégeot, D. Oehlrich, F. Rombouts, *J. Org. Chem.* **2013**, *78,* 4615-4619.

9 (a) S. Z. Zard, *Chem. Soc. Rev.* **2008**, *37,* 1603-1618; (b) W. C. Danen, F. A. Neugebauer, *Angew. Chem. Int. Ed.* **1975**, *14,* 783-789; (c) L. Stella, *Angew. Chem. Int. Ed.* **1983**, *22,* 337-350.

10 (a) H. Lu, C. Li, *Tetrahedron Lett.* **2005**, *46,* 5983-5985. (b) R. Alonso, P. J. Campos, B. Garcia, M. A. Rodriguez, *Org. Lett.* **2006**, *8,* 3521-3523.

11 M. E. Wolff, *Chem. Rev.* **1963**, *63*, 55-64.

12 Å. Sjöholm, M. Hemmerling, N. Pradille, P. Somfai, *J. Chem. Soc., Perkin Trans. 1,* **2001**, 891-899.

13 The reaction with *N*-stannylaminyl radicals, see; (a) M. Frankel, D. Wagner, D.

Gertner, A. Zikha, *J. Organomet. Chem.* **1967**, *7*, 518-520; (b) M. C. Samano, M. J. Robins, *Tetrahedron Lett.* **1991**, *32,* 6293-6296; (c) N. E. Poopeiko, T. I. Pricota, I. A. Mikhailopulo, *Synlett* **1991**, 342; (d) S. Kim, G. H. Joe, J. Y. Do, *J. Am. Chem. Soc.* **1993**, *115,* 3328-3329; (e) S. Kim, G. H. Joe, J. Y. Do, *J. Am. Chem. Soc.* **1994**, *116,* 5521-5522; (f) S. Kim, J. Y. Do, *J. Chem. Soc., Chem. Commun.* **1995**, 1607-1608; (g) S. Kim, S. S. Kim, H. S. Seo, K. S. Yoon, *Tetrahedron* **1995**, *51,* 8437-8446; (h) H.-S. Dang, B. P. Roberts, *J. Chem. Soc., Perkin Trans. 1* **1996**, 1493-1498; (i) S. Kim, K. M. Yeon, K. S. Yoon, *Tetrahedron Lett.* **1997**, *38,* 3919-3922; (j) A. M. Hornemann, I. Lundt, *J. Org. Chem.* **1998**, *63,* 1919-1928; (k) P. C. Montevecchi, M. L. Navacchia, P. Spagnolo, *Eur. J. Org. Chem.* **1998**, 1219-1226; (l) D. S. Hays, G. C. Fu, *J. Org. Chem.* **1998**, *63,* 2796-2797; (m) A. J. Moreno-Vargas, P. Vogel, *Tetrahedron Lett.* **2003**, *44,* 5069-5073; (n) L. Benati, G. Bencivenni, R. Leardini, M. Minozzi, D. Nanni, R. Scialpi, P. Spagnolo, G. Zanardi, C. Rizzoli, *Org. Lett.* **2004**, *6,* 417-420; (o) M. Zlotorzynska, H. Zhai, G. M. Sammis, *J. Org. Chem.* **2010**, *75,* 864-872.

14 (a) J. Hartung, *Eur. J. Org. Chem.* **2001**, 619-632. (b) J. Hartung, T. Gottwald, K. Špehar, *Synthesis* **2002**, *11*, 1469-1498 and referenced there in.

15 (a) D. H. R. Barton, B. Lacher, S. Z. Zard, *Tetrahedron* **1987**, *43,* 4321-4328; (b) A. L. J. Beckwith, S. A. M. Duggan, *J. Chem, Soc., Perkin Trans. 2.* **1994**, 1509-1518.

16 (a) Y. Yasu, T. Koike, M. Akita, *Adv. Synth. Catal.* 2**012**, *354,* 3414-3420; (b) H. Huang, G. Zhang, L. Gong, S. Zhang, Y. Chen, *J. Am. Chem. Soc.* **2014**, *136,* 2280-2283; (c) J. C. Tellis, D. N. Primer, G. A. Molander, *Science* **2014**, *345*, 433-437; (d) D. N. Primer, I. Karakaya, J. C. Tellis, G. A. Molander, *J. Am. Chem. Soc.* **2015**, *137,* 2195-2198; (e) O. Gutierrez, J. C. Tellis, D. N. Primer, G. A.

Molander, *J. Am. Chem. Soc.* **2015**, *137,* 4896-4899; (f) I. Karakaya, D. N. Primer, G. A. Molander, *Org. Lett.* **2015**, *17,* 3294-3297; (g) Y. Yamashita, J. C. Tellis, G. A. Molander, *Proc. Natl. Acad. Sci. U.S.A.* **2015**, *112*, 12026-12029; (h) H. Huang, K. Jia, Y. Chen, *Angew. Chem. Int. Ed.* **2015**, *54,* 1881-1884.

17 (a) V. Corcé, L.-M. Chamoreau, E. Derat, J.-P. Goddard, C. Ollivier, L. Fensterbank, *Angew. Chem. Int. Ed.* **2015**, *54,* 11414-11418; (b) L. Chennnberg, C. Lévêque, V. Corcé, A. Baralle, J.-P. Goddard, C. Ollivier, L. Fensterbank, *Synlett* **2016**, *27*, 731-735; (c) C. Lévêque, L. Chenneberg, V. Corcé, J.-P. Goddard, C. Olliver, L. Fensterbank, *Org. Chem. Front.* **2016**, *3*,462-465; (d) J.-P. Goddard, C. Ollivier, L. Fensterbank, *Acc. Chem. Res.* **2016**, *49*, 1924-1936; (e) C. Lévêque, L. Chenneberg, V. Corcé, C. Ollivier, L. Fensterbank, *Chem. Commun.* **2016**, *52,* 9877-9880;

18 (a) T. Koike, M. Akita, *Acc. Chem. Res*, **2016**, *49*, 1937-1945; (b) I. Ghosh, L. Marzo, A. Das, R. Shaikh, B. König, *Acc. Chem. Res.* **2016**, *49,* 1566-1577 and references therein.

19 Y. Yasu, T. Koike, M. Akita, *Angew. Chem. Int. Ed.* **2012**, *51,* 9567-9571.

Chapter 2

Hydro-aminomethylation and -alkoxymethylation of Olefins with Organotrifluoroborate by Photoredox Catalysis

ABSTRACT: Photocatalytic hydro-aminomethylation and -alkoxymethylation of olefins with the corresponding heteroatom-substituted methyltrifluoroborates have been developed. Reactive carbon radicals adjacent to the nitrogen and oxygen atoms can be easily generated from the corresponding organotrifluoroborates via visible-light-induced SET processes of the photoredox catalysis, *i.e.* reductive quenching cycle. This methodology provides a new strategy for the introduction of amino- and alkoxy-methyl groups onto electron-deficient C=C bonds and constitutes a facile entry into synthetically useful γ–aminobutyric acid (GABA) derivatives such as baclofen.

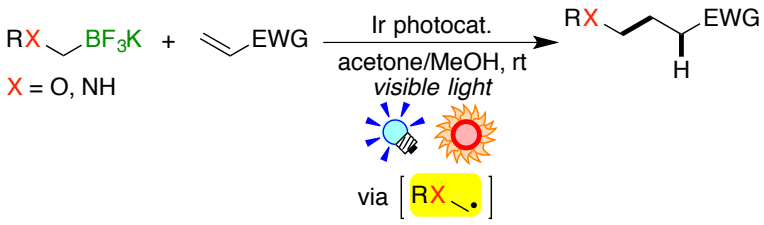

2.1 Introduction

Introduction of heteroatom-functional groups to organic skeleton is significantly important and essential in the field of organic synthesis. For synthesis of alkyl amines or ethers, S_N2 reactions of alkyl halide with alcohol or amine are of the top priority, because such reactions have been studied extensively. The classical synthetic methods involve Williamson ether synthesis and Gabriel synthesis.

The synthetic method to be chosen is also dependent on the availability of the reactants. If the desired alkyl halide and alcohol or amine are not readily available, alternatives to the above-mentioned S_N2 reactions should be searched or developed. Alkenes are a class of abundant chemical feedstocks and could be candidates for the alternatives, if conversion methods are established. For ether synthesis, simple acid-catalyzed addition of alcohol produces branched internal ethers following the Markovnikov addition, whereas the versatile radical addition to electron-deficiend alkenes, so-called Giese reaction (Scheme 2.1)[1] would afford linearly extended derivatives due to the reaction features as discussed in Chapter 1. Taking account of this situation, the author expected that ethers or amines can be prepared by the addition reactions of *N*- or *O*-containing carbon centered radicals.

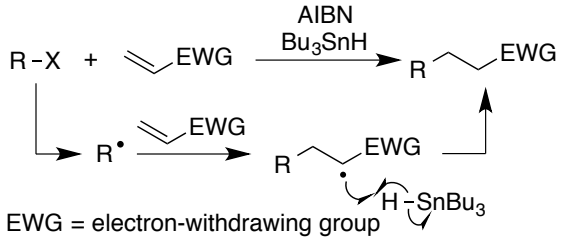

Scheme 2.1 Giese reaction.

In Chapter 2, the author describes the results of hydro-aminomethylation and hydro-alkoxymethylation of alkenes with the corresponding organotrifluoroborates by photoredox catalysis to afford ethers and amines with linearly extended carbon chains.

In these catalysis, the *O*- and *N*-groups are introduced to the γ position with respect to the alkene substituent EWG.

Photoredox catalyzed reaction of amines and ethers

Oxidation chemistry of ethers and amines has been studied extensively and established.[2] For example, interconversion of the cation radical of amine with relevant reactive *N*-containing reactive species such as α-aminoalkyl radical, iminium cation, and azomethine ylid via a series of transformations including deprotonation, hydrogen atom abstraction, and 1e-oxidation is shown in Scheme 2.2 (a). On the other hand, oxidation of ether gives a few reactive intermediate. Oxonium ion is a major intermediates for transformations of cationic oxygen radical radical via H-abstraction or deprotonation and 1e-oxidation under highly oxidative conditions (Scheme 2.2 (b)).

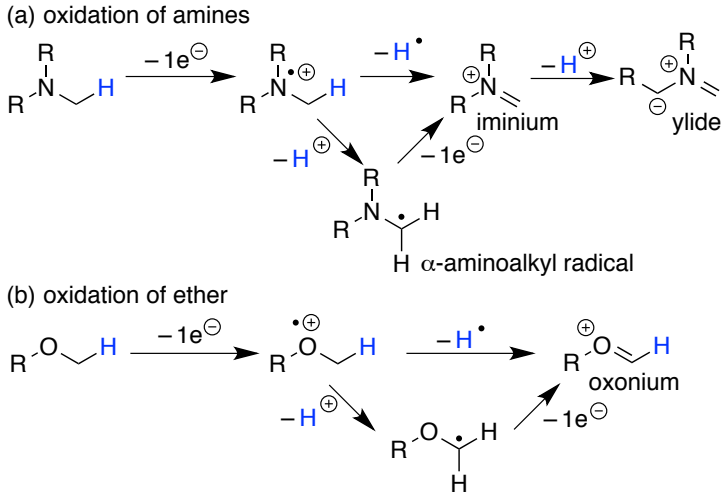

Scheme 2.2 Oxidation of amine and ether.

1e-Redox processes by photoredox catalysis are expected to trigger the above-mentioned interconversions of amines and ethers.

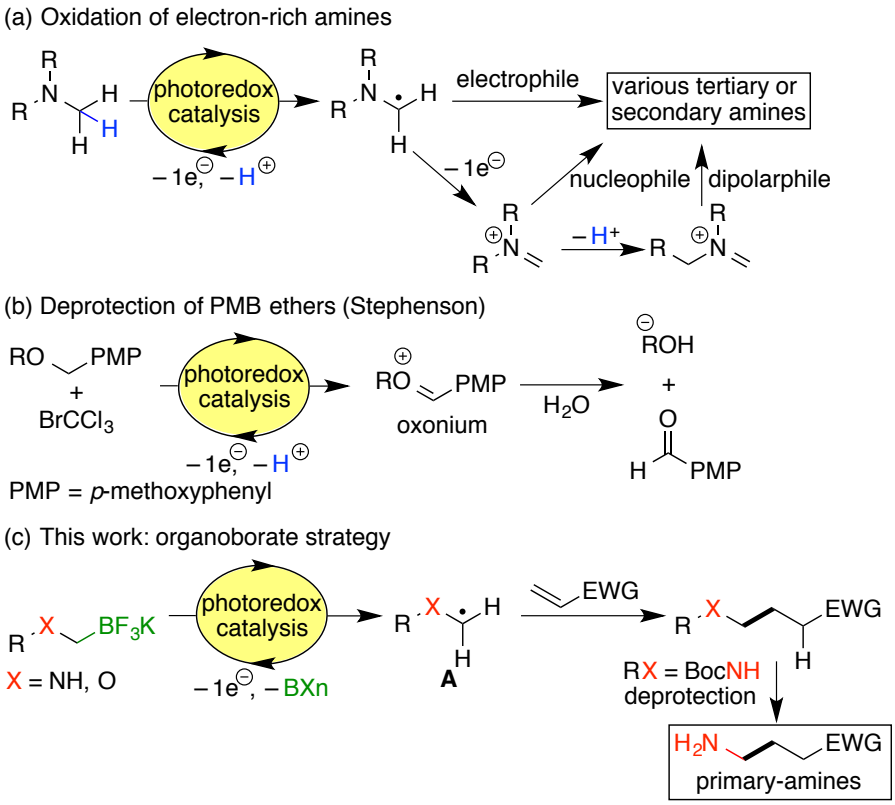

Scheme 2.3 Photoredox-catalyzed transformation of amines and ethers.

For the past few years, photoredox catalysis has become a powerful tool for oxidative transformation of electron-rich amines such as tertiary amine and enamine under visible light irradiation.[3-7] Reactive chemical species such as radicals, iminium ions, and azomethine ylides, can be generated through photoredox-catalyzed single electron transfer (SET) processes at the amine moiety and are converted to diverse nitrogen-containing products (Scheme 2.3 (a)). While previous reports mainly describe synthesis of tertiary or secondary amines, an access to useful primary amines has not been well-documented.[8]

On the other hand, functionalization of ethers by photoredox catalysis is limited. In 2011, the group of Stephenson reported photocatalytic deprotection of *p*-methoxybenzyl (PMB) ethers *via* oxonium species formed via a 2e-oxidation process (Scheme 2.3(b)).[9]

In contrast, oxidative generation of alkoxymethyl radicals[10] *via* a photoredox process has not been reported yet.

In Chapter 1 the author showed that organoborates can serve as electron donors as well as organic radical precursors by the action of the Ir photoredox catalyst, $[Ir(dF(CF_3)ppy)_2(bpy)](PF_6)$ (**Ir-3**) and $[Ir(dF(CF_3)ppy)_2(dtbbpy)](PF_6)$ (**Ir-4**),[11] of which the photoexcited species have the reduction potentials sufficient to oxidize organoborates.[2e,12] *N*-Protected aminomethyl- and alkoxymethyl-trifluoroborates have been developed and are known as easy-to-handle organometallic reagents.[13] Thus, the author envisioned that photoredox catalysis can generate heteroatom-functionalized carbon radical **A** from the corresponding organotrifluoroborates and induce hydro-aminomethylation and hydro-alkoxymethylation of electron-deficient olefins (Scheme 2.3 (c)). Furthermore, the author has extended this photocatalytic aminomethylation to synthesis of a bioactive γ-aminobutyric acid (GABA), which is a motif of baclofen.[14,] The present method provide a new strategy for access to molecules bearing the primary aminomethyl moiety.

2.2. Results and discussion

2.2.1 Hydro-aminomethylation by photoredox catalysis

2.2.1.1 Photocatalytic hydro-aminomethylation of methyl acrylate

The author initially examined the photocatalytic reaction of potassium Boc-protected aminomethyltrifluoroborate (**1a**) with methyl acrylate (**2a**) in the presence of the Ir photoredox catalyst **Ir-3** (2 mol%) in the mixed solvent system, acetone-d_6/CD_3OD (1/1), under visible light irradiation (blue LEDs: λ_{max} = 425 nm) for 1 h. As a result, the corresponding aminomethylated product **3aa** was formed in 92% yield as determined by ^{1}H NMR spectroscopy (entry 1 in Table 2.1 and Figure 2.1).

Table 2.1 Optimization of the photocatalytic hydro-aminomethylation.

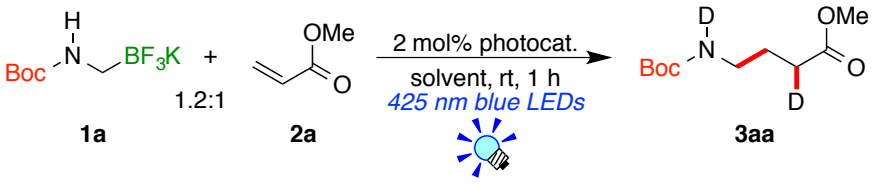

photocatalysts

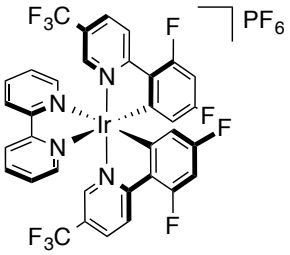

Ir-3

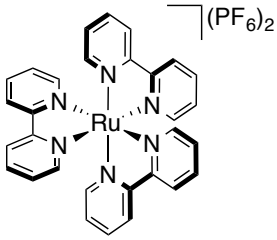

Ru-1

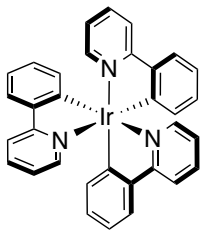

Ir-1

entry	photocatalyst	solvent	yield of **5ae**[b]/%
1	**Ir-3**	acetone-d_6/CD_3OD (1/1)	92
2	**Ir-3**	acetone-d_6/D_2O (1/1)	43
3	**Ir-3**	DMSO-d_6/CD_3OD (1/1)	59
4	**Ir-3**	CD_3CN/CD_3OD (1/1)	42
5	**Ir-3**	acetone-d_6	55
6	**Ir-3**	CD_3OD	72
7	**Ru-1**	acetone-d_6/CD_3OD (1/1)	0
8	**Ir-1**	acetone-d_6/CD_3OD (1/1)	0
9[c]	**Ir-3**	acetone-d_6/CD_3OD (1/1)	0
10	None	acetone-d_6/CD_3OD (1/1)	0

[a] Reaction conditions: A reaction mixture of **4a** (0.06 mmol), **2e** (0.05 mmol), photocatalyst (0.001 mmol) and solvent (0.5 mL) was irradiated by 3W blue LEDs (λ = 425 ± 15 nm) for 1 h at room temperature. [b] Yields were determined by ^{1}H NMR spectroscopy. [c] The reaction was conducted in the dark.

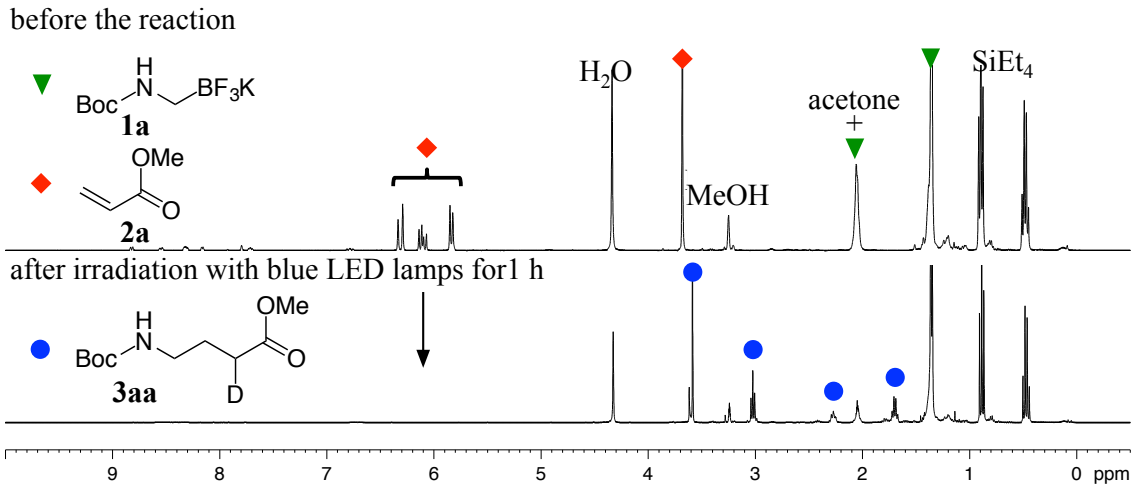

Figure 2.1 ^{1}H NMR Spectra of the reaction of **1a** with **2a**

(in acetone-d_6/CD_3OD (1/1), at 400 MHz, at rt)

As shown in Figure 2.1, alkene **2a** was completely converted within 1 h to give the aminomethylated product **3aa** exclusively. Among the solvent systems examined (entry 2–6), a mixture of acetone-d_6 and CD_3OD turned out to be the best. It should be noted that the typical photoredox catalysts $[Ru(bpy)_3](PF_6)_2$ (**Ru-1**) and *fac*-$[Ir(ppy)_3]$ (**Ir-1**) (ppy = 2-phenylpyridine) did not afford the product at all (entries 7 and 8).[15] It is notable that the product **3aa** was not obtained either in the dark or in the absence of the photocatalyst (entries 9 and 10), strongly supporting that the photoexcited species of the photoredox catalyst plays a key role in the reaction.

Next, the protective groups on the nitrogen atom were investigated as shown in Scheme 2.4. The reaction of aminomethyltrifluoroborate protected by *para*-tolyloxycarbonyl group (**1b**) with methyl acrylate (**2a**) under the above-mentioned optimal conditions afforded the corresponding aminomethylated product **3ba** in 87% NMR yield, but this reaction required a reaction time (3 h) longer than that of the reaction of **1a** (1 h). Yield and efficiency of the reaction of the Ts-protected

aminomethylborate (**1c**) (Ts = *para*-toluenesulfonyl) were significantly deteriorated (**3ca**: 58% NMR yield, 24 h). Furthermore, the reaction of potassium phthalimidomethyltrifluoroborate (**1d**) gave only a trace amount of the coupling product (**3da**). As shown in Scheme 2.4, cyclic voltammograms for *N*-protected substrate (**1a**–**d**) exhibited broad irreversible oxidation waves at +0.74 V, +0.76 V, +0.98 V, and +0.90 V (*vs*. [Cp_2Fe] in MeCN), respectively. In contrast to **1c** and **1d**, oxidation potentials of **1a** and **1b** are substantially lower than the reduction potential of the photoexcited catalyst **Ir-3*** (= +0.91 V).[12] In addition, under the above-mentioned reaction conditions, **1c** and **1d** were not completely dissolved. These factors might cause the significant decline in the efficiency of the reactivity of **1c** and **1d**. Thus, potassium Boc-protected amionomethyltrifluoroborate **1a** proved to be the best aminomethylborate reagent in terms of yield and efficiency.

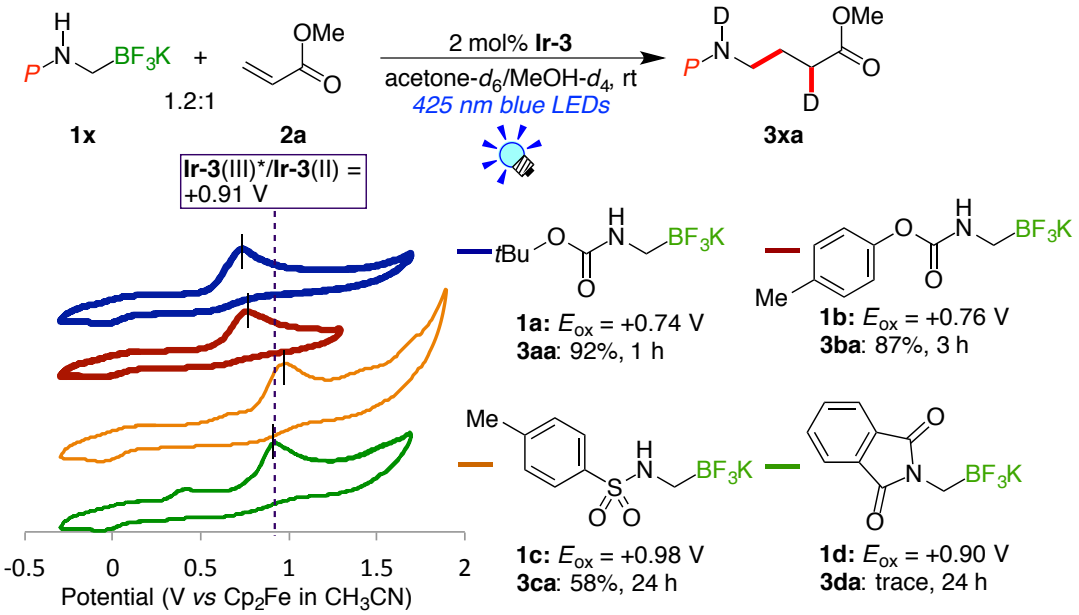

CV conditions: observed as 2 mM acetonitrile solution; $[NBu_4](PF_6)$ = 0.1 M; Ag/AgCl = electrode; reported with respect to the $[FeCp_2]/[FeCp]^+$ couple.

Scheme 2.4 Examination of protective groups on the nitrogen atom in aminomethyltrifluoroborates.

2.2.1.2 Scope and limitation of hydro-aminomethylation of olefins

Table 2.2 Scope of the photocatalytic hydro-aminomethylation.[a, b]

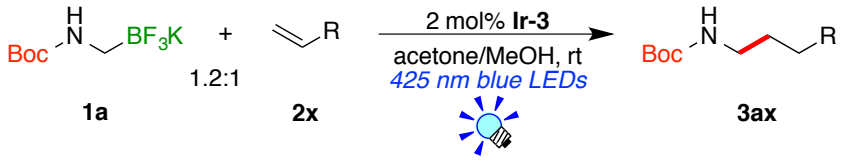

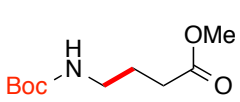
3aa: 85%,4 h

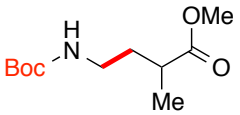
3ab: 85%, 4 h

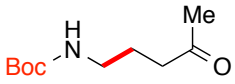
3ac: 54%, 4 h

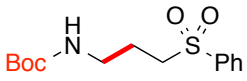
3ad: 79%, 6 h

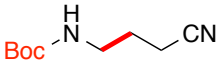
3ae: 69%, 6 h

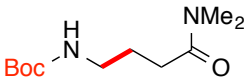
3af: 31%, 4 h

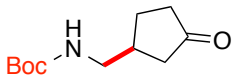
3ag: 54%, 10 h

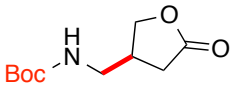
3ah: 33%,24 h

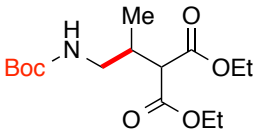
3ai: 85%, 4 h

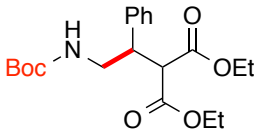
3aj: 91%, 48 h

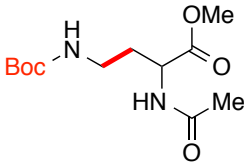
3ak: 68%, 4 h

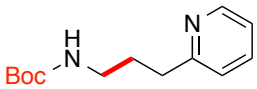
3al: 79%, 24 h

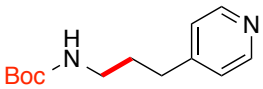
3am: 88%, 24 h

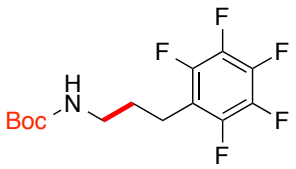
3an: 60%, 24 h

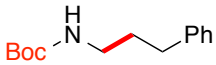
3ao: 5%. 24 h

[a] Reaction conditions; A reaction mixture of **4a** (0.48 mmol), **2x** (0.40 mmol), photocatalyst **Ir-3** (4.0 μmol), degassed acetone (2.0 mL) and MeOH (2 mL) was irradiated by 3 W blue LEDs (λ = 425 ± 15 nm) at room temperature. [b] Yields of isolated products. [c] **Ir-3** (5 mol%) was used.

The scope of the present photocatalytic aminomethylation of olefins with **1a** is summarized in Table 2.2. Typical electron-deficient alkenes such as methyl acrylate (**2a**), methyl methacrylate (**2b**), methyl vinyl ketone (**2c**), phenyl vinyl sulfone (**2d**), and acrylonitrile (**2e**) produced the corresponding aminomethylated products in good yields (54–85% isolated yields, 4–6 h). The reaction of *N,N*-dimethyl acrylamide (**2f**) gave the

product **3af** in a lower yield (31%). Cyclic enones such as 2-cyclopentenone (**2g**) and 2,5-dihydro-2-furanone (**2h**) reacted slowly to give the products **3ag** and **3ah** in moderate yields (**3ag**: 54%, 10 h, **3ah**: 33%, 24 h) probably due to the substitution at the reaction site.

To expand the scope, alkenes bearing two electron-withdrawing groups were examined. Ethylidenemalonic acid diethyl ester (**2i**) readily reacted with **1a** (4 h) to give the product **3ai** in 85% isolated yield. Furthermore, to our delight, benzylidenemalonic acid diethyl ester (**2j**), an alkene bearing a more bulky substituent at the reaction site, was also a substrate suitable for the present photocatalytic transformation. The reaction required a longer time (48 h) and a higher catalyst loading (5 mol%) but afforded the product **3aj** in an excellent yield (91% isolated yield). As further extension of the olefin substrate, enamides and aromatic alkenes were also examined. The reaction of 2-acetylaminoacrylic acid methyl ester (**2k**) smoothly proceeded to give the corresponding C–C coupled product **3ak** in 68% yield. 2-Vinylpyridine (**2l**), 4-vinylpyridine (**2m**) and 2,3,4,5,6-pentafluorostyrene (**2n**) afforded the corresponding aminomethylated products (**3al**, **3am**, **3an**) in high yields (60–88%, 24 h). In contrast, the reaction of electron-rich alkene such as styrene (**2o**) resulted in a low yield (5%, 24 h) partly because a side reaction of **2o** giving the cyclobutane **2o'** proceeded (Scheme 2.5).[16] These results show that *N*-Boc-aminomethyl radical is highly nucleophilic and electron-deficient olefins with various functional groups such as ester, ketone, sulfone, nitrile, amide, pyridyl, and perfluoroaryl groups can be applied to the present photocatalytic aminomethylation.

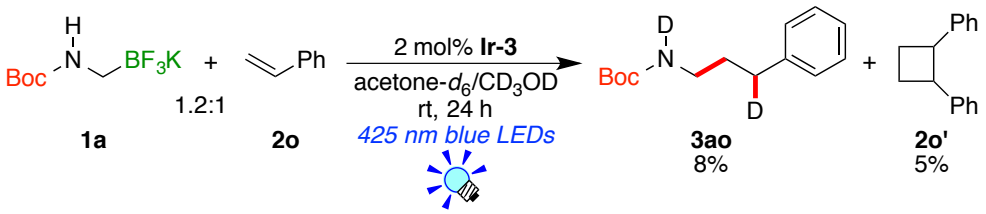

Scheme 2.5 NMR experiment of **2o**

2.2.1.3 Application to the synthesis of GABA derivative

Encouraged by the aminomethylation of **2j**, the author extended this transformation to the reaction of a benzylidenemalonic acid ester derivative (**2p**) (Scheme 2.6 (a)). The aminomethylation of **2p** gave the γ-amino acid derivative **3ap** in 89% yield. Subsequent acid-mediated deprotection produced hydrochloric acid salt of racemic baclofen (98% yield), which is a well-known muscle relaxer and antispastic agent. This two-step synthesis of γ-aminobutylic acid derivatives is superior to the method reported by MacMillan's group (Scheme 2.6 (b)) (in total 3 steps including photoredox reaction with Boc-protected gycine).[17] This result suggests that γ-amionobutyric acid (GABA) derivatives are readily accessible by the consecutive processes consisting of photocatalytic aminomethylation and deprotection under acidic conditions. It is noteworthy that this reaction sequence is synthetically equivalent to primary *aminomethylation of olefin*, which remained to be solved.

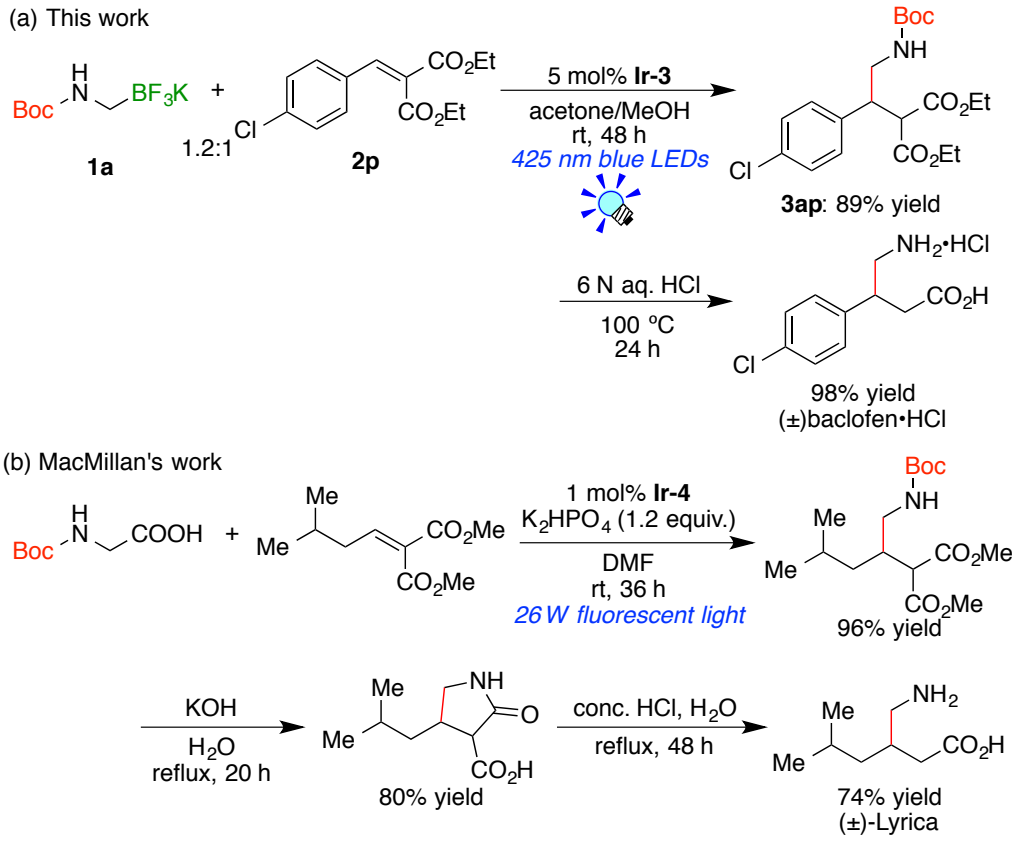

Scheme 2.6 Application to the synthesis of the baclofen motif.

2.2.1.4 Sunlight-driven reaction

Finally, the present photocatalytic system can harness ambient sunlight as the light source instead of blue LED lamps. (Scheme 2.7).

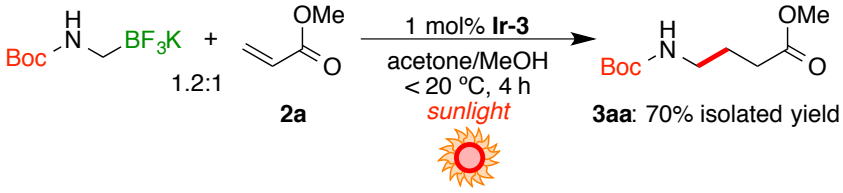

Scheme 2.7 Sunlight-driven reaction.

2.2.2 Hydro-alkoxymethylation by photoredox catalysis

2.2.2.1 Photocatalytic hydro-alkoxymethylation of 2-cyclopentenone

The author initially examined the photocatalytic reaction of potassium 4-methoxyphenoxymethyltrifluoroborate **4a** (1.2 equiv.)[10] with 2-cyclopentenone **2g** using the photocatalysts **Ru-1**, **Ru-2**, **Ir-2**, and **Ir-4** (2 mol%) in a mixture of acetone-d_6 and CD_3OD (1/1) under visible light irradiation (blue LEDs: λ_{max} = 425 nm) for 24 h (entries 1-4 in Table 2.3). The hydroalkoxymethylated product **5ag** was formed for all entries but the choice of the photocatalyst turned out to be crucial. Of the catalysts examined the Ir photocatalyst **Ir-4** gave the best result to afford the product **5ag** in 99% yield as determined by ^{1}H NMR spectroscopy (entry 1). A significant solvent effect was observed for the present reaction (entries 5-8). Although **4a** was slightly soluble in the mixed solvent system consisting of acetone and MeOH, the mixed solvent resulted in the best efficiency. The reaction under air caused a decrease of the yield of **5ag** (entry 9) because unclear side reactions occured. It is notable that product **5ag** was formed neither in the dark nor in the absence of a photocatalyst (entries 10 and 11), strongly supporting that the photoexcited species of the photoredox catalyst are involved in the reaction.

Table 2.3 Optimization studies

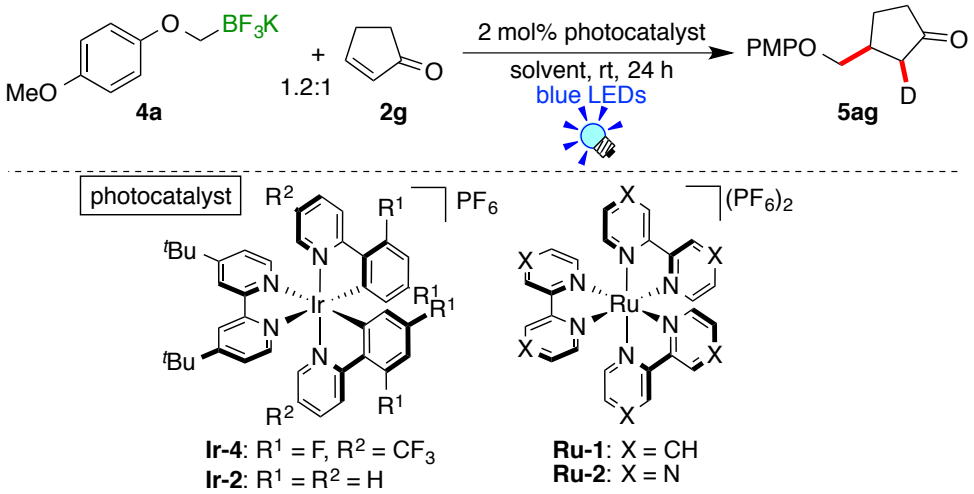

entry	photocatalyst	solvent	yield of **3aa**[b]/%
1	**Ir-4**	acetone-d_6/CD_3OD(1/1)	99
2	**Ir-2**	acetone-d_6/CD_3OD (1/1)	61
3	**Ru-1**	acetone-d_6/CD_3OD (1/1)	17
4	**Ru-2**	acetone-d_6/CD_3OD (1/1)	25
5	**Ir-4**	acetone-d_6	48
6	**Ir-4**	CD_3OD	54
7	**Ir-4**	DMSO-d_6/CD_3OD (1/1)	68
8	**Ir-4**	MeCN-d_3/CD_3OD (1/1)	76
9[c]	**Ir-4**	acetone-d_6/CD_3OD (1/1)	46
10[d]	**Ir-4**	acetone-d_6/CD_3OD (1/1)	0
11	none	acetone-d_6/CD_3OD (1/1)	0

PMP = *p*-methoxyphenyl. [a] Reaction conditions: A reaction mixture of **4a** (0.06 mmol), **5g** (0.05 mmol), photocatalyst (0.001 mmol) and solvent (0.5 mL) was irradiated by 3W blue LEDs (λ = 425 ± 15 nm) for 24 h at room temperature. [b] Yields were determined by ^{1}H NMR spectroscopy. [c] Under air. [d] The reaction was conducted in the dark.

2.2.2.2 Scope and limitation of hydro-alkoxymethylation of olefins

Table 2.4 Scope of hydro-alkoxymethylation[a]

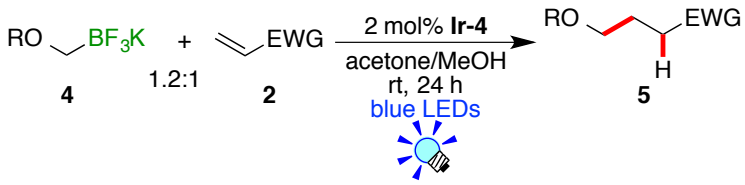

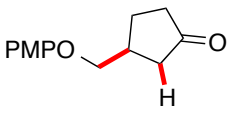

5ag: 94%

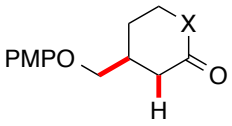

5aq (X = CH_2): 67%
5ar (X = O): 62%

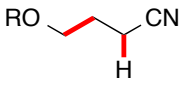

5ae (R = PMP): 97%
5be (R = Ph): 45%
5ce (R = Bn): 68%
5de (R = PMB): 82%

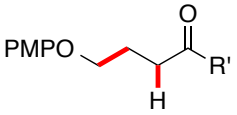

5aa (R' = OMe): 74%
5af (R' = NMe_2): 58%

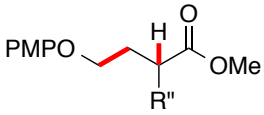

5ab(R" = Me): 99%
5ak (R" = NHAc): 65%

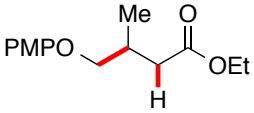

5as: 27%[b]

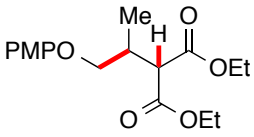

5ai: 76%

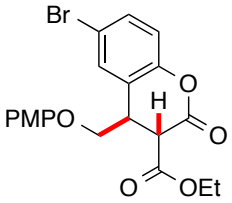

5at: 50%

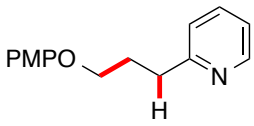

5al: 70%

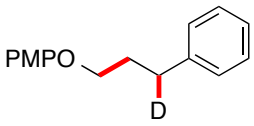

5ao: 17%[b]

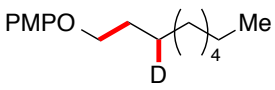

5au: trace[b]

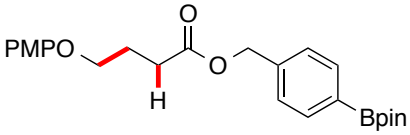

5av: 56%

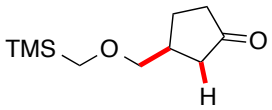

5gg: 42%

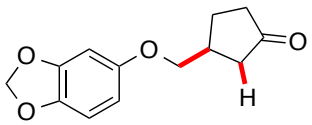

5eg: 78%

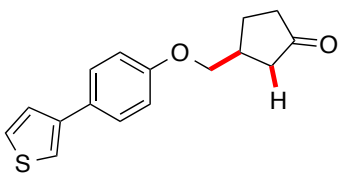

5fg: 47%

[a] Reaction conditions: A reaction mixture of **4** (0.24 mmol), olefins **2** (0.2 mmol), **Ir-4** (0.004 mmol) dissolved in degassed acetone (1 mL) and MeOH (1 mL) was irradiated by 3 W blue LEDs (λ = 425 ± 15 nm) for 24 h at room temperature. Olefins were completely consumed and isolated yields are shown, unless otherwise noted. Isolated yields of some of the products are low due to loss during the chromatographic purification process. [b] The reaction was not completed under these reaction conditions. Yields were determined by ^{1}H NMR spectroscopy.

The scope of the present photocatalytic hydro-alkoxymethylation is summarized in Table 2.4. Under the optimized conditions, the reaction of **4a** with **2g**, 2-cyclohexenone **2q** and 5,6-dihydro-*2H*-pyran-2-one **2r** smoothly afforded the corresponding hydroalkoxymethylated products (**5ag**, **5aq** and **5ar**) in 94%, 67% and 62% yields, respectively. This reaction could be applied to acyclic olefins such as acrylonitrile **2e**, methyl acrylate **2a**, *N,N*-dimethylacrylamide **2f**, methyl methacrylate **2b** and 2-acetamidoacrylic acid methyl ester **2t** to give the products **5aa**, **5af**, **5ab** and **5at** obtained in moderate to good yields (58–99% yields). Remarkable steric hindrance due to the Me group at the reaction site, however, was observed for the reaction of ethyl crotonate **2s** (27% NMR yield). To expand the scope, olefins bearing two electron-withdrawing groups were examined. Ethylidenemalonic acid diethyl ester **2i** and 6-bromocoumarin-3-carboxylic acid ethyl ester **2t** readily reacted with **4a** to give the products **5ai** and **5at** in 76% and 50% yields, respectively. In addition, 2-vinylpyridine **2l** was applicable to this photocatalytic system to afford **5al** in 70% yield. These results show that the present photocatalytic reaction is highly tolerant to a wide variety of functional groups. But electron rich olefin such as styrene **2o** and unactivated olefin such as 1-octene **2u** turned out to be unsuitable for this reaction (**5ao**; 17% yield and **3au**; trace).

Site-specific generation of C-radicals is important for modern radical reactions. The present photocatalytic hydroalkoxymethylation exhibited site-selective reactions at the C–BF_3K moiety for **2v**, which contains two different kinds of B-functional groups, *i.e.* BF_3 and Bpin. The reaction of **4a** with **2v** to provide the coupling product **5av** resulting from exclusive reaction at the BF_3 moiety. Furthermore, the $SiMe_3$ group in **5g** was not affected by the present reaction. These results show that the BF_3K reacts in preference to TMS and Bpin groups, which are susceptible to other oxidative conversions to

generate C–radicals.[19]

Furthermore, the scope of the alkoxyl groups in the **4** was investigated (Table 2.4). The reactions of alkoxymethylborates with phenyl (**4b**), benzyl (**4c**), and *p*-methoxybenzyl groups (**4d**) with **2e** resulted in low yields of coupling products **5**, while the reactions with acrylonitrile **2e** afforded products **5be**, **5ce** and **5de** in good yields (45–82%). For the alkoxy substituents, *p*-methoxyphenyl group showed the best reactivity when compared with the non-substituted phenyl derivative **4d** and benzyl derivative **4c**. In addition, sesamoxymethylborate **4e** and 4-(3-thienyl)phenoxyborate **4f** reacted with **2g** to give the products (**5eg** and **5fg**) in 78% and 47% yields, respectively. Strong electron donating to the alkoxymethyl radical increased the yield of products.

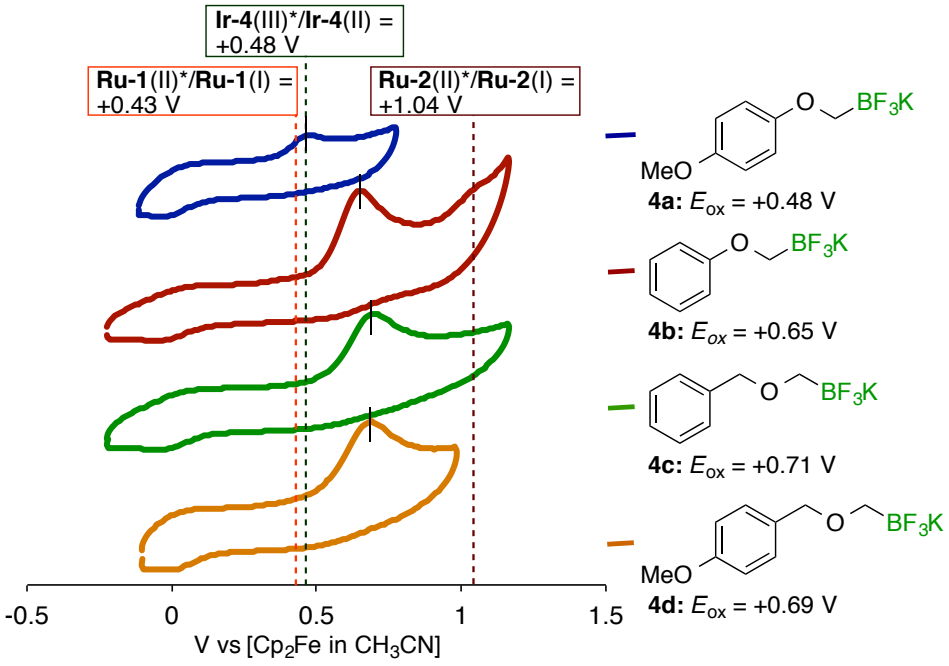

Conditions: observed as 2 mM acetonitrile solution; $[NBu_4](PF_6)$ = 0.1 M; Ag/AgCl =electrode; reported with respect to the $[FeCp_2]/[FeCp_2]^+$ couple.

Figure 2.2 Cyclic voltammograms for alkoxymethylborates

Cyclic voltammograms of alkoxymethylborates (**4a**, **4b**, **4c** and **4d**) shown in Figure 2.2 contain irreversible oxidation waves at +0.48 V (**4a**), +0.65V (**4b**), +0.71 V (**4c**) and

+0.69 V (**4d**). Although, judging from the oxidation potentials, only **4a** can be oxidized the photoredox catalyst, the others **4a-d** turn out to be also oxidized by ***Ir-4**. As a result, **4a** can be oxidized by ***Ir-4** (cf. reduction potential ***Ir-4**: +0.48 V)[12] efficiently. In addition, although **4b**, **4c** and **4d** have high reduction potential, the present reaction proceeded with these alkoxymethylborates. Because photocatalyst has broad redox potential due to its vibrational level, oxidation potential of photocatalyst and reduction potential of the reagent are overlapped. Hence, the photoexcited ***Ir-4** can oxidize the alkoxymethylborates. On the other hand, **Ru-1** (E_{ox} = +0.43 V)[16a] having similar oxidation potential of **Ir-4** afforded low yield. As described in chapter 1, the life time of excited **Ir-4** (τ = 2.3 μs) is longer than that of **Ru-1** and **Ru-2** (τ = 1.1 and 0.74 μs). The author presumed that the longer life time of excited species of ***Ir-4** led to smooth the present reaction.[20]

This scope for hydro-alkoxymethylation is comparable to the hydro-aminomethylation described in section 2.2.1, and the later is more effective than former despite the higher oxidation potential of **1a**. This result is presumably ascribed to the solubility of the borate. The aminoderivative **1a** completely dissolves in acetone/MeOH, while *p*-methoxyphenoxymethyltrifluoroborate is sparingly soluble in organic solvent.

2.2.2.3 Sunlight-driven reaction

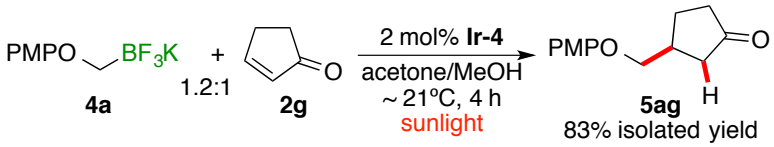

Scheme 2.8 Hydroalkoxymethylation under sunlight

It should be noted that the present photocatalytic system can harness natural sunlight as a light source as noted for the nitrogen analogue (Scheme 2.7). Sunlight induced the reaction more efficiently than blue LEDs did to complete the reaction of **4a** with **2g** within 4 h (Scheme 2.8).

2.2.3 Experiments for analysis of reaction mechanism

To gain insight into the reaction mechanism, several experiments including CV measurements (Scheme 2.4 and Figure 2.1), Stern-Volmer plots and the intermittently irradiation experiments were investigated.

The Stern-Volmer plots for quenching of the photoexcited photocatalyst ***Ir*** (***Ir-3** and ***Ir-4**) by the action of organoborates (**1a** and **4a**) and **2** (Figure 2.3) show that ***Ir*** is not quenched by **2** but by organoborates (**1a** and **4a**), indicating that the initial electron transfer event occurs between the photoexited photocatalyst ***Ir*** and organoborates.

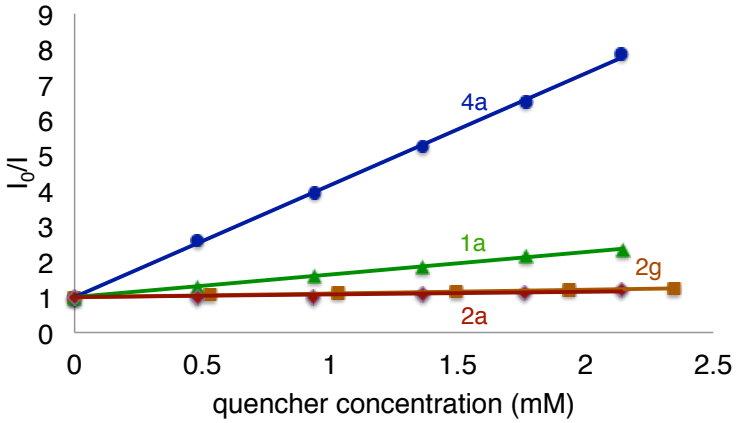

1a and **2g**: Intensities of the emission at 476 nm were recorded upon excitation of a DMSO solution of **Ir-3** at 379 nm.
4a and **2g**: Intensities of the emission at 480 nm were recorded upon excitation of a DMSO solution of **Ir-4** at 400 nm

Figure 2.3 Stern-Volmer studies of photocatalyst **Ir-4**

Next, the author conducted the photocatalytic reaction under periodic visible light irradiation (Figure 2.4). It was observed that the reaction proceeded steadily upon blue LED irradiation but, in the dark, ceased. It suggested that a radical chain mechanism was not involved as a main process.

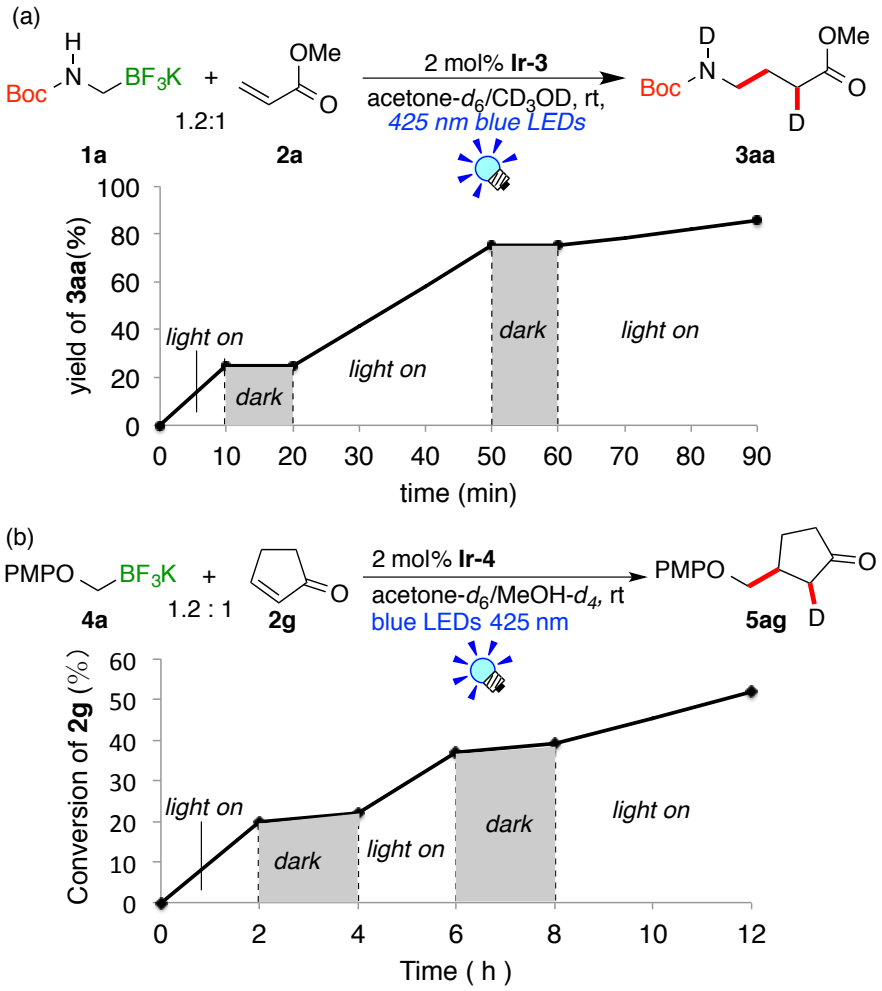

Figure 2.4 Photocatalytic reaction under periodic visible light irradiation

A plausible reaction mechanism for the present hydro-alkoxymethylation and hydro-aminomethylation following the reductive quenching cycle is illustrated in Scheme 2.9. First, the photocatalyst $\boldsymbol{Ir^{III}}$ (**Ir-3** and **Ir-4**) is excited by visible light irradiation (blue LEDs or sunlight) to generate the excited species $\boldsymbol{*Ir^{III}}$, which

undergoes 1e-oxidation of amino- or alkoxy-methyltrifluoroborates **1** to generate, together with the reduced $\boldsymbol{Ir^{II}}$ species, an amino- or alkoxy-methyl radical **A** via a B-C bond cleavage process with formal elimination of a "BF_3" species. This STE process is supported by the luminescent quenching experiments and comparison of the redox properties of organoborate **1a** with that of ***Ir*** suggests that **1a** and **4a** can be oxidized by photoexcited $\boldsymbol{*Ir^{III}}$ as described above. The generated heteroatom-functionalized carbon radical reacts with electron-deficient alkene **2** to afford the C–C coupling adduct **6**, reduction of which by $\boldsymbol{Ir^{II}}$ (path a) followed by protonation by the solvent gives the product **3** or **5** together with the ground state $\boldsymbol{Ir^{III}}$ to complete the catalytic cycle. There is an alternative pathway, where **6** reacts with **1** or **4** to give an amino- or alkoxy-methyl radical (path b), leading to the product **3** or **5** (radical chain mechanism). This mechanism, however, may not be a major reaction pathways as judged by the periodic irradiation experiment.

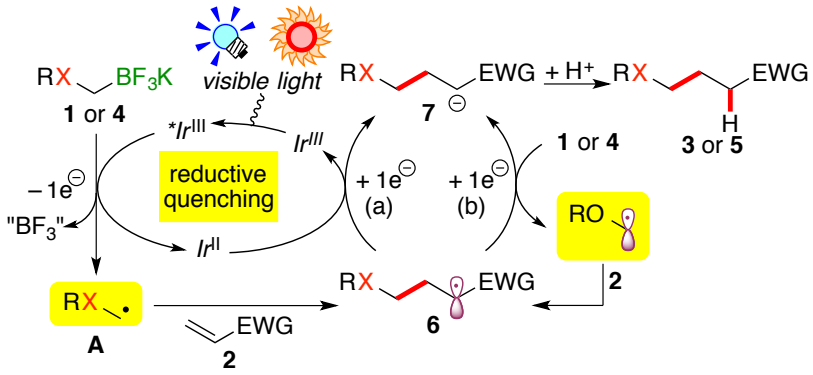

Scheme 2.9 A plausible reaction mechanism

Notably, homo-coupling products of aminomethyl and alkoxymethyl radicals, which are typical byproducts of benzyl radical, were not detected at all[20] (Scheme 2.10). The author considered the following two factors. (i) The carbon radical species with electron donation of adjacent nitrogen and oxygen atoms preferentially add to olefins. (ii) In

radical-radical reactions, one radical is essential to be long lifetime (persistent)[22]. The benzyl radical is a long-lived (τ = 1.4 μs) species[23] to cause the generation of homo-coupling product.

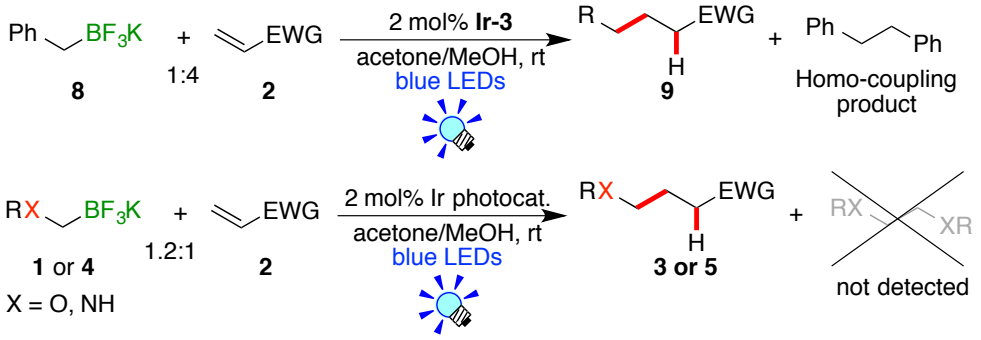

Scheme 2.10 Homo-coupling reaction of organoborates

2.3 Conclusion

The author has developed the photocatalytic hydro-aminomethylation and -alkoxymethylation of olefins with the corresponding organotrifluoroborates. The carbon radical adjacent to nitrogen- and oxygen-atom is reactive enough to couple with electron-deficient olefins. In hydro-aminomethylation, this reaction is regarded as a formal net primary aminomethylation when combined with the deprotection process. The present protocol provides us with a new strategy for the synthesis of biologically active γ-aminobutyric acid (GABA) derivatives. In hydro-alkoxymethylation, this new reaction serves as a method for functionalization of the carbon atoms adjacent to the oxygen atoms of ethers.

2.4 Experimental

General

$[Ru(bpy)_3](PF_6)_2$ (**Ru-1**),[24a] $[Ru(bpz)_3](PF_6)_2$ (**Ru-2**),[24a] *fac*-$[Ir(ppy)_3]$ (**Ir-1**),[24b] $[Ir(ppy)_2(dtbbpy)](PF_6)$ (**Ir-2**),[24c] $[Ir(dF(CF_3)ppy)_2(bpy)](PF_6)$ (**Ir-3**),[12a] $[Ir(dF(CF_3)ppy)_2(dtbbpy)](PF_6)$ (**Ir-4**),[12b] potassium *N*-Boc-protected aminomethyltrifluoroborate (**4a**)[13e], potassium phthalimidomethyltrifluoroborate (**4d**)[10f], potassium (4-methylphenyl)sulfonamide–methyltrifluoroborate (**4c**)[10b] and (4-chloro-benzylidene)malonate

(**2p**)[25] were prepared according to the reported procedures. Olefins **2a, 2b, 2c, 2e, 2f, 2g, 2m, 2o, 2q, 2r** and **2t** were purchased from TCI, **2u** purchased from Wako and **2d, 2h, 2i, 2j, 2k, 2l, 2m,** and **2s** were purchased from Aldrich. B-compound **2v** was prepared according to the reported literature procedure.[11a] Catalytic reactions were performed under an atmosphere of nitrogen using standard Schlenk techniques unless otherwise noted. Solvents were dried by standard procedures (acetone (K_2CO_3)), distilled and stored under nitrogen. Methanol (dehydrated solvent purchased from KANTO CHEMICAL CO., INC.) was degassed with a ultrasonic bath, and stored under N_2 atmosphere. Thin-layer chromatography was performed on silica gel TLC plates (60 F_{254}, Merck). Column chromatography was performed using Fuji Silysia silica gel FL100D (neutral) and Merck aluminium oxide 90 standardized. Visible light irradiation was performed with Relyon LED lamps (3 W×2: λ = 425 nm ± 15 nm). ^{1}H NMR spectra were acquired on JEOL AL 300 (300 MHz) and Bruker AVANCE-400 spectrometers (400 MHz). NMR Chemical shifts were referenced to residual protio impurities in the deuterated solvents. Electrochemical measurements were recorded on a Hokutodenkou HZ-5000 analyzer (observed in 0.002 M CH_3CN; $[(NBu_4)PF_6]$ = 0.1 M; Ag/AgCl = electrode; reported with respect to the $[FeCp_2]/[FeCp_2]^+$ couple). Emission spectra were recorded at room temperature by SHIMADZU RF-5300PC. HRMS (ESI-TOF Mass) spectra were obtained with a Bruker microTOF II spectrometer.

Purification of products (**3ab, 3ac, 3ad, 3ae, 3af, 3ag, 3ai, 3aj, 3ak, 3al, 3am, 3ba, 3ca**) was performed by flash column chromatography with aluminum oxide (aluminium oxide 90 standardized (Merck)) deactivated by 7wt% water.

Procedure for synthesis of potassium 4-methylphenoxycarbonylaminomethyltrifluoroborate (1b)

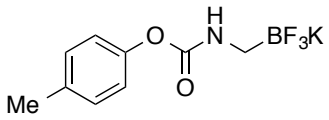

The titled compound was prepared by the modified procedures reported by G. A. Molander *et al.*[26]

Freshly prepared KHMDS (11% in toluene, *ca*. 0.5 M) (10mL) dissolved in dry THF (10 mL) was added dropwise to a solution of 2-chloromethyl-4,4,5,5-tetramethyl-1,3,2-dioxaborolane (0.919 g, 5.16 mmol) in dry THF (10 mL) cooled at -78 ºC. After stirring for 15 min, the cooling bath was removed and the mixture was stirred for an additional 2 h at rt. Then dry MeOH (0.4 mL) was added at 0 ºC. After the mixture was stirred in an ice bath for an additional 2 h at 0 ºC, *p*-tolyl chloroformate (1.81 g, 10.6 mmol) was added. The reaction was warmed to rt by removing the ice bath and stirred for 24 h. The reaction mixture was concentrated under reduced pressure to remove the volatiles. The residue was diluted with MeOH (10 mL) and cooled to 0 ºC before addition of a saturated aqueous solution of KHF_2 (1.55 g, 20.0 mmol). The mixture was stirred for 30 min at 0 ºC, and then dried under reduced pressure. The residue was dissolved in hot acetone and filtered. After the solvent was removed from the filtrate, the residue was washed with Et_2O and dried under *in vacuo*. The product was obtained in 51% yield (0.712 g, 2.63 mmol) as a white solid.

^{1}H NMR (400 MHz, DMSO-d_6, rt) δ 7.12 (d, *J* = 7.6, 2H), 6.91 (d, *J* = 7.6 Hz, 2H), 5.66 (brs, 1H), 2.27 (s, 3H), 1.97 (m, 2H). **^{13}C NMR** (100 MHz, DMSO-d_6, rt) δ 155.1, 149.4, 133.2, 129.3, 121.4, 20.3. **^{11}B NMR** (128 MHz, DMSO-d_6, rt) δ 3.42**. ^{19}F NMR** (376 MHz, DMSO-d_6, rt) δ -142.9. **HRMS** (ESI-TOF) calculated for $[C_{20}H_{10}O_2NBF_3]^-$ requires 232.0764, found 232.0764.

Typical procedures for NMR experiments (reaction conditions in Table 2.1 and Figure 2.1)

*Photocatalytic hydro-aminomethylation of methyl acrylate (**2a**)*

To methyl acrylate (**2a**) (4.7 mg, 54.6 μmol) dissolved in a mixture of deuterated acetone (0.25 mL)-deuterated MeOH (0.25 mL) in an NMR tube, potassium *tert*-butoxycarbonylaminomethyltrifluoroborate (**1a**) (14.5 mg, 61.2 μmol), $[Ir(dF(CF_3)ppy)_2(bpy)](PF_6)$ (**Ir-3**) (1.1 mg, 1.09 μmol) and tetraethylsilane (an internal standard) were added under N_2. The mixture was degassed by three freeze-pump-thaw cycles. The reaction was carried out at room temperature (in a water bath) under irradiation of visible light (placed at a distance of 2~3 cm from the blue LED lamp: $h\nu$ = 425 ± 15 nm). Then the reaction mixture was

analyzed by ^{1}H NMR spectroscopy.

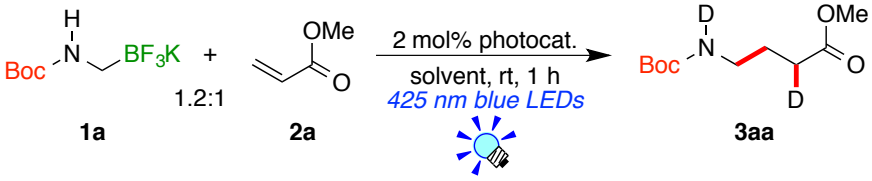

General procedure for the photocatalytic reaction of aminomethyltrifluoroborates with olefins (reaction conditions in Table 2.2)

Under N_2, to olefin (**2**) (0.40 mmol) dissolved in a mixture of acetone (2.0 mL)-MeOH (2.0 mL) in a 20 mL-Schlenk tube were added potassium *tert*-butoxycarbonylaminomethyltrifluoroborate (**1a**) (0.48 mmol) and [Ir(dF(CF$_3$)ppy)$_2$(bpy)](PF$_6$) (**Ir-3**) (8 μmol). The mixture was degassed by three freeze-pump-thaw cycles. The tube was placed at a distance of 2-3 cm from the blue LED lamp ($h\nu$ = 425 ± 15 nm). The resulting mixture was stirred at room temperature (water bath) under visible light irradiation. Then, the reaction mixture was concentrated *in vacuo*. Products were extracted with CH_2Cl_2, dried (Na_2SO_4) and filtered. The filtrate was concentrated *in vacuo* and the residue was purified by flash column chromatography on aluminium oxide (treated with 7.0wt% water) (hexane:EtOAc = 10:1).

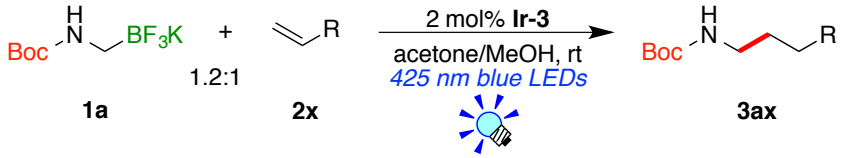

Methyl 4-*tert*-butoxycarbonylaminobutanoate (3aa)

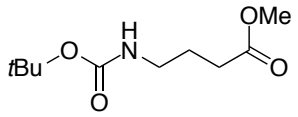

The reaction of methyl acrylate (**2a**) (32.8 mg, 0.381 mmol), **1a** (113.9 mg, 0.480 mmol) and **Ir-3** (8.2 mg, 8.12 μmol) following the general procedures afforded **3aa** (74.2 mg, 85% yield, reaction time = 4 h) as a pale yellow oil after purification with flash column chromatography on aluminium oxide (hexane:EtOAc = 10:1). Spectral data is in agreement with the literature.[27a]

^{1}H NMR (400 MHz, $CDCl_3$, rt) δ 4.67 (brs, 1H), 3.65 (s, 3H), 3.13 (m, 2H), 2.33 (t, ^{3}J = 7.2 Hz, 2H), 1.78 (m, 2H), 1.40 (s, 9H).

Methyl 4-*tert*-butoxycarbonylamino-2-methyl-butanoate (3ab)

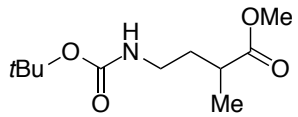

The reaction of methyl methacrylate (**2b**) (40.3 mg, 0.403 mmol), **1a** (113.7 mg, 0.480 mmol) and **Ir-3** (8.3 mg, 8.22 μmol) following the general procedures afforded **3ab** (79.2 mg, 85% yield, reaction time 4 h) as a pale yellow oil after purification with column chromatography on aluminium oxide (treated with 7.0wt% water) (hexane:EtOAc = 10:1).

^{1}H NMR (400 MHz, $CDCl_3$, rt) δ 4.60 (brs, 1H), 3.66 (s, 3H), 3.12 (m, 2H), 2.49 (m, 1H), 1.83 (m, 1H), 1,61 (m 1H), 1.41 (s, 9H), 1.16 (d, ^{3}J = 7.2 Hz, 3H). **^{13}C NMR** (100 MHz, $CDCl_3$, rt) δ 176.8, 156.0, 79.3, 51.8, 38.7, 37.2, 34.0, 28.5, 17.2. **HRMS** (ESI-TOF) calculated for $[C_{11}H_{21}NO_4+Na]^+$ requires 254.1363, found 254.1363.

***tert*-Butoxycarbonylaminnopentan-4-on (3ac)**

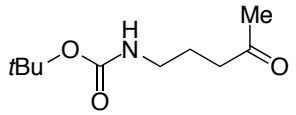

The reaction of methyl vinyl ketone (**2c**) (28.4 mg, 0.405 mmol), potassium **1a** (113.9 mg, 0.480 mmol) and **Ir-3** (8.0 mg, 7.92 μmol) following the general procedures afforded **3ac** (44.0 mg, 54% yield, reaction time was 4 h) as a pale yellow oil after purification with column chromatography on aluminium oxide (treated with 7.0wt% water) (hexane:EtOAc = 10:1).
^{1}H NMR (400 MHz, $CDCl_3$, rt) δ 4.57 (brs, 1H), 3.12 (m, 2H), 2.45 (t, ^3J = 7.2 Hz, 2H), 2.15 (s. 3H), 1.75 (tt, ^3J = 7.2 Hz, ^3J = 7.2 Hz, 2H), 1.44 (s, 9H). **^{13}C NMR** (100 MHz, $CDCl_3$, rt) δ 208.4, 156.2, 79.4, 40.9, 40.2, 30.0, 28.5, 24.3. **HRMS** (ESI-TOF) calculated for $[C_{10}H_{19}O_3N+Na]^+$ requires 224.1257, found 224.1263.

***tert*-Butyl 3-benzensulfonylpropylcarbamate (3ad)**

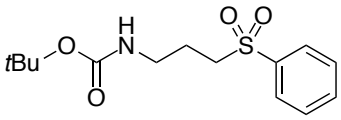

The reaction of phenyl vinyl sulfone (**2d**) (67.4 mg, 0.401 mmol), potassium **1a** (113.9 mg, 0.480 mmol) and **Ir-3** (8.0 mg, 7.92 μmol) following the general procedures afforded **3ad** (94.4 mg, 79% yield, reaction time was 6 h) as a white solid after purification with column chromatography on aluminium oxide (treated with 7.0wt% water) (hexane:EtOAc = 10-5:1).
^{1}H NMR (400 MHz, $CDCl_3$, rt) δ 7.91 (d, ^3J = 7.6 Hz, 2H), 7.66 (t, ^3J = 7.6 Hz, 1H), 7.57 (dd, ^3J = 7.6 Hz, ^3J = 7.6 Hz, 2H), 4.65 (brs, 1H), 3.23 (m, 2H), 3.13 (t, ^3J = 7.6 Hz, 2H), 1.92 (m, 2H), 1.41 (s, 9H). **^{13}C NMR** (100 MHz, $CDCl_3$, rt) δ 156.0, 139.3, 133.9, 129.5, 128.1, 79.8, 53.9, 39.0, 28.5, 23.8. **HRMS** (ESI-TOF) calculated for $[C_{14}H_{21}O_4NS+Na]^+$ requires 322.1083, found 322.1086.

***tert*-Butyl *N*-3-cyanopropylcarbamate (3ae)**

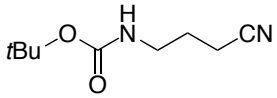

The reaction of acrylonitrile (**2e**) (21.4 mg, 0.403 mmol), **1a** (113.8 mg, 0.480 mmol) and **Ir-3** (8.2 mg, 8.12 μmol) following the general procedures afforded **4ae** (51.6 mg, 69% yield, reaction time was 6 h) as a pale yellow oil after purification with column chromatography on aluminium oxide (treated with 7.0wt% water) (hexane:EtOAc = 10:1).
^{1}H NMR (400 MHz, $CDCl_3$, rt) δ 4.66 (brs, 1H), 3.25 (m, 2H), 2.40 (t, ^3J = 7.2 Hz, 2H), 1.87 (m, 2H), 1.44 (s, 9H). **^{13}C NMR** (100 MHz, $CDCl_3$, rt) δ 156.1, 119.3, 79.9, 39.5, 28.5, 26.3, 14.8. **HRMS** (ESI-TOF) calculated for $[C_9H_{16}O_2N_2+Na]^+$ requires 207.1104, found 207.1105.

***N*-*tert*-butyloxycarbonyl-γ-aminobutyric acid *N',N'*-dimethylamide (3af)**

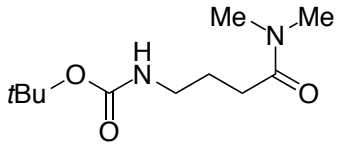

The reaction of *N,N*-dimethylacrylamide (**2f**) (40.1 mg, 0.405 mmol), **1a** (113.9 mg, 0.480 mmol) and **Ir-3** (8.2 mg, 8.12 μmol) following the general procedures afforded **3af** (29.3 mg, 31% yield, reaction time = 4 h) as a pale yellow oil after purification with column chromatography on aluminium oxide (treated with 7.0wt% water) (hexane:EtOAc = 10:1). Spectral data is in agreement with the literature.[27b]

^{1}H NMR (400 MHz, $CDCl_3$, rt) δ 4.44 (brs, 1H), 3.17 (t, ^3J = 6.8 Hz, 2H), 2.97 (s, 6H), 2.36 (t, ^3J = 6.8 Hz, 2H), 1.83 (tt, ^3J = 6.8 Hz, ^3J = 6.8 Hz, 2H), 1.43 (s, 9H).

***tert*-Butyl 3-oxocyclopentylmethylcarbamate (3ag)**

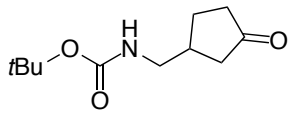

The reaction of 2-cyclopenten-1-one (**2g**) (32.9 mg, 0.401 mmol), potassium **1a** (114.1 mg, 0.481 mmol) and [Ir(dF(CF_3)ppy)$_2$(bpy)](PF_6) (**Ir-3**) (8.2 mg, 8.12 μmol) following the general procedures afforded **3ag** (46.3 mg, 54% yield, reaction time = 10 h) as a pale yellow oil after purification with column chromatography on aluminium oxide (treated with 7.0wt% water) (hexane:EtOAc = 10:1).
^{1}H NMR (400 MHz, $CDCl_3$, rt) δ 4.67 (brs, 1H), 3.19 (m, 2H), 2.38 (m, 1H), 2.31 (m, 2H), 2.16 (m, 2H), 1.90 (m, 1H), 1.61 (m, 1H), 1.44 (s, 9H). **^{13}C NMR** (100 MHz, $CDCl_3$, rt) δ 218.3, 156.1, 79.7, 44.8, 42.8, 38.1, 37.8, 28.5, 26.9. **HRMS** (ESI-TOF) calculated for $[C_{11}H_{19}NO_3+Na]^+$ requires 236.1257, found 236.1256.

4-(*tert*-Butoxycarbonylaminomethyl)tetrahydrofuran-2(3H)-one (3ah)

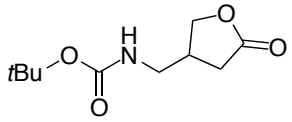

The reaction of γ-crotonolactone (**2h**) (33.4 mg, 0.397 mmol), **1a** (113.6 mg, 0.479 mmol) and **Ir-3** (8.3 mg, 8.22 μmol) following the general procedures afforded **3ah** (26.3 mg, 33% yield, reaction time = 24 h) as a pale yellow oil after purification with column chromatography on aluminium oxide (hexane:EtOAc = 10:1).
^{1}H NMR (400MHz, $CDCl_3$, rt) δ 4.76 (brs, 1H), 4.38 (m, 1H), 4.08 (m, 1H), 3.22 (m, 2H), 2.79 (m, 1H), 2.61 (m, 1H), 2.32 (m, 1H), 1.44 (s, 9H). **^{13}C NMR** (100 MHz, $CDCl_3$, rt) δ 176.5, 156.2, 80.2, 71.1, 42.7, 36.3, 32.1, 28.5. **HRMS** (ESI-TOF) calculated for $[C_{10}H_{17}O_4N+Na]^+$ requires 238.1050, found 238.1050.

Diethyl 2-*tert*-butoxycarbonylamino-1-methylethylmalonate (3ai)

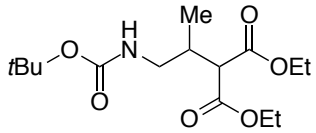

The reaction of diethyl ethylidenmalonate (**2i**) (74.7 mg, 0.401 mmol), **1a** (113.6 mg, 0.479 mmol) and **Ir-3** (8.1 mg, 8.02 μmol) following the general procedures afforded **3ai** (108.9 mg, 85% yield, reaction time = 4 h) as a colorless oil after purification with column chromatography on aluminium oxide (treated with 7.0wt% water) (hexane:EtOAc = 10:1).
^{1}H NMR (400 MHz, $CDCl_3$, rt) δ 4.71 (brs, 1H), 4.20 (q, ^3J = 7.2 Hz, 2H), 4.19 (q, ^3J = 7.2 Hz, 2H), 3.30 (d, ^3J = 7.6 Hz, 1H), 3.16 (m, 2H), 2.45 (m, 1H), 1.43 (s, 9H), 1.26 (t, ^3J = 7.2 Hz, 6H), 1.01 (d, ^3J = 7.2 Hz, 3H). **^{13}C NMR** (100 MHz, $CDCl_3$, rt) δ 168.9, 168.7, 156.1, 79.4, 61.5, 61.5, 55.3, 44.4, 34.3, 28.5, 15.7, 14.2. **HRMS** (ESI-TOF) calculated for $[C_{15}H_{27}NO_6+Na]^+$ requires 340.1731, found 340.1731.

Diethyl 2-*tert*-butoxycarbonylamino-1-phenylethylmalonate (3aj)

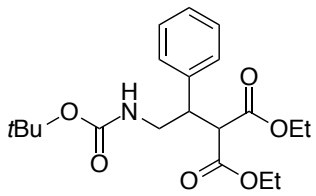

The reaction of diethyl benzylidenmalonate (**2j**) (114.0 mg, 0.402 mmol), **1a** (114.0 mg, 0.480 mmol) and **Ir-3** (20.1 mg, 19.9 μmol) following the general procedures afforded **3aj** (138.3 mg, 91% yield, reaction time = 48 h) as a pale yellow solid after purification with column chromatography on aluminium oxide (treated with 7.0wt% water) (hexane:EtOAc = 15:1).
^{1}H NMR (400 MHz, $CDCl_3$, rt) δ 7.31 (m, 2H), 7.23 (m, 3H), 4.43 (brs, 1H), 4.27 (q, ^3J = 7.2 Hz, 2H), 3.93 (m, 2H), 3.73 (d, 10.4 Hz, 1H). 3.64 (m, 1H), 3.54 (m, 1H), 3.43 (m, 1H), 1.40 (s, 9H), 1.32 (t, ^3J = 7.2 Hz, 3H), 0.99 (t, ^3J = 7.2 Hz, 3H). **^{13}C NMR** (100 MHz, $CDCl_3$, rt) δ 168.3, 167.7, 139.1, 130.2, 128.8, 128.5, 127.6, 79.4, 61.9, 61.4, 55.9, 45.6, 44.2, 28.5, 14.2, 13.8. **HRMS** (ESI-TOF) calculated for $[C_{20}H_{29}O_6N+Na]^+$ requires 402.1887, found 402.1887.

Methyl-2-acetamido-4-(*tert*-butoxycarbonylamino)butanoate (3ak)

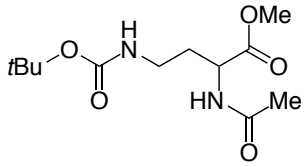

The reaction of methyl 2-acetamidoacrylate (**2k**) (57.0 mg, 0.398 mmol), **1a** (113.6 mg, 0.479 mmol), **Ir-3** (8.1 mg, 8.02 μmol) following the general procedures afforded **3ak** (74.7 mg, 68% yield, reaction time = 4 h) as a pale yellow solid after purification with column chromatography on aluminium oxide (treated with 7.0wt% water) (hexane:EtOAc = 10-1:1).
^{1}H NMR (400 MHz, $CDCl_3$, rt) δ 6.41 (brs, 1H), 5.12 (brs, 1H), 4.66 (m, 1H), 3.74 (s, 3H), 3.39 (m, 1H), 2.96 (m, 1H), 2.04 (m, 1H), 2.04 (s, 3H), 1.77 (m,1H), 1.43 (s, 9H).
^{13}C NMR (100 MHz, $CDCl_3$, rt) δ 173.1, 170.4, 156.2, 79.5, 52.7, 49.9, 36.6, 33.2, 28.6, 23.3. **HRMS** (ESI-TOF) calculated for $[C_{12}H_{22}N_2O_5+Na]^+$ requires 297.1421, found 297.1421.

***tert*-Butyl 3-pyridine-2-ylpropylcarbamate (3al)**

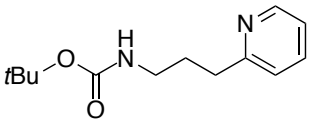

The reaction of 2-vinylpyridine (**2l**) (42.0 mg, 0.399 mmol), **1a** (113.6 mg, 0.479 mmol), **Ir-3** (8.3 mg, 8.22 μmol) following the general procedures afforded **3al** (74.9 mg, 79% yield, reaction time = 24 h) as a pale yellow oil after purification with column chromatography on aluminium oxide (treated with 7.0wt% water) (hexane:EtOAc = 3:1).
^{1}H NMR (400 MHz, $CDCl_3$, rt) δ 8.50 (brd, ^3J = 4.8 Hz, 1H), 7.58 (dt, ^3J = 7.6 Hz, ^4J = 1.6 Hz, 1H), 7.14 (d, ^3J = 7.6 Hz, 1H), 7.10 (dt, ^3J = 4.8 Hz, ^4J = 1.6 Hz, 1H), 4.78 (brs, 1H), 3.16 (dt, ^3J = 6.4 Hz, ^3J = 6.4 Hz, 2H), 2.82 (t, ^3J = 7.2 Hz, 2H), 1.92 (quint, ^3J = 7.2 Hz, 2H), 1.43 (s, 9H). **^{13}C NMR** (100 MHz, $CDCl_3$, rt) δ 161.5, 156.2, 149.4, 136.6, 123.0, 121.3, 79.2, 40.3, 35.6, 30.0, 28.6. **HRMS** (ESI-TOF) calculated for $[C_{13}H_{20}O_2N_2+Na]^+$ requires 259.1417, found 259.1417.

***tert*-Butyl 3-pyridine-4-ylpropylcarbamate (3am)**

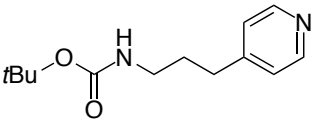

The reaction of 4-vinylpyridine (**2m**) (42.5 mg, 0.404 mmol), **1a** (113.7 mg, 0.480 mmol), **Ir-3** (8.2 mg, 8.12 μmol) following the general procedures afforded **4am** (84.5 mg, 88% yield, reaction time = 24 h) as a pale yellow oil after purification with column chromatography on aluminium oxide (treated with 7.0wt% water) (hexane:EtOAc = 10-1 : 1).
^{1}H NMR (400 MHz, $CDCl_3$, rt) δ 8.49 (d, ^3J = 5.6 Hz, 2H), 7.13 (d, ^3J = 5.2 Hz, 2H), 4.57 (brs, 1H), 3.17 (m, 2H), 2.64 (t, ^3J = 8.0 Hz, 2H), 1.83 (m, 2H), 1.44 (s, 9H). **^{13}C NMR** (100 MHz, $CDCl_3$, rt) δ 156.1, 150.8, 149.8, 124.0, 79.5, 40.2, 32.5, 30.8, 28.5. **HRMS** (ESI-TOF) calculated for

$[C_{13}H_{20}N_2O_2+Na]^+$ requires 259.1417, found 259.1417.

***tert*-Butyl 3-pentafluorophenylpropylcarbamate (3an)**

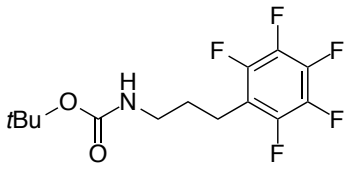

The reaction of 2,3,4,5,6-pentafluorostyrene (**2n**) (77.3 mg, 0.398 mmol), **1a** (113.7 mg, 0.480 mmol) and **Ir-3** (8.2 mg, 8.12 μmol) following the general procedures afforded **3an** (78.1 mg, 60% yield, reaction time = 24 h) as a white solid after purification with PTLC on silica gel (hexane:EtOAc = 4:1).
^{1}H NMR (400 MHz, $CDCl_3$, rt) δ 4.59 (brs, 1H), 3.15 (m, 2H), 2.73 (t, ^3J = 7.6 Hz, 2H), 1.78 (m, 2H), 1.44 (s, 9H). **^{13}C NMR** (100 MHz, $CDCl_3$, rt) δ 155.9, 146.2 (m), 143.8 (m), 140.9 (m), 138.6 (m), 136.2 (m), 114.5 (m) 79.3, 39.8, 29.5, 28.3, 19.6.
^{19}F NMR (376 MHz, $CDCl_3$, rt) δ -145.5 (dd, ^3J = 21.4 Hz, ^3J = 21.8 Hz, 2F), -158.9 (t, ^3J = 20.7 Hz, 1F), -164.0 (m, 2F). **HRMS** (ESI-TOF) calculated for $[C_{14}H_{16}O_2N_2F_5+Na]^+$ requires 348.0993, found 348.0993.

***tert*-Butyl 3-phenylpropylcarbamate (3ao)**

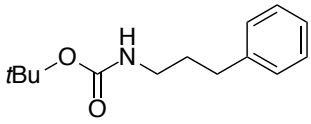

The reaction of styrene (**2o**) (41.5 mg, 0.398 mmol), **1a** (114.3 mg, 0.482 mmol) and **Ir-3** (7.9 mg, 7.82 μmol) following the general procedures afforded **3ao** (4.9 mg, 5% yield, reaction time was 24 h) as a colorless oil after purification with PTLC on silica gel (hexane/EtOAc = 5 : 1). Spectral data is in agreement with the literature.[27c]
^{1}H NMR (400 MHz, $CDCl_3$, rt) δ 7.28 (m, 2H), 7.19 (m, 3H), 4.52 (brs, 1H), 3.15 (m, 2H), 2.64 (t, ^3J = 8.0 Hz, 2H), 1.81 (quintet, J = 7.2 Hz, 2H), 1.44 (s, 9H).

Methyl 4-(4-methylphenoxycarbonylamino)butanoate (5be)

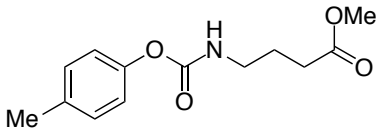

The reaction of methyl acrylate (**2a**) (33.3 mg, 0.387 mmol), Potassium 4-methylphenoxycarbonylaminomethyltrifluoroborate (**1b**) (130.7 mg, 0.482 mmol) and **Ir-3** (8.0 mg, 7.92 μmol) following the general procedures afforded **3ba** (55.0 mg, 57% yield, reaction time was 6 h) as a pale yellow solid after purification with column chromatography on aluminium oxide (treated with 7.0wt% water) (hexane:EtOAc = 10-5:1).
^{1}H NMR (400 MHz, $CDCl_3$, rt) δ 7.14 (d, ^3J = 8.0 Hz, 2H), 6.99 (d, ^3J = 8.4 Hz, 2H), 5.17 (brs, 1H), 3.69 (s, 3H), 3.31 (m, 2H), 2.42 (t, ^3J = 7.2 Hz, 2H), 2.33 (s, 3H), 1.91 (m, 2H). **^{13}C NMR** (100 MHz, $CDCl_3$, rt) δ 173.8, 155.0, 149.0, 135.0, 129.9, 121.4, 51.8, 40.8, 31.4, 25.1, 20.9. **HRMS** (ESI-TOF) calculated for $[C_{13}H_{17}O_4N+Na]^+$ requires for 274.1050, found 274.1051.

Methyl 4-tosylaminobutyrate (3ca)

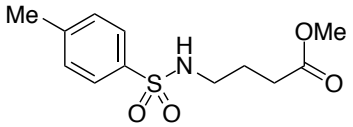

The reaction of methyl acrylate (**2a**) (33.0 mg, 0.384 mmol), Potassium

4-methylphenylsulfonamidomethyltrifluoroborate (**1c**) (130.7 mg, 0.482 mmol) and **Ir-3** (8.2 mg, 8.12 μmol) following the general procedures afforded **3ca** (33.7 mg, 32% yield, reaction time was 24 h) as a colorless oil after purification with column chromatography on aluminium oxide (treated with 7.0wt% water) (hexane:EtOAc = 5-3:1).
^{1}H NMR (400 MHz, $CDCl_3$, rt) δ 7.73 (d, ^3J = 8.0 Hz, 2H), 7.30 (d, ^3J = 8.0 Hz, 2H), 4.84 (brs, 1H), 3.64 (s, 3H), 2.98 (m, 2H), 2.42 (s, 3H), 2.35 (t, ^3J = 7.2 Hz, 2H), 1.79 (m, 2H). **^{13}C NMR** (100 MHz, $CDCl_3$, rt) δ 173.65, 143.5, 137.2, 129.9, 127.2, 52.8, 42.7, 31.1, 24.9, 21.6. **HRMS** (ESI-TOF) calculated for $[C_{12}H_{17}O_4N+Na]^+$ requires for 294.0770, found 294.0773.

Sunlight driven reaction

A cylindrical vessel (diameter: 4.5 cm, depth: 1.5 cm) was used for photoreaction under sunlight. To a mixture of acetone (2.0 mL) and MeOH (2.0 mL) solution of methyl acrylate (**2a**) (34.2 mg, 0.397 mmol) in the vessel, potassium *tert*-butoxycarbonylaminomethyltrifluoroborate (**1a**) (114.1 mg, 0.481 mmol) and $[Ir(dF(CF_3)ppy)_2(bpy)](PF_6)$ (**Ir-3**) (3.9 mg, 3.86 μmol) were added under N_2. The mixture was degassed by three freeze-pump-thaw cycles. The reaction mixture was exposed to sunlight around 20 ºC for 4 h (March 6th, 2014). After workup, **3aa** was obtained as oil in 70% yield.

Synthesis of Baclofen

Diethyl 2-(*tert*-butoxycarbonylamino)-1-(*p*-chlorophenyl)ethylmalonate (3ap)

To an acetone (2.0 mL)-MeOH (2.0 mL) solution of diethyl (4-chloro-benzylidene)malonate (**2p**) (113.3 mg, 0.401 mmol) in a 20mL-Schlenk tube, **1a** (114.4 mg, 0.483 mmol) and **Ir-3** (19.9 mg, 19.7 μmol) were added under N_2. The mixture was degassed by three freeze-pump-thaw cycles. The tube was placed at a distance of 2~3 cm from blue LED lamps ($h\nu$ = 425 ± 15 nm). The resulting mixture was stirred for 48 h at room temperature (in a water bath) under visible light irradiation. Then, the reaction mixture was concentrated *in vacuo*. Products were extracted with CH_2Cl_2, dried over Na_2SO_4 and filtered. The filtrate was concentrated *in vacuo* and the residue was purified by column chromatography on aluminum oxide (treated with 7.0wt % water) (hexane:EtOAc = 10:1). The product **3ap** was obtained in 89% yield (147.5 mg, 0.356 mmol) as a white solid.

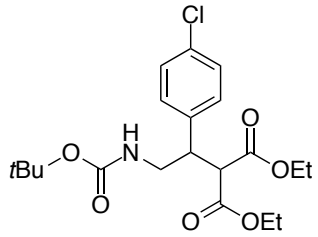

^{1}H NMR (400 MHz, $CDCl_3$, rt) δ 7.28 (d, ^3J = 8.4 Hz, 2H), 7.17 (d, ^3J = 8.0 Hz, 2H), 4.41 (brs, 1H), 4.24 (q, ^3J = 7.2 Hz, 2H), 3.94 (m, 2H), 3.67 (d, ^3J = 6.4 Hz, 1H), 3.60 (m, 1H), 3.49 (m, 1H), 3.38 (m, 1H), 1.37 (s, 9H), 1.29 (t, ^3J = 7.2 Hz, 3H), 1.01 (t, ^3J = 7.2 Hz, 3H). **^{13}C NMR** (100 MHz, $CDCl_3$, rt) δ 168.1, 167.5, 155.7, 137.7, 133.4, 129.9, 128.9, 79.6, 62.0, 61.6, 55.7, 45.1, 44.0, 28.4, 14.2, 13.9. **HRMS** (ESI-TOF) calculated for $[C_{20}H_{28}ON_6Cl+Na]^+$ requires 436.1497, found 436.1485.

The aminomethylated product (**3ap)** (147.5 mg, 0.356 mmol) and 6 N HCl aqueous solution (4 mL) were mixed in a 20 mL Schlenk-tube. After the mixture was refluxed for 24 h at 100 ºC, the reaction mixture was filtered, and the volatiles were removed under reduced pressure to give baclofen hydrochloride as a white solid in 98% yield.

General procedure for synthesis of alkoxymethyltrifluoroborates

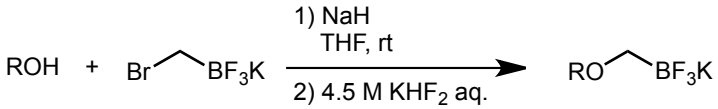

A 100 mL 2-neck round-bottom flask was charged with NaH (3.0 eq.) and dry THF under N_2. Alcohol (3.0 eq.) was added dropwise to the suspension via syringe at 0 ºC. The mixture was stirred for 15 min and then for 30 min at rt. Potassium bromomethyltrifluoroborate (1.0 eq.) was added to the mixture in one portion at 0 ºC. The reaction mixture was stirred at rt for the reaction time described in the literature[13a]. The mixture was quenched by adding saturated aq. KHF_2 solution (4.5 M). The reaction mixture was stirred for 30 min at rt, and then the resultant suspension was dried *in vacuo*. The crude solid was extracted with hot acetone and the filtrate was concentrated. The precipitated pure compound was washed with CH_2Cl_2, dried *in vacuo* and obtained as a white solid.

Potassium (*p*-methoxyphenoxy)methyltrifluorobarate (4a)

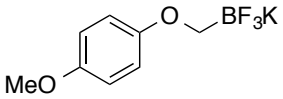

The reaction of *p*-methoxyphenol (1.87 g, 15 mmol), NaH (60% dispersion in mineral oil) (0.608 g, 15 mmol), THF (25 mL) and potassium bromomethyltrifluoroborate (1.02 g, 5.0 mmol) following the general procedures afforded **4a** (0.418 g, 34%, reaction time = 3 days) as a white solid.
^{1}H NMR (400 MHz, DMSO-d_6, rt): d 6.76 (m, 2H), 6.76 (m, 2H), 3.66 (s, 3H), 2.88 (brs, 2H). **^{13}C NMR** (100 MHz, DMSO-d_6, rt): d 156.2, 151.9, 114.3, 114.2, 55.3. **^{11}B NMR** (128 MHz, DMSO-d_6, rt) d 3.15. **^{19}F NMR** (376 MHz, DMSO-d_6, rt) d -141.7. **HRMS** (ESI-TOF): calculated for $[C_8H_9BF_3O]^-$ requires 205.0655, found 205.0638.

Potassium (3,4-methylenedioxyphenoxy)methyltrifluoroborate (4e)

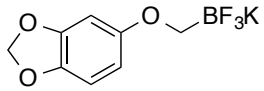

The reaction of sesamol (1.25 g, 9.05 mmol), NaH (60% dispersion in mineral oil) (0.367 g, 9.18 mmol), THF (15 mL) and potassium bromomethyltrifluoroborate (0.609 g, 3.03 mmol) following the general procedures afforded **4e** (0.635 g, 81%, reaction time = 2 days) as a pale brown solid.
^{1}H NMR (400 MHz, DMSO-d_6, rt): d 6.71 (d, J = 8.4 Hz, 1H), 6.49 (d, J = 2.4, 1H), 6.26 (dd, ^3J = 8.4 Hz, ^4J = 2.4 Hz, 1H), 5.89 (s, 2H), 2.89 (brs, 2H). **^{13}C NMR** (100 MHz, DMSO-d_6. rt) d 157.9, 147.7, 139.7, 107.9, 104.7, 100.6, 97.0. **^{11}B NMR** (128 MHz, DMSO-d_6, rt) d 2.31. **^{19}F NMR** (376 MHz, DMSO-d_6, rt) d -141.7. **HRMS** (ESI-TOF): calculated for $[C_8H_7BF_3O_3]^-$ requires 219.0447, found 219.0447.

Potassium (4-(3-thienyl)phenoxy)methyltrifluoroborate (4f)

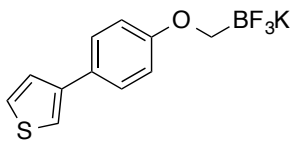

The reaction of 4-(3-thienyl)phenol (1.03 g, 5.84 mmol), NaH (60% dispersion in mineral oil) (0.238 g, 5.95 mmol) and potassium bromomethyltrifluoroborate (0.403 g, 2.01 mmol) following the general procedures afford **4f** (0.113 g, 19%, reaction time = 3 days) as a white solid.
^{1}H NMR (400 MHz, DMSO-d_6, rt) d 7.64 (m, 1H), 7.56 (m, 3H), 7.46 (m, 1H), 6.89 (m 2H), 2.99 (brs, 2H). **^{13}C NMR** (100 MHz, DMSO-d_6, rt) d 161.6, 141.9, 127.0, 126.7, 126.1, 118.5, 114.3. **^{11}B**

NMR (128 MHz, DMSO-d_6, rt) d 2.66. **^{19}F NMR** (376 MHz, DMSO-d_6, rt) d -141.7.
HRMS (ESI-TOF): calculated for $[C_{11}H_9BF_3OS]^-$ requires 295.0763, found 295.0766.

Potassium (2-(trimethylsilyl)methoxy)methyltrifluoroborate (4g)

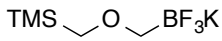

The reaction of trimethylsilylmethanol (0.619 g, 5.94 mmol), NaH (60% dispersion in mineral oil) (0.241 g, 6.03 mmol), potassium bromomethyltrifluoroborate (0.401 g, 2.00 mmol) following the general procedures afforded **4g** (0.145 g, 32%, reaction time = 7 h) as a white solid.
^{1}H NMR (400 MHz, CD_3OD, rt) d 3.17 (s, 2H), 2.83 (brq, J = 6.0 Hz, 2H), 0.04 (s, 9H). **^{13}C NMR** (100 MHz, CD_3OD, rt), d 66.9, -2.32. **^{11}B NMR** (128 MHz, DMSO-d_6, rt) d 2.60. **^{19}F NMR** (376 MHz, DMSO-d_6, rt) d -140.7. **HRMS** (ESI-TOF): calculated for $[C_5H_{13}BF_3OSi]^-$ requires 185.0788, found 185.0783.

Typical procedures for NMR experiments (reaction conditions in Table 2.3)
*photocatalytic alkoxymethylation of 2-cyclopenten-1-one (**2g**)*

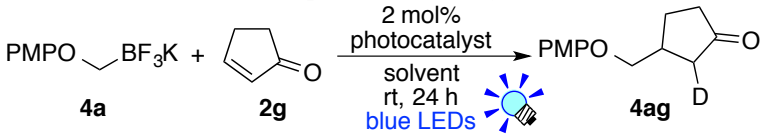

To a solution (0.5 mL) of 2-cyclopenten-1-one (**2g**) (4.1 mg, 50.0 mmol) in an NMR tube, potassium 4-methoxyphenoxymethyltrifluoroborate (**4a**) (14.4 mg, 59.0 mmol), photocatalyst (1 mmol) and tetraethylsilane (an internal standard) were added under N_2. The mixture was degassed by three freeze-pump-thaw cycles. The reaction was carried out at room temperature (water bath) under visible light irradiation (placed at a distance of ~3 cm from blue LED lamps: $h\nu$ = 425 ± 15 mm). The reaction was followed by ^{1}H NMR spectroscopy.

General procedure for the photocatalytic reaction of electron deficient alkenes with Alkoxymethyltrifluoroborates (reaction conditions in Table 2.4)

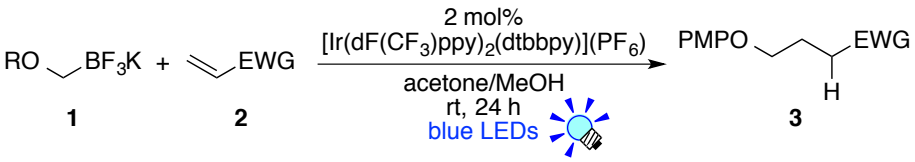

To olefin (**2**) (0.20 mmol) dissolved in a mixture of acetone (1.0 mL) and MeOH (1.0 mL) in a 20 mL-Schlenk tube, alkoxymethyltrifluoroborate (**1**) (0.24 mmol) and photocatalyst (4 mmol) were added under N_2. The mixture was degassed by three freeze-pump-thaw cycles. The reaction was carried out at room temperature (water bath) under visible light irradiation (placed at a distance of ~3 cm from blue LED lamps: $h\nu$ = 425 ± 15 nm). The resulting mixture was stirred for 24 h and concentrated *in vacuo*. The residue was purified by column chromatography to afford 1,4-addition product (**3**).

3-(*p*-Methoxyphenoxymethyl)cyclopentan-1-one (5ag)

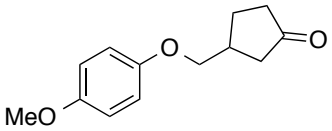

The reaction of 2-cyclopenten-1-one (**2g**) (15.1 mg, 0.184 mmol), potassium (4-methoxyphenoxy)methyltrifluoroborate (**4a**) (53.3 mg, 0.218 mmol) and $[Ir(dF(CF_3)ppy)_2(dtbbpy)](PF_6)$ (**Ir-4**) (4.4 mg, 3.91 mmol) following the general procedures afforded **5ag** (38.2 mg, 94% yield) as a pale yellow oil after purification with column chromatography on silica gel (hexane:EtOAc = 10:1).

^{1}H NMR (400 MHz, $CDCl_3$, rt): δ 6.83 (m, 4H), 3.89 (d, 2H), 3.77 (s, 3H), 2.69 (m, 1H), 2.42 (m, 2H), 2.19 (m, 3H), 1.85 (m, 1H). **^{13}C NMR** (100 MHz, $CDCl_3$, rt): d 218.6, 154.2, 153.1, 115.7, 114.9, 71.7, 55.9, 42.0, 38.0, 36.7, 26.2. **HRMS** (ESI-TOF): calculated for $[C_{13}H_{16}O_3+Na]^+$ requires 243.0992, found 243.0996.

3-(*p*-Methoxyphenoxymethyl)cyclohexan-1-one (5aq)

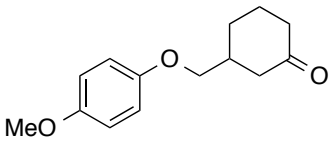

The reaction of 2-cyclohexen-1-one (**2q**) (19.5 mg, 0.203 mmol), potassium (4-methoxyphenoxy)methyltrifluoroborate (**4a**) (58.5 mg, 0.240 mmol) and $[Ir(dF(CF_3)ppy)_2(dtbbpy)](PF_6)$ (**Ir-4**) (4.5 mg, 4.00 mmol) following the general procedures afforded **5aq** (31.7 mg, 67% yield) as a pale yellow oil after purification with preparative TLC on silica gel (hexane:EtOAc = 3:1).
^{1}H NMR (400 MHz, $CDCl_3$, rt): δ 6.82 (m, 4H), 3.82 (d, 2H), 3.81 (s, 3H), 2.54 (m, 1H), 2.33 (m, 3H), 2.11 (m, 1H), 2.03 (m, 1H), 1.72 (m, 2H), 1.59 (m, 1H). **^{13}C NMR** (100 MHz, $CDCl_3$, rt): δ 211.0, 154.2, 153.2, 72.5, 55.9, 44.8, 41.5, 39.1, 28.2, 25.0. **HRMS** (ESI-TOF): calculated for $[C_{14}H_{18}O_3+Na]^+$ requires 257.1148, found 257.1156.

Tetrahydro-(4-(4-methoxyphenoxy)methyl)-*2H*-pyran-2-one (5ar)

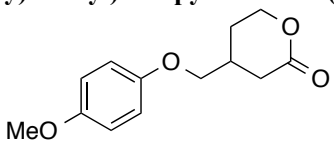

The reaction of 5,6-dihydro-*2H*-pyran-2-one (**2r**) (19.7 mg, 0.200 mmol), potassium (4-methoxyphenoxy)methyltrifluoroborate (**4a**) (58.7 mg, 0.241 mmol) and $[Ir(dF(CF_3)ppy)_2(dtbbpy)](PF_6)$ (**Ir-4**) (4.5 mg, 4.00 mmol) following the general procedures afforded **5ar** (29.6 mg, 62% yield) as a pale yellow oil after purification with column chromatography on silica gel (hexane:EtOAc = 10:1).
^{1}H NMR (400 MHz, $CDCl_3$, rt): δ 6.83 (m, 4H), 4.47 (m, 1H), 4.36 (m, 1H), 3.84 (m, 2H), 3.77 (s, 3H), 2.75(m, 1H), 2.49(m, 2H), 2.09 (m, 1H), 1.80 (m, 1H). **^{13}C NMR** (100 MHz, $CDCl_3$, rt): δ 171.1, 154.4, 152.8, 115.7, 114.9, 71.6, 68.1, 55.9, 32.9, 31.6, 25.9. **HRMS** (ESI-TOF): calculated for $[C_{13}H_{16}O_4+Na]^+$ requires 259.0941, found 259.0954.

4-(4-Methoxyphenoxy)butanenitrile (5ae)

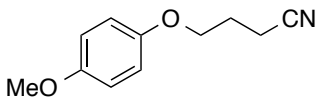

The reaction of acrylonitrile (**2e**) (11.2 mg, 0.211 mmol), potassium (*p*-methoxyphenoxy)methyltrifluoroborate (**4a**) (58.8 mg, 0.241 mmol) and $[Ir(dF(CF_3)ppy)_2(dtbbpy)](PF_6)$ (**Ir-4**) (4.4 mg, 3,91 mmol) following the general procedures afford **5ae** (39.2 mg, 97% yield) as a pale yellow oil after purification with column chromatography on silica gel (hexane:EtOAc = 10:1).

^{1}H NMR (400 MHz, $CDCl_3$, rt) δ 6.84 (m, 4H), 4.04 (t, *J* = 6.0, 2H), 3.77 (s, 3H), 2.58 (t, *J* = 7.2, 2H), 2.11 (m, 2H). **^{13}C NMR** (100 MHz, $CDCl_3$, rt) δ 154.4, 152.7, 119.3, 115.8, 114,9, 66.3, 55.9, 25.8, 14.3. **HRMS** (ESI-TOF): calculated for $[C_{11}H_{13}NO_2+Na]^+$ requires 214.0838, found 214.0847.

***N*,*N*-Dimethyl-4-(4-methoxypheoxy)-butanamide (5af)**

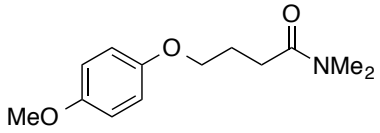

The reaction of *N*,*N*-dimethylacrylamide (**2f**) (19.9 mg, 0.201 mmol), potassium (4-methoxyphenoxy)methyltrifluoroborate (**4a**) (58.6 mg, 0.240 mmol) and $[Ir(dF(CF_3)ppy)_2(dtbbpy)](PF_6)$ (**Ir-4**) (4.5 mg, 4.00 mmol) following the general procedures afforded **5af** (27.6 mg, 58% yield) as a pale yellow oil after purification with column chromatography on aluminium oxide (hexane:EtOAc = 10:1).
^{1}H NMR (400 MHz, $CDCl_3$, rt) δ 6.82 (m, 1H), 3.97 (t, *J* = 5.8 Hz, 2H), 3.76 (s, 3H), 3.00 (s, 3H), 2.95 (s, 3H), 2.51 (t, *J* = 7.2, 2H), 2.10 (m, 2H). **^{13}C NMR** (100 MHz, $CDCl_3$, rt) δ 172.5, 154.0, 153.2, 115.6, 114.8, 67.9, 55.9, 37.3, 35.5, 29.6, 25.1. **HRMS** (ESI-TOF): calculated for $[C_{13}H_{19}NO_3+Na]^+$ requires 260.1257, found 260.1263.

Methyl 2-methyl-4-(4-methoxyphenoxy)butanoate (5ab)

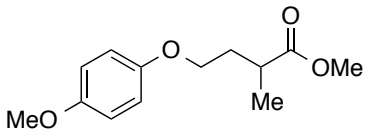

The reaction of methyl methacrylate (**2b**) (19.1 mg, 0.191 mmol), potassium (4-methoxyphenoxy)methyltrifluoroborate (**4a**) (57.1 mg, 0.234 mmol) and $[Ir(dF(CF_3)ppy)_2(dtbbpy)](PF_6)$ (**Ir-4**) (4.3 mg, 3.83 mmol) following the general procedures afforded **5ab** (44.9 mg, 99% yield) as a pale yellow oil after purification with column chromatography on silica gel (hexane:EtOAc = 10:1).
^{1}H NMR (400 MHz, $CDCl_3$, rt) δ 6.82 (s, 4H), 3.94 (t, ^3J = 6.4 Hz, 1H), 3.94 (t, ^3J = 6.4 Hz, 1H), 3.76 (s, 3H), 3.68 (s, 3H), 2.74 (m, 1H), 2.16 (m, 1H), 1.86 (m, 1H), 1.23 (d, ^3J = 7.2, 3H). **^{13}C NMR** (400 MHz, $CDCl_3$, rt) δ 176.9, 154.0, 153.2, 115.7, 114.8, 66.4, 55.9, 51.7, 36.5, 33.3, 17.3. **HRMS** (ESI-TOF): calculated for $[C_{14}H_{18}O_4+Na]^+$ requires 261.1097, found 261.1105.

Methyl 2-acetamido-4-(4-methoxyphenoxy)butanoate (5ak)

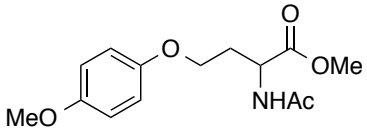

The reaction of methyl 2-acetamidoacrylate (**2k**) (28.7 mg, 0.201 mmol), potassium (4-methoxyphenoxy)methyltrifluoroborate (**4a**) (58.7 mg, 0.241 mmol) and $[Ir(dF(CF_3)ppy)_2(dtbbpy)](PF_6)$ (**Ir-4**) (4.4 mg, 3.91 mmol) following the general procedures afforded **5ak** (36.3 mg, 65% yield) as a pale yellow solid after purification with column chromatography on aluminium oxide. (hexane:EtOAc = 10:1).
^{1}H NMR (400 MHz, $CDCl_3$, rt) δ 6.80 (m, 4H), 6.39 (brd, *J* = 6.8 Hz, 1H), 4.75 (dt, ^2J = 7.2 Hz, ^3J = 5.6 Hz, 1H), 3.98 (m, 2H), 3.76 (s, 3H), 3.75 (s, 3H), 2.30 (m, 2H), 2.02 (s, 3H). **^{13}C NMR** (100 MHz, $CDCl_3$, rt) δ 172.7, 170.0, 154.4, 152.7, 115.7, 114.9, 65.2, 55.9, 52.6, 50.6, 31.5, 23.3. **HRMS** (ESI-TOF): calculated for $[C_{14}H_{19}NO_5+Na]^+$ requires 304.1155, found 304.1162.

Diethyl 2-(4-methoxyphenoxy)malonate (5ai)

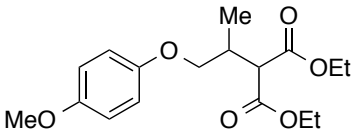

The reaction of diethyl ethylidenmalonate (**2i**) (32.4 mg, 0.205 mmol), potassium (*p*-methoxyphenoxy)methyltrifluoroborate (**4a**) (58.5 mg, 0.240 mmol) and $[Ir(dF(CF_3)ppy)_2(dtbbpy)](PF_6)$ (**Ir-4**) (4.4 mg, 3.91 mmol) following the general procedures afford **5ai** (50.4 mg, 76% yield) as a pale yellow oil after purification with column chromatography on silica gel (hexane:EtOAc = 10:1).

^{1}H NMR (400 MHz, $CDCl_3$, rt) δ 6.83 (m, 4H), 4.19 (m, 4H), 3.89 (m, 2H), 3.77 (s, 3H), 3.58 (d, ^3J = 7.6 Hz, 1H), 2.72 (m, 1H), 1.26 (t, J = 7.2 Hz, 3H), 1.22 (t, J = 7.2 Hz, 3H), 1.14 (d, J = 6.8 Hz, 3H). **^{13}C NMR** (100 MHz, $CDCl_3$, rt) δ 168.9, 168.7, 154.1, 153.2, 115.8, 114.8, 71.2, 61.4, 55.9, 54.3, 33.8, 14.9, 14.2, 14.2. **HRMS** (ESI-TOF): calculated for $[C_{17}H_{24}O_6+Na]^+$ requires 347.1465, found 347.1465.

6-Bromo-3-ethoxycarbonyl-4-(4-methoxyphenoxymethyl)-3,4-dihydrocoumarin (5at)

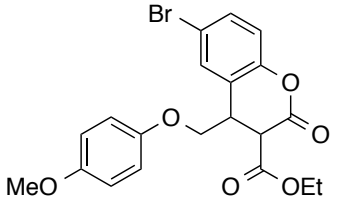

The reaction of ethyl 6-bromocoumarin-3-carboxylate (**2t**) (59.6 mg, 0.201 mmol), potassium (*p*-methoxyphenoxy)methyltrifluoroborate (**4a**) (58.9 mg, 0.241 mmol) and $[Ir(dF(CF_3)ppy)_2(dtbbpy)](PF_6)$ (**Ir-4**) (4.4 mg, 3.91 mmol) following the general procedures afforded **5at** (42.4 mg, 50% yield) as a pale yellow oil after purification with preparative TLC on silica gel (hexane:EtOAc = 3:1).

^{1}H NMR (400 MHz, $CDCl_3$, rt) δ 7.42 (m, 2H), 6.99 (m, 1H), 6.78 (m 4H), 4.12 (m, 2H), 4.11 (m, 1H), 4.04 (m, 2H), 3.81 (m, 1H), 3.75 (s, 3H), 1.15 (t, J = 7.2 Hz, 3H). **^{13}C NMR** (100 MHz, $CDCl_3$, rt) δ 166.9, 163.1, 154.8, 152.2, 150.9, 132.6, 131.5, 123.0, 119.0, 117.5, 115.9, 114.9, 70.7, 62.8, 55.9, 49.3, 40.1, 14.0. **HRMS** (ESI-TOF): calculated for $[C_{20}H_{19}BrO_6+Na]^+$ requires 457.0257, found 457.0256.

2-(3-(4-Methoxyphenoxy)propyl)pyridine (5al)

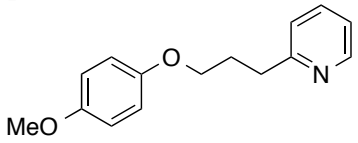

The reaction of 2-vinylpyridine (**2l**) (21.5 mg, 0.204 mmol), potassium (*p*-methoxyphenoxy)methyltrifluoroborate (**4a**) (58.3 mg, 0.239 mmol) and $[Ir(dF(CF_3)ppy)_2(dtbbpy)](PF_6)$ (**Ir-4**) (4.4 mg, 3.91 mmol) following the general procedures afforded **5al** (34.9 mg, 70% yield) as a pale yellow oil after purification with column chromatography on aluminium oxide (hexane:EtOAc = 10:1).

^{1}H NMR (400 MHz, $CDCl_3$, rt) δ 8.54 (m, 1H), 7.59 (m, 1H), 7.18 (m, 1H), 7.11 (m, 1H), 6.82 (m, 4H), 3.96 (t, J = 6.4 Hz, 2H), 3.76 (s, 3H), 2.98 (t, J = 7.6 Hz, 2H), 2.20 (m, 2H). **^{13}C NMR** (100 MHz, $CDCl_3$, rt) δ 161.6, 154.0, 153.4, 149.5, 136.5, 123.1, 121.1, 115.7, 114.8, 68.0, 55.9, 34.9, 29.4. **HRMS** (ESI-TOF): calculated for $[C_{15}H_{17}NO_2+Na]^+$ requires 266.1151, found 266.1153.

(4-Boronic pinacol ester)benzyl (4-methoxyphenoxy)butanoate (5av)

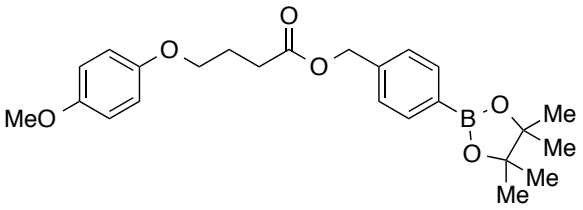

The reaction of (*p*-acrylate)methylphenylboronic acid pinacol ester (**2v**) (58.0 mg, 0.201 mmol), potassium (*p*-methoxyphenoxy)methyltrifluoroborate (**4a**) (58.5 mg, 0.240 mmol), $[Ir(dF(CF_3)ppy)_2(dtbbpy)](PF_6)$ (**Ir-4**) (4.4 mg, 3.91 mmol) following the general procedures afforded **5av** (49.4 mg, 56% yield) as a pale yellow solid after purification with column chromatography on silica gel (hexane:EtOAc = 20:1).
^{1}H NMR (400 MHz, $CDCl_3$, rt) δ 7.79 (d, J = 8.4 Hz, 2H), 7.34 (d, J = 8.4 Hz, 2H), 6.83 (m, 4H), 5.14 (s, 2H), 3.94 (t, J = 6.0, 2H), 3.76 (s, 3H), 2.57 (t, J = 7.2, 2H), 2.10 (m, 2H), 1.34 (s, 12H). **^{13}C NMR** (100 MHz, $CDCl_3$, rt) δ 173.2, 154.1, 153.2, 139.1, 135.2, 127.4, 115.7, 114.9, 84.0, 67.6, 66.3, 55.9, 31.0, 25.0, 24.9. **HRMS** (ESI-TOF): calculated for $[C_{24}H_{31}BO_6+Na]^+$ requires 449.2110, found 449.2111.

3-((Trimethylsilylmethyloxy)methyl)cyclopentan-1-one (5gg)

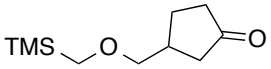

The reaction of 2-cyclopenten-1-one (**2g**) (17.6 mg, 0.214 mmol), potassium (2-(trimethylsilyl)methoxy)methyltrifluroborate (**4g**) (57.7 mg, 0.257 mmol), $[Ir(dF(CF_3)ppy)_2(dtbbpy)](PF_6)$ (**Ir-4**) (4.5 mg, 4.00 mmol) following the general procedures afforded **5gg** (20.7 mg, 48% yield) as a pale yellow solid after purification with column chromatography on silica gel (hexane:EtOAc = 10:1).
^{1}H NMR (400 MHz, $CDCl_3$, rt) δ 5.60 (d, J = 5.6 Hz, 2H), 3.09 (s, 2H), 2.48 (m, 1H), 2.31 (m, 2H), 2.09 (m, 1H), 0.01 (s, 9H). **^{13}C NMR** (100 MHz, $CDCl_3$, rt) δ 219.7, 78.7, 65.6, 42.2, 38.1, 36.9, 26.3, 1.16, -2.96. **HRMS** (ESI-TOF): calculated for $[C_{10}H_{20}O_2Si+Na]^+$ requires 223.1125, found 223.1151.

3-((3,4-Methylenedioxyphenoxy)methyl)cyclopenten-1-one (5eg)

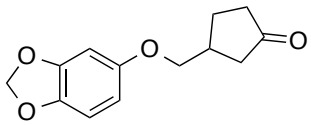

The reaction of 2-cyclopenten-1-one (**2g**) (16.1 mg, 0.196 mmol), potassium (3,4-methylenedioxyphenoxy)methyltrifluoroborate (**4e**) (62.0 mg, 0.240 mmol) and $[Ir(dF(CF_3)ppy)_2(dtbbpy)](PF_6)$ (**Ir-4**) (4.5 mg, 4.00 mmol) following the general procedures afforded **5gg** (37.0 mg, 78% yield) as a pale orange solid after purification with column chromatography on silica gel (hexane:EtOAc = 10:1).
^{1}H NMR (400 MHz, $CDCl_3$, rt) δ 6.69 (d, J = 8.4 Hz, 1H), 6.48 (d, J = 2.4, 1H), 6.30 (dd, ^3J = 8.4 Hz, ^4J = 2.4 Hz, 1H), 5.91 (s, 2H), 3.90 (d, J = 2.0 Hz, 2H), 2.68 (m, 1H), 2.40 (m, 2H), 2.23 (m, 2H), 2.12 (m, 1H), 1.83 (m, 1H). **^{13}C NMR** (100 MHz, $CDCl_3$, rt) δ 218.5, 154.5, 148.5, 142.0, 108.1, 105.9, 101.3, 98.3, 72.0, 41.9, 38.0, 36.6, 26.2. **HRMS** (ESI-TOF): calculated for $[C_{13}H_{14}O_4+Na]^+$ requires 257.0784, found 257.0785.

3-(4-(3-Thienyl)phenoxy)methyl)cyclopentan-1-one (5fg)

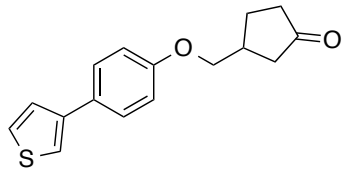

The reaction of 2-cyclopenten-1-one (**2g**) (16.8 mg, 20.5 mmol), potassium 4-(3-thionyl)phenoxymethyltrifluoroborate (**4f**) (71.1 mg, 0.240 mmol), $[Ir(dF(CF_3)ppy)_2(dtbbpy)](PF_6)$ (**Ir-4**) (4.4 mg, 3.91 mmol) following the general procedures afforded **4fg** (24.4 mg, 47% yield) as a pale yellow solid after purification with column chromatography on silica gel (hexane:EtOAc = 10:1-5:1).
^{1}H NMR (400 MHz, $CDCl_3$, rt) δ 7.52 (m, 2H), 7.36 (m, 3H), 6.92 (m, 2H), 4.02 (d, J = 6.0 Hz, 2H), 2.73 (m 1H), 2.44 (m, 2H), 2.27 (m, 2H), 2.17 (m, 1H), 1.88 (m, 1H). **^{13}C NMR** (400 MHz, $CDCl_3$, rt) δ 218.5, 158.2, 142.1, 129.3, 127.7, 126.4, 126.2, 119.2, 114.9, 71.0, 41.9, 38.1, 36.6, 26.2. **HRMS** (ESI-TOF): calculated for $[C_{16}H_{16}O_2S+Na]^+$ requires 295.0766, found 295.0766.

4-(4-Methoxybenzyloxy)butylonitrile (5de)

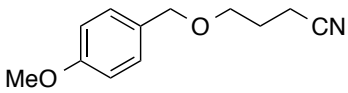

The reaction of acrylonitrile (**2e**) (10.8 mg, 0.204 mmol), potasssium (4-methoxybenzyloxy)methyltrifluoroborate (**4d**) (62.0 mg, 0.240 mmol), $[Ir(dF(CF_3)ppy)_2(dtbbpy)](PF_6)$ (**Ir-4**) (4.4 mg, 3.91 mmol) following the general procedures afforded **5de** (31.1 mg, 68% yield) as a pale yellow solid after purification with column chromatography on silica gel (hexane:EtOAc = 10:1).
^{1}H NMR (400 MHz, $CDCl_3$, rt) δ 7.27 (m, 2H), 6.91 (d, 2H), 4.47 (s, 2H), 3.83 (s, 3H), 3.57 (t, ^3J = 5.8 Hz, 2H), 2.49 (t, ^3J = 7.2 Hz, 2H), 1.95 (m, 2H). **^{13}C NMR** (100 MHz, $CDCl_3$, rt) δ 159.5, 130.2, 129.4, 119.6, 114.0, 73.0, 67.4, 55.4, 26.0, 14.3. **HRMS** (ESI-TOF): calculated for $[C_{12}H_{15}NO_2+Na]^+$ requires 228.0995, found 228.0912.

Sunlight-driven reaction

A cylindrical vessel (diameter: 4.5 cm, depth: 1.5 cm) was used for photoreaction under sunlight. To 2-cyclopentenone (**2g**) (16.0 mg, 0.195 mmol) dissolved in a mixture of acetone (1.0 mL) and MeOH (1.0 mL) placed in the vessel, **4a** (57.0 mg, 0.234 mmol) and **Ir-4** (4.4 mg, 3.91 mmol) were added under N_2. The mixture was degassed freeze-pump-thaw cycles. The reaction mixture was exposed to sunlight for 4 h around 21 ºC (in November 15th, 2012). After workup, **5ag** was obtained as oil (35.8 mg, 83% yield).

2.5 References

1 (a) B. Giese, *Angew. Chem. Int. Ed.* **1983**, *22,* 753-764; (b) W. Zhang, *Tetrahedron* **2001**, *57,* 7237-7262; (c) G. S. C. Srikanth, S. L. Castle, *Tetrahedron* **2005**, *61,* 10377-10441.

2 (a) S. Murahashi, D. Zhang, *Chem. Soc. Rev.* **2008**, *37,* 1490-1501; (b) C.-J. Li, *Acc. Chem. Res.* **2009**, *42,* 335-344; (c) C. J. Scheuermann, *Chem. Asian. J.* **2010**, *5,* 436-451; (d) C. S. Yeung, V. M. Dong, *Chem. Rev.* **2011**, *111,* 1215-1292.

3 For selected recent reviews on photoredox catalysis, see: (a) T. P. Yoon, M. A. Ischay, J. Du, *Nat. Chem.* **2010**, *2,* 527-532; (b) J. M. R. Narayanam, C. R. J. Stephenson, *Chem. Rev.* **2011**, *40,* 102-113; (c) J. Xuan, W.-J. Xiao, *Angew. Chem. Int. Ed.* **2012**, *51,* 6828-6838; (d) L. Shi, W. Xia, *Chem. Soc. Rev.* **2012**, *41,* 7687-7696; (e) C. K. Prier, D. A. Rankic, D. W. C. MacMillan, *Chem. Rev.* **2013**, *113,* 5322-5363; (f) Y. Xi, H. Yi, A. Lei, *Org. Biomol. Chem.* **2013**, *11,* 2387-2403; (g) D. P. Hari, B. König, *Angew. Chem. Int. Ed.* **2013**, *52,* 4734-4743; (h) M. Reckenthäler, A. G. Griesbeck, *Adv. Synth. Catal.* **2013**, *355,* 2727-2744; (i) J. Hu, J. Wang, T. H. Nguyen, N. Zheng, *Beilstein J. Org. Chem.* **2013**, *9,* 1977-2001; (j) M. N. Hopkinson, B. Sahoo, J.-L. Li, F. Glorius, *Chem. Eur. J.* **2014**, *20,* 3874-3886; (k) T. Koike, M. Akita, *Top. Catal.* **2014**, *57,* 967-974; (l) D. M. Schultz, T. P. Yoon, *Science* **2014***, 343,* 1239176-1-1239176-8.

4 For selected reports on the generation of aminoalkyl radical by photoredox catalysis, see: (a) A. McNally, C. K. Prier, D. W. C. MacMillan, *Science* **2011**, *334,* 1114-1117; (b) P. Kohls, D. Jadhav, G. Pandey, O. Reiser, *Org. Lett.* **2012**, *14,* 672-675; (c) Y. Miyake, K. Nakajima, Y. Nishibayashi, *J. Am. Chem. Soc.* **2012**, *134,* 3338-3341; (d) S. Cai, X. Zhao, X. Wang, Q. Liu, Z. Li, D. Z. Wang, *Angew. Chem. Int. Ed.* **2012**, *51,* 8050-8053; (e) X. Ju, D. Li, W. Li, W. Yu, F. Bian, *Adv. Synth. Catal.* **2012**, *354,* 3561-3567; (f) S. Zhu, A. Das, L. Bui, H. Zhou, D. P. Curran, M. Rueping, *J. Am. Chem. Soc.* **2013**, *135,* 1823-1829.

5 Foe selected reports on the generation of iminium ions by photoredox catalysis, see: (a) A. G. Condie, J. C. González-Gómez, C. R. J. Stephenson, *J. Am. Chem. Soc.* **2010**, *132,* 1464-1465; (b) M. Rueping, C. Vila, R. M. Koenigs, K. Poscharny, D. C. Fabry, *Chem. Commun.* **2011**, *47,* 2360-2362; (c) M. Rueping, S. Zhu, R. M. koenigs, *Chem. Commun.* **2011**, *47,* 8679-8681; (d) J. Xuan, Y. Cheng, J. An, L.-Q.

Lu, X.-X. Zhang, W.-J. Xiao, *Chem. Commun.* **2011**, *47,* 8337-8339; (e) D. P. Hari, B. König, *Org. Lett.* **2011**, *13,* 3852-3855; (f) Y. Pan, C. W. Kee, L. Chen, C.-H. Tan, *Green Chem.* **2011**, *13,* 2682-2685; (g) Q. Liu, Y.-N. Li, H.-H. Zhang, B. Chen, C.-H. Tung, L.-Z. Wu, *Chem. Eur. J.* **2012**, *18,* 620-627; (h) D. B. Freeman, L. Furst, A. G. Condie, C. R. J. Stephenson, *Org. Lett.* **2012**, *14,* 94-97; (i) G. Zhao, C. Yang, L. Guo, H. Sun, C. Chen, W. Xia, *Chem. Commun.* **2012**, *48,* 2337-2339; (j) S. Maity, M. Zhu, R. S. Shinadery, N. Zheng, *Angew. Chem. Int. Ed.* **2012**, *51,* 222-226; (k) S. Zhu, M. Rueping, *Chem. Commun.* **2012**, *48,* 11960-11962; (l) Q.-Y. Meng, J.-J. Zhong, Q. Liu, X.-W. Gao, H.-H. Zhang, T. Lei, Z.-J. Li, K. Feng, B. Chen, C.-H. Tung, L.-Z. Wu, *J. Am. Chem. Soc.* **2013**, *135,* 19052-19055.

6 For selected reports on generation of azomethine ylides by photoredox catalysis, see: (a) Y.-Q. Zou, L.-Q. Lu, L. Fu, N.-J. Chang, J.Rong, J.-R. Chen, W.-J. Xiao, *Angew. Chem. Int. Ed.* **2011**, *123,* 7171-7175; (b) M. Rueping, D. Leonori, T. Poisson, *Chem. Commun.* **2011**, *47,* 9615-9617.

7 For selected reports on oxidation of enemines by photoredox catalysis, see: (a) T. Koike, M. Akita, *Chem. Lett.* **2009**, *38,* 166-167; (b) Y. Yasu, T. Koike, M. Akita, *Chem. Commun.* **2012**, *48,* 5355-5357; (c) M. T. Pirnot, D. A. Rankic, D. B. C. Martin, D. W. C. MacMillan, *Science* **2013**, *339,* 1593-1596; (d) F. R. Petronijević, M. Nappi, D. W. C. MacMillan, *J. Am. Chem. Soc.* **2013**, *135,* 18323-18326; (e) J. A. Terrett, M. D. Clift, D. W. C. MacMillan, *J. Am. Chem. Soc.* **2014**, *136,* 6858-6861

8 (a) Z. Zuo, D. W. C. MacMillan, *J. Am. Chem. Soc.* **2014**, *136,* 5257-5260; (b) L. J. Allen, P. J. Cabrera, M. Lee, M. S. Sanford, *J. Am. Chem. Soc.* **2014**, *136,* 5607-5610.

9 J. W. Trucker, J. M. R. Narayanam, P. S. Shah, C. R. J. Stepehnson, *Chem.*

Commun. **2011**, *47,* 5040-5042.

10 (a) T. Iwahama, S. Sakaguchi, Y. Ishii, *Chem. Commun.* **2000**, 613-614; (b) K.-i. Yamada, Y. Yamamoto, K. Tomioka, *J. Synth. Org. Chem. Jpn.* **2004**, *62*, 1158-1165; (c) S.-Y. Zhang, F.-M. Zhang, Y. -Q. Tu, *Chem. Soc. Rev.* **2011**, *40,* 1937-1949.

11 (a) Y. Yasu, T. Koike, M. Akita, *Adv. Synth. Catal.* **2012**, *354,* 3414-3420; (b) T. Koike, M. Akita, *Synlett* **2013**, *24,* 2492-2505.

12 The photoexcited states of $[Ir(dF(CF_3)ppy)_2(bpy)](PF_6)$ (**Ir-3**) and $[Ir(dF(CF_3)ppy)_2(dtbbpy)](PF_6)$ (**Ir-4**) are strong oxidants ($E_{1/2}$ = +0.91 V and +0.48 V *vs* $[Cp_2Fe]$, respectively); see: (a) D. Hanss, J. C. Freys, G. Bernardine, O. S. Wenger, *Eur. J. Inorg. Chem.* **2009**, 4850-4859; (b) M. S. Lowry, J. I. Goldsmith, J. D. Slinker, R. Rohl, R. A. Pascal, G. G. Malliaras, S. Bernhard, *Chem. Mater.* **2005**, *17,* 5712-5719.

13 (a) G. A. Molander, B. Candurk, *Org. Lett.* **2008**, *10,* 2135-2138; (b) G. A. Molander, N. Fleury-Brégeot, M.-A. Hiebel, *Org. Lett.* **2011**, *13,* 1694-1697; (c) G. A. Molander, V. Colombel, A. Braz, *Org. Lett.* **2011**, *13,* 1852-1855; (d) G. A. Molander, F. Beaumard, *Org. Lett.* **2011**, *13,* 3948-3951; (e) G. A. Molander, I. Shin, *Org. Lett.* **2011**, *13,* 3956-3959; (f) N. Murai, M. Miyano, M. Yonaga, K. Tanaka, *Org. Lett.* **2012**, *14,* 2818-2821; (g) G. A. Molander, I. Shin, *Org. Lett.* **2012**, *14,* 4458-4461; (h) R. Devulapally, N. Fleury-Brégeot, G. A. Molander, D. G. Seapy, *Tetrahedron Lett.* **2012**, *53,* 1051-1055; (i) G. A. Molander, S. R. Wisniewski, *J. Am. Chem. Soc.* **2012**, *134,* 16856-16868. (j) G. A. Molander, I. Shin, *Org. Lett.* **2013**, *15,* 2534-2537.

14 (a) P. Berthelot, C. Vaccher, N. Flouquet, M. Debaert, M. Luyckx, C. Brunet, *J. Med. Chem.* **1991**, *34,* 2557-2560; (b) G. Costantino, A. Macchiarulo, A. E.

Guadix, R. Pellicciari, *J. Med. Chem.* **2001**, *44,* 1827-1832; (c) M. Ordóñez, C. Cativiela, *Tetrahedron Asymmetry* **2007**, *18,* 3-99 (d) C. Shao, H.-J. Yu, N.-Y. Wu, P. Tian, R. Wang, C.-G. Feng, G.-Q. Lin, *Org. Lett.* **2011**, *13,* 788-791.

15 The photoexcited states of $[Ru(bpy)_3](PF_6)_2$ (**1c**) and *fac*-$[Ir(ppy)_3]$ (**1d**) are weaker oxidants ($E_{1/2}$ = +0.36 V and –0.10V *vs.* $[Cp_2Fe]$, respectively) than **1a**; see: (a) K. Kalyanasundaram, *Coord. Chem. Rev.* **1982**, *46,* 159-244; (b) L. Flamigni, A. Barbieri, C. Sabatini, B. Ventura, F. Barigelletti, *Top. Curr. Chem.* **2007**, *281,* 143-203.

16 The group of Yoon reported on the [2+2] cycloaddition of electron-rich styrenes by photoredox catalysis. An analogous product was observed in the present reaction. M. A. Ischay, M. A. Ischay, M. S. Ament, T. P. Yoon, *Chem. Sci.* **2012**, *3,* 2807-2811.

17 L. Chu, C. Ohta, Z. Zuo, D. W. C. MacMillan, *J. Am. Chem. Soc*, **2014**, *136*, 10886-10889.

18 The present aryloxymethylation is regarded as hydroxymethylation because the aryloxy group can be deprotected by treatment with cerium(IV) ammonium nitrate (CAN). T. Mikami, M. Harada, K. Narasaka, *Chem. Lett.* **1999**, 425-426.

19 For selected reports on oxidative transformation of organoboronic acids and α-silylethers, see: (a) H. C. Brown, N. C. Hébert, C. H. Snyder, *J. Am. Chem. Soc.* **1961**, *83,* 1001-1002; (b) G. Gutenberger, E. Steckhan, S. Blechert, *Angew. Chem. Int. Ed.* **1998**, *37,* 660-662; (c) J.-i. Yoshida, K. Kataoka, R. Horcajada, A. Nagaki, *Chem. Rev.* **2008**, *108,* 2265-2299; (d) Y. Fujiwara, V. Domingo, I. B. Seiple, R. Gianatassio, M. D. Bel, P. S. Baran, *J. Am. Chem. Soc.* **2011**, *133,* 3292-3295.

20 J. R. Ochola, M. O. Wolf, *Org. Biomol. Chem.* **2016**, *14,* 9088-9092.

21 Homocoupling products were apparently observed in photoredox-catalyzed

benzylation with benzylborates. To prevent this, an excess amount of alkenes with respect to borates was used as in ref. *11a*.

22 (a) A. Studer, *Chem. Eur. J.* **2001**, *7,* 1159-1164; (b) H. Fischer, *Chem. Rev.* **2001**, *101,* 3581-3610; (c) K. S. Forsaneanu, J. C. Scaiano, *Helv. Chem. Acta* **2006**, *89*, 2473-2482; (d) A. Studer, D. P. Curran, *Angew. Chem. Int. Ed.* **2016**, *55,* 58-102.

23 T. Okamura, K. Obi, I. Tanaka, *Chem. Phys. Lett*. **1974**, *26*, 218-220.

24 (a) H. B. Ross, M. Boldaji, D. P. Rilema, C. B. Blanton and R. P. White, *Inorg, Chem.* **1989**, *28*, 1013-1021; (b) A. B. Tamayo, B. D. Alleyne, P. I. Djurovich, S. Lamansky, I. Tsyba, N. N. Ho, R. Bau, M. E. Thompson, *J. Am. Chem. Soc.* **2003**, *125,* 7377-7387; (c) J. D. Slinker, Alon. A. Gorodetsky, M. S. Lowry, J. Wang, S. Parker, R. Rohl, S. Bernhard and G. G. Malliaras. *J. Am. Chem. Soc.* **2004**, *126*, 2763-2767.

25 I. Meskini, L. Toupet, M. Daoudi, A. Kerbal, T. B. Hadda, *J. Chem. Crystallogr* **2011***, 41,* 891-894.

26 G. A. Molander and M.-A. Hiebel, *Org. Lett*. **2010**, *12*, 4876-4879.

27 (a) E. Barbayianni, I. Fotakopoulou, M. Schmidt, V. Constantinou-Kokotou, U. T. Bornscheuer, G. Kokotos, *J. Org. Chem.* **2005**, *70*, 8730-8733; (b) G. P. Dado, S. H. Gellman, *J. Am. Chem. Soc*. **1994**, *116*, 1054-1062; (c) D. A. Everson, B. A. Jones and D. J. Weix, *J. Am. Chem. Soc.* **2012**, *134*, 6146-6159.

Chapter 3

Regiospecific Intermolecular Aminohydroxylation of Olefins by Photoredox Catalysis

ABSTRACT: A regiospecific aminohydroxylation of olefins by photoredox catalysis has been developed. *N*-Protected 1-amionopyridinium salts are the key compounds and serve as *N*-centered radical precursors by the action of Ir photocatalysts, *fac*-[Ir(ppy)$_3$] (**Ir-1**) and [Ir(ppy)$_2$(dtbbpy)](PF$_6$) (**Ir-2**). Furthermore, a variety of *N*-protected iminopyridinium ylides also serve as *N*-centered radical precursors by the dual Ir photoredox/Sc(OTf)$_3$ catalysis. The present photocatalytic systems allows us to synthesize vicinal aminoalcohol derivatives from olefins bearing various functional groups under mild reaction conditions.

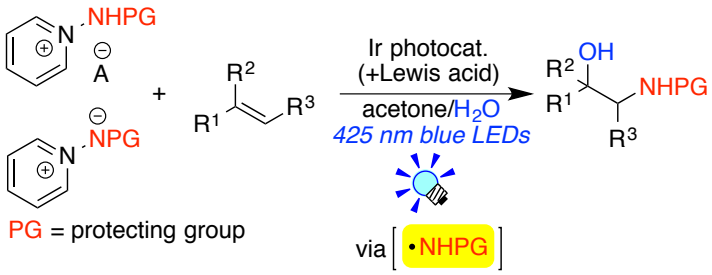

3.1 Introduction

In chapter 2, the author described that amine and ether compounds are obtained by C-C coupling of amino- and alkoxy-methytrifluoroborates with olefins by the action of reductive quenching cycles of photoredox catalysis. In this chapter the author has made another approach for synthesis of amine compounds via C-N bond formation with *N*-centered radicals. Together with ate precursors, onium precursors are also popular and diverse. When onium precursors are used as radical precursors, reaction systems following oxidative quenching cycle are expected to perform the task. On the other hand, in the author's laboratory, trifluoromethylative difunctionalization of alkenes with electrophilic trifluoromethylating reagents has been studied extensively as described in Chapter 1. Taking account of these situations, the author initiated the study with the aim of aminative heterodifunctionalization of olefins, in particular, aminohydroxylation, which is the major subject of the present chapter (Scheme 3.1).

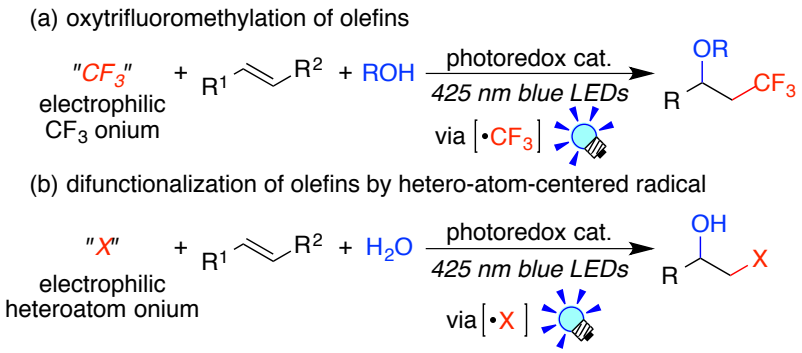

Scheme 3.1 Photoredox catalyzed difunctionalization of olefins via oxidative quenching cycle.

Vicinal aminoalcohol skeletons are ubiquitous in biologically active natural compounds and drugs.[2] Aminohydroxylation of olefins has been regarded as one of effective accesses to vicinal aminoalcohols. Various types of catalytic

amionooxygenation of olefins have been reported so far (Scheme 3.2).[3,4] Yoon's group reported aminooxygenation of olefin with oxaziridine. The use of copper and iron catalysts leads to the products with the contrasting regioselectivity (Scheme 3.2 (a)).[4m,4rq] Stahl's group developed palladium-catalyzed aminoacetoxylation of alkene with phthalimide via aminopalladation (Scheme 3.2 (c)).[4f]

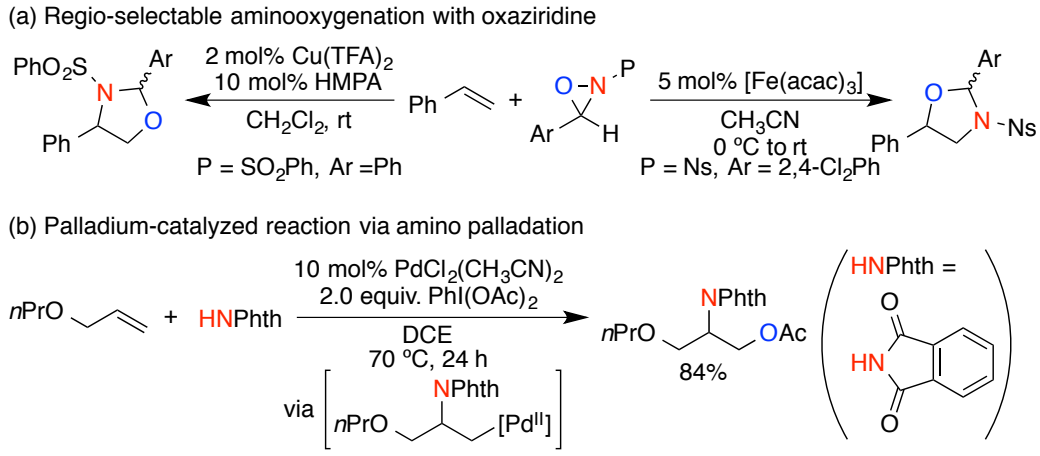

Scheme 3.2 Example of catalytic aminooxygenation of olefins.

One of the most reliable methods for intermolecular aminohydroxylation of olefins is the Os-catalyzed system, which was originally developed by Sharpless et al..[5,6] However, the reported methods usually use the potentially toxic Os catalyst. In addition, regioselectivity with respect to addition of the amino and hydroxyl groups to the internal C=C bond is frequently unsatisfactory (Scheme 3.3 (a)).[6e] Although the regioselectivity of aminohydroxylation with bromamine-T was advanced recently (Scheme 3.3 (b)),[7] it has been difficult to predict regioselectivity. Thus, development of new methodologies for easy-to-use and selective aminohydroxylation of olefin is still highly desirable.

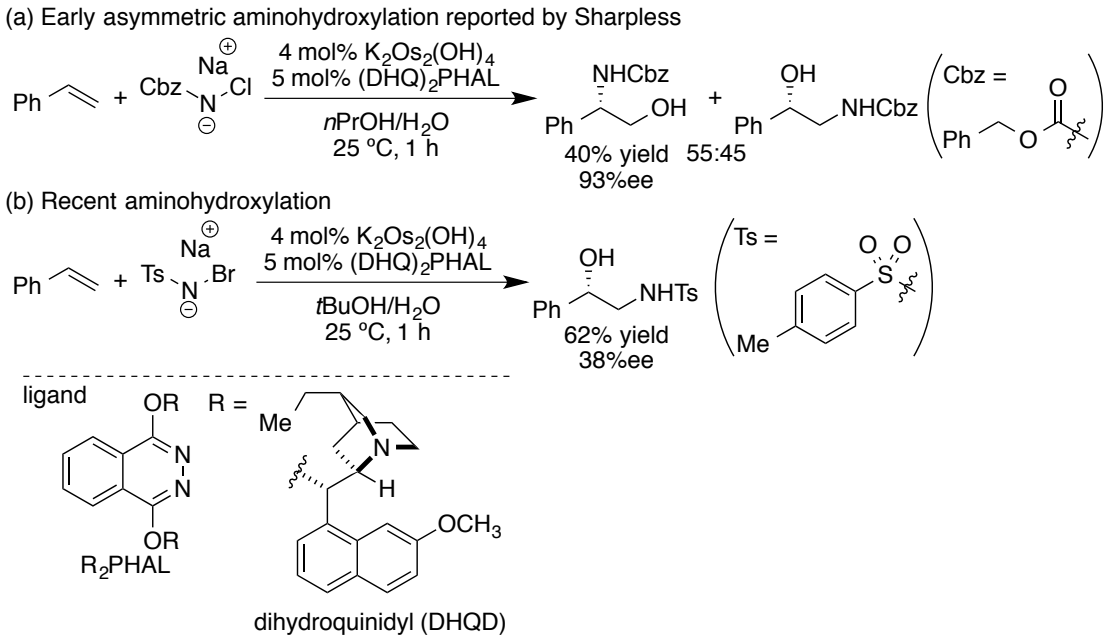

Scheme 3.3 Osmium-catalyzed aminohydroxylation of olefins.

In recent years, photoredox catalysis has opened a new field in synthetic organic chemistry.[8] The reactions involving carbon radicals are the center of research. Photoredox-catalyzed reactions of nitrogen-centered radicals have also attracted a considerable interest of synthetic chemists.[9] Various types of reactions via nitrogen-centered radical species such as hydrogen atom abstraction[10] and radical amination of arenes[11] and olefins[12] are important for construction of carbon-nitrogen bonds as described in chapter 1. The author realized that development of efficient ways to generate *N*-centered radicals is essential for the success of the reactions described above.

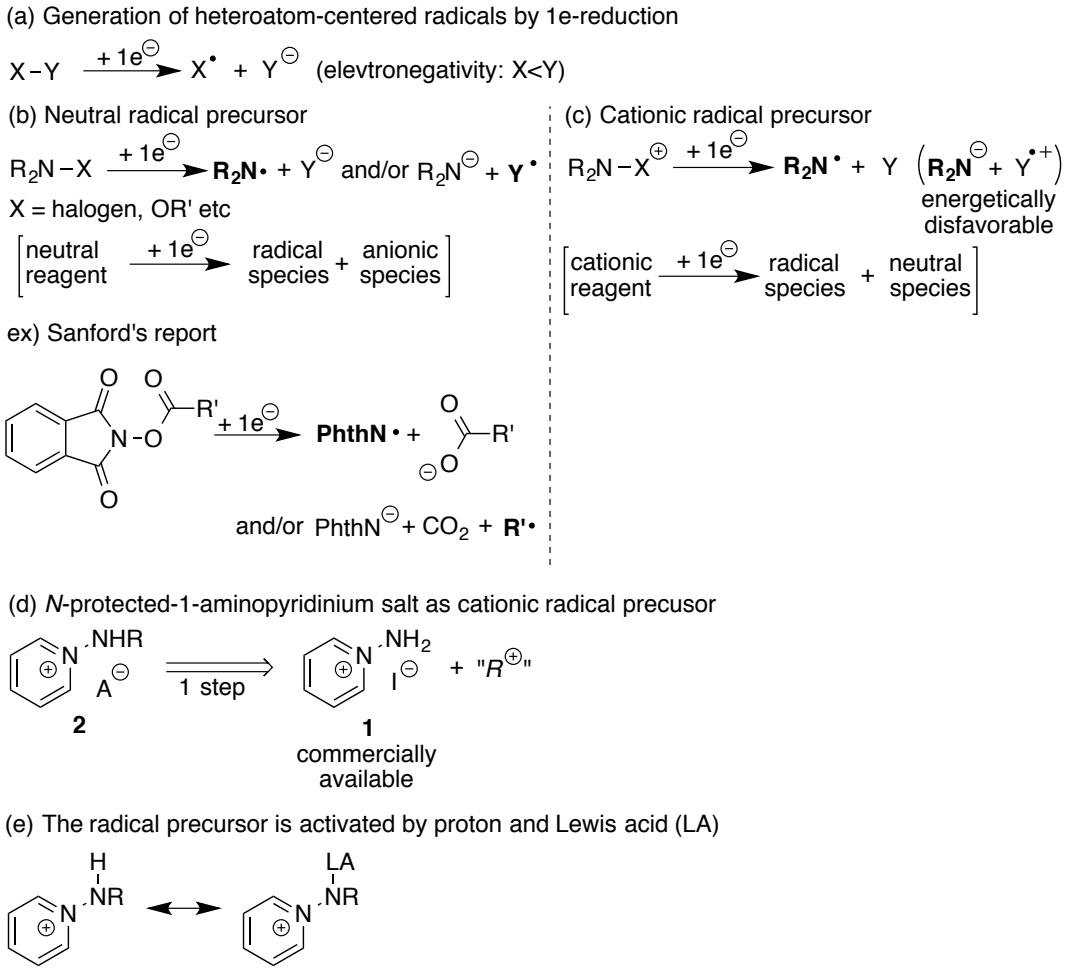

Scheme 3.4 Concept for *N*-centered radical precursor.

One electron reduction of unsymmetrical precursor X-Y occurs to the direction, where the more electronegative moiety carries the negative charge (Scheme 3.4 (a)). Therefore, *O*- or *N*- containing groups or halogens are used as the leaving group Y.

Sanford's group reported generation of phthalimidyl radical (PhthN$^{\bullet}$) from *N*-acyloxyphthalimides by photoredox catalyzed 1-e reduction (Scheme 3.4 (a) ex.).[9g] Electron-withdrawing R' group caused to generate carboxylate and the PhthN$^{\bullet}$ radical. By contrast, the reaction of substrates with ordinary alkyl groups (R') caused formation of phthalimide and carboxyl radical (R'COO$^{\bullet}$), which readily underwent decarboxylation to form alkyl radical (R'$^{\bullet}$). These results indicate that the balance of the

degrees of electron-withdrawing nature between the amine group and the leaving group is important for selective generation of amidyl radical.

To solve the "direction" problem it is essential to introduce much more electronegative group as Y. One of the solutions is the use of a neutral leaving group, which is more stable than the anionic leaving groups containing O, N or X moieties. Such types of precursors are regarded as "onium species". In the case of nitrogen-centered radicals (Scheme 3.4 (c)), the N-Y bond is cleaved to generate the neutral nitrogen-centered radicals and the neutral species, because the other cleavage the pair of the ionized species, i.e. amide anion and the cation radical $[Y\text{-}R]^{+\bullet}$. Because the latter combination is energetically highly unfavorable, the former process generating the *N*-centered radical should occur exclusively. Then the author proposed *N*-protected-1-aminopyridinium salt **2** (Scheme 3.4 (d)) because of the following three reasons: (i) The salt **2** can be readily synthesized from commercially available 1-aminopyridinium iodide (**1**). (ii) Pyridinium moiety is good electron acceptor. (iii) It is possible to introduce various protecting groups on the nitrogen atom.

Herein the author describes novel photoredox-catalyzed regiospecific three-component aminohydroxylation of olefins with aminopyridinium salts. Because the salts can be regarded as a protonated form of the ylide, the author also examined activation of the ylide with a Lewis acid in place of proton, a Brønsted acid.

3.2 Results and discussion

3.2.1 Aminohydroxylation of olefins with *N*-protected aminopyridinium salts by photoredox catalysis

3.2.1.1 Synthesis of amidyl radical precursors

First of all, the author designed electrophilic amine reagents as precursors for

N-centered radicals. 1-Aminopyridinium iodide (**1**) is a commercially available chemical, derivatives of which have been used as building blocks for *N*-containing heterocycles.[13] Its primary amine moiety was modified by acid chloride or acid anhydride having R group with different electronic features (Scheme 3.5). The obtained *N*-(*p*-toluenesulfonylamino)-pyridinium tetrafluoroborate (**2a**), *N*-(2,3,4,5,6-pentafluorobenzoylamino)-pyridinium triflate (**2b**), *N*-(benzyloxycarbonylamino)-pyridinium triflate (**2c**), and *N*-(trifluoroacetyl)-pyridinium triflate (**2d**)[14] turned out to be shelf-stable chemicals.

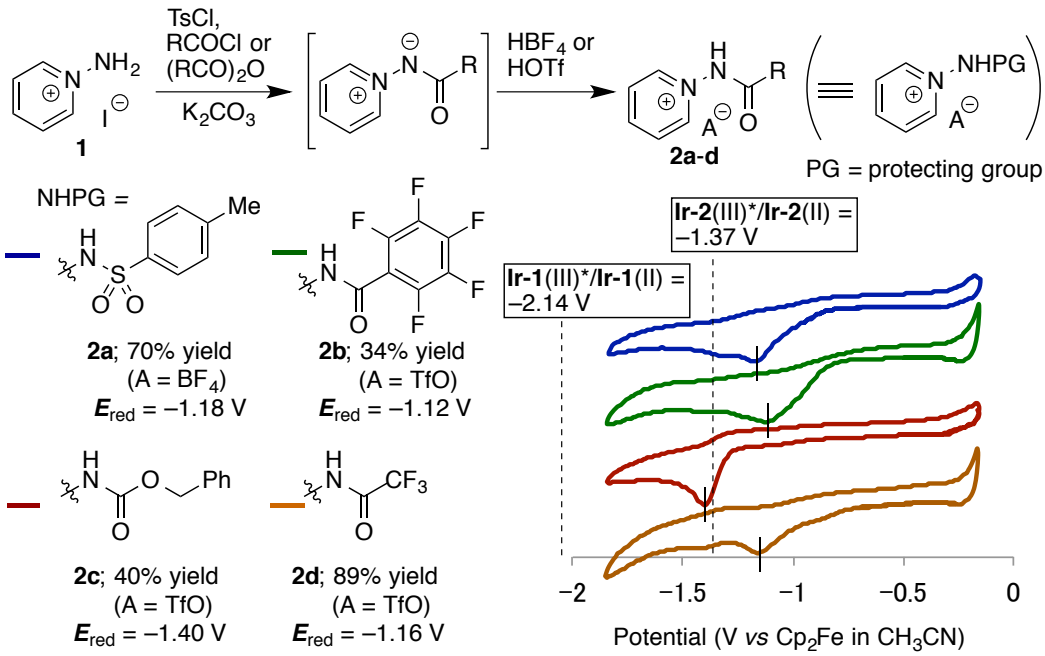

CV conditions: observed as 2 mM acetonitrile solutions; $[NBu_4](PF_6)$ = 0.1 M; Ag/AgCl =electrode; reported with respect to the $[FeCp_2]/[FeCp_2]^+$ couple.

Scheme 3.5 Synthetic scheme for electrophilic amine reagents (**2a-2d**) and their reduction potentials.

Reduction potentials of the aminating reagents (**2a-d**) were first investigated by CV measurements. Irreversible reduction waves were observed at –1.18 V (**2a**), –1.12 V (**2b**), –1.40 V (**2c**), and –1.16 V (**2d**) (vs. $FeCp_2$), respectively. When compered with

the oxidation potentials of the photoexcited catalysts ($E_{1/2}$ (***Ir-1**) = –2.14 V, $E_{1/2}$ (***Ir-2**) = –1.37 V),[15] the pyridinium salts **2a-d** may be readily reduced by these photocatalysts.[16] Almost at the same time, the group of Studer reported similar *N*-radical precursors synthesized from the pyrylium salt and hydrazine derivatives. Secondary-amidyl or imidyl radicals were successfully generate upon photochemical 1e-reduction of them to undergo amidation and imidation of arenes (Scheme 3.6).[9l]

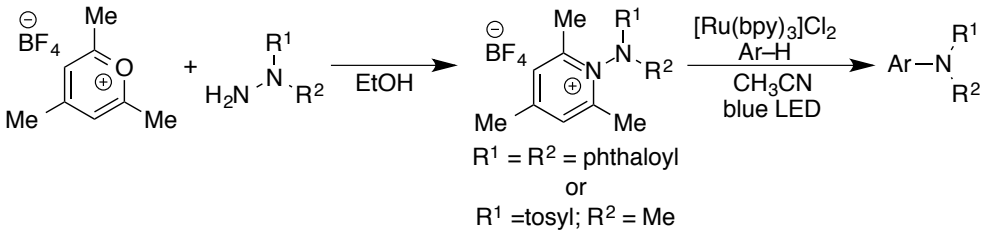

Scheme 3.6 Amidation or imidation of arenes and heteroarenes.

3.2.1.2 Photocatalytic aminohydroxylation of styrene with aminopyridinium salts

With these reagents in hand, the author commenced examination of photocatalytic aminohydroxylation of styrene (**3a**) in the presence of 2 mol% of *fac*-[Ir(ppy)$_3$] (**Ir-1**) in a mixed solvent system consisting of acetone-d_6 and D_2O under visible light irradiation with 425 nm blue LEDs. The reaction conditions are similar to those of trifluoromethylative difunctionalization. Through elaborated exploration of the amine sources (entries 1–7 in Table 4.1), he found the *N*-Ts protected 1-aminopyridinium salt (**2a**) produced 2-(*N*-Ts-amino)-1-phenylethanol (**4aa**) as a single product in an excellent yield and efficiency (98%, 2 h, Figure 3.1, entry 2 in Table 3.1). The reactants **2a** and **3a** were almost converted within 2 hours. The product **2aa** identified by comparison with the reported data[22a] turned out to be the vicinal aminoalcohol, where the *N*-group and the OH group were introduced to the β and α positions of styrene **2a**, respectively, in a regiospecific manner.

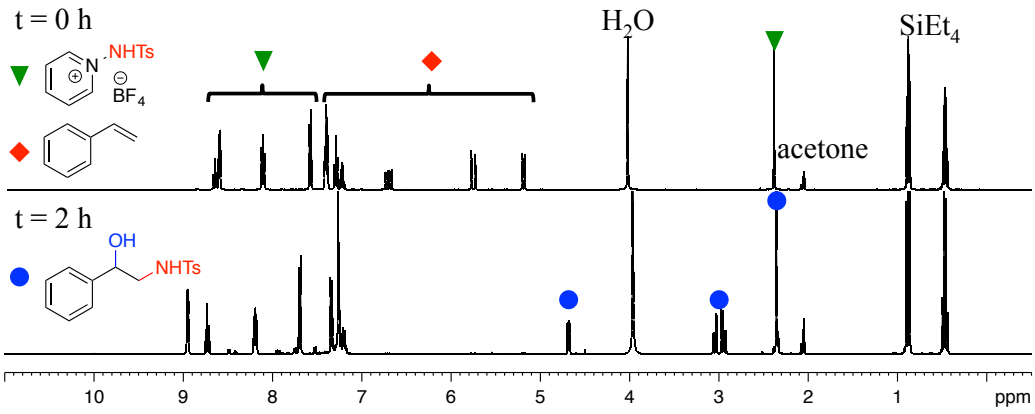

Figure 3.1 ^{1}H NMR Spectra of a reaction mixture of **2a** with **3a** before and after irradiation for 2 hours in acetone-d_6/D_2O (9/1) at 400 MHz at rt).

Unprotected 1-amino-pyridinium salt (**1**) did not react at all (entry 1, Table 3.1). The pyridinium salt **2b** was less effective but afforded **4ba** in 87% yield. In addition,the pyridinium salts **2c** and **2d** were much less effective to afford the **4ca** and **4da** in low yields (entries 3–5, Table 3.1). It should be noted that classical electrophilic nitrogen sources such as chloramine-T (**2e**) and alkoxyamine derivative (**2f**) turned out to be sluggish under the present photocatalytic conditions (entries 6 and 7, Table 3.1).

For other photoredox catalysts, $[Ir(ppy)_2(dtbbpy)](PF_6)$ (**Ir-2**) showed high activity similar to that of *fac*-$[Ir(ppy)_3]$ (**Ir-1**), whereas $[Ru(bpy)_3](PF_6)_2$ (**Ru-1**) ($E_{1/2}$ (***Ru-1**) = –1.24 V) turned out to be sluggish (entries 8 and 9, Table 3.1). The trend of the reactivity of photocatalyst is similar to that for the reactions described in chapter 2. Although the author can not clarify the reason of different reactivity in terms of redox potentials and life time of photocatalysts, electron transfer efficiency may affect the reaction.

Finally, the present reaction did not proceed at all either in the dark or in the absence of a photocatalyst (entries 10 and 11, Table 3.1). These results indicate that the Ir photocatalyst and visible light are essential for the efficient photocatalytic

amionhydroxylation.

Table 3.1 Optimization of the photocatalytic aminohydroxylation.[a]

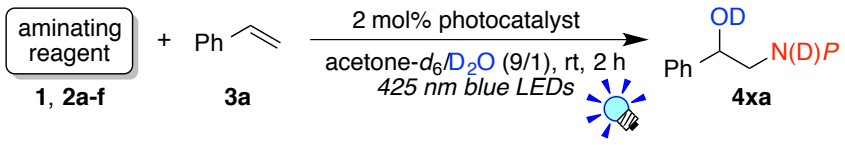

entry	aminating reagent **1** or **2x**	photocatalyst	yield of **9xa**[b]/%
1	**1**	*fac*-[Ir(ppy)$_3$] (**Ir-1**)	0
2	**2a**	**Ir-1**	98
3[c]	**2b**	**Ir-1**	87
4[c]	**2c**	**Ir-1**	44
5[c]	**2d**	**Ir-1**	7
6[c]	TsNNaCl•3H$_2$O (**2e**)	**Ir-1**	0
7[c]	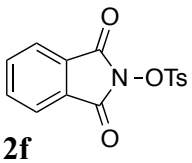 **2f**	**Ir-1**	23
8	**2a**	[Ru(bpy)$_3$](PF$_6$)$_2$ (**Ru-1**)	35
9	**2a**	[Ir(ppy)$_2$(dtbbpy)](PF$_6$) (**Ir-2**)	97
10	**2a**	–	0
11[d]	**2a**	**Ir-1**	0

[a] Reaction conditions: A reaction mixture of aminating reagent (0.05 mmol), **3a** (0.05 mmol), photocatalyst (1.0 μmol) and solvent (0.5 mL) was irradiated by 3W blue LEDs (λ = 425 ± 15 nm) for 4 h at room temperature. [b] Yields were determined by ^{1}H NMR spectroscopy using SiEt$_4$. [c] Reaction time = 24 h. [d] The reaction was conducted in the dark.

3.2.1.3 Scope and limitation of amionohydroxylation with 2a

Table 3.2. Scope of the photocatalytic aminohydroxylation[a,b]

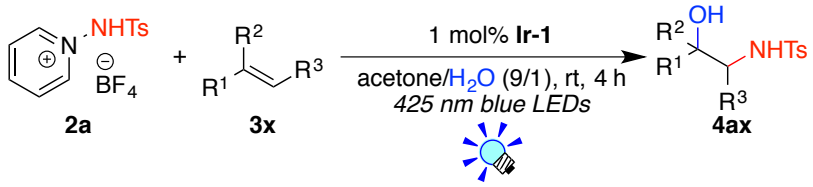

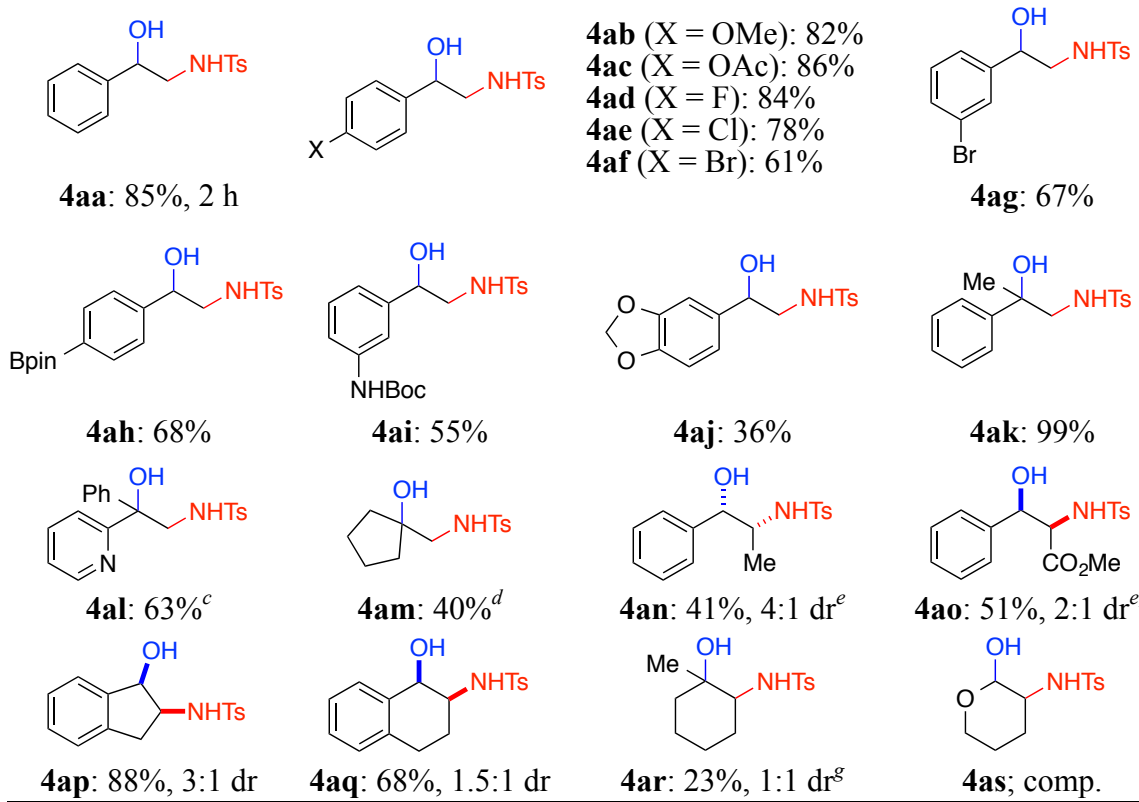

[a] Reaction conditions: A reaction mixture of **2a** (0.48 mmol), **3x** (0.40 mmol), photocatalyst (4.0 μmol) and solvent (4.0 mL) was irradiated by 3W blue LEDs (λ = 425 ± 15 nm) for 4 h at room temperature. Diastereomer ratios (dr) were determined by ^{1}H NMR spectra of crude reaction mixtures. [b] Yields of isolated products. [c] Reaction time = 10 h. [d] 1.5 equiv of **2a** with respect to olefin was used. [e] [Ir(ppy)$_2$(dtbbpy)](PF$_6$) (**Ir-2**) (2 mol%) was used and the reaction time was 12 h. [f] 1.8 equiv. of **2a** with respect of olefin was used. [g] reaction time = 8 h.

The scope of the present photocatalytic aminohydroxylation is summarized in Table 3.2. Styrene **3a** and its derivatives bearing OMe (**3b**), OAc (**3c**; Ac = acetyl), F (**3d**), Cl (**3e**), Br (**3f**,**g**), Bpin (**3h**; boronic acid pinacol ester), NHBoc (**3i**; Boc = *tert*-butoxycarbonyl), and methylenedioxy groups (**3i**) on the benzene ring produced the

corresponding amionoalcohols (**4aa**–**aj**) in 36–86% yields in a regiospecific manner.

Furthermore, α-substituted styrenes such as α-methylstyrene (**3k**) and α-pyridylstyrene (**3l**) were converted to the aminoalcohols bearing tertiary alcohol moieties in good yields (**4ak**: 99%, **4al**: 63%) exclusively. In addition, an aliphatic alkene, methylenecyclopentane (**3m**), could be also applied to the present photocatalytic system.

The reactions of internal alkenes such as *E*-β-methylstyrene (**3n**), methyl cinnamate (**3o**), indene (**3p**), 1,2-dihydronaphtharene (**3q**), and 1-methylcyclohexene (**3r**), also proceeded in a regiospecific manner but the products were obtained as mixtures of two diastereomers, (**4an**: 41%, 4:1 dr, **4ao**: 51%, 2:1 dr, **4ap**: 88%, 3:1 dr, **4aq**: 68%, 1.5:1 dr, **4ar**: 23%, 1:1 dr). The reaction of 3,4-dihydro-*2H*-pyran (**3s**) afforded to complicated mixture of products. It is noteworthy that a variety of functional groups such as halogens (**3d**–**g**), ester (**3c**,**o**), boronic acid pinacol ester (**3h**), *N*-protected amine (**3i**), pyridine (**3l**), and acetal (**3j**) groups were tolerable with the present reaction. Thus, the present aminohydroxylation turns out to be a regiospecific reaction for both terminal and internal alkenes regardless of the acyclic and cyclic structures.

3.2.1.4 Gram-scale aminohydroxylation

As a demonstration of scalability, aminohydroxylation of 4-methoxystyrene (**3b**) with **2a** was carried out on a gram scale. As a result, the product **4ab** was isolated in a 76% yield (1.22 g) (Scheme 3.5).

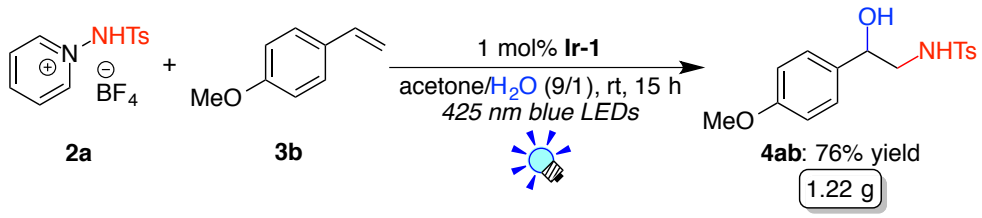

Scheme 3.5. A gram-scale reaction

3.2.2 Aminohydroxylation of olefins with *N*-protected iminopyridinium ylide by dual photoredox and Lewis acid catalysis

While *N*-Ts-protected aminopyridinium salt **2a** was an effective radical precusor to afford the corresponding vicinal aminoalcohol **4ax**, the Ts group is not always easily removed from the products (Scheme 3.7). On the other hand, 1-aminopyridinium precursors with readily removable protective groups such as trifluoroacetyl group could be also prepared, but the photocatalytic aminohydroxylation turned out to be sluggish (Table 3.1, entry 5).

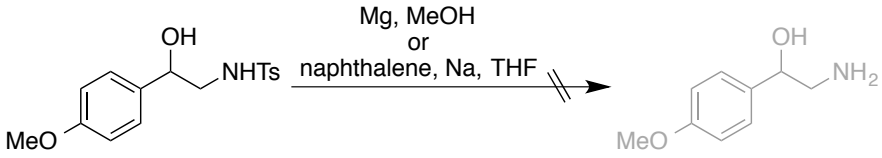

Scheme 3.7 Approach for deprotection of Ts group.

Aminopyridinium salt **2** is regarded as a protonated form of iminopyridinium ylide **5**. The author envisaged that ylide **5** may be able to be activated by the action of a Lewis acid instead of Brønsted acid, H^+. (Scheme 3.8).

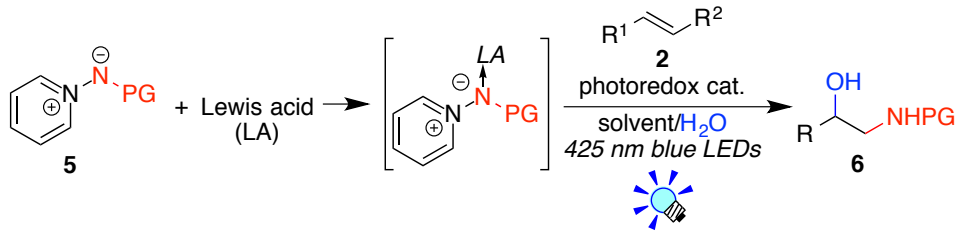

3.8 Photocatalytic and Lewis acid catalytic aminohydroxylation olefins

3.2.2.1 Synthesis of *N*-protected aminopyridinium ylides

When the final protonation process of the synthesis of the aminopyridinium salts (Scheme 3.9) was omitted, the zwittweionic ylide **5** were obtained as shelf-stable chemicals (**5a**; *N*-(Trifluoroacetyl)iminopyridinium ylide, **5b**; *N*-(benzoyl)iminopyridinium ylide, **5c**; *N*-(*tert*-butoxycarbonyl)iminopyridinium ylide, **5d**; *N*-(2,2,2-trichloroethoxycarbonyl)iminopyridnium ylide, and **5e**; *N*-(allyloxycarbonyl)iminopyridinium ylide).

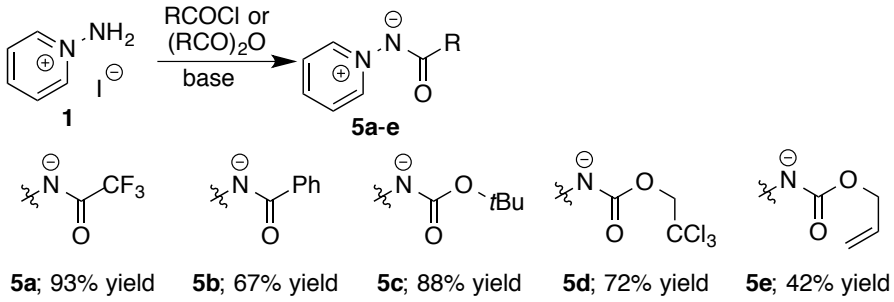

Scheme 3.9 Synthesis of iminopyridinium ylide.

3.2.2.2 Photocatalytic aminohydroxylation of styrene with iminopyridinium ylides

The author examined the reaction conditions for the photocatalytic aminohydroxylation of styrene (**3a**) with *N*-TFAc-protected iminopyridinium ylide (**5a**) (TFAc = trifluoroacetyl) in the presence of *fac*-[Ir(ppy)$_3$] (**Ir-1**) (2 mol%) (Table 3.3). When **5a** was used as it was, the reaction did not proceed at all (entry 1).

Table 3.3 Optimization of the photocatalytic aminohydroxylation.[a]

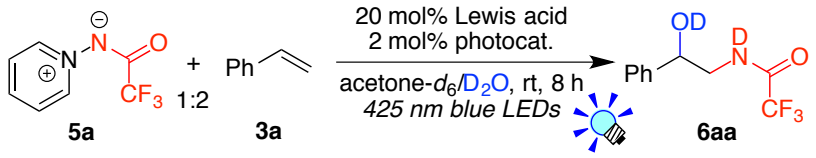

entry	photocatalyst	**5a**/**3a**	additive	yield of **6aa**[b]/%
1	*fac*-[Ir(ppy)$_3$] (**Ir-1**)	0.5	–	0
2	**Ir-1**	0.5	Sc(OTf)$_3$	74
3	**Ir-1**	0.5	Y(OTf)$_3$	72
4	**Ir-1**	0.5	La(OTf)$_3$	36
5	**Ir-1**	0.5	Zn(OTf)$_2$	49
6	[Ru(bpy)$_3$](PF$_6$)$_2$ (**Ru-1**)	0.5	Sc(OTf)$_3$	trace
7	[Ir(ppy)$_2$(dtbbpy)](PF$_6$) (**Ir-2**)	0.5	Sc(OTf)$_3$	8
8	**Ir-1**	1.0	Sc(OTf)$_3$	41
9	**Ir-1**	2.0	Sc(OTf)$_3$	63
10	–	0.5	Sc(OTf)$_3$	0
11[c]	**Ir-1**	0.5	Sc(OTf)$_3$	0

[a] Reaction conditions: A reaction mixture of **5a** (0.05 mmol), **3a** (0.10 mmol), photocatalyst (1.0 μmol), Lewis acid (0.01 mmol) and solvent (0.5 mL) was irradiated by 3W blue LEDs (λ = 425 ± 15 nm) for 8 h at room temperature. [b] Yields were determined by ^{1}H NMR spectroscopy using SiEt$_4$ as an internal standard. [c] The reaction was conducted in the dark.

To his delight, addition of a catalytic amount of Sc(OTf)$_3$ (20 mol%) to **5a** dramatically enhanced the yield of 2-aminoalcohol **6aa** to 74% as determined by ^{1}H NMR (entry 2). Investigation with other Lewis acid catalysts proved that Sc(OTf)$_3$ is the best option from the viewpoints of efficiency and yield (entries 3–5). Sc(OTf)$_3$ is the strongest Lewis acid among those of Lewis acid in presence of water because (i) Sc(OTf)$_3$ is hard and (ii) high exchange rata constants for substitution of water prevents hydrolysis and promote the reaction cycle.[16] For the photocatalyst, *fac*-[Ir(ppy)$_3$] (**Ir-1**) turned out to be the best (entries 6 and 7). Furthermore, addition of an extra amount of olefin **3a**

improved the yields (entries 8 and 9). To be noted is that the present reaction did not proceed at all either in the absence of the photocatalyst or in the dark (entries 10 and 11).

3.2.2.3 Scope and limitation of aminohydroxylation by dual catalysis

With the optimal reaction conditions in hand, the author investigated the scope of the present dual catalytic aminohydroxylation.

Table 3.4 Scope of the photocatalytic aminohydroxylation with **5a**.

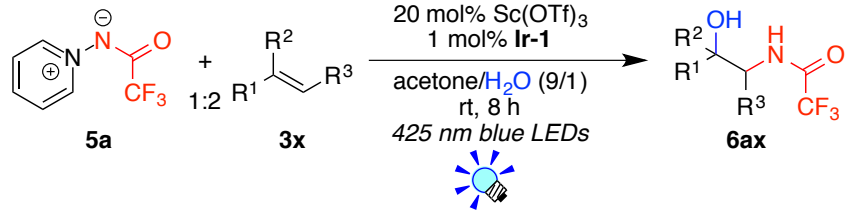

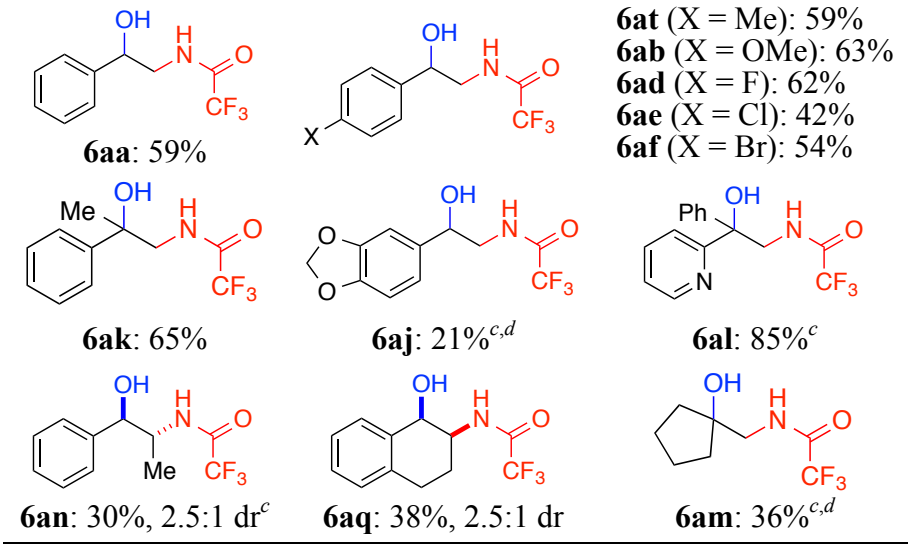

[a] Reaction conditions: A reaction mixture of **5a** (0.40 mmol), **3x** (0.80 mmol), **Ir-1** (4.0 μmol), $Sc(OTf)_3$, acetone (3.6 mL) and H_2O (0.4 mL) was irradiated by 3W blue LEDs (λ = 425 ± 15 nm) at room temperature for 8 h. Diastereomer ratios (dr) were determined by ^1H NMR spectra of crude reaction mixtures. [b] Yields of isolated products. [c] Reaction time = 24 h. [d] 2 mol% of *fac*-[$Ir(ppy)_3$] was used.

Styrenes bearing an electron-donating group (Me (**5s**) and OMe (**5b**)) and an

electron-withdrawing group (F (**5d**), Cl (**5e**), and Br (**5f**)) on the benzene ring, and α-methylstyrene (**5k**) afforded the corresponding products in 42–65% isolated yields. In addition, methylenedioxy (**3j**) and pyridyl (**3l**) groups were tolerated with the present reaction system (**6aj**: 21%, **6al**: 85%) but the former reaction was very slow. Furthermore, reactions of internal olefins such as β-methylstyrene (**3n**) and 1,2-dihydronaphthalene (**3q**) produced aminoalcohols in 30% (**6an**) and 38% yields (**6aq**), respectively. An aliphatic olefin, methylenecyclopentane (**3m**), could also be applied to the present aminohydroxylation (**6am**: 36% yield) but a considerable amount of *N*-(cyclopent-1-en-lymethyl)-2,2,2-trifluoroacetamide (**7am**) was formed as a by-product (Scheme 3.10).

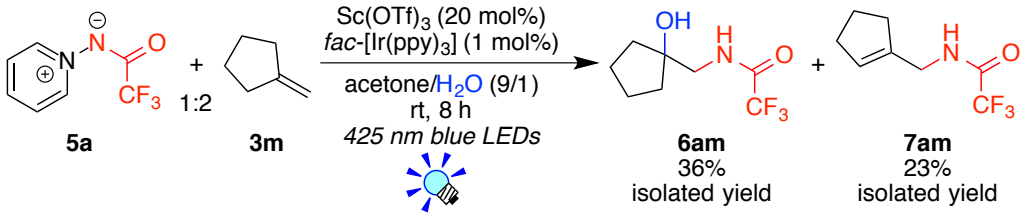

Scheme 3.10 Aminohydroxylation of methylenecyclopentane **3m** with **5a**.

The author supposed that the protective group on the nitrogen atom affects not only the efficiency of the radical generation but also the stability and reactivity of the *N*-centered radicals (Scheme 3.11).

As a result, common amide and carbamate groups can be incorporated into the iminopyridinium ylide scaffolds **5x** as shown in Scheme 3.11. The result of the *N*-Bz-protected reagent (**5b**) took a longer time (24 h) and afforded the corresponding product (**6ba**) in a moderate yield (45%). It was found that **5c**, **5d**, and **5e** served as *N*-centered radical sources in manner similar to **5a** (**6ca**: 58%, **6da**: 54% and **6ea**: 43%, 8 h). Thus, various types of *N*-protected aminoalcohols have become accessible.

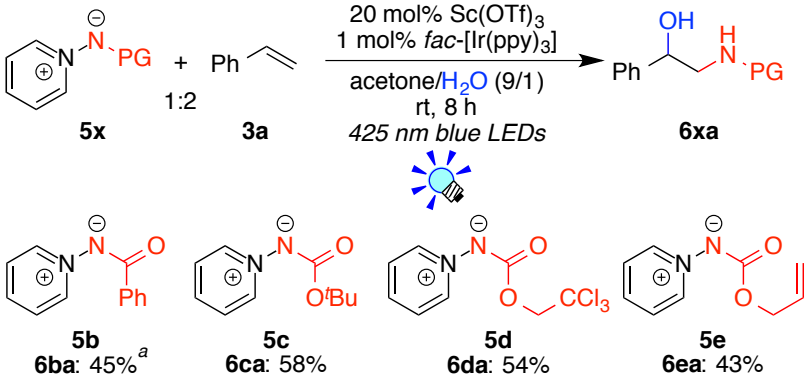

Scheme 3.11 The scope for the protective groups on the nitrogen atom in **5**

Reaction conditions: A reaction mixture of **5x** (0.40 mmol), **3a** (0.80 mmol), **Ir-1** (4.0 μmol) acetone (3.6 mL) and H_2O (0.4 mL) was irradiated by 3W blue LEDs (λ = 425 ± 15 nm) e for 8 h at room temperatur. Yields of isolated products. [a] Reaction time was 24 h.

3.2.2.4 Deprotection of the *N*-protected aminoalcohol products

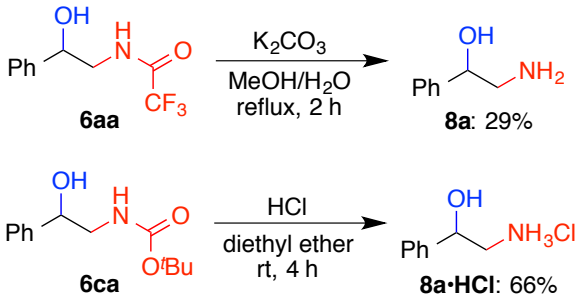

Scheme 3.12 Deprotection of the *N*-protected aminoalcohol products.

The obtained amide and carbamate derivatives **6** can be deprotected by further treatment to afford free primary amines **8** (Scheme 3.12).[17] For example, the TFAc derivative **6aa** was deprotected under basic conditions, *i.e.* by treatment with K_2CO_3, to afford 2-amino-1- phenylethanol **8a** in a 29% yield.[17c] On the other hand, the *N*-Boc-derivative **6ca** was deprotected under acidic conditions, *i.e.* by exposure to ethereal HCl solution, to furnish the salt **8a•HCl** in a 66% isolated yield.[17e] Thus free

β-hydroxylated primary amines **6** can be synthesized from olefins **3** by the present photoredox-catalyzed aminohydroxylation followed by deprotection under conditions appropriate for the functional groups in the molecule.

3.2.3 Experiments for analysis of reaction mechanism

3.2.3.1 Mechanistic study on aminohydroxylation with 2a

To gain insight into the reaction mechanism, the author examined the photocatalytic reaction of cyclopropane derivative (**3u**) which may undergo ring opening when the reaction involves a radical intermediate. It turned out that the ring-opened, linear product **9u** was obtained in a 72% isolated yield, suggesting the occurrence of the radical intermediate with the radical center located at the α-position of the cyclopropane ring (Scheme 3.12 (a)). In addition, the reaction of cyclohexene (**3v**) gave the cyclized product **10v** in a 37% yield. This product is reminiscent of HAS (homolytic aromatic substitution) reaction of the radical intermediate resulting from addition of the $TsNH^{\bullet}$ radical to cyclohexene (Scheme 3.12 (b)). These results strongly support that radical intermediates are involved in the present reactions. Furthermore, aminohydroxylation of *E*- and *Z*-β-methylstyrene (*E*-**2n** and *Z*-**2n**) afforded the products **3bn** with essentially the same diastereoselectivities (4:1; Table 3.2 and Scheme 3.12(c)), indicating that the same intermediate was formed irrespective of the starting *E*- and *Z*-alkenes.

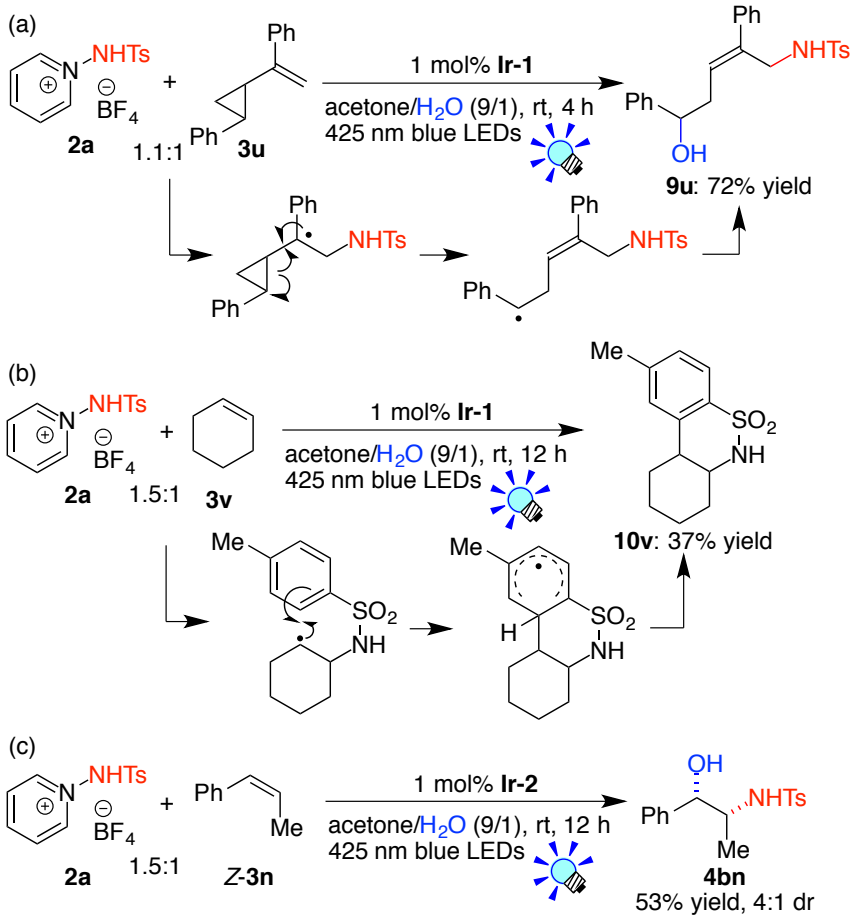

Scheme 3.13 Reference experiments. with **2a**.

The relation of the reduction potential (described in scheme 3.5) and reactivity of *N*-protected aminopyridinium salt **2** (results of Table 3.1) is shown in Figure 3.2. Pyridinium salts **2a** (E_{red} = –1.18 V) and **2b** (–1.12 V) afforded the products **4aa** and **4ba** in good yields but the reaction of **2b** took longer time (24 h). In addition, despite the low reduction potential of **2b**, the reaction was sluggish. On the other hand, pyridinium salt **2c** is more difficult to be reduced by ***Ir-1** than **2d** but the reaction of **2c** afforded the corresponding product in moderate yield. These results indicated that the ease of generation of amidyl radical is not always correlated to the reduction potential.

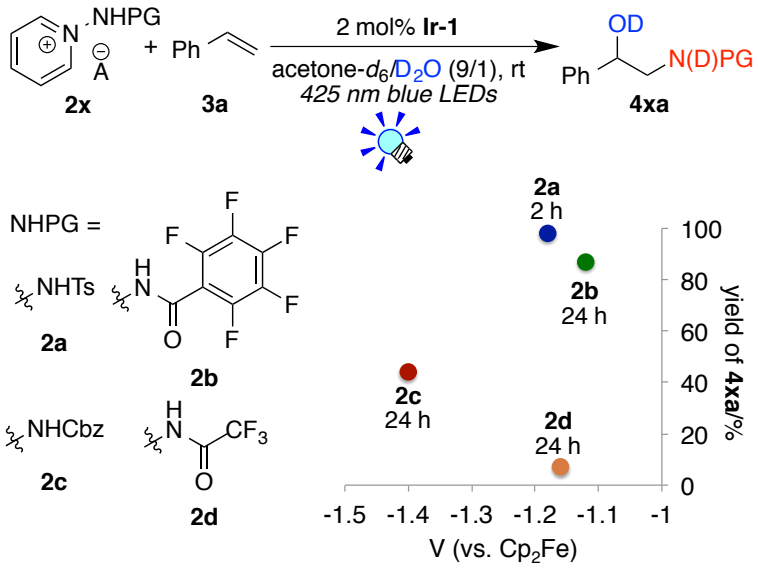

Figure 3.2 Reduction potentials of **2** and yield of **4**

The Stern-Volmer plots for quenching of the photoexited catalyst ***Ir-1** by the action of **2a** and **3a** (Figure 3.3) revealed that ***Ir-1** was not quenched by **3a** but by **2a**, indicating that electron transfer event occurs between the ***Ir-1** and **2a**.

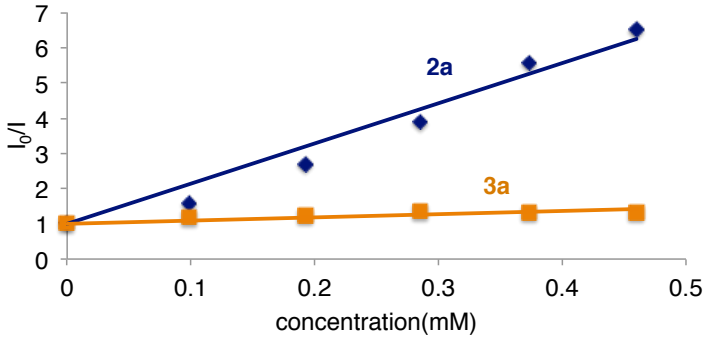

Intensities of the emission at 520 nm were recorded upon excitation of an acetone solution of **Ir-1** at 374 nm

Figure 3.3 Stern-Volmer studies for photocatalyst **Ir-1**

The author conducted the photocatalytic aminohydroxylation of styrene under periodic visible light irradiation (Scheme 3.13). It was observed that the reaction

proceeded only during the blue LED irradiation, suggesting that a radical chain mechanism was not involved as a main process.

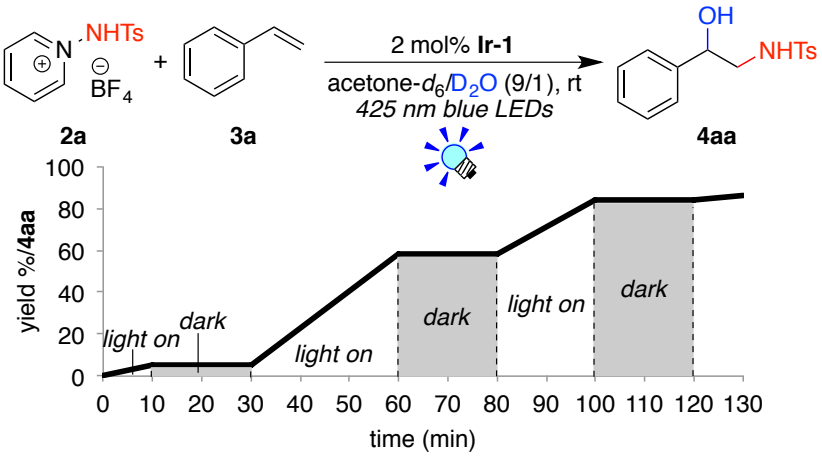

Scheme 3.14 Photocatalytic reaction of **2a** and **3a** under periodic visible light irradiation

On the basis of these observations, a plausible reaction mechanism is shown in Scheme 3.14. The mechanism is also based on that for trifluoromethylative difunctionalization of olefins. Firstly, the photocatalyst $\boldsymbol{Ir^{III}}$ is excited by visible light to give the excited species $\boldsymbol{*Ir^{III}}$, which undergoes SET to amionopyridinium **2** to afford stabilized radical **2** and highly oxidizable Ir species $\boldsymbol{Ir^{IV}}$. Radical **2** fragmentates into the amidyl radical and pyridine.[18] The generated amidyl radical reacts with alkene **3** in a regiospecific manner to yield the benzyl radical intermediate **11**, which is oxidized by the strongly oxidizing Ir species $\boldsymbol{Ir^{IV}}$ to afford β-aminocarbocationic intermediate **12** and to regenerate the ground state Ir photocatalyst $\boldsymbol{Ir^{III}}$. Finally, the carbocationic intermediate **12** is susceptible to nucleophilic attack of H_2O to produce 1,2-aminoalcohol **4**. The regiochemistry is determined at the stage of the radical addition to olefin, *i.e.* the β−attack giving the more stable benzyl radical intermediate is

more favorable the α attack.

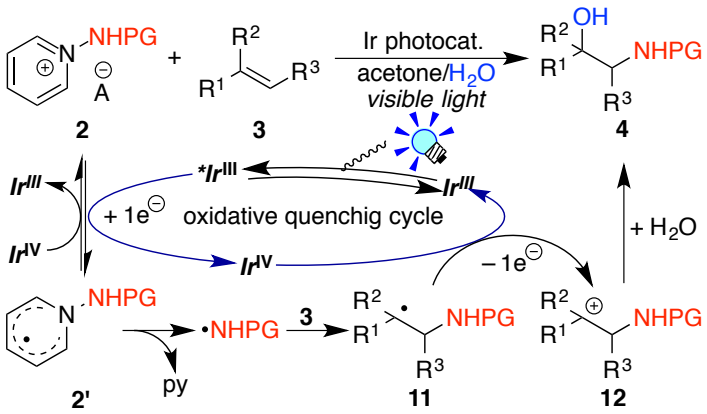

Scheme 3.15 A plausible reaction mechanism.

3.2.3.2 Mechanic study on aminohydroxylation by dual catalysis

The author also carried out mechanistic studies on the dual catalytic aminohydroxylation of olefins (Figure 3.4).

Photocatalytic reaction of cyclopropane derivative (**3u**) afforded the linear product **11u** indicating that radical intermediates are involved and that the radical center is located at the α–position of the cyclopropane ring, *i.e.* α–position of the benzene ring (Figure 3.4 (a)). Periodic visible light irradiation (Figure 3.4 (b)) gave the similar results as documented in Scheme 3.14. Furthermore, the Stern-Volmer plots for the photoexited photocatalyst ***Ir-1** by the action of **5a**, $Sc(OTf)_3$, **3a,** and a mixture of **10a** and $Sc(OTf)_3$ (Figure 3.4 (c)) revealed that not only **3a** but also $Sc(OTf)_3$ or the mixture served as effective quenchers.

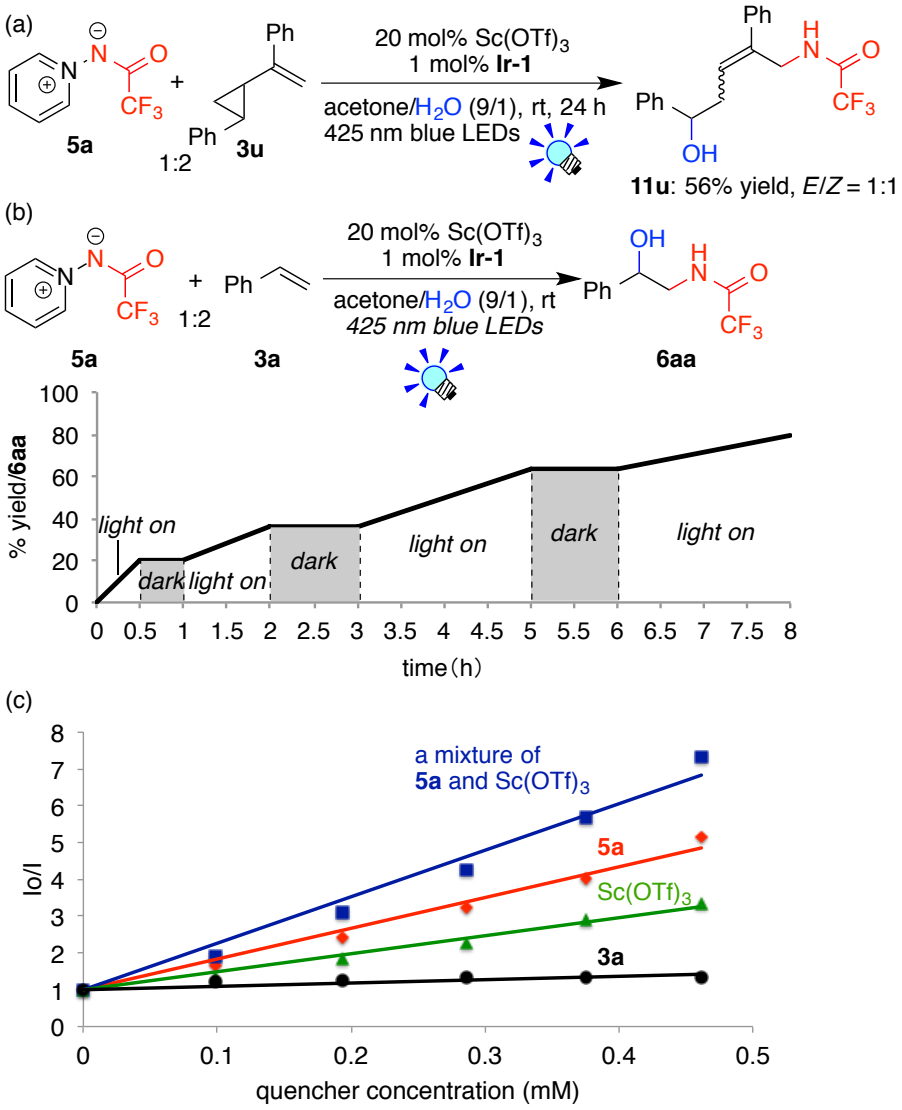

(c) Intensities of the emission at 520 nm were recorded upon excitation of an acetone solution of **Ir-1** at 374 nm.

Figure 3.4 Reference experiments with **5a**.

When $Sc(OTf)_3$ was added, the ^1H NMR signals for the pyridinium part **5a** were shifted to the lower field upon gradually addition of 0→20→50→100→200 mol% of $Sc(OTf)_3$ (δ_H 8.33 (*p*) → 8.42 → 8.53 → 8.59 → 8.61; 8.02 (*m*) → 8.09 → 8.17 → 8.20 → 8.21), indicating that there is some interaction **5a** with $Sc(OTf)_3$ (Figure 3.5).

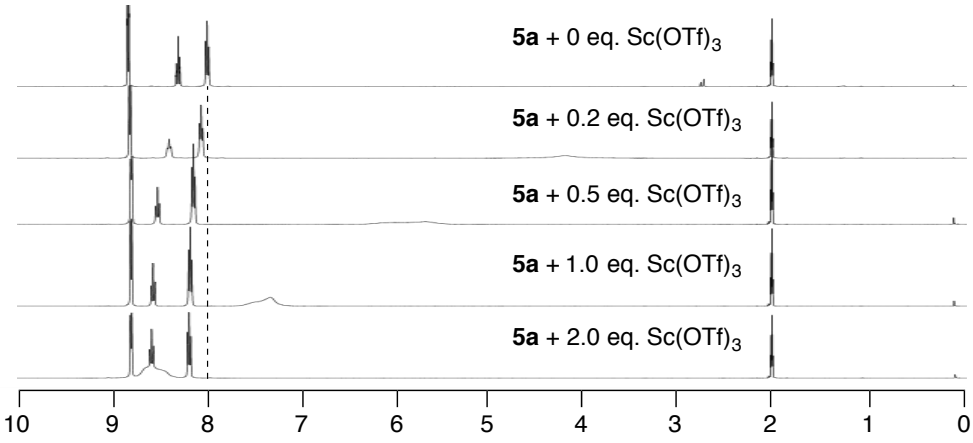

Figure 3.5 ^{1}H NMR shift of **5a** by gradually additional $Sc(OTf)_3$ in acetone-d_6 at 400 MHz at rt

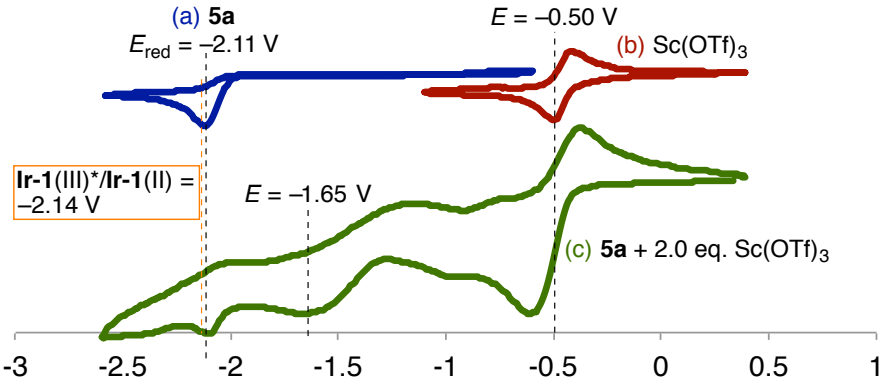

CV conditions: observed as 2 mM acetone solutions; $[NBu_4](PF_6)$ = 0.1 M; Ag/AgCl =electrode; reported with respect to the $[FeCp_2]/[FeCp_2]^+$ couple.

Figure 3.6 CV experiments.

The CV measurements of **5a**, $Sc(OTf)_3$ and a mixture of **5a** and $Sc(OTf)_3$ shown in Figure 3.6. The neutral ylide **5a** is difficult to be reduced by ***Ir-1** than the protonated aminopyridinium salt **2d** (E_{red} = –1.16 V) (Scheme 3.5). A reversible wave of $Sc(OTf)_3$ observed around –0.5 V suggests an electron transfer event occurs between ***Ir-1** and $Sc(OTf)_3$. Furthermore, CV measurement of a mixture of **5a** and $Sc(OTf)_3$ resulted that

the redox potential was confirmed around –2.1 V and –0.5 V which are considered to be derived from **5a** and $Sc(OTf)_3$ respectively. In addition, a new broadening wave was confirmed –1.65 V. The author guesses the reduction wave is derived from the product formed by the interaction of **5a** and $Sc(OTf)_3$, but the activated species can not be distinguished exactly. More detail analysis of the reaction mechanism is necessary.

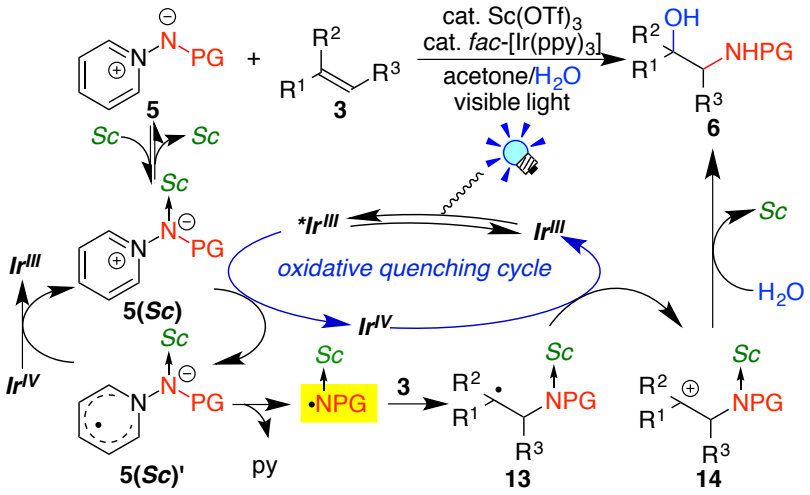

Scheme 3.16 Plausible reaction mechanism.

On the basis of the experimental results obtained and previous section, a plausible reaction mechanism is shown in Scheme 3.16. First, **5** is activated by $Sc(OTf)_3$ to form adduct **5(*Sc*)**. The photoexcited Ir species (***Ir*^{III}**) undergoes SET to **5(*Sc*)** to give the radical **5(*Sc*)'** and converts to the highly oxidized Ir species ***Ir*^{IV}**. Radical **5(*Sc*)'** fragmentates into *N*-centered radical and pyridine. The *N*-centered radical adds to olefin **3** to yield radical intermediate **13**, which is oxidized by the ***Ir*^{IV}** species to afford carbocationic intermediate **14** and regenerate the ground state ***Ir*^{III}** species. Finally, nucleophilic attack of water to carbocationic intermediate **14** furnishes aminohydroxylated product **6** and regenerates the scandium catalyst.

3.3 Conclusion

The author has developed a novel and simple strategy for regiospecific synthesis of 1,2-amionoalcohol derivatives by photoredox catalysis. Well-designed *N*-protected 1-amino-pyridinium salts serve both as an electron acceptor and as an efficient amidyl radical precursor by the action of the photoredox catalysis. Moreover, the author has developed a new strategy for introduction of a variety of protected amino functional groups to alkene by the dual Ir photoredox/$Sc(OTf)_3$ catalysis. Iminopyridinium ylide can serve as an efficient *N*-centered radical precursor when combined with the $Sc(OTf)_3$ and *fac*-[$Ir(ppy)_3$] catalysis under visible light irradiation. The present photocatalytic systems enable regiospecific intermolecular three-component aminohydroxylation of olefins bearing a wide variety of functionalities through radical processes.

3.4 Experimental

General

Materials and Methods

fac-[$Ir(ppy)_3$] (**Ir-1**),[19a] [$Ru(bpy)_3$](PF_6)$_2$ (**Ru-1**)[19b] and [$Ir(ppy)_2$(dtbbpy)](PF_6) (**Ir-2**)[15c] were prepared according to the reported procedures. 1-Aminopyridinium iodide (**1**) was purchased from TCI. Olefins **3a, 3b, 3d, 3e, 3f, 3g, 3k, *E*-3n, 3o, 3p, 3q, 3s** and **3t** were purchased from TCI. Olefins **3c, 3m, 3r** and **3v** were purchased from Aldrich. Olefin ***Z*-3n** was purchased from Wako. They were used without further purification. Substrates **3h**,[20a] **3i**[20b] and **3j**[20c] were prepared according to the reported literatures. ^{1}H NMR spectra were acquired on a Bruker AVANCE-400 (400 MHz) and a Bruker AVANCE-HD500 (500 MHz). Recycled GPC was performed with a JAI LC-9201R/U. Other conditions were the same as those described in previous chapters.

Procedure for the synthesis of *N*-protected aminopyridinium salts

1-(p-Toluenesulfonylamino)-pyridinium tetrafluoroborate (2a)

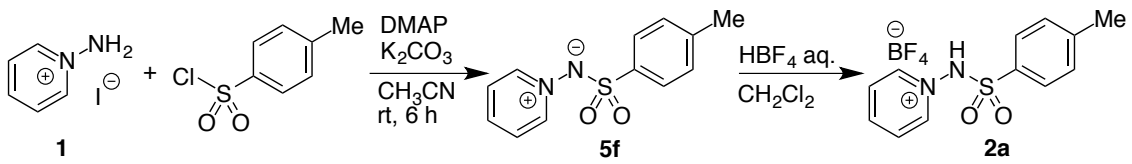

To a mixture of 1-aminopyridinium iodide (**1**) (1.67 g, 7.51 mmol) and distilled-CH_3CN (60 mL) was added 4-dimethylaminopyridine (DMAP) (91.8 mg, 0.748 mmol), potassium carbonate (3.75 g, 27.1 mmol) and *p*-toluenesulfonyl chloride (1.42 g, 7.47 mmol) at 0 ˚C under N_2. Then, the cooling bath was removed and the reaction mixture was stirred for 6 h at rt. The suspension was filtered and the filtrate was concentrated *in vacuo*. The residue was extracted with CH_2Cl_2 and filtered. After the

solvent was removed under reduced pressure, the crude product was purified by flash column chromatography on Fuji Silysia silica gel FL100D (CH_2Cl_2:MeOH = 10:1) and washed with a small amount of CH_2Cl_2 to afford ylide **5f** as a pale orange solid (1.34 g, 5.39 mmol, 72% yield). Spectral data was in agreement with the reported literature.[21a]
^{1}H NMR (400 MHz, $CDCl_3$, rt) δ 8.46 (d, ^3J = 5.2 Hz, 2H; $C_5H_3H_2N$), 7.97 (t, ^3J = 8.0 Hz, 1H; $C_5H_4H_1N$), 7.60 (m, 4H; $C_5H_3H_2N$, $SO_2C_6H_2H_2CH_3$), 7.17 (d, ^3J = 8.0 Hz, 2H; $SO_2C_6H_2H_2CH_3$), 2.35 (s, 3H; $SO_2C_6H_4CH_3$).

To a CH_2Cl_2 solution of **5f** (1.34 g, 5.39 mmol) was added to tetrafluoroboric acid solution (42wt.% in H_2O) (1.27 g, 6.97 mmol) at rt. The mixture was stirred for 30 min to precipitate the product, which was collected by filtration, washed with diethyl ether and pentane, and dried *in vacuo*. The title product **2a** was obtained as a white solid (1.77 g, 5.26 mmol, 96% yield).
^{1}H NMR (400 MHz, CD_3CN, rt) δ 10.36 (brs, 1H; N*H*), 8.64 (t, ^3J = 7.6 Hz, 1H; $C_5H_4H_1N$), 8.37 (d, ^3J = 7.2 Hz, 2H; $C_5H_3H_2N$), 8.03 (t, ^3J = 7.6 Hz, 2H; $C_5H_3H_2N$), 7.59 (d, ^3J = 8.4 Hz, 2H; $SO_2C_6H_2H_2CH_3$), 7.46 (d, ^3J = 8.4 Hz, 2H; $SO_2C_6H_2H_2CH_3$), 2.48 (s, 3H; $SO_2C_6H_4CH_3$). **^{13}C NMR** (125 MHz, CD_3CN, rt) δ 149.4, 149.0, 146.4, 131.9, 130.7, 130.4, 129.7. 21.9. **Elemental analysis.** Calcd. For $C_{12}H_{13}BF_4N_2O_2S$: C, 42.88; H, 3.90; N, 8.33. Found: C, 42.59; H, 3.67; N, 8.27.

1-(2,3,4,5,6-Pentafluorobenzoylamino)-pyridinium trifluoromethansulfonate (2b)

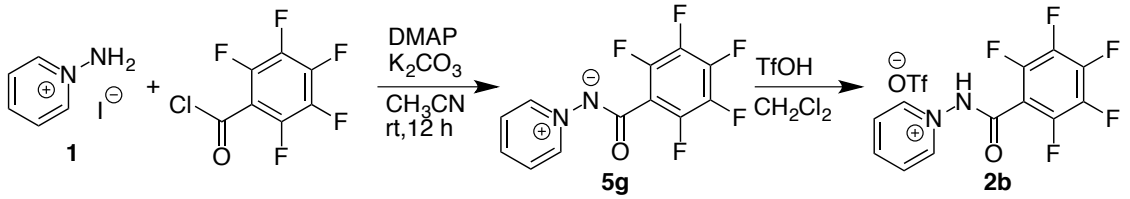

To a mixture of **1** (1.12 g, 5.04 mmol) and distilled CH_3CN (40 mL) was added potassium carbonate (2.09 g, 15.1 mmol) and pentafluorobenzoyl chloride (1.17 g, 5.08 mmol) in an ice bath under N_2. Then, the cooling bath was removed and the reaction mixture was stirred for 12 h at rt. The suspension was concentrated *in vacuo* and the residue was extracted with CH_2Cl_2 and filtered. After the volatiles were removed under reduced pressure, the crude product was purified by flash column chromatography on Fuji Silysia silica gel FL100D (CH_2Cl_2:MeOH = 20:1) to afford ylide **5g** as a yellow solid (0.558 g, 1.94 mmol, 38% yield).
^{1}H NMR (400 MHZ, $CDCl_3$, rt) δ 8.86 (dd, ^3J = 6.8 Hz, ^4J = 1.2 Hz, 2H; $C_5H_3H_2N$), 8.03 (t, ^3J = 8.0 Hz, 1H; $C_5H_4H_1N$), 7.76 (dd, ^3J = 7.2 Hz, ^3J = 7.2 Hz, 2H; $C_5H_3H_2N$). **^{13}C NMR** (125 MHz, $CDCl_3$, rt) δ 163.0, 145.2-143.3 (m), 143.1, 142.1-140.1 (m), 138.6, 138.6-136.6 (m), 126.6, 114.9. **^{19}F NMR** (376 MHz, $CDCl_3$, rt) δ -143.3 (m, 2F), -156.9 (t, ^3J = 20.7 Hz, 1F), -163.5 (m, 2F). **HRMS** (ESI-TOF) calculated for $[C_{12}H_5F_5N_2O+Na]^+$ requires 311.0214, found 311.0214.

To a CH_2Cl_2 solution of **5g** (0.558 g, 1.94 mmol) was added trifluoromethanesulfonic acid (0.417 g, 1.99 mmol) in an ice bath. Then, the cooling bath was removed and the reaction mixture was stirred for 1 h at rt. The volatile compounds were removed under reduced pressure and the residue was washed with diethyl ether and pentane and dried *in vacuo*. The title product **2b** was obtained as a white solid (0.766 g, 1.75 mmol, 34% total yield).
^{1}H NMR (400 MHz, $CDCl_3$, rt) δ 13.7 (brs, 1H; N*H*), 8.94 (m, 2H; $C_5H_2H_2HN$), 8.64 (m, 1H; $C_5H_2H_2HN$), 8.20 (m, 1H; $C_5H_2H_2HN$). **^{13}C NMR** (125 MHz, CD_3CN, rt) δ 157.4, 149.5, 147.5, 147.2-145.2 (m), 146.0-143.9 (m), 140.2-138.1 (m), 130.3, 121.7 (q, ^1J = 317.9 Hz), 108.1(m). **^{19}F NMR** (376 MHz, $CDCl_3$, rt) δ –78.6 (s, 3F; CF_3SO_3), –138.0 (m, 2F; $C_6F_2F_1F_2$), –145.8 (m, 1F; $C_6F_2F_1F_2$), –159.3 (m, 2F; $C_6F_2F_1F_2$). **HRMS** (ESI-TOF) calculated for $[C_{12}H_6F_5N_2O]^+$ requires 289.0395, found 289.0397.

1-(Benzyloxycarbonylamino)-pyridinium trifluoromethansulfonate (2c)

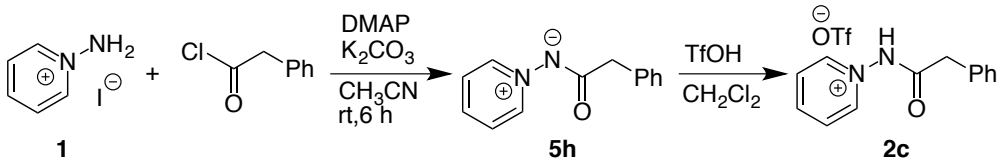

To a mixture of **1** (0.559 g, 2.52 mmol) and distilled CH_3CN (20 mL) was added DMAP (32.9 mg, 0.268 mmol), potassium carbonate (1.12 g, 8.10 mmol) and benzyl chloroformate (0.435 g, 2.55 mmol) in an ice bath under N_2. Then, the cooling bath was removed and the reaction mixture was stirred for 6 h at rt. The suspension was concentrated *in vacuo*. The residue was extracted with CH_2Cl_2 and filtered. The filtrate was concentrated under reduced pressure and the crude product was through flash column chromatography on Fuji Silysia silica gel FL100D (CH_2Cl_2:MeOH = 10:1). To a CH_2Cl_2 solution of the product was added trifluoromethanesulfonic acid (126 μL) and the mixture was stirred for 1 h. Furthermore, to the reaction mixture was added diethyl ether to precipitate the title compound. The suspension was filtered, washed with diethyl ether and pentane and dried *in vacuo*. The title product (**2c**) was obtained as a brown solid (0.378 g, 1.00 mmol, 40% yield).
^{1}H NMR (400 MHz, CD_3CN, rt) δ 10.6 (brs, 1H; N*H*), 8.79 (m, 2H; $C_5H_2HH_2N$), 8.65 (m, 1H; $C_5H_2HH_2N$), 8.14 (m, 2H; $C_5H_2HH_2N$), 7.43 (m, 5H; C_6H_5), 5.29 (s, 2H; $CO_2CH_2C_6H_5$). **^{13}C NMR** (125 MHz, CD_3CN, rt) δ 155.0, 148.7, 147.6, 136.0, 129.9, 129.7, 129.7, 129.4, 121.9 (q, ^1J = 318.2 Hz), 70.1. **HRMS** (ESI-TOF) calculated for $[C_{13}H_{13}N_2O_2]^+$ requires 229.0972, found 229.0979.

1-(Trifluoroacetyl)-pyridinium trifluoromethanesulfonate (2d)

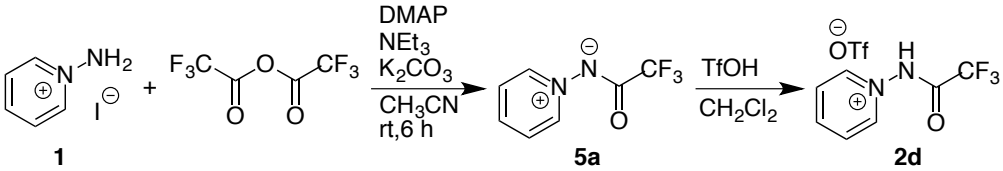

To a mixture of **1** (0.555 g, 2.50 mmol) and distilled CH_3CN (20 mL) was added triethylamine (0.510 g, 5.04 mmol), 4-dimethylaminopyridine (29.9 mg, 0.243 mmol) and trifluoroacetic anhydride (0.580 g, 2.76 mmol) in an ice bathe under N_2. Then, the cooling bath was removed and the reaction mixture was stirred at rt for 6 h. Moreover, potassium carbonate (1.03 g, 7.26 mmol) was added and the reaction mixture was stirred for additional 2 h at rt. The suspension was concentrated *in vacuo*. The residue was extracted with CH_2Cl_2 and filtered. After volatile compounds were removed under reduced pressure, the crude product was purified by flash column chromatography on Fuji Silysia silica gel FL100D (CH_2Cl_2:MeOH = 20:1) to afford **5a** as a white solid (0.441 g, 2.32 mmol, 93% yield).
^{1}H NMR (400 MHz, $CDCl_3$, rt) δ 8.77 (dd, ^3J = 7.2 Hz, ^4J = 1.2 Hz, 2H; $C_6H_2HH_2N$), 8.06 (m, 1H; $C_6H_2H_2HN$), 7.77 (dd, ^3J = 7.2 Hz, ^3J = 7.2 Hz, 2H; $C_6H_2H_2HN$). **^{13}C NMR** (125 MHz, $CDCl_3$, rt) δ 162.4 (q, ^2J = 33.4 Hz), 142.9, 139.2, 126.8, 118.4 (q, ^1J = 285.3 Hz) **^{19}F NMR** (376 MHz, $CDCl_3$, rt) δ –75.5. **HRMS** (ESI-TOF) calculated for $[C_7H_5F_3N_2O+Na]^+$ requires 213.0246, found 213.0246.

To a CH_2Cl_2 (10 mL) solution of **5a** (0.440 g, 2.32 mmol), cooled in an ice bath, was added trifluoromethanesulfonic acid (212 μL, 2.40 mmol). Then the cooling bath was removed and the reaction mixture was stirred for 1 h at rt. The mixture was concentrated under reduced pressure and the residue was washed with diethyl ether and pentane and dried *in vacuo*. The title product (**2d**) was obtained as a white solid (0.753 g, 2.21 mmol, 89% total yield).
^{1}H NMR (400 MHz, CD_3CN, rt) δ 12.3 (brs, 1H; N*H*), 8.87 (m, 2H; $C_6H_2HH_2N$), 8.73 (m, 1H; $C_6H_2HH_2N$), 8.23 (m, 2H; $C_6H_2HH_2N$). **^{13}C NMR** (125 MHz, CD_3CN, rt) δ 156.5 (q, ^2J = 40.9 Hz), 150.1, 147.2, 130.5, 121.7 (q, ^1J = 317.8 Hz), 116.1 (q, ^1J = 284.9 Hz). **^{19}F NMR** (376 MHz, $CDCl_3$, rt) δ –75.6, –79.9. **HRMS** (ESI-TOF) calculated for $[C_7H_6N_2O]^+$ requires 191.0427, found 191.0427.

Preparation of alkenes (3l and 3u)
Synthesis of 1-(2-pyridyl)-1-phenylethene (3l)

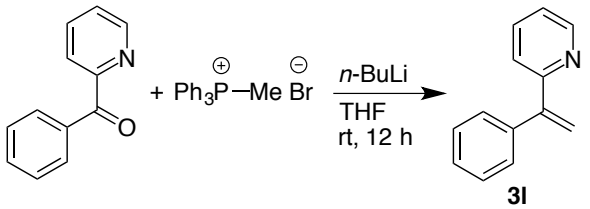

3l

To an anhydrous THF (30 mL) solution of methyltriphenyl phosphonium bromide (5.36 g, 15.0 mmol), *n*-butyl lithium in hexane (1.60 M) (9.3 mL, 14.9 mmol) was added dropwise at 0 ºC. After stirring for 30 min, an anhydrous THF solution (30 mL) of 2-benzoylpyridine (2.76 g, 15.0 mmol) was added dropwise for 30 min. The reaction mixture was stirred for 12 h at rt and then treated with saturated ammonium chloride solution. The product was extracted with EtOAc (20 mL x 3), and then the combined organic layer was washed with brine, dried over Na_2SO_4, filtered and concentrated *in vacuo*. The crude mixture was purified by flash column chromatography on silica gel (Hexane:EtOAc = 5:1) to afford the title product (2.18 g, 80 %). Spectral data was in agreement with that reported the literature.[21b]

^{1}H NMR (400 MHz, $CDCl_3$, rt) δ 8.63 (m, 1H; C_5HH_3N), 7.61 (m, 1H; C_5HHH_2N), 7.34 (m, 5H; C_6H_5), 7.24 (m, 1H; C_5H_2HHN), 7.19 (m, 1H; C_5H_3HN), 5.98 (d, ^2J = 1.2 Hz, 1H; C=C*H*H), 5.59 (d, ^2J = 1.6 Hz, 1H; C=CH*H*).

Synthesis of 1-phenyl-1-(*E*-2-phenylpropyl)ethene (3u)

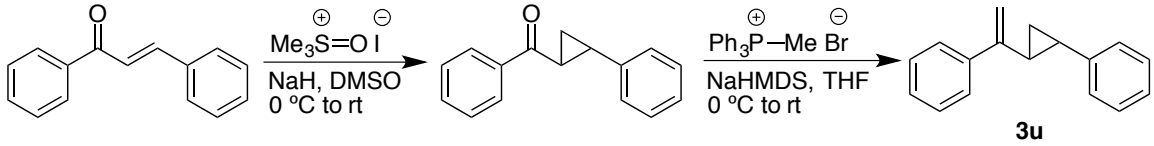

3u

Phenyl(2-phenylcyclopropyl)methanone

Sodium hydride (0.96 g, 24.0 mmol, 1.2 eq., 60% dispersion in paraffin liquid) placed in a two-necked round flask was washed with hexane (under N_2). Then, dry DMSO (35 mL) and trimethylsulfoxonium iodide (4.84 g, 22.0 mmol, 1.1 eq.) was added to the flask under N_2. The flask was immersed in an ice bath and a solution of chalcone (4.17 g, 20.0 mmol, 1.00 eq.) in dry DMSO (10 mL) was added to the reaction mixture. The reaction mixture was extracted with ether then concentrated. The crude product was purified by flash column chromatography (hexane : ether = 19 : 1) to afford the cyclopropane product (1.79 g, 40% yield). Spectral data is in agreement with that reported the lieterature.[21c]

^{1}H NMR (500 MHz, $CDCl_3$, rt) δ 8.00 (m, 2H; Ar), 7.57 (m, 1H; Ar), 7.47 (m, 2H; Ar), 7.32 (m, 2H; Ar), 7.24 (m, 1H; Ar), 7.19 (m, 2H; Ar), 2.91 (m, 1H; COC*H*), 2.71 (m, 1H; C_6H_5CH), 1.93 (m, 1H; C_6H_5CHCHH), 1.57 (m, 1H; C_6H_5CHCHH).

1-Phenyl-1-(trans-2-phenylcyclopropyl)ethene (3u)

To a mixture of dry-THF (35 mL) and sodium bis(trimethylsilyl)amide (10 mL, 1.00 M in THF) was added a THF (15 mL) solution of the cyclopropane (1.79 g, 80.3 mmol) at 0 ºC. After stirring for 15 min, the reaction mixture was warmed up to room temperature and stirred for an additional 6 h. The mixture was partially purified through silica-pad (Et_2O was used as an eluent). The eluate was concentrated *in vacuo* then purified by flash column chromatography (hexane) to afford **3u**. Spectral data is in agreement with the literature.[21d]

^{1}H NMR (400 MHz, $CDCl_3$, rt) δ 7.53 (dd, ^3J = 8.2 Hz, ^4J = 1.4 Hz, 2H; Ar), 7.33-7.25 (m, 5H; Ar), 7.22-7.16 (m, 2H; Ar), 5.38 (s, 1H; CC*H*H), 5.06 (s, 1H; CCH*H*), 2.05-1.95 (m, 2H; C_6H_5CHCHC), 1.45 (m, 1H; C_6H_5CHCHH), 1.31 (m, 1H; C_6H_5CHCHH).

Typical NMR experimental procedure

*Photocatalytic aminohydroxylation of styrene (**3a**)*

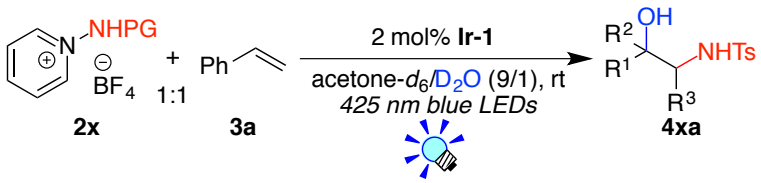

Under N_2, to **3a** (50.0 μmol) dissolved in a mixture of deuterated acetone (0.45 mL) and D_2O (0.05 mL) in an NMR tube, **2x** (50.0 μmol), **Ir-1** (1.00 μmol) and tetraethylsilane (an internal standard) were added. The mixture was degassed by three freeze-pump-thaw cycles. The reaction was carried out at room temperature (water bath) under irradiation of visible light (placed at a distance of 2-3 cm from the blue LED lamp: $h\nu = 425 \pm 15$ nm). Then the reaction was followed by ^{1}H NMR spectroscopy.

General procedure for the photocatalytic aminohydroxylation of olefins with 7a

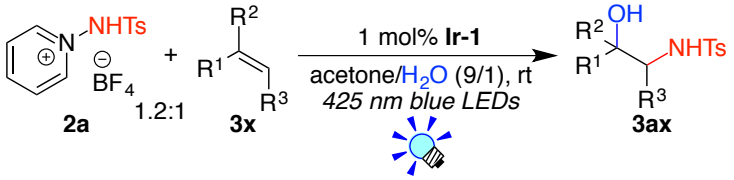

Under N_2, to alkene (**3x**) (0.40 mmol) dissolved in a mixture of acetone (3.6 mL) and H_2O (0.4 mL) in a 20 mL-Schlenk tube, **2a** (0.44 mmol) and **Ir-1** (4 μmol) were added. The mixture was degassed by three freeze-pump-thaw cycles. The tube was placed at a distance of 2-3 cm from blue LED lamp (hν = 425 ± 15 nm). The resulting mixture was stirred at room temperature (water bath) under visible light irradiation. Then, the reaction mixture was concentrated *in vacuo* to remove volatile compounds. Products were extracted with CH_2Cl_2, dried (Na_2SO_4) and filtered. The filtrate was concentrated under reduced pressure and purified by flash column chromatography on silica gel to give **4ax**.

***N*-(2-Hydroxy-2-phenylethyl)-4-methylbenzene sulfonamide (4aa)**

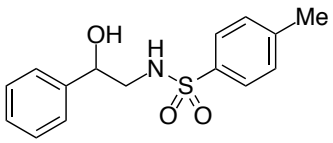

The reaction of styrene (**3a**) (42.4 mg, 0.407 mmol), **2a** (150.4 mg, 0.447 mmol) and **Ir-1** (2.7 mg, 4.13 μmol) following the general procedures afforded **4aa** (100.2 mg, 85% yield, reaction time = 2 h) as a white solid after purification with flash column chromatography on Fuji Silysia silica gel FL100D (hexane:EtOAc = 3 : 1). Spectral data is in agreement with the reported literature.[22a]

^{1}H NMR (400 MHz, $CDCl_3$, rt) δ 7.73 (d, ^3J = 8.0 Hz, 2H; $SO_2C_6H_2H_2CH_3$), 7.35-7.27 (m, 7H; Ar), 5.00 (m, 1H; N*H*), 4.79 (m, 1H; HOC*H*CH_2NH), 3.25 (m, 1H; HOCHC*H*HNH), 3.03 (m, 1H; HOCHCH*H*NH), 2.48 (s, 1H; O*H*), 2.42 (s, 3H; $SO_2C_6H_4CH_3$).

***N*-(2-Hydroxy-2-(4-methoxyphenyl)ethyl)-4-methylbenzene sulfonamide (4ab)**

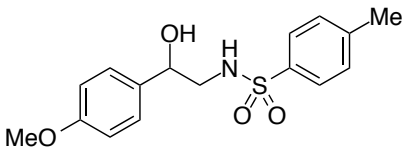

The reaction of 4-methoxystyrene (**3b**) (53.3 mg, 0.397 mmol), **2a** (147.5 mg, 0.439 mmol) and **Ir-1** (2.7 mg, 4.13 μmol) following the general procedures afforded **4ab** (104.4 mg, 82% yield, reaction time = 4 h) as a white solid after purification with column chromatography on Fuji Silysia silica gel FL100D (hexane:EtOAc = 3 : 1).
^{1}H NMR (400 MHz, $CDCl_3$, rt) δ 7.72 (d, ^3J = 8.4 Hz, 2H; $SO_2C_6H_2H_2CH_3$), 7.29 (d, ^3J = 8.0 Hz, 2H; $SO_2C_6H_2H_2CH_3$), 7.19 (d, ^3J = 8.4 Hz, 2H; $CH_3OC_6H_2H_2$), 6.85 (d, ^3J = 8.8 Hz, 2H; $CH_3OC_6H_2H_2$), 4.95 (m, 1H; N*H*), 4.73 (m, 1H; HOC*H*CH_2NH), 3.79 (s, 3H; C$H_3$$OC_6H_4$), 3.20 (m, 1H; HOCHCH*H*NH), 3.02 (m, 1H; HOCHC*H*HNH), 2.42 (s, 3H; $SO_2C_6H_4CH_3$), 2.38 (brd, ^3J = 3.6 Hz, 1H; O*H*). **^{13}C NMR** (400 MHz, $CDCl_3$, rt) δ 159.5, 143.6, 136.8, 133.0, 129.9, 127.3, 127.2, 114.1, 72.4, 55.4, 50.3, 21.6. **HRMS** (ESI-TOF) calculated for $[C_{16}H_{19}NO_4S+Na]^+$ requires 280.0387, found 280.0383.

***N*-(2-Hydroxy-2-(4-acetoxyphenyl)ethyl)-4-methylbenzene sulfonamide (4ac)**

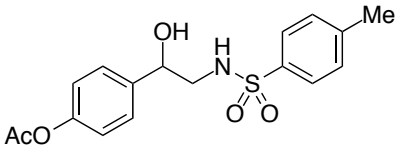

The reaction of 4-acetoxystyrene (**3c**) (64.8 mg, 0.400 mmol), **2a** (148.2 mg, 0.441 mmol) and **Ir-1** (2.6 mg, 3.97 μmol) following the general procedures afforded **4ac** (118.8 mg, 86% yield, reaction time = 4 h) as a white solid after purification with column chromatography on Fuji Silysia silica gel FL100D (hexane:EtOAc = 3 : 1).
^{1}H NMR (400 MHz, $CDCl_3$, rt) δ 7.72 (d, ^3J = 7.6 Hz, 2H; $SO_2C_6H_2H_2CH_3$), 7.30 (d, ^3J = 7.6 Hz, 4H; $CH_3COOC_6H_4$), 7.05 (d, ^3J = 7.6 Hz, 2H; $SO_2C_6H_2H_2CH_3$), 4.92 (m, 1H; N*H*), 4.80 (m, 1H; HOC*H*CH_2NH), 3.23 (m, 1H; HOCHC*H*HNH), 3.00 (m 1H; HOCHCH*H*NH), 2.72 (brs, 1H; O*H*), 2.42 (s, 3H; C$H_3$$COOC_6H_4$), 2.29 (s, 3H; $SO_2C_6H_4CH_3$). **^{13}C NMR** (125 MHz, $CDCl_3$, rt) δ 169.7, 150.5, 143.8, 138.6, 136.7, 130.0, 127.2, 127.1, 121.9, 72.4, 50.3, 21.7, 21.2. **HRMS** (ESI-TOF) calculated for $[C_{17}H_{19}NO_5S+Na]^+$ requires 372.0876, found 372.0872.

***N*-(2-Hydroxy-2-(4-fluorophenyl)ethyl)-4-methylbenzene sulfonamide (4ad)**

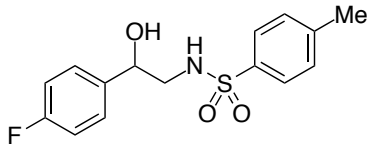

The reaction of 4-fluorostyrene (**3d**) (49.3 mg, 0.404 mmol), **2a** (148.2 mg, 0.441 mmol) and **Ir-1** (2.6 mg, 3.97 μmol) following the general procedures afforded **4ad** (105.5 mg, 84% yield, reaction time = 4 h) as a white solid after purification with column chromatography on Fuji Silysia SCAVENGER NH SILICA (hexane:EtOAc = 2 :1 – 1 : 3).
^{1}H NMR (400 MHz, $CDCl_3$, rt) δ 7.72 (d, ^3J = 8.4 Hz, 2H; $SO_2C_6H_2H_2CH_3$), 7.30 (d, ^3J = 8.0 Hz, 2H; $SO_2C_6H_2H_2CH_3$), 7.26 (m, 2H; $C_6H_2H_2F$), 7.00 (m, 2H; $C_6H_2H_2F$), 5.05 (brs, 1H; N*H*), 4.80 (m, 1H; HOC*H*CH_2NH), 3.21 (m, 1H; HOCHC*H*HNH), 3.00 (m, 1H; HOCHCH*H*NH), 2.61 (brs, 1H; O*H*), 2.42 (s, 3H; $SO_2C_6H_4CH_3$). **^{13}C NMR** (125 MHz, $CDCl_3$, rt) δ 162.7 (d, ^1J = 245 Hz), 143.9, 136.8, 136.7 (d, ^4J = 3.1 Hz), 130.0, 127.7 (d, ^3J = 8.3 Hz), 127.2, 115.7 (d, ^2J = 21.3 Hz), 72.3, 50.4, 21.7. **HRMS** (ESI-TOF) calculated for $[C_{15}H_{16}FNO_3S+Na]^+$ requires 332.0727, found 332.0727.

***N*-(2-Hydroxy-2-(4-chlorophenyl)ethyl)-4-methylbenzene sulfonamide (4ae)**

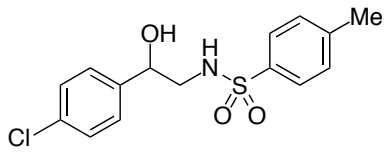

The reaction of 4-chlorostyrene (**3e**) (56.0 mg, 0.404 mmol), **2a** (148.5 mg, 0.442 mmol) and **Ir-1** (2.7 mg, 4.12 μmol) following the general procedures afforded **4ae** (103 mg, 78% yield, reaction time = 4 h) as a white solid after purification with column chromatography on Fuji Silysia SCAVENGER NH SILICA (hexane:EtOAc = 2:1–1:3).
^{1}H NMR (400 MHz, $CDCl_3$, rt) δ 7.71 (d, ^3J = 8.4 Hz, 2H; $SO_2C_6H_2H_2CH_3$), 7.29 (m, 4H; C_6H_4Cl), 7.22 (d, ^3J = 8.4 Hz, 2H; $SO_2C_6H_2H_2CH_3$), 5.02 (t, ^3J = 6.8 Hz, 1H; N*H*), 4.80 (m, 1H; HOC*H*CHHNH), 3.22 (m, 1H; OHCHC*H*HNH), 2.99 (m, 1H; HOCHCH*H*NH), 2.62 (brs, 1H; O*H*), 2.42 (s, 3H; $SO_2C_6H_4CH_3$). **^{13}C NMR** (125 MHz, $CDCl_3$, rt) δ 143.9, 139.4, 136.7, 134.1, 130.0, 128.9, 127.4, 127.2, 72.3, 50.3, 21.9. **HRMS** (ESI-TOF) calculated for $[C_{15}H_{16}ClNO_3S+Na]^+$ requires 348.0432, found 348.0432.

***N*-(2-Hydroxy-2-(4-bromophenyl)ethyl)-4-methylbenzene sulfonamide (4af)**

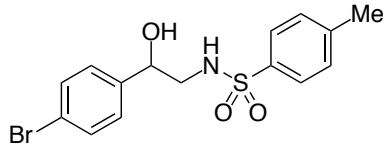

The reaction of 4-bromostyrene (**3f**) (73.6 mg, 0.402 mmol), **2a** (148.1 mg, 0.441 mmol) and **Ir-1** (2.3 mg, 3.52 μmol) following the general procedures afforded **4af** (90.6 mg, 61% yield, reaction time = 4 h) as a white solid after purification with column chromatography on Fuji Silysia silica gel FL100D (hexane:Et_2O = 5–1:1).
^{1}H NMR (400 MHz, $CDCl_3$, rt) δ 7.71 (m, 2H; $SO_2C_6H_2H_2CH_3$), 7.45 (m, 2H; $BrC_6H_2H_2$), 7.30 (m, 2H; $SO_2C_6H_2H_2CH_3$), 7.17 (m, 2H; $BrC_6H_2H_2$), 4.83-4.77 (m, 2H; HOC*H*CH_2N*H*) (overlapped), 3.24 (m, 1H; HOCHC*H*HNH), 3.00 (m, 1H; HOCHCH*H*NH), 2.43 (s, 3H; $SO_2C_6H_4CH_3$), 2.38 (m, 1H; O*H*). **^{13}C NMR** (125 MHz, $CDCl_3$, rt) δ 143.9, 139.9, 136.8, 131.9, 130.0, 127.7, 127.2, 122.3, 72.4, 50.2, 21.7. **HRMS** (ESI-TOF) calculated for $[C_{15}H_{16}BrNO_3+Na]^+$ requires ,391.9926 found 391.9924.

***N*-(2-Hydroxy-2-(3-bromophenyl)ethyl)-4-methylbenzene sulfonamide (4ag)**

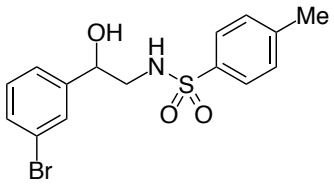

The raection of 3-bromostyrene (**3g**) (72.7 mg, 0.397 mmol), **2a** (147.9 mg, 0.440 mmol) and **Ir-1** (2.8 mg, 4.28 μmol) following the general procedures afforded **4ag** (98.9 mg, 67% yield, reaction time = 4 h) as a white solid after purification with column chromatography on Fuji Silysia SCAVENGER NH SILICA (hexane:EtOAc = 2:1–1:2).
^{1}H NMR (400 MHz, $CDCl_3$, rt) δ 7.72 (d, ^3J = 8.4 Hz, 2H; $SO_2C_6H_2H_2CH_3$), 7.44 (s, 1H; C_6HH_3Br), 7.41 (m, 1H; C_6HHH_2Br), 7.31 (d, ^3J = 8.0 Hz, 2H; $SO_2C_6H_2H_2CH_3$), 7.20 (m, 2H; $C_6H_2H_2B$), 4.90 (m, 1H; N*H*), 4.79 (m, 1H; HOC*H*CHHNH), 3.25 (m, 1H; HOCHC*H*HNH), 3.00 (m, 1H; HOCHCH*H*NH), 2.50 (d, ^3J = 2.8 Hz, 1H; O*H*), 2.43 (s, 3H; $SO_2C_6H_4CH_3$). **^{13}C NMR** (125 MHz, $CDCl_3$, rt) δ 143.9, 143.2, 136.7, 131.4, 130.4, 130.0, 129.1, 127.2, 124.7, 122.9, 72.3, 50.3, 21.7. **HRMS** (ESI-TOF) calculated for $[C_{15}H_{16}BrNO_3S+Na]^+$ requires 393.9906, found 393.9907.

***N*-(2-Hydroxy-2-(4-(3,3,4,4,-tetramethyl-2,5-dioxa-1-boryl)phenyl)ethyl)-4-methylbenzene sulfonamide (4ah)**

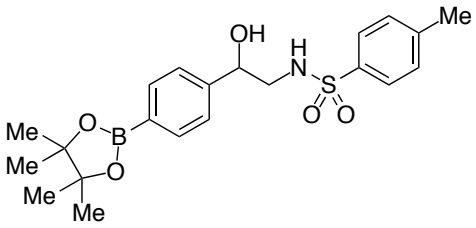

The reaction of *p*-(4,4,5,5-tetramethyl-1,3,2-dioxaborolan-2-yl)styrene (**3h**) (92.7 mg, 0.403 mmol), **2a** (147.9 mg, 0.440 mmol) and **Ir-1** (2.9 mg, 4.43 μmol) following the general procedures afforded **4ah** (113.7 mg, 68% yield, reaction time = 4 h) as a white solid after purification with column chromatography on silica gel (hexane:EtOAc = 3 : 1) and recrystallization with CH_2Cl_2 and hexane.
^{1}H NMR (400 MHz, $CDCl_3$, rt) δ 7.77 (d, ^3J = 8.0 Hz, 2H; pinBC$_6$*H*$_2$H$_2$), 7.71 (d, ^3J = 8.4 Hz, 2H; $SO_2C_6H_2H_2CH_3$), 7.28 (d, ^3J = 8.4 Hz, 2H; $SO_2C_6H_2H_2CH_3$), 7.28 (d, ^3J = 8.0 Hz, 2H; pinBC$_6$H$_2$*H*$_2$), 4.87 (m, 1H; N*H*), 4.81 (m, 1H; HOC*H*CH$_2$NH), 3.25 (m, 1H; HOCHC*H*HNH), 3.01 (m, 1H; HOCHCH*H*NH), 2.43 (brs, 1H; O*H*), 2.42 (s, 3H; $SO_2C_6H_4CH_3$), 1.34 (s, 12H; $C_6H_{12}O_2B$). **^{13}C NMR** (100 MHz, $CDCl_3$, rt) δ 143.9, 143.8, 136.8, 135.3, 129.9, 127.2, 125.2, 84.1, 72.9, 50.3, 25.0, 21.7. **HRMS** (ESI-TOF) calculated for $[C_{21}H_{28}BNO_5S+Na]^+$ requires 440.1677, found 440.1677.

***N*-(2-Hydroxy-2-(3-*N*-(*tert*-butoxycarbonyl)ethyl)-4-methylbenzene sulfonamide (4ai)**

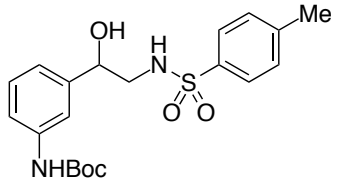

The reaction of *N*-(*tert*-butoxycarbonyl)-3-vinylaniline (**3i**) (88.3 mg, 0.403 mmol), **2a** (148.0 mg, 0.440 mmol) and **Ir-1** (2.7 mg, 4.13 μmol) following the general procedures afforded **4ai** (89.5 mg, 55% yield, reaction time = 4 h) as a white solid after purification with column chromatography on Fuji Silysia SCAVENGER NH SILICA (hexane:EtOAc = 2:1–1:2).
^{1}H NMR (400 MHz, $CDCl_3$, rt) δ 7.72 (d, ^3J = 8.4 Hz, 2H; $SO_2C_6H_2H_2CH_3$), 7.34 (s, 1H; C$_6$*H*$_3$NH), 7.29 (d, ^3J = 8.0 Hz, 2H; $SO_2C_6H_2H_2CH_3$), 7.24 (m, 2H; C$_6$H*H*$_2$HNH), 6.94 (m, 1H; C$_6$HH$_2$*H*NH), 6.48 (s, 1H; N*H*CO$_2$CC$_3$H$_9$), 4.88 (m, 1H; N*H*SO$_2$C$_6$H$_4$CH$_3$), 4.75 (m, 1H; HOC*H*CHHNH), 3.25 (m, 1H; HOCHC*H*HNH), 3.03 (m, 1H; OHCHCH*H*NH), 2.46 (d, ^3J = 3.6 Hz; O*H*), 2.42 (s, 1H: $SO_2C_6H_4CH_3$), 1.51 (s, 9H; $SO_2C_6H_2H_2CH_3$). **^{13}C NMR** (125 MHz, $CDCl_3$, rt) δ 152.8, 143.7, 142.0, 138.8, 136.9, 129.9, 129.5, 127.2, 120.6, 118.5, 116.0, 80.9, 72.7, 50.2, 28.5, 21.7. **HRMS** (ESI-TOF) calculated for $[C_{20}H_{26}N_2O_5S+Na]^+$ requires 429.1455, found 429.1455.

***N*-(2-hydroxy-2-(2,4-methylenedioxyohenyl)ethyl)-4-methylbenzenesulfonamide (4aj)**

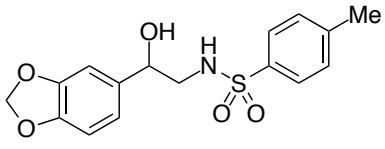

The reaction of 5-ethenyl-1,3-benzodioxide (**3j**) (59.4 mg, 0.401 mmol), **2a** (148.4 mg, 0.442 mmol) and **Ir-1** (2.6 mg, 3.97 μmol) following the general procedures afforded **4aj** (48.9 mg, 36% yield, reaction time = 12 h) as a white solid after purification with column chromatography on Fuji Silysia SCAVENGER NH SILICA (hexane:EtOAc = 2:1–1:2). The obtained solid was washed with

a little amount of diethyl ether to afford 1st crop (29.1 mg). Furthermore, the washing liquid was dried *in vacuo*. The residue was reprecipitated from CH_2Cl_2 and pentane to afford 2nd crop (19.8 mg).
^{1}H NMR (400 MHz, $CDCl_3$, rt) δ 7.73 (d, ^3J = 8.0 Hz, 2H; $SO_2C_6H_2H_2CH_3$), 7.30 (d, ^3J = 8.0 Hz, 2H; $SO_2C_6H_2H_2CH_3$), 6.74 (m, 3H; $C_6H_3OCH_2O$), 5.95 (s, 2H; $C_6H_3OCH_2O$), 4.81 (m, 1H; N*H*), 4.70 (m, HOC*H*CHHNH), 3.19 (m, 1H; HOCHC*H*HNH), 3.01 (m, 1H; HOCHCH*H*NH), 2.43 (s, 3H; $SO_2C_6H_2H_2CH_3$), 2.25 (d, 1H; O*H*). **^{13}C NMR** (125 MHz, $CDCl_3$, rt) δ 148.1, 147.7, 143.8, 136.9, 134.9, 130.0, 127.5, 119.5, 108.5, 106.4, 101.3, 72.8, 50.3, 21.7. **HRMS** (ESI-TOF) calculated for $[C_{16}H_{17}FNO_5S+Na]^+$ requires 358.0720, found 358.0720.

***N*-(2-Hydroxy-2-phenylpropyl)-4-methylbenzene sulfonamide (4ak)**

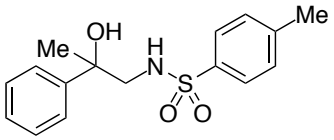

The reaction of α-methylstyrene (**3k**) (49.1 mg, 0.415 mmol), **2a** (147.4 mg, 0.439 mmol) and **Ir-1** (2.7 mg, 4.13 μmol) following the general procedures afforded **4ak** (125.1 mg, 99% yield, reaction time = 4 h) as a colorless oil after purification with flash column chromatography on Fuji Silysia silica gel FL100D (hexane:EtOAc = 3:1).
^{1}H NMR (400 MHz, $CDCl_3$, rt) δ 7.67 (d, ^3J = 8.4 Hz, 2H; $SO_2C_6H_2H_2CH_3$), 7.37-7.26 (m, 7H; Ar), 4.68 (m, 1H; N*H*), 3.21 (m, 1H; HOC(CH_3)C*H*HNH), 3.12 (m, 1H; HOC(CH_3)CH*H*NH), 2.47 (s, 1H; O*H*), 2.42 (s, 3H; $SO_2C_6H_4CH_3$), 1.55 (s, 3H; CCH_3). **^{13}C NMR** (125 MHz, $CDCl_3$, rt) δ 144.9, 143.7, 136.7, 129.9, 128.7, 127.6, 127.2, 124.9,73.8, 54.0, 27.6, 21.7. **HRMS** (ESI-TOF) calculated for $[C_{16}H_{19}NO_3S+Na]$ requires 328.0978, found 328.0972.

***N*-(2-Hydroxy-2-phenyl-2-(pyridine-2-yl))ethyl)-4-methylbenzene sulfonamide (4al)**

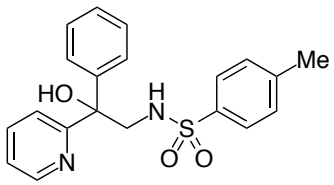

The reaction of 1-(2-pyridyl)-1-phenylethene (**3l**) (73.5 mg, 0.406 mmol), **2a** (147.9 mg, 0.440 mmol) and **Ir-1** (2.5 mg, 3.82 μmol) following the general procedures afforded **4al** (94.3 mg, 63% yield, reaction time = 10 h) as a white solid after purification with column chromatography on Fuji Silysia silica gel FL60D (hexane:EtOAc = 5:1).
^{1}H NMR (400 MHz, $CDCl_3$, rt) δ 8.48 (m, 1H; C_5HH_3N), 7.70-7.65 (m, 3H; $SO_2C_6H_2H_2CH_3$ and C_5NHHH_2 were overlappped), 7.42 (m, 3H; $C_6H_2H_3$), 7.28 (m, 4H; $SO_2C_6H_2H_2CH_3$ and $C_6H_2H_3$), 7.23 (m, 2H; $C_5H_2H_2N$), 5.58 (s, 1H; O*H*), 5.07 (m, 1H; N*H*), 3.88 (dd, ^2J = 12.4 Hz, ^3J = 7.2 Hz, 1H; HOCC*H*HNH), 3.47 (dd, ^2J = 15.5 Hz, ^3J = 5.6 Hz, 1H; HOCCH*H*NH), 2.41 (s, 3H; $SO_2C_6H_4CH_3$). **^{13}C NMR** (125 MHz, $CDCl_3$, rt) δ 161.2, 147.6, 143.6, 143.3, 137.6, 137.0, 129.9, 128.6, 127.8, 127.2, 125.8, 122.8, 121.7, 77.1, 51.7, 21.6. **HRMS** (ESI-TOF) calculated for $[C_{20}H_{20}N_2O_3S+Na]^+$ requires 391.1087, found 391.1090.

***N*-((1-hydroxycyclopentyl)methyl)-4-methylbenenesulfonamine (4am)**

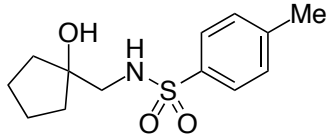

The reaction of methylene cyclopentene (**3m**) (32.5 mg, 0.396 mmol), **2a** (201.5 mg, 0.600 mmol) and **Ir-1** (2.8 mg, 4.28 μmol) following the general procedures afforded **4am** (43.1 mg, 40% yield, reaction time = 4 h) as a white solid after purification with column chromatography on Fuji Silysia silica gel FL100D (hexane:EtOAc = 3:1) and GPC($CHCl_3$). **^{1}H NMR** (400MHz, $CDCl_3$, rt) δ 7.75 (d, ^3J = 8.0 Hz, 2H; $SO_2C_6H_2H_2CH_3$), 7.31 (d, ^3J = 8.0 Hz, 2H; $SO_2C_6H_2H_2CH_3$), 4.97 (t, ^3J = 6.0 Hz, 1H; N*H*), 2.97 (d, ^3J = 6.4 Hz, 2H; HOCCH_2NH), 2.43 (s, 3H; $SO_2C_6H_4CH_3$), 1.78 (m, 2H; C_5H_8), 1.75 (s, 1H; O*H*), 1.61 (m, 6H; C_5H_8). **^{13}C NMR** (125 MHz, $CDCl_3$, rt) δ 143.6, 136.8, 129.9, 127.2, 81.6, 52.1, 38.3, 24.0, 21.7. **HRMS** (ESI-TOF) calculated for $[C_{13}H_{19}NO_3S+Na]^+$ requires 292.0978, found 292.0977.

_N_-(2-Hydroxy-1-methyl-2-phenylethyl)-4-methylbenzenesulfonamide (4an)

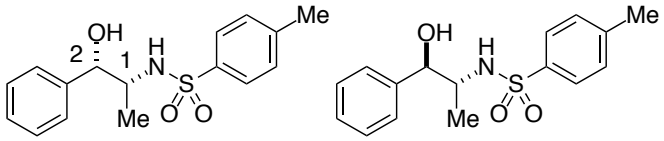

(1*R**,2*S**)-**4an** (1*R**,2*R**)-**4an**

Reaction of *E*-β-methylstyrene (*E*-**3n**): The reaction of *E*-β-methylstyrene (***E*-3n**) (46.8 mg, 0.396 mmol), **2a** (161.3 mg, 0.480 mmol) and **Ir-2** (7.4 mg, 8.10 μmol) following the general procedures afforded diastereomer mixtures of **4an** (49.6 mg, 41% yield, reaction time = 12 h) as a white solid after purification through washing with 0.5 M NaOHaq. and subsequent column chromatography on Fuji Silysia silica gel FL100D (hexane:EtOAc = 4:1). Diastereomer ratio (4:1) was determined by ^{1}HNMR analysis of the unpurified product mixture.

Reaction of *Z*-β-methylstyrene Z-**3n**): The reaction of *Z*-β-methylstyrene (***Z*-3n**) (47.7 mg, 0.404 mmol), **2a** (161.5 mg, 0.480 mmol) and **Ir-2** (7.5 mg, 8.21 μmol) following the general procedures afforded **4an** (65.7 mg, 53% yield, reaction time = 12 h) as a white solid after purification through washing with 0.5 M NaOHaq. and subsequent column chromatography on Fuji Silysia silica gel FL100D (hexane:EtOAc = 4:1). Diastereomer ratio (4:1) was determined by ^{1}HNMR analysis of the unpurified product mixture. The spectral data was identical with the reported literatures.[22b, 22c]

^{1}H NMR (400 MHz, $CDCl_3$, rt) (1*R**,2*S**)-**4an** (major isomer) δ 7.77 (d, ^3J = 7.6 Hz, 2H; $SO_2C_6H_2H_2CH_3$), 7.34-7.22 (m, 7H; Ar), 4.82 (d, ^3J = 8.8 Hz, 1H; HOC*H*CH(CH_3)NH), 4.77 (s, 1H; N*H*), 3.58 (m, 1H; HOCHC*H*(CH_3)NH), 2.54 (m, 1H; O*H*), 2.42 (s, 3H; $SO_2C_6H_4CH_3$), 0.85 (d, ^3J = 6.8 Hz, 3H; HOCHCH(CH_3)NH). (1*R**,2*R**)-**4an** (minor isomer) δ 7.66 (d, ^3J = 8.4 Hz, 2H; $SO_2C_6H_2H_2CH_3$), 7.34-7.22 (m, 7H; Ar), 4.85 (s, 1H; N*H*), 4.50 (d, ^3J = 6.4 Hz, 1H; HOC*H*CH(CH_3)NH)、3.44 (m, 1H; HOCHC*H*(CH_3)NH), 2.58 (m, 1H; O*H*), 2.41 (s, 3H; $SO_2C_6H_4CH_3$), 0.97 (d, ^3J = 6.4 Hz, 3H; HOCHCH(CH_3)NH).

Methyl 2-(*N*-*p*-toluenesulfonyl)amino-3-hydroxy-3-phenyl)propionate (4ao)

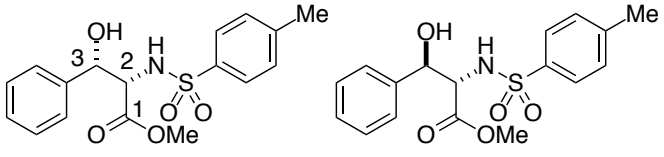

(1*R**,2*R**)-**4ao** (1*R**,2*R**)-**4ao**

The reaction of methyl cinnamate (**3o**) (64.7 mg, 0.399 mmol), **2a** (242.1 mg, 0.720 mmol) and **Ir-2** (7.2 mg, 8.0 μmol) following the general procedures afforded diastereomer mixtures of **4ao** (70.7 mg, 51% yield, reaction time = 12 h) as a white solid after purification with column chromatography on Fuji Silysia silica gel FL60D (hexane:EtOAc = 4:1). Diastereomer ratio (2:1) was determined by ^{1}HNMR analysis of the unpurified product mixture. The spectral data of diastereomers were identical with the reported literature.[22d]

(2*R**,3*R**)-**4ao** (major isomer) **^{1}H NMR** (400 MHz, $CDCl_3$, rt) δ 7.69 (d, ^3J = 8.4 Hz, 2H; $SO_2C_6H_2H_2CH_3$), 7.32-7.20 (m, 7H; $SO_2C_6H_2H_2CH_3$ and C_6H_5 were overlapped), 5.33 (d, ^3J = 9.2 Hz, 1H; N*H*), 5.07 (m, 1H; HOC*H*CHNH), 4.26 (dd, ^3J = 9.2 Hz,^{2} = 4.0 Hz 1H; HOCHC*H*NH),

3.44 (s, 3H; CO_2CH_3), 3.04 (d, ^3J = 6.8 Hz, 1H; O*H*), 2.41 (s, 3H; $SO_2C_6H_4CH_3$). **^{13}C NMR** (125 MHz, $CDCl_3$, rt) δ 169.4, 144.1, 138.5, 136.3, 129.9, 128.6, 128.6, 127.4, 126.3, 74.3, 61.3, 52.6, 21.7.
(2*R**,3*S**)-**4ao** (minor isomer) δ 7.51 (d, ^3J = 8.4 Hz, 2H, $SO_2C_6H_2H_2CH_3$), 7.32-7.20 (m, 5H; C_6H_5), 7.16 (d, ^3J = 8.0 Hz, 2H; $SO_2C_6H_2H_2CH_3$), 5.39 (d, ^3J = 10.0 Hz, 1H; N*H*), 5.03 (m, 1H; HOC*H*CHNH), 4.10 (dd, ^3J = 9.6 Hz, ^2J = 4.0 Hz, 1H; HOCHC*H*NH), 3.50 (s, 3H; CO_2CH_3), 2.65 (d, ^3J = 3.6 Hz, 1H; O*H*), 2.38 (s, 3H; $SO_2C_6H_4CH_3$). **^{13}C NMR** (125 MHz, $CDCl_3$, rt) δ 170.5, 143.6, 138.7, 136.7, 129.6, 128.6, 128.5, 127.2, 126.3, 74.3, 62.0, 52.8, 21.6. **HRMS** (ESI-TOF) calculated for $[C_{17}H_{19}NO_5S+Na]^+$ requires 372.0876, found 372.0875.

***N*-(1-Hydroxy-indan-2-yl)-toluene-4-sulfonamide (4ap)**

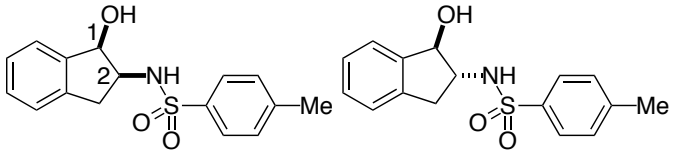

(1*R**,2*R**)-**4ap** (1*R**,2*R**)-**4ap**

The reaction of indene (**3p**) (47.0 mg, 0.405 mmol), **2a** (147.5 mg, 0.439 mmol) and **Ir-1** (2.8 mg, 4.28 μmol) following the general procedures afforded diastereomer mixtures of **4ap** (107.6 mg, 88% yield, reaction time = 4 h) as a white solid after purification with column chromatography on silica gel (hexane:EtOAc = 10:1). Diastereomer ratio (3:1) was determined by ^{1}HNMR analysis of the unpurified product mixture. The spectral data of diastereomers were identical with the reported literature.[22e]
(1*R**,2*S**)-**4ap** (major isomer) **^{1}H NMR** (400 MHz, $CDCl_3$, rt) δ 7.82 (m, 2H; $SO_2C_6H_2H_2CH_3$), 7.36-7.09 (m, 6H; Ar), 5.42 (d, ^3J = 8.4 Hz, 1H; N*H*), 4.77 (t, ^3J = 5.2 Hz, 1H; HOC*H*CHNH), 3.97 (m, 1H; HOCHC*H*NH), 3.02 (m, 1H; HNCHC*H*H), 2.87 (m, 1H; HNCHCH*H*), 2.45 (s, 3H; $SO_2C_6H_4CH_3$), 2.17 (d, ^3J = 5.2 Hz, 1H; O*H*). (1*R**,2*R**)-**4ap** (minor isomer) **^{1}H NMR** (400 MHz, $CDCl_3$, rt) δ 7.82 (m, 2H; $SO_2C_6H_2H_2CH_3$), 7.36-7.09 (m, 6H; Ar), 5.23 (d, ^3J = 6.0 Hz, 1H; N*H*), 5.10 (dd, ^3J = 6.4 Hz, ^3J = 4.4 Hz, 1H; HOC*H*CHNH), 3.66 (m, 1H; HOCHC*H*NH), 3.28 (d, ^3J = 4.4 Hz, 1H; O*H*), 3.08 (m, 1H; HNCHC*H*H). 2.67 (m, 1H; HNCHCH*H*), 2.43 (s, 3H; $SO_2C_6H_4CH_3$).

2-(4-Methylbenzenesulfonylamino)-1,2,3,4-tetrahydronaphthol (4aq)

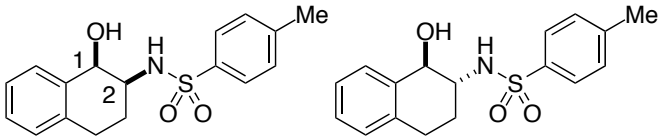

(1*R**,2*R**)-**4aq** (1*R**,2*R**)-**4aq**

The reaction of 1,2-dihydronaphthalene (**3q**) (51.7 mg, 0.397 mmol), **2a** (148.1 mg, 0.441 mmol) and **Ir-1** (2.7 mg, 4.12 μmol) following the general procedures afforded **4aq** (single diastereomer of (1*R**,2*S**)-**4aq**: 25.0 mg, 20% and diastereomer mixtures: 60.9 mg, 48%, total yield; 85.9 mg, 68%, reaction time = 12 h) as a white solid after purification through washing with 0.5 M NaOHaq. and subsequent column chromatography on Fuji Silysia silica gel FL60D (hexane:EtOAc = 5:1). Diastereomer ratio (1.5:1) was determined by ^{1}HNMR analysis of the unpurified product mixture. The structure of major diastereomer was confirmed by single-crystal X-ray analysis *vide infra*.
(1*R**,2*S**)-**4aq** (major isomer)**^{1}H NMR** (400 MHz, $CDCl_3$, rt) δ 7.81 (d, ^3J = 8.4 Hz, 2H; $SO_2C_6H_2H_2CH_3$), 7.32 (d, ^3J = 7.6 Hz, 2H; $SO_2C_6H_2H_2CH_3$), 7.26-7.09 (m, 4H; C_6H_4), 5.11 (d, ^3J = 8.4 Hz, 2H; N*H*), 4.49 (m, 1H; HOC*H*CHNH), 3.57 (m, 1H; HOCHC*H*NH), 2.82 (m, 2H; $C_6H_4CH_2CH_2$), 2.44 (s, 3H; $SO_2C_6H_4CH_3$), 2.00-1.81 (m, 2H; $C_6H_4CH_2CH_2$), 1.85 (d, ^3J = 6.0 Hz, 1H; O*H*). **^{13}C NMR** (125 MHz, $CDCl_3$, rt) δ 143.6, 138.3, 136.1, 135.7, 130.1, 130.0, 129.0, 128.8, 127.2, 126.7, 68.8, 53.9, 28.0, 24.8, 21.7.
(1*R**,2*R**)-**4aq** (minor isomer) **^{1}H NMR** (400 MHz, $CDCl_3$, rt) δ 7.80 (d, ^3J = 8.0 Hz, 2H; $SO_2C_6H_2H_2CH_3$), 7.45 (m, 1H; C_6H_4), 7.31 (d, ^3J = 8.0 Hz, 2H; $SO_2C_6H_2H_2CH_3$), 7.22-7.16 (m, 2H;

C_6H_4), 7.07 (m, 1H; C_6H_4), 4.95 (d, ^3J = 6.4 Hz, 1H; N*H*), 4.51 (m, 1H; HOC*H*CHNH), 3.36 (m, 1H, HOCHC*H*NH), 2.80 (m, 2H; $C_6H_4CH_2CH_2$), 2.43 (s, 3H; $SO_2C_6H_4CH_3$), 2.43 (1H; O*H*), 2.11-2.01 (m 1H; $C_6H_4CH_2CHH$), 1.76-1.72 (m, 1H; $C_6H_4CH_2CHH$). **^{13}C NMR** (125 MHz, $CDCl_3$, rt) δ 143.9, 137.2, 136.3, 135.3, 130.0, 128.6, 128.1, 128.0, 127.4, 126.7, 72.4, 56.8, 27.2, 26.8, 21.7. **HRMS** (ESI-TOF) calculated for $[C_{17}H_{19}NO_3S+Na]^+$ requires 340.0978, found 340.0979.

2-(4-Methylbenzenesulfonylamino)-1-methylcyclohexanol (4ar)

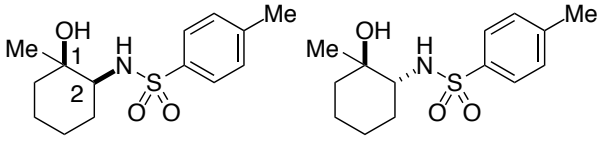

(1*R**,2*R**)-**4ar** (1*R**,2*R**)-**4ar**

The reaction of 1-methyl-1-cyclohexene (**3r**) (38.9 mg, 0.404 mmol), **2a** (148.0 mg, 0.440 mmol) and **Ir-1** (2.6 mg, 3.97 μmol) following the general procedures afforded diastereomer mixtures of **4ar** (26.8 mg, 23% yield, reaction time = 8 h) as a colorless oil after purification with column chromatography on Fuji Silysia silica gel FL60D (hexane:EtOAc = 4:1) and GPC($CHCl_3$). Diastereomer ratio (1:1) was determined by ^{1}HNMR analysis of the unpurified product mixture.
^{1}H NMR (400MHz, $CDCl_3$, rt) (1*R**,2*S**)-**4ar** or (1*R**,2*R**)-**4ar** δ 7.78 (m, 2H; $SO_2C_6H_2H_2CH_3$), 7.32 (m, 2H; $SO_2C_6H_2H_2CH_3$), 4.46 (d, ^3J = 7.6 Hz, 1H; N*H*), 3.02 (m, 1H; C*H*NHSO$_2$), 2.43 (s, 3H; $SO_2C_6H_4CH_3$), 2.39 (s, 1H; O*H*), 1.71 (m, 1H), 1.60 (m, 2H), 1.41 (m, 3H), 1.15 (m, 2H), 1.14 (s, 3H; HOCCH_3). (1*R**,2*S**)-**4ar** or (1*R**,2*R**)-**4ar** δ 7.75 (m, 2H; $SO_2C_6H_2H_2CH_3$), 7.29 (m, 2H; $SO_2C_6H_2H_2CH_3$), 4.71 (d, ^3J = 9.2 Hz, 1H; N*H*), 3.02 (m, 1H; C*H*NHSO$_2$), 2.42 (s, 3H; $SO_2C_6H_4CH_3$), 1.71 (m, 1H), 1.60 (m, 2H), 1.41 (m, 3H), 1.32 (s, 1H; O*H*), 1.15 (m, 2H), 1.14 (s, 3H; HOCCH_3). **^{13}C NMR** (125 MHz, $CDCl_3$, rt) (1*R**,2*S**)-**4ar** or (1*R**,2*R**)-**4ar** δ 148.1, 147.7, 143.8, 136.9, 134.9, 130.0, 127.2, 119.5, 108.5, 106.4, 101.3, 72.8, 50.3, 21.7. **HRMS** (ESI-TOF) calculated for $[C_{14}H_{21}NO_3S+Na]^+$ requires 306.1134, found 306.1134.

Procedure for the synthesis of *N*-protected iminopyridinium ylide
***N*-benzoyliminopyridinium ylide (10b)**

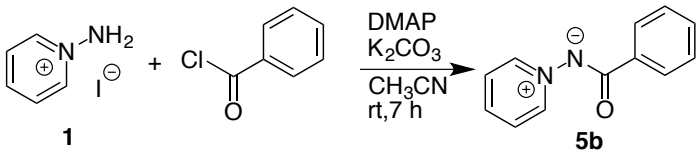

1 **5b**

To a dry-CH_3CN (40 mL) solution of 1-aminopyridinium iodide (**1**) (1.12 g, 5.02 mmol) was added 4-dimethylaminopyridine (DMAP) (59.9 mg, 0.490 mmol), potassium carbonate (2.08 g, 15.0 mmol), and benzoylchloride (724.4 mg, 5.15 mmol). Then, the reaction mixture was stirred for 7 h at rt. The suspension was concentrated *in vacuo*. The product was extracted with CH_2Cl_2 and filtered. After the filtrate was evaporated under reduced pressure, the crude product was purified by flash column chromatography on Fuji Silysia silica gel FL100D (CH_2Cl_2:MeOH = 20:1) to afford **5b** as a white solid (668 mg, 3.37 mmol, 67% yield). The spectral data was identical with the reported literatures[23].
^{1}H NMR (400 MHz, $CDCl_3$) δ 8.85 (m, 2H; $NC_5H_2HH_2$), 8.16 (m, 2H; $C_6H_2H_3$), 7.92 (m, 1H; $NC_5H_2HH_2$), 7.68 (m, 2H; $NC_5H_2HH_2$), 7.42 (m, 3H; $C_6H_2H_3$).

***N*-(tert-Butoxycarbonyl)iminopyridinium ylide (5c)**

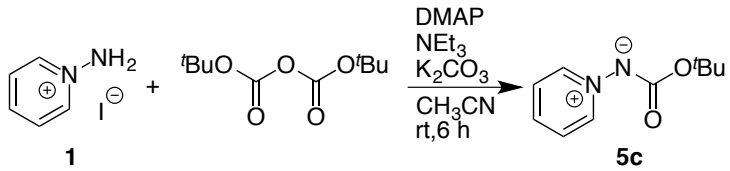

1 **5c**

Under N_2 at 0 ºC, to a dry-CH_3CN (100 mL) solution of **1** (5.0103 g, 22.6 mmol) was added triethylamine (6.3 mL, 45 mmol), DMAP (276 mg, 2.26 mmol), and di-*tert*-butoxy dicarbonate (5.07 g, 23.3 mmol). The cooling bath was removed and the reaction mixture was stirred for 6 h at rt. Then, potassium carbonate (9.32 g, 67.5 mmol) was added and the reaction mixture was stirred for additional 2 h at rt. The suspension was concentrated *in vacuo*. The product was extracted with CH_2Cl_2 and filtered. After the filtrate was evaporated under reduced pressure, the crude product was purified by flash column chromatography on Fuji Silysia silica gel FL60D (CH_2Cl_2:MeOH = 20:1) and recrystallized from CH_2Cl_2 and hexane to afford the three crops of **5c** as a white solid (total, 3.86 g, 19.9 mmol, 88% yield).
^{1}H NMR (400 MHz, $CDCl_3$) δ 8.83 (m, 2H; $C_5H_2H\mathit{H}_2N$), 7.71 (m, 1H; $C_5H_2\mathit{H}H_2N$), 7.51 (m, 2H; $C_5\mathit{H}_2HH_2N$), 1.50 (s, 9H; $C(C\mathit{H}_3)_3$). **^{13}C NMR** (125 MHz, $CDCl_3$) δ 163.4, 142.3, 134.6, 125.8, 77.9, 28.9. **HRMS** (ESI-TOF) calculated for [$C_{10}H_{14}N_2O_2$+Na] requires 217.0947, found 217.0948.

***N*-(2,2,2-trichloroethoxycarbonyl)iminopyridinium ylide (5d)**

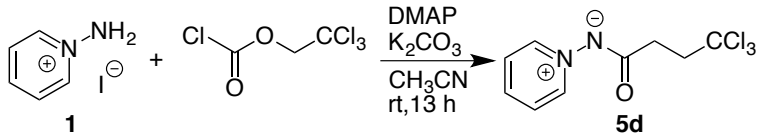

1 **5d**

Under N_2 at 0 ºC, to a dry-CH_3CN (50 mL) solution of **1** (1.12 g, 5.02 mmol) was added DMAP (64.3 mg, 0.526 mmol), potassium carbonate (2.03 g 14.7 mmol), and 2,2,2-trichloroethyl chloroformate (1.01 g, 4.76 mmol). The cooling bath was removed and the reaction mixture was stirred for 13 h at rt. After the same workup as in **5b**, the crude product was purified by flash column chromatography on Fuji Silysia silica gel FL100D (CH_2Cl_2:MeOH = 20:1) to afford **5d** as a white solid (0.924 g, 3.43 mmol, 72%).
^{1}H NMR (400 MHz, $CDCl_3$) δ 8.87 (d, ^3J = 6.0 Hz, 2H; $C_5H_2H\mathit{H}_2N$), 7.87 (t, ^3J = 7.6 Hz, 1H; $C_5H_2\mathit{H}H_2N$), 7.64 (m, 2H; $C_5\mathit{H}_2HH_2N$), 4.80 (s, 2H; $C\mathit{H}_2CCl_3$). **^{13}C NMR** (125 MHz, $CDCl_3$) δ 162.0, 142.6, 136.3, 126.3, 96.8, 74.8. **HRMS** (ESI-TOF) calculated for [$C_8H_7Cl_3N_2O_2$+Na] requires 290.9465, found 290.9465.

***N*-(Allyloxycarbonyl)iminopyridinium ylide (5e)**

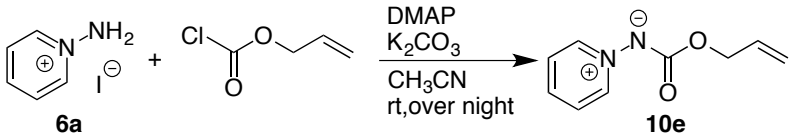

6a **10e**

To a dry-CH_3CN (40 mL) solution of **1** (1.12 g, 5.02 mmol) was added DMAP (60.5 mg, 0.493 mmol), potassium carbonate (2.12 g, 15.3 mmol), and allyl chloroformate (587 mg, 4.86 mmol). The reaction mixture was stirred for overnight at rt. After the same workup as in **5b**, the crude product was purified by flash column chromatography on Fuji Silysia silica gel FL60D (Hexane:EtOAc = 1:1−CH_2Cl_2:MeOH = 20:1) to afford **10e** as a dull red oil (377 mg, 2.12 mmol, 42% yield).
^{1}H NMR (400 MHz, $CDCl_3$) δ 8.86 (d, ^3J = 6.0 Hz, 2H; $C_5HH_2\mathit{H}_2N$), 7.80 (t, ^3J = 7.6 Hz, 1H; $C_5\mathit{H}H_2H_2N$), 7.58 (m, 2H; $C_5H\mathit{H}_2H_2N$), 6.03 (m, 1H; CH_2=C$\mathit{H}$$CH_2O$), 5.28 (m, 2H; C$\mathit{H}_2$=$CHCH_2O$), 4.63 (m, 2H; CH_2=$CHC\mathit{H}_2O$). **^{13}C NMR** (125 MHz, $CDCl_3$) δ 163.4, 142.5, 135.4, 134.3, 126.0,

116.7, 65.3. **HRMS** (ESI-TOF) calculated for [$C_9H_{10}N_2O_2$+Na] requires 201.0634, found 201.0637.

General procedures for photocatalytic amionohydroxylation of alkenes with ylide 5x

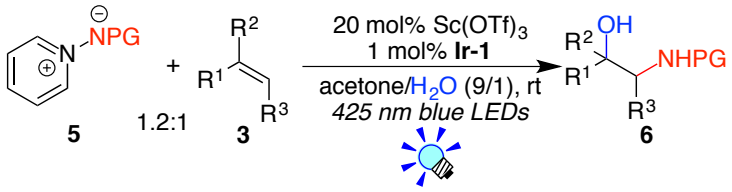

Under N_2, to alkene (**3**) (0.80 mmol) dissolved in a mixture of acetone (3.6 mL) and H_2O (0.4 mL) in a 20 mL-Schlenk tube, ylide **5** (0.40 mmol), **Ir-1** (4 µmol), and $Sc(OTf)_3$ (80 µmol) were added. The mixture was degassed by three freeze-pump-thaw cycles. The tube was placed at a 2-3 cm from blue LED lamps. The resulting mixture was stirred at room temperature (in a water bath) under visible light irradiation. Then, the resulting mixture was concentrated *in vacuo* to remove volatile compounds. The crude product was purified by flash column chromatography on silica gel to give **6**.

***N*-(2-Hydroxy-2-phenylethyl)-2,2,2-trifluoroacetylamide(6aa)**

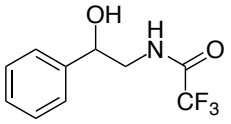

The reaction of **5a** (75.9 mg, 0.399 mmol), styrene (**4a**) (82.7 mg, 0.794 mmol), $Sc(OTf)_3$ (38.9 mg, 79.0 µmol), and **Ir-1** (2.7 mg, 4.12 µmol) following the general procedures afforded **6aa** (56.7 mg, 61% yield, reaction time = 8 h) as a white solid after purification with flash column chromatography on Fuji Silysia SCAVENGER NH SILICA (hexane:EtOAc = 8:1−5:1−3:1). Spectral data is in agreement with the reported data.[24a]
^{1}H NMR (400 MHz, $CDCl_3$) d 7.42-7.34 (m, 5H; C_6H_5), 6.77 (brs, 1H; N*H*), 4.90 (m, 1H; HOC*H*CHHNH), 3.83 (m, 1H; HOCHC*H*HNH), 3.38 (m, 1H; HOCHCH*H*NH), 2.23 (brs, 1H; O*H*).

***N*-(2-Hydroxy-2-(4-methylphenyl)ethyl)- 2,2,2-trifluoroacetamide (6at)**

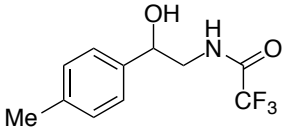

The reaction of **5a** (76.5 mg, 0.402 mmol), 4-methylstyrene (**3s**) (94.9 mg, 0.803 mmol), $Sc(OTf)_3$ (39.7 mg, 80.7 µmol), and **Ir-1** (2.6 mg, 3.97 µmol) following the general procedures afforded **6as** (59.1 mg, 59% yield, reaction time = 8 h) as a colorless oil after purification with flash column chromatography on Fuji Silysia SCAVENGER NH SILICA (hexane:EtOAc = 5:1).
^{1}H NMR (400 MHz, $CDCl_3$) δ 7.25 (d, ^3J = 8.0 Hz, 2H; $C_6H_2H_2$), 7.20 (d, ^3J = 8.0 Hz, 2H; $C_6H_2H_2$), 6.75 (brs, 1H; N*H*), 4.85 (m, 1H; HOC*H*CHHNH), 3.80 (m, 1H; HOCHC*H*HNH), 3.37 (m, 1H; HOCHCH*H*NH), 2.36 (s, 3H; $CH_3C_6H_4$), 2.14 (brs, 1H; O*H*). **^{13}C NMR** (125 MHz, $CDCl_3$) δ 157.6 (q, ^2J = 36.9 Hz), 138.6, 137.7, 129.6, 125.8, 116.0 (q, ^1J = 285.9), 72.4, 46.7, 21.3. **^{19}F NMR** (376 MHz, $CDCl_3$) δ –77.2. **HRMS** (ESI-TOF) calculated for [$C_{11}H_{12}F_3NO_2$+Na] requires 270.0712, found 270.0712.

***N*-(2-Hydroxy-2-(4-methoxyphenyl)ethyl)- 2,2,2-trifluoroacetamide (6ab)**

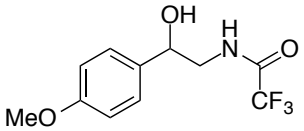

The reaction of **5a** (75.8 mg, 0.399 mmol), 4-methoxystyrene (**3b**) (107.4 mg, 0.800 mmol), $Sc(OTf)_3$ (40.1 mg, 81.5 µmol), and **Ir-1** (2.5 mg, 3.82 µmol) following the general procedures afforded **6ab** (66.6 mg, 63% yield, reaction time = 8 h) as a pale yellow solid after purification with

flash column chromatography on Fuji Silysia SCAVENGER NH SILICA (hexane:EtOAc = 8:1–5:1–3:1).
^{1}H NMR (400 MHz, CDCl3) δ 7.28 (d, ^3J = 8.4 Hz, 2H; $C_6H_2H_2$), 6.91 (d, ^3J = 8.8 Hz, 2H; $C_6H_2H_2$), 6.74 (brs, 1H; N*H*), 4.83 (m, 1H; HOC*H*CHHNH), 3.81 (s, 3H; $CH_3OC_6H_4$), 3.78 (m, 1H; HOCHC*H*HNH), 3.37 (m, 1H; HOCHCH*H*NH), 2.21 (brs, 1H; O*H*). **^{13}C NMR** (125 MHz, $CDCl_3$) δ 159.9, 157.5 (q, ^2J = 36.9 Hz), 132.8, 127.2, 116.0 (q, ^1J = 284.6 Hz), 114.4, 72.2, 55.5, 46.7. **^{19}F NMR** (376 Hz, $CDCl_3$) δ –77.2. **HRMS** (ESI-TOF) calculated for [$C_{11}H_{12}F_3NO_3$+Na] requires 286.0661, found 286.0662.

***N*-(2-Hydroxy-2-(4-fluorolphenyl)ethyl)-2,2,2-trifluoroacetamide (6ad)**

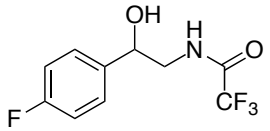

The reaction of **5a** (76.3 mg, 0.401 mmol), 4-fluorostyrene (**3d**) (97.8 mg, 0.801 mmol), $Sc(OTf)_3$ (38.4 mg, 78.0 μmol), and **Ir-1** (2.7 mg, 4.12 μmol) following the general procedures afforded **6ad** (62.9 mg, 62% yield, reaction time = 8 h) as a white solid after purification with flash column chromatography on Fuji Silysia SCAVENGER NH SILICA (hexane:EtOAc = 10:1–5:1–3:1).
^{1}H NMR (400 MHz, $CDCl_3$) δ 7.34 (m, 2H; $FC_6H_2H_2$), 7.07 (m, 2H; $FC_6H_2H_2$), 6.80 (brs, 1H; N*H*), 4.88 (m, 1H; HOC*H*CHHNH), 3.78 (m, 1H; HOCHC*H*HNH), 3.35 (m, 1H; HOCHCH*H*NH), 2.45 (brs, 1H; O*H*). **^{13}C NMR** (125 MHz, $CDCl_3$) δ 162.8 (d, ^1J = 245.5 Hz), 157.8 (q, ^2J = 37.0 Hz), 136.5 (^4J = 3.1 Hz), 127.6 (d, ^3J = 8.25 Hz), 115.9 (q, ^1J = 285.6 Hz), 115.8 (d, ^2J = 21.4 Hz), 71.9, 46.8. **^{19}F NMR** (376 MHz, $CDCl_3$) δ –75.9, –113.3 (m). **HRMS** (ESI-TOF) calculated for [$C_{10}H_9F_4NO_2$+Na] requires 274.0462, found 274.0462.

***N*-(2-Hydroxy-2-(4-chlorolphenyl)ethyl)-2,2,2-trifluoroacetamide (6ae)**

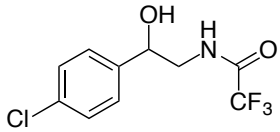

The reaction of **5a** (76.7 mg, 0.403 mmol), 4-chlorostyrene (**3e**) (110.7 mg, 0.799 mmol), $Sc(OTf)_3$ (38.9 mg, 79.0 μmol), and **Ir-1** (2.6 mg, 3.97 μmol) following the general procedures afforded **6ae** (45.6 mg, 42% yield, reaction time = 8 h) as a colorless oil after purification with flash column chromatography on Fuji Silysia SCAVENGER NH SILICA (hexane:EtOAc = 20:1–5:1).
^{1}H NMR (400 MHz, $CDCl_3$) δ 7.37 (m, 2H; $ClC_6H_2H_2$), 7.32 (m, 2H; $ClC_6H_2H_2$), 6.73 (brs, 1H; N*H*), 4.90 (m, 1H; HOC*H*CHHNH), 3.80 (m, 1H; HOCHC*H*HNH), 3.35 (ddd, ^2J = 13.6 Hz, ^3J = 8.4, 4.2 Hz, 1H; HOCHCH*H*NH), 2.26 (brs, 1H; O*H*). **^{13}C NMR** (125 MHz, $CDCl_3$) δ 157.8 (q, ^2J = 37.1 Hz), 139.2, 134.4, 129.1, 127.2, 115.9 (q, ^1J = 285.6 Hz), 71.9, 46.8. **^{19}F NMR** (376 MHz, $CDCl_3$) δ –77.2. **HRMS** (ESI-TOF) calculated for [$C_{10}H_9ClF_3NO_2$+Na] requires 290.0166, found 290.0165.

***N*-(2-Hydroxy-2-(4-bromophenyl)ethyl)-2,2,2-trifluoroacetamide (11af)**

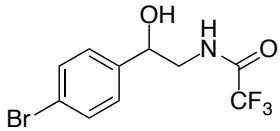

The reaction of **5a** (76.1 mg, 0.400 mmol), 4-bromostyrene (**3f**) (146.4 mg, 0.800 mmol), $Sc(OTf)_3$ (39.2 mg, 79.7 μmol), and **Ir-1** (2.8 mg, 4.28 μmol) following the general procedures afforded **6af** (67.3 mg, 54% yield, reaction time = 8 h) as a white solid after purification with flash column chromatography on Fuji Silysia SCAVENGER NH SILICA (hexane:EtOAc = 5:1–3:1).
^{1}H NMR (400 MHz, $CDCl_3$) δ 7.52 (d, ^3J = 8.4 Hz, 2H; $BrC_6H_2H_2$), 7.26 (d, ^3J = 8.4 Hz, 2H; $BrC_6H_2H_2$), 6.73 (brs, 1H; N*H*), 4.88 (m, 1H; HOC*H*CHHNH), 3.80 (m, 1H; HOCHC*H*HNH), 3.35 (m,1H; HOCHCH*H*NH), 2.29 (brs, 1H; O*H*). **^{13}C NMR** (125 MHz, $CDCl_3$) δ 157.7 (q, ^2J = 37.0

Hz), 139.7, 132.1, 127.5, 122.6, 115.9 (q, ^1J = 286.0 Hz), 72.0, 46.7. **^{19}F NMR** (376 MHz, $CDCl_3$) δ –77.2. **HRMS** (ESI-TOF) calculated for [$C_{10}H_9BrF_3NO_2$+Na] requires 333.9661, found 333.9661.

***N*-(2-Hydroxy-2-(phenylethyl)-2,2,2-trifluoroacetamide (6ak)**

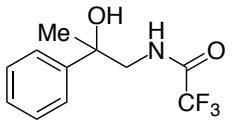

The reaction of **5a** (76.2 mg, 0.401 mmol), α-methylstyrene (**3k**) (94.8 mg, 0.802 mmol), $Sc(OTf)_3$ (39.7 mg, 80.7 μmol), and **Ir-1** (2.6 mg, 3.97 μmol) following the general procedures afforded **6ak** (64.6 mg, 65% yield, reaction time = 8 h) as a white solid after purification with flash column chromatography on Fuji Silysia SCAVENGER NH SILICA (hexane:EtOAc = 5:1).
^{1}H NMR (400 MHz, $CDCl_3$) δ 7.45 (m, 2H; $C_6H_2H_2H$), 7.39 (m, 2H; $C_6H_2H_2H$), 7.31 (m, 1H; $C_6H_2H_2H$), 6.60 (brs, 1H; N*H*), 3.75 (dd, ^2J = 13.6 Hz, ^3J = 6.4 Hz, 1H; OHCC*H*HNH), 3.53 (dd, ^2J = 13.6 Hz, ^3J = 5.2 Hz; OHCCH*H*NH), 1.66 (brs, 1H; O*H*), 1.62 (brs, 3H; CH_3C). **^{13}C NMR** (125 MHz, $CDCl_3$) δ 157.9 (q, ^2J = 37.0 Hz), 144.4, 128.7, 127.7, 124.8, 115.9 (q, ^1J = 285.7 Hz), 74.2, 50.5, 27.4. **^{19}F NMR** (376 MHz, $CDCl_3$) δ –77.2. **HRMS** (ESI-TOF) calculated for [$C_{11}H_{10}F_3NO_4$+Na] requires 300.0454, found 300.0455.

***N*-(2-Hydroxy-2-(2,4-methylenedioxyophenyl)ethyl-4-methyl-2,2,2-trifluoroacetamide (6aj)**

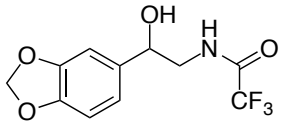

The reaction of **5a** (76.2 mg, 0.401 mmol), 5-ethynyl-1,3-benzodioxide (**3j**) (117.9 mg, 0.796 mmol), $Sc(OTf)_3$ (39.1 mg, 79.4 μmol), and **Ir-1** (5.1 mg, 7.79 μmol) following the general procedures afforded **6aj** (23.3 mg, 21% yield, reaction time = 24 h) as a pale yellow oil after purification with flash column chromatography on Fuji Silysia silica gel (hexane:EtOAc = 10:1–5:1).
^{1}H NMR (400 MHz, $CDCl_3$) δ 6.86 (s, 1H; C_6HHH), 6.81 (m, 2H; C_6H*HH*), 6.74 (brs, 1H; N*H*), 5.98 (s, 2H; OCH_2O), 4.80 (m, 1H; HOC*H*CH_2NH), 3.77 (m, 1H; HOCHC*H*HNH), 3.34 (m, 1H; HOCHCH*H*NH), 2.24 (brs, 1H; O*H*). **^{13}C NMR** (125 MHz, $CDCl_3$) δ 157.6 (q, ^2J = 36.9 Hz), 148.2, 147.8, 134.7, 119.4, 116 (q, ^1J = 285.8 Hz), 108.6, 106.3, 101.4, 72.3, 46.8. **^{19}F NMR** (376 MHz, $CDCl_3$) δ –77.2. **HRMS** (ESI-TOF) calculated for [$C_{11}H_{10}F_3NO_4$+Na] requires 300.0454, found 300.0455.

***N*-((2-Hydroxy-2-phenyl-2-(pyridine-2-yl))ethyl-4-methylbenzene)-2,2,2-trifluoroacetamide (6al)**

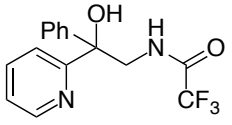

The reaction of **5a** (76.3 mg, 0.401 mmol), 1-(2-pyridyl)-1-phenylethene (**3l**) (145.2 mg, 0.801 mmol), $Sc(OTf)_3$ (40.3 mg, 81.9 μmol), and **Ir-1** (2.7 mg, 4.12 μmol) following the general procedures afforded **6al** (105.9 mg, 85% yield, reaction time = 24 h) as a white solid after purification with flash column chromatography on Fuji Silysia SCAVENGER NH SILICA (hexane : EtOAc = 10:1–5:1).
^{1}H NMR (400 MHz, $CDCl_3$) δ 8.54 (m, 1H; C_5HHH_2N), 7.70 (m, 1H; C_5H*H*H_2N), 7.49 (d, ^3J = 7.2 Hz, 2H; $C_6H_2H_3$), 7.41-7.25 (m, 5H; C_5HHH_2N and $C_6H_2H_3$ were overlapped), 6.87 (brs, 1H; N*H*), 6.17 (brs, 1H; O*H*), 4.32 (dd, ^2J = 13.6 Hz, ^3J = 7.2 Hz, 1H; OHCC*H*HNH), (dd, ^2J = 13.6 Hz, ^3J = 4.8 Hz, 1H; OHCCH*H*NH). **^{13}C NMR** (125 MHz, $CDCl_3$) δ 160.1, 157.4 (q, ^2J = 37.0 Hz), 147.7, 142.7, 137.8, 128.8, 128.1, 125.8, 123.2, 120.9, 115.8 (q, ^1J = 286.0 Hz), 77.1, 47.9. **^{19}F NMR** (376 MHz, $CDCl_3$) δ –77.4. **HRMS** (ESI-TOF) calculated for [$C_{15}H_{13}F_3N_2O_2$+Na] requires 333.0821,

found 333.0820.

***N*-(2-Hydroxy-1-methyl-2-phenylethyl)-2,2,2-trifluoroacetamide (6an)**

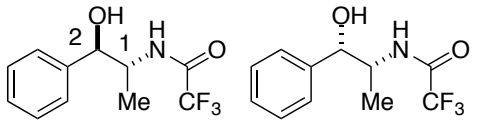

(1*R**,2*S**)-**6an** (1*R**,2*R**)-**6an**

The reaction of **5a** (75.9 mg, 0.399 mmol), *trans*-β-methylstyrene (**3n**) (94.3 mg, 0.798 mmol), $Sc(OTf)_3$ (39.7 mg, 80.7 μmol), and **Ir-1** (2.6 mg, 3.97 μmol) following the general procedures afforded **6an** (30 mg, 30% yield, reaction time = 24 h) as a white solid after purification with flash column chromatography on Fuji Silysia silica gel FL60D (hexane:EtOAc = 5:1).
(1*R**,2*R**)-**11an** (major isomer): **^{1}H NMR** (400 MHz, $CDCl_3$) δ 7.35 (m, 5H; C_6H_5), 6.55 (brs, 1H; N*H*), 4.75 (m, 1H; HOC*H*CHNH), 4.25 (m, 1H; HOCHC*H*NH), 2.24 (brs, 1H; O*H*), 1.31 (d, ^3J = 6.8 Hz, 3H; CHCH_3). **^{13}C NMR** (125 MHz, $CDCl_3$) δ 157.0 (q, ^2J = 36.8 Hz), 140.7, 128.8, 128.7, 126.0, 115.9 (q, ^1J = 286.3 Hz), 75.9, 51.7, 17.5. **^{19}F NMR** (376 MHz, $CDCl_3$) δ –77.3. **HRMS** (ESI-TOF) calculated for [$C_{11}H_{12}F_3NO_2$+Na] requires 270.0712, found 270.0713.
(1*R**,2*S**)-**11an** (minor isomer): **^{1}H NMR** (400 MHz, $CDCl_3$, rt) δ 7.35 (m, 5H; C_6H_5), 6.67 (brs, 1H; N*H*), 4.94 (m, 1H; HOC*H*CHNH), 4.31 (m, 1H; HOCHC*H*NH), 2.40 (brs, 1H; O*H*), 1.06 (d, ^3J = 6.8 Hz, 3H; CHCH_3). The spectral data of (1*R**,2*S**)-**11an** was identical with the reported data.[25b]

***N*-(1-hydroxy-1,2,3,4-tetrahydronaphthalen-2-yl)-2,2,2-trifluoroacetamide (6aq)**

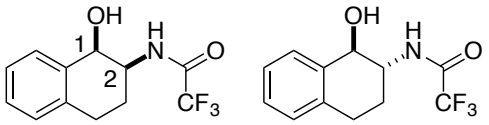

(1*R**,2*R**)-**6aq** (1*R**,2*R**)-**6aq**

The reaction of **5a** (76.1 mg, 0.400 mmol), 1,2-dihydronaphthalene (**3q**) (104.7 mg, 0.804 mmol), $Sc(OTf)_3$ (38.7 mg, 78.6 μmol), and **Ir-1** (2.8 mg, 4.28 μmol) following the general procedures afforded **6aq** (single diastereomer of (1*R**,2*S**)-**6aq** fraction: 11.8 mg, 11% yield, diastereomer mixture fraction: 18.4 mg, 18% yield, and single diastereomer of (1*R**,2*R**)-**6aq** fraction: 8.6 mg, 8% yield, total yiled: 38.8 mg, 37%, reaction time = 8 h) as each white solid after purification with flash column chromatography on Fuji Silysia silica gel FL60D (hexane:EtOAc = 10:1−5:1). Diastereomer ratio (2.5:1) was determined by ^{1}H NMR analysis of the crude product before chromatography. The structure of major diastereomer was confirmed by single-crystal X-ray analysis.
(1*R**,2*S**)-**6aq** (major isomer): **^{1}H NMR** (400 MHz, $CDCl_3$) δ 7.32 (m, 1H; C_6HH_2H), 7.27 (m, 2H; C_6HH_2H), 7.18 (m, 1H; C_6HH_2H), 7.04 (brs, 1H; N*H*), 4.74 (d, ^3J = 4.4 Hz, 1H; HOC*H*CHNH), 4.24 (m, 1H; HOCHC*H*NH), 2.95 (m, 2H; $C_6H_4CH_2$), 2.01 (m, 2H; HNCHCH_2CH_2), 1.78 (brs, 1H; O*H*). **^{13}C NMR** (125 MHz, $CDCl_3$) δ 156.9 (q, ^2J = 36.6 Hz), 135.84, 135.77, 130.2, 129.3, 129.2, 126.9, 116.0(q, ^1J = 286.3 Hz), 68.2, 50.4, 28.1, 23.1. **^{19}F NMR** (376 MHz, $CDCl_3$) δ –77.2.
(1*R**,2*R**)-**6aq** (minor isomer): **^{1}H NMR** (400 MHz, $CDCl_3$) δ 7.53 (m, 1H; C_6HH_2H), 7.27 (m, 2H; C_6HH_2H), 7.14 (m, 1H; C_6HH_2H), 6.43 (brs, 1H; N*H*), 4.66 (d, ^3J = 7.6 Hz, 1H; HOC*H*CHNH), 4.15 (m, 1H; HOCHC*H*NH), 3.02 (m, 1H; C_6H_4CHH), 2.88 (m, 1H; C_6H_4CHH). 2.31 (m, 1H; HNCHC*H*HCH$_2$), 2.23 (brs, 1H; OH), 1.91 (m, 1H; HNCHC*H*HCH$_2$). **^{13}C NMR** (125 MHz, $CDCl_3$) δ 157.9 (q, ^2J = 36.9 Hz), 136.5, 135.2, 128.8, 128.4, 127.9, 127.0, 115.9 (q, ^1J = 286.3 Hz), 72.3, 54.0, 27.2, 26.0. **^{19}F NMR** (376 MHz, $CDCl_3$) δ –77.1. **HRMS** (ESI-TOF) calculated for [$C_{12}H_{12}F_3NO_2$+Na] requires 282.0712, found 282.0712.

_N_-((1-Hydroxycyclopentyl)methyl)-2,2,2-trifluoroacetamide (6am) and _N_-(cyclopent-1-en-ylmethyl)-2,2,2-trifluoroacetamide (7am)

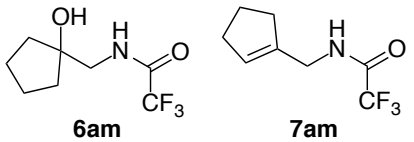

6am **7am**

The reaction of **5a** (76.4 mg, 0.402 mmol), methylenecyclopentane (**3m**) (66.1 mg, 0.805 mmol), $Sc(OTf)_3$ (39.5 mg, 80.3 μmol), and *fac*-$[Ir(ppy)_3]$ (5.2 mg, 7.94 μmol) following the general procedures afforded **6am** (30.7 mg, 36% yield, reaction time = 24 h) as a white solid and **7am** (18.2 mg, 23% yield) as a colorless oil after purification with flash column chromatography on Fuji Silysia silica gel FL60D (hexane:EtOAc = 10:1−5:1).

6am: **^{1}H NMR** (400 MHz, $CDCl_3$) δ 6.78 (brs, 1H; NH), 3.47 (d, ^3J = 5.6 Hz, 2H; HOCCH_2NH), 1.82 (m, 2H; cyclopentyl), 1.70 (m, 6H; cyclopentyl). 1.61 (brs, 1H; O*H*). **^{13}C NMR** (125 MHz, $CDCl_3$) δ 157.9 (q, ^2J = 37.0 Hz), 116.1 (q, ^1J = 285.8 Hz), 81.8, 48.6, 38.2, 23.8. **^{19}F NMR** (376 MHz, $CDCl_3$) δ −77.2. **HRMS** (ESI-TOF) calculated for $[C_8H_{12}F_3NO_2$+Na] requires 234.0712, found 234.0713.

7am: **^{1}H NMR** (400 MHz, $CDCl_3$) δ 6.42 (brs, 1H; N*H*), 5.59 (t, ^3J = 1.6 Hz, 1H; C=C*H*CH_2), 4.02 (d, ^3J = 5.6 Hz, 2H; CCH_2NH), 2.34 (m, 2H; CHC$H_2$$CH_2$), 2.29 (m, 2H; CC$H_2$$CH_2$), 1.93 (m, 2H; CCH_2C$H_2$$CH_2$). **^{13}C NMR** (125 MHz, $CDCl_3$) δ 157.2 (q, ^2J = 36.6 Hz), 138.8, 127.8, 116.0 (q, ^1J = 286.1 Hz), 40.3, 33.4, 32.4, 23.4. **^{19}F NMR** (376 MHz, $CDCl_3$) δ −77.2. **HRMS** (ESI-TOF) calculated for $[C_8H_{10}F_3NO$+Na] requires 216.0607, found 216.0604.

(*Z*)-*N*-(5-hydroxy-2,5-diphenylpent-2-ene-1-yl)-4-methylbenzenesulfonamide (9u)

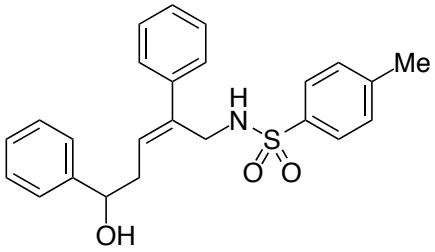

The reaction of 1-phenyl-2-(1-phenylethenyl)cycloprapane (**3u**) (88.0 mg, 0.399 mmol), **2a** (147.9 mg, 0.440 mmol) and **Ir-1** (2.6 mg, 3.97 μmol) following the general procedures afforded **9u** (117.3 mg, 72% yield, reaction time = 4 h) as a white solid after purification with column chromatography on Fuji Silysia silica gel FL60D (hexane:EtOAc = 4:1). The structure was confirmed by single-crystal X-ray analysis *vide infra*.

^{1}H NMR (400 MHz, $CDCl_3$, rt) δ 7.74 (d, ^3J = 8.0 Hz, 2H; $SO_2C_6H_2H_2CH_3$), 7.39-7.23 (m, 12H; Ar), 5.90 (t, ^3J = 8.0 Hz, 1H; C_6H_5CC*H*CH_2), 5.32 (m, 1H; N*H*), 4.81 (t, ^3J = 6.0 Hz, 1H; C*H*OH), 3.86 (m, 2H; CH_2NH), 2.46 (dd, ^3J = 8.4 Hz, ^3J = 6.0 Hz, 2H; HOCHCH_2), 2.45 (s, 3H; $SO_2C_6H_4CH_3$), 2.07 (brs, 1H; O*H*). **^{13}C NMR** (125 MHz, $CDCl_3$, rt) δ 143.8, 143.5, 140.7, 137.7, 136.6, 129.7, 128.8, 128.6, 128.1, 127.6, 127.5, 126.2, 125.7, 73.5, 42.0, 38.5, 21.7. **HRMS** (ESI-TOF) calculated for $[C_{24}H_{25}NO_3S$+Na]$^+$ requires 430.1447, found 430.1445.

1-Methyl-6a,7,8,9,10,10a-hexahydro-6*H*-dibenzo[*c*,*e*][1,2]thiazine 5,5-dioxide (10v)

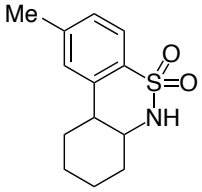

The reaction of cyclohexene (**3v**) (33.2 mg, 0.404 mmol), **2a** (201.9 mg, 0.601 mmol) and **Ir-1** (2.6 mg, 3.97 μmol) following the general procedures afforded **10v** (37.4 mg, 37% yield, reaction time was 12 h) as a white solid after purification with column chromatography on Fuji Silysia silica gel FL60D (hexane:EtOAc = 10:1). The structure was confirmed by single-crystal X-ray analysis *vide infra*.

^{1}H NMR (400 MHz, $CDCl_3$, rt) δ 7.73 (d, ^3J = 8.4 Hz, 2H; SO_2C_6HHH), 7.19 (m, 2H; SO_2C_6HHH), 4.28 (d, ^3J = 11.6 Hz, 1H), 3.53 (m, 1H; NHC*H*), 2.62 (m, 1H; C_6H_3CH), 2.52 (m, 1H; C_6H_3CHCHH), 2.39 (s, 3H; $C_6H_3CH_3$), 2.15 (m, 1H; NHCHC*H*H), 1.92 (m, 2H; $NHCH_2CHHCHHCH$), 1.48 (m, 3H; NHCHCH*H*CH*H*CH*H*), 1.38 (m, 1H; C_6H_3CHCHH). **^{13}C NMR** (125 MHz, $CDCl_3$, rt) δ 142.8, 138.7, 135.3, 128.2, 126.8, 124.5, 57.9, 42.7, 33.7, 29.5, 25.8, 25.3, 21.9. **HRMS** (ESI-TOF) calculated for $[C_{13}H_{17}NO_2S+Na]^+$ requires 274.0872, found 274.0873.

***N*-(2-Hydroxy-2-phenylethyl)-2,3,4,5,6-Pentafluoro-benzamide (4ba)**

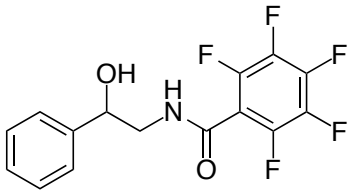

The reaction of styrene (**3a**) (45.9 mg, 0.441 mmol), **2b** (175.4 mg, 0.400 mmol) and **Ir-1** (2.7 mg, 4.12 μmol) following the general procedures afforded **4ba** (74.9 mg, 56% yield, reaction time = 12 h) as a white solid after purification with column chromatography on Fuji Silysia silica gel FL60D (hexane:EtOAc = 3:1).

^{1}H NMR (400 MHz, $CDCl_3$, rt) δ 7.40 (m, 4H; C_6H_4H), 7.34 (m, 1H; C_6H_4H), 6.34 (brs, 1H; N*H*), 4.97 (m, 1H; HOC*H*CHHNH), 3.96 (m, 1H; HOCHC*H*HNH), 3.51 (m, 1H; HOCHCH*H*NH), 2.45 (brs, 1H; O*H*). **^{19}F NMR** (376 MHZ, $CDCl_3$, rt) δ –141.5 (m), –151.7 (m), –161.2 (m). **^{13}C NMR** (125 MHz, CD_3OD, rt) δ 159.9, 146.1-144.1 (m), 144.3-142.3 (m), 143.7, 139.8-137.8 (m), 129.4, 128.8, 127.3, 113.5 (m), 73.2, 48.5. **HRMS** (ESI-TOF) calculated for $[C_{12}H_5F_5N_2OS+Na]^+$ requires 311.0214, found 311.0214.

***N*-(2-Hydroxy-2-phenylethyl)benzamide (6ba)**

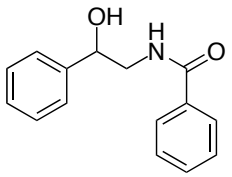

The reaction of 1-benzoyliminopyridinium ylide (**5b**) (79.5 mg, 0.401 mmol), styrene (**3a**) (83.1 mg, 0.798 mmol), $Sc(OTf)_3$ (38.9 mg, 79.0 μmol), and **Ir-1** (2.6 mg, 3.97 μmol) following the general procedures afforded **6ba** (43.4 mg, 45% yield, reaction time = 24 h) as a white solid after purification with flash column chromatography on Fuji Silysia silica gel (hexane:EtOAc = 5:1). The spectral data was identical with the reported data.[24c]

^{1}H NMR (400 MHz, $CDCl_3$) δ 7.76 (d, ^3J = 7.2 Hz, 2H; $C_6H_2H_3$), 7.75-7.29 (m, 8H; Ar), 6.56 (brs, 1H; N*H*), 4.98 (m, 1H; HOC*H*CH_2NH), 3.94 (m, 1H; HOCHC*H*HNH), 3.54 (m, 1H; HOCHCH*H*NH), 3.22 (brs, 1H; O*H*).

***tert*-Butyl N-(2-hydroxy-2-phenylethyl)carbamate (6ca)**

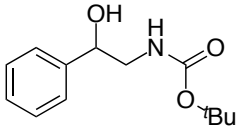

The reaction of *N-tert*-butoxycarbonyliminopyridinium ylide (**5c**) (78.0 mg, 0.402 mmol), **3a**

(83.4 mg, 0.801 mmol), $Sc(OTf)_3$ (39.7 mg, 80.7 μmol), and **Ir-1** (2.6 mg, 3.97 μmol) following the general procedures afforded **6ca** (55.2 mg, 58% yield, reaction time = 8 h) as a white solid after purification with flash column chromatography on Fuji Silysia SCAVENGER NH SILICA (hexane:EtOAc = 5:1). The spectral data was identical with the reported data.[24d]
^{1}H NMR (400 MHz, $CDCl_3$) δ 7.35 (m, 4H; Ar), 7.28 (m, 1H; Ar), 4.92 (brs, 1H; N*H*), 4.83 (m, 1H; HOC*H*CH_2), 3.49 (m, 1H; HOCHC*H*HNH), 3.26 (m, 1H; HOCHCH*H*NH), 3.01 (brs, 1H; O*H*), 1.45 (s, 9H; OC($C*H_3$)$_3$.

2-(2,2,2-Trichloroethoxycarbonylamino)-1-phenylethanol (6da)

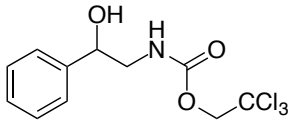

The reaction of 1-2,2,2-trichloroethoxycarbonyliminopyridinium ylide (**5d**) (108.2 mg, 0.401 mmol), **3a** (83.3 mg, 0.800 mmol), $Sc(OTf)_3$ (38.6 mg, 78.4 μmol), and **Ir-1** (2.6 mg, 3.97 μmol) following the general procedures afforded **6da** (67.3 mg, 54% yield, reaction time = 8 h) as a white solid after purification with flash column chromatography on Fuji Silysia SCAVENGER NH SILICA (hexane:EtOAc = 10:1–5:1–3:1).
^{1}H NMR (400 MHz, $CDCl_3$) δ 7.38-7.29 (m, 5H; Ar), 5.44 (brs, 1H; N*H*), 4.87 (m, 1H; HOC*H*CHHNH), 4.73 (s, 2H; CH_2CCl_3), 3.61 (m, 1H; HOCHC*H*HNH), 3.37 (m, 1H; HOCHCH*H*NH), 2.49 (brs, 1H; OH). **^{13}C NMR** (125 MHz, $CDCl_3$) δ 155.3, 141.3, 128.8, 128.4, 126.0, 95.6, 74.8, 73.5, 48.6. **HRMS** (ESI-TOF) calculated for [$C_{11}H_{12}Cl_3NO_3$+Na] requires 339.9775, found 339.9773.

2-(Allyloxycarbonylamino)-1-phenylethanol (6ea)

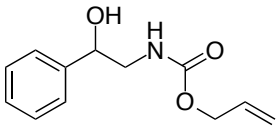

The reaction of *N*-allyloxycarbonyliminopyridinium ylide (**5e**) (71.3 mg, 0.400 mmol), **3a** (83.6 mg, 80.3 mmol), $Sc(OTf)_3$ (39.4 mg, 80.1 μmol), and **Ir-1** (2.8 mg, 4.28 μmol) following the general procedures afforded **6ea** (37.8 mg, 43% yield, reaction time = 8 h) as a white solid after purification with flash column chromatography on Fuji Silysia SCAVENGER NH SILICA (hexane:EtOAc = 5:1–3:1).
^{1}H NMR (400 MHz, $CDCl_3$) δ 7.37 (m, 4H; Ar), 7.32 (m, 1H; Ar), 5.92 (m, 1H; CH_2=C*H*CH_2O), 5.27 (m, 2H; CH_2=CHCH_2O), 5.13 (brs, 1H; N*H*), 4.85 (m, 1H; HOC*H*CH_2NH), 4.58 (m, 2H; CH_2=CHCH_2O), 3.56 (m, 1H; HOCHC*H*HNH), 3.32 (m, 1H; HOCHCH*H*NH), 2.71 (brs, 1H; O*H*).
^{13}C NMR (125 MHz, $CDCl_3$) δ 157.2, 141.7, 132.9, 128.7, 128.1, 126.0, 118.0, 73.8, 66.0, 48.6.
HRMS (ESI-TOF) calculated for [$C_{12}H_{15}F_3NO_3$+Na] requires 244.0944, found 244.0943.

Gram-scale aminohydroxylation of 4-methoxystyrene (3b)

To 4-methoxystyrene (**3b**) (0.671 g, 5.00 mmol) dissolved in a distilled-acetone (22.5 mL) and H_2O (degassed by N_2 bubbling) (2.5 mL) in a 50 mL-Schlenk tube, **2a** (1.85 g, 5.50 mmol) and **Ir-1** (32.8 mg, 50 μmol) were added under N_2. The tube was placed at a distance of 2~3 cm from the blue LED lamps (hν = 425 ± 15 nm). The resulting mixture was stirred at room temperature (water bath) under visible light irradiation for 15 h. Then, the reaction mixture was concentrated *in vacuo*. Products were extracted with CH_2Cl_2, dried (Na_2SO_4) and filtered. The filtrate was concentrated under reduced pressure. The residue was purified by flash column chromatography on Fuji Silysia silica gel FL60D (hexane:EtOAc = 5:1–3:1–2:1) to afford the product **4ab** (1.22 g, 76%).

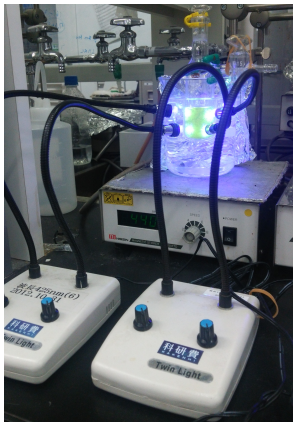

Deprotection of 6aa and 6ca

*Deprotection of **6aa** under basic conditions*

This deprotection was conducted according to the modified Nordlander's report.[25a] A mixture of **6aa** (63.0 mg, 0.270 mmol) and potassium carbonate (201 mg, 1.49 mmol) dissolved in MeOH (10 mL)-H_2O (0.6 mL) was reflux for 2 h. After cooling to room temperature, the mixture was concentrated *in vacuo*. Then, H_2O was poured into the mixture and extracted with CH_2Cl_2. The organic layer was washed with brine, dried over Na_2SO_4 and filtered. The filtrate was concentrated *in vacuo* to afford the 2-amion-1-phenylethanol (**8a**) (10.9 mg, 29% yield). The spectral data was identical with the reported data[25b].

^{1}H NMR (400 MHz, $CDCl_3$) δ 7.34 (m, 4H; Ar), 7.29 (m, 1H; Ar), 4.68 (dd, ^3J = 8.0 Hz, ^3J = 3.6 Hz, 1H; HOC*H*), 3.05 (dd, ^3J = 12.8 Hz, ^3J = 3.6 Hz, 1H; HNC*H*H), 2.85 (dd, ^3J = 12.8 Hz, ^3J = 8.0 Hz, 1H; HNCH*H*), 2.00 (brs, 3H; O*H* and NH_2 are overlapped).

*Deprotection of **6ca** under acidic conditions*

To **6ca** (55.2 mg, 0.233 mmol) was added hydrogen chloride (1.0 M in diethyl ether solution) under 0 ºC. The cooling bath was removed and the reaction mixture was stirred for 4 h at rt. Then, the mixture was concentrated *in vacuo*. The residue was washed with CH_2Cl_2 and dried *in vacuo* to afford **8a•HCl** (26.8 mg, 66% yield). The spectral data was identical with the reported data.[26c]

^{1}H NMR (400 MHz, DMSO-d_6) δ 8.15 (brs, 3H; NH_3Cl), 7.38 (m, 4H; Ar), 7.31 (m, 1H; Ar), 6.08 (brs, 1H; O*H*), 4.84 (dd, ^3J = 5.6 Hz, ^3J = 3.2 Hz, 1H; HOC*H*), 3.00 (m, 1H; H_3NC*H*H), 2.82 (m, 1H; H_3NCH*H*).

Luminescence quenching experiments (Figure 3.3, 3.4)

General experimental procedure: A solution of the Ir catalyst was prepared as to show the absorbance 0.1 exitation wavelength and degassed by three freeze-pump-thaw cycles in a 1 cm quartz cell equipped with an sphere moiety for freeze. The solution of quencher was added to the solution of the Ir catalyst before measurement of emission intensities.

Crystallographic data for 2a, (1*R**,2*S**)**-4an,** (1*R**2*S**)**-4aq, 9u, 10v,** (1*R**,2*S**)**-6aq**

Diffraction measurements were made on a Bruker SMART APEX II ULTRA/CCD. Intensity measurements were performed using monochromated (doubly curved silicon crystal) Mo-Kα-radiaiton (0.71073 Å) from a sealed microfocus tube. Data were acquired using three sets of Omega scans at different Phi settings. The frame width was 0.5 º. The crystallographic data are summarized in Table S4.1-6. The structural analysis was performed on an APEX2 software for preliminary determination of the unit cell. Determination of integrated intensities and unit cell refinement were performed using SAINT. Unless otherwise stated, all non-hydrogen atoms were refined anisotropically by full-matrix least-square techniques based on F^2. All hydrogen atoms were fixed at the calculated positions.

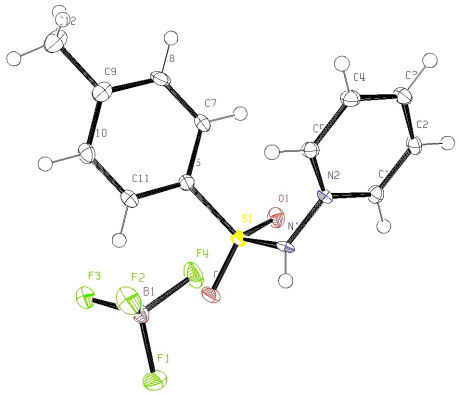

Figure S3.1. Crystal structure of **2a**

Table S3.1. Crystal data and structure refinement for 2a.

Identification code	KM960
Chemical formula	$C_{12}H_{13}BF_4N_2O_2S$
Formula weight	336.11
Temperature	90(2) K
Wavelength	0.71073 Å
Crystal size	0.024 x 0.095 x 0.128 mm
Crystal system	triclinic
Space group	P -1
Unit cell dimensions	a = 6.763(3) Å α = 92.242(5)° b = 8.057(3) Å β = 104.039(5)° c = 13.404(5) Å γ = 95.626(5)°
Volume	703.7(5) Å^3
Z	2
Density (calculated)	1.586 g/cm^3
Absorption coefficient	0.283 mm^{-1}
F(000)	344
Theta range for data collection	1.57 to 25.02°
Index ranges	-8<=h<=7, -9<=k<=9, -10<=l<=15
Reflections collected	3092
Independent reflections	2364 [R(int) = 0.0127]
Coverage of independent reflections	95.7%
Absorption correction	multi-scan
Max. and min. transmission	0.9930 and 0.9650
Refinement method	Full-matrix least-squares on F^2
Refinement program	SHELXL-2013 (Sheldrick, 2013)
Function minimized	Σ w(F$_o^2$ - Fc^2)^2
Data / restraints / parameters	2364 / 0 / 200
Goodness-of-fit on F^2	1.143
Final R indices	2103 data; I>2σ(I) R1 = 0.0482, wR2 = 0.1272 all data R1 = 0.0534, wR2 = 0.1296
Weighting scheme	w=1/[σ^2(F$_o^2$)+(0.0349P)^2+2.4236P] where P=(F$_o^2$+2F$_c^2$)/3
Largest diff. peak and hole	0.720 and -0.729 eÅ^{-3}
R.M.S. deviation from mean	0.081 eÅ^{-3}

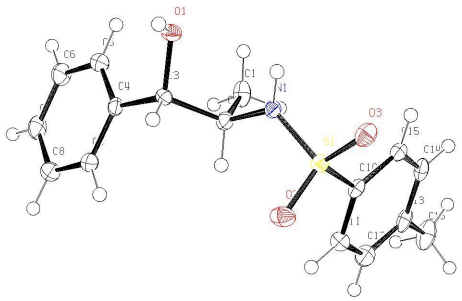

Figure S3.2. Crystal structure of **(1*R**,2*S**)-4an**

Table S3.2. Crystal data and structure refinement for (1*R,2*S**)-4an.**

Identification code	KM1112
Chemical formula	$C_{16}H_{19}NO_3S$
Formula weight	305.38
Temperature	90(2) K
Wavelength	0.71073 Å
Crystal size	0.044 x 0.072 x 0.316 mm
Crystal system	monoclinic
Space group	P 1 21/c 1
Unit cell dimensions	a = 10.7866(13) Å α = 90° b = 6.1972(8) Å β = 94.8720(10)° c = 23.326(3) Å γ = 90°
Volume	1553.6(3) Å^3
Z	4
Density (calculated)	1.306 g/cm^3
Absorption coefficient	0.218 mm^{-1}
F(000)	648
Theta range for data collection	1.75 to 25.03°
Index ranges	-11<=h<=12, -7<=k<=7, -27<=l<=19
Reflections collected	6583
Independent reflections	2687 [R(int) = 0.0164]
Coverage of independent reflections	97.7%
Absorption correction	multi-scan
Max. and min. transmission	0.9900 and 0.9340
Refinement method	Full-matrix least-squares on F^2
Refinement program	SHELXL-2013 (Sheldrick, 2013)
Function minimized	Σ w(F$_o^2$ - Fc^2)^2
Data / restraints / parameters	2687 / 0 / 193
Goodness-of-fit on F^2	1.273
Final R indices	2538 data; I>2σ(I) R1 = 0.0414, wR2 = 0.1201 all data R1 = 0.0431, wR2 = 0.1209
Weighting scheme	w=1/[σ^2(F$_o^2$)+(0.0097P)^2+3.5508P] where P=(F$_o^2$+2F$_c^2$)/3
Largest diff. peak and hole	0.595 and -0.660 eÅ^{-3}
R.M.S. deviation from mean	0.064 eÅ^{-3}

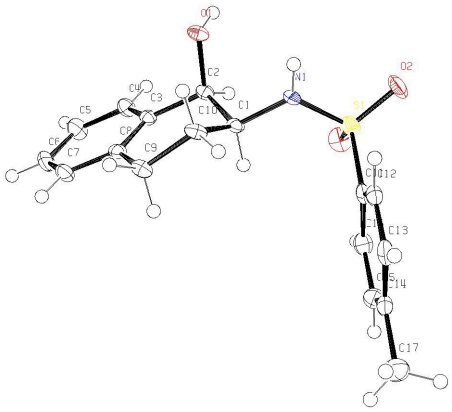

Figure S3.3. Crystal structure of **(1*R**2*S**)-4aq**

Table S3.3. Crystal data and structure refinement for (1*R2*S**)-4aq.**

Identification code	KM1140	
Chemical formula	$C_{17}H_{19}NO_3S$	
Formula weight	317.39	
Temperature	90(2) K	
Wavelength	0.71073 Å	
Crystal size	0.018 x 0.071 x 0.266 mm	
Crystal system	monoclinic	
Space group	P 1 21/c 1	
Unit cell dimensions	a = 11.751(3) Å	α = 90°
	b = 6.2897(15) Å	β = 94.964(3)°
	c = 21.205(5) Å	γ = 90°
Volume	1561.4(6) Å^3	
Z	4	
Density (calculated)	1.350 g/cm^3	
Absorption coefficient	0.219 mm^{-1}	
F(000)	672	
Theta range for data collection	1.93 to 25.03°	
Index ranges	-10<=h<=13, -7<=k<=7, -25<=l<=21	
Reflections collected	6582	
Independent reflections	2725 [R(int) = 0.0354]	
Coverage of independent reflections	98.9%	
Absorption correction	multi-scan	
Max. and min. transmission	0.9960 and 0.9440	
Refinement method	Full-matrix least-squares on F^2	
Refinement program	SHELXL-2013 (Sheldrick, 2013)	
Function minimized	$\Sigma\, w(F_o^2 - Fc^2)^2$	
Data / restraints / parameters	2725 / 0 / 201	
Goodness-of-fit on F^2	1.933	
Final R indices	2209 data; I>2σ(I)	R1 = 0.0501, wR2 = 0.0993
	all data	R1 = 0.0622, wR2 = 0.1017
Weighting scheme	$w=1/[\sigma^2(F_o^2)]$ where $P=(F_o^2+2F_c^2)/3$	
Largest diff. peak and hole	0.491 and -0.550 eÅ^{-3}	
R.M.S. deviation from mean	0.065 eÅ^{-3}	

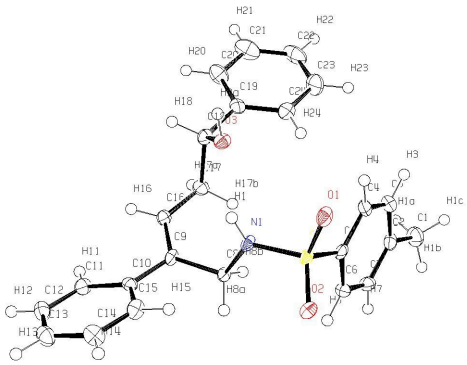

Figure S3.4. Crystal structure of **9u**

Table S3.4. Crystal data and structure refinement for 9u.

Identification code	KM1092
Chemical formula	$C_{25}H_{27}Cl_2NO_3S$
Formula weight	492.43
Temperature	90(2) K
Wavelength	0.71073 Å
Crystal size	0.038 x 0.088 x 0.195 mm
Crystal system	monoclinic
Space group	P 1 21/c 1
Unit cell dimensions	a = 11.7804(16) Å α = 90°
	b = 27.069(4) Å β = 90°
	c = 15.069(2) Å γ = 90°
Volume	4805.3(11) Å^3
Z	8
Density (calculated)	1.361 g/cm^3
Absorption coefficient	0.384 mm^{-1}
F(000)	2064
Theta range for data collection	1.50 to 25.03°
Index ranges	-9<=h<=14, -32<=k<=26, -17<=l<=17
Reflections collected	12090
Independent reflections	4693 [R(int) = 0.0305]
Coverage of independent reflections	55.4%
Absorption correction	multi-scan
Max. and min. transmission	0.9860 and 0.9290
Refinement method	Full-matrix least-squares on F^2
Refinement program	SHELXL-2013 (Sheldrick, 2013)
Function minimized	Σ w(F$_o^2$ - F$_c^2$)^2
Data / restraints / parameters	4693 / 0 / 581
Goodness-of-fit on F^2	0.999
Final R indices	4060 data; I>2σ(I) R1 = 0.0666, wR2 = 0.1962
	all data R1 = 0.0731, wR2 = 0.2015
Weighting scheme	w=1/[σ^2(F$_o^2$)+(0.1283P)^2+12.6085P] where P=(F$_o^2$+2F$_c^2$)/3
Absolute structure parameter	0.0(0)
Largest diff. peak and hole	0.826 and -0.470 eÅ^{-3}
R.M.S. deviation from mean	0.104 eÅ^{-3}

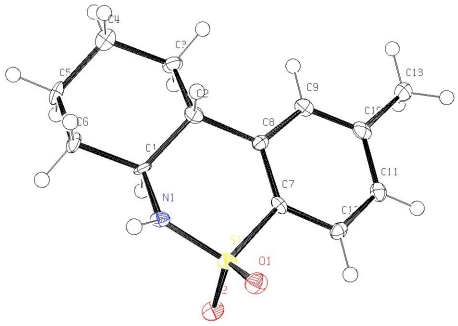

Figure S3.5. Crystal structure of **10v**

Table S3.5. Crystal data and structure refinement for 10v.

Identification code	KM1014_2	
Chemical formula	$C_{13}H_{17}NO_2S$	
Formula weight	251.33	
Temperature	90(2) K	
Wavelength	0.71073 Å	
Crystal size	0.010 x 0.080 x 1.021 mm	
Crystal system	orthorhombic	
Space group	P n a 21	
Unit cell dimensions	a = 29.943(3) Å	α = 90°
	b = 7.8956(8) Å	β = 90°
	c = 5.1010(5) Å	γ = 90°
Volume	1206.0(2) Å^3	
Z	4	
Density (calculated)	1.384 g/cm^3	
Absorption coefficient	0.258 mm^{-1}	
F(000)	536	
Theta range for data collection	1.36 to 25.02°	
Index ranges	-31<=h<=35, -7<=k<=9, -6<=l<=6	
Reflections collected	5459	
Independent reflections	2107 [R(int) = 0.0150]	
Coverage of independent reflections	99.6%	
Absorption correction	multi-scan	
Max. and min. transmission	0.9970 and 0.7790	
Refinement method	Full-matrix least-squares on F^2	
Refinement program	SHELXL-2013 (Sheldrick, 2013)	
Function minimized	$\Sigma\, w(F_o^2 - Fc^2)^2$	
Data / restraints / parameters	2107 / 1 / 155	
Goodness-of-fit on F^2	1.226	
Final R indices	2095 data; I>2σ(I)	R1 = 0.0493, wR2 = 0.1185
	all data	R1 = 0.0495, wR2 = 0.1186
Weighting scheme	$w=1/[\sigma^2(F_o^2)+(0.0270P)^2+3.3018P]$ where $P=(F_o^2+2F_c^2)/3$	
Absolute structure parameter	0.3(0)	
Largest diff. peak and hole	0.621 and -0.365 eÅ^{-3}	
R.M.S. deviation from mean	0.078 eÅ^{-3}	

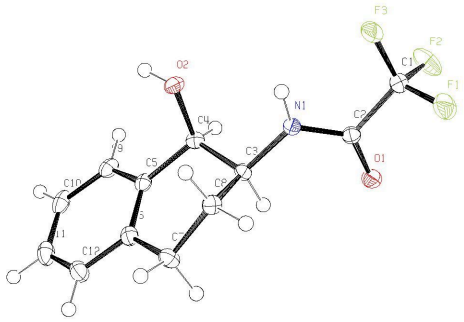

Figure S3.6. Crystal structure of 0f (1*R**,2*S**)-**6aq**

Table S3.6. Sample and crystal data for KM1539_1.

Identification code	KM1539_1
Chemical formula	$C_{12}H_{12}F_3NO_2$
Formula weight	259.23
Temperature	90(2) K
Wavelength	0.71073 Å
Crystal size	0.080 x 0.201 x 0.207 mm
Crystal system	monoclinic
Space group	P 1 21/c 1
Unit cell dimensions	a = 12.2403(8) Å α = 90°
	b = 10.6582(7) Å β = 110.0580(10)°
	c = 9.3065(7) Å γ = 90°
Volume	1140.48(14) Å^3
Z	4
Density (calculated)	1.510 g/cm^3
Absorption coefficient	0.135 mm^{-1}
F(000)	536
Theta range for data collection	1.77 to 25.02°
Index ranges	-10<=h<=14, -12<=k<=12, -11<=l<=6
Reflections collected	5289
Independent reflections	2003 [R(int) = 0.0111]
Coverage of independent reflections	99.4%
Absorption correction	multi-scan
Max. and min. transmission	0.9890 and 0.9730
Refinement method	Full-matrix least-squares on F^2
Refinement program	SHELXL-2013 (Sheldrick, 2013)
Function minimized	Σ w(F$_o^2$ - Fc^2)^2
Data / restraints / parameters	2003 / 0 / 164
Goodness-of-fit on F^2	1.056
Final R indices	1919 data; I>2σ(I) R1 = 0.0281, wR2 = 0.0746
	all data R1 = 0.0291, wR2 = 0.0755
Weighting scheme	w=1/[σ^2(F$_o^2$)+(0.0357P)^2+0.5600P] where P=(F$_o^2$+2F$_c^2$)/3
Largest diff. peak and hole	0.262 and -0.247 eÅ^{-3}
R.M.S. deviation from mean	0.037 eÅ^{-3}

3.5 References

1 Y. Yasu, T. Koike, M. Akita, *Angew. Chem. Int. Ed.* **2012**, *51,* 9567-9571.

2 (a) D. J. Ager, I. Prakash, D. R. Schaad, *Chem. Rev.* **1996**, *96,* 835-875; (b) S. C. Bergmeier, *Tetrahedron* **2000**, *56,* 2561-2576; (c) O. K. Karjalainen, A. M. P. Koskinen, *Org. Biomol. Chem.* **2012**, *10,* 4311-4326.

3 For recent reviews on metal-catalyzed aminooxygenation, see: (a) S. R. Chemler, *Org. Biomol. Chem.* **2009**, *7,* 3009-3019; (b) F. Cardona, A. Goti, *Nat. Chem.* **2009**, *1,* 269-275; (c) T. J. Donohoe, C. K. A. Callens, A. Flores, A. R. Lacy, A. H. Rathi, *Chem. Eur. J.* **2011**, *17,* 58-76; (d) K. S. Williamson, D. J. Michaelis, T. P. Yoon, *Chem. Rev.* **2014**, *114,* 8016-8036.

4 For selected reports on aminooxygenation, see: (a) M. Noack, R. Göttlich, *Chem. Commun.* **2002***,* 536-537; (b) A. Padwa, T. Stengel, *Org. Lett.* **2002**, *4,* 2137-2139; (c) E. Levites-Agababa, E. Menhaji, L. N. Perlson, C. M. Rojas, *Org. Lett.* **2002**, *4,* 2137-2139; (d) E. J. Alexanian, C. Lee, E. J. Sorensen, *J. Am. Chem. Soc.* **2005**, *127,* 7690-7691; (e) P. Szolcsényi, T. Gracza, *Chem. Commun.* **2005**, 3948-3950; (f) G. Liu, M. S. S. Stahl, *J. Am. Chem. Soc.* **2006**, *128,* 7179-7181; (g) L. V. Desai, M. S. Sanford, *Angew. Chem. Int. Ed.* **2007**, *119,* 5839-5842; (h) D. J. Michaelis, C. J. Shaffer, T. P. Yoon, *J. Am. Chem. Soc.* **2007**, *129,* 1866-1867; (i) P. H. Fuller, J.-W. Kim, S. R. Chemler, *J. Am. Chem. Soc.* **2008**, *130,* 17638-17639; (j) B. M. Cochran, F. E. Michael, *Org. Lett.* **2008**, *10,* 5039-5042; (k) H.-C. Xu, K. D. Moeller, *J. Am. Chem. Soc.* **2008**, *130,* 13542-13543; (l) M. C. Paderes, S. R. Chemler, *Org. Lett.* **2009**, *11,* 1915-1918; (m) D. J. Michaelis, K. S. Williamson, T. P. Yoon, *Tetrahedron* **2009**, *65,* 5118-5124 (n) K. Muñiz, A. Iglesias, Y. Fang, *Chem. Commun.* **2009**, *11,* 5591-5593; (o) S. Beaumont, V. Pons, P. Retailleau, R. H. Dodd, P. Dauban, *Angew. Chem. Int. Ed.* **2010**, *49,* 1634-1637; (p) D. E.

Mancheno, A. R. Thornton, A. H. Stoll, A. Kong, S. B. Blakey, *Org. Lett.* **2010**, *12,* 4110-4113; (q) D. J. Wardrop, E. G. Bowen, R. E. Forslund, A. D. Sussman, S. L. Weerasekera, *J. Am. Chem. Soc.* **2010**, *132,* 1188-1189; (r) K. S. Williamson, T. P. Yoon, *J. Am. Chem. Soc.* **2010**, *132,* 4570-4572; (s) V. A. Schmidt, E. J. Alexanian, *J. Am. Chem. Soc.* **2011**, *133,* 11402-11405; (t) T. de Haro, C. Nevado, *Angew. Chem. Int. Ed.* **2011**, *50,* 906-910; (u) K. S. Williamson, T. P. Yoon, *J. Am. Chem. Soc.* **2012**, *134,* 12370-12373; (v) G.-S. Liu, Y.-Q. Zhang, Y.-A. Yuan, H. Xu, *J. Am. Chem. Soc.* **2013**, *135,* 3343-3346; (w) D.-F. Lu, C.-L. Zhu, Z.-X. Jia, H. Xu, *J. Am. Chem. Soc.* **2014**, *136,* 13186-13189; (x) Y. Li, M. Hartmann, C. G. Daniliuc, A. Studer, *Chem. Commun.* **2015**, *51,* 5706-5709.

5 For selected reviews on Os-catalyzed aminohydroxylation, see: (a) O. Reiser, *Angew. Chem. Int. Ed. Engl.* **1996**, *35,* 1308-1309; (b) P. O'Brien, *Angew. Chem. Int. Ed.* **1999**, *38,* 326-329; (c) D. Nilov, O. Reiser, *Adv. Synth. Catal.* **2002**, *344,* 1169-1173; (d) J. A. Bodkin, M. D. McLeod, *J. Chem. Soc. Perkin Trans. 1* **2002**, 2733-2746; (e) K. Muñiz, *Chem. Soc. Rev.* **2004**, *33,* 166-174; (f) S. D. R. Christie, A.D. Warrington, *Synthesis* **2008**, 1325-1341.

6 K. B. Sharpless, A. O. Chong, K. Oshima, *J. Org. Chem.* **1976**, *41,* 177-179; (b) G. Li, H.-T. Chang, K. B. Sharpless, *Angew. Chem. Int. Ed. Engl.* **1996**, *35,* 451-454; (c) G. Li, H. H. Angert, K. B. Sharpless, *Angew. Chem. Int. Ed. Engl.* **1996**, *35,* 2813-2817; (d) M. Bruncko, G. Schlingloff, K. B. Sharpless, *Angew. Chem. Int. Ed. Engl.* **1997**, *109,* 1580-1583; (e) K. Laxma, K. B. Sharpress, *J. Am. Chem. Soc.* **1998**, *120,* 1207-1217.

7 A. J. Borah, P. Phukan, *Tetrahedron Lett.* **2014**, *55,* 713-715.

8 For selected reviews on photoredox catalysis, see: (a) T. P. Yoon, M. A. Ischay, J. Du, *Nat. Chem.* **2010**, *2,* 527-532; (b) J. M. R. Narayanam, C. R. J. Stephenson,

Chem. Soc. Rev. **2011**, *40,* 102-113; (c) J. Xuan, W.-J. Xiao, *Angew. Chem. Int. Ed.* **2012**, *51,*6828-6838; (d) C. K. Prier, D. A. Rankic, D. W. C. MacMillan, *Chem. Rev.* **2013**, *113,* 5322-5363; (e) D. P. Hari, B. König, *Angew. Chem. Int. Ed.* **2013**, *52,* 4734-4743; (f) M. Reckenthäler, A. G. Griesbeck, *Adv. Synth. Catal.* **2013**, *355,* 2727-2744; (g) M. N. Hopkinson, B. Sahoo, J.-L. Li, F. Glorius, *Chem. Eur. J.* **2014**, *20,* 3874-3886; (h) T. Koike, M. Akita, *Inorg. Chem. Front.* **2014**, *20,* 3874-3886.

9 For related reviews, see: (a) J. Hu, J. Wang, T. H. Nguyen, N. Zheng, *Beilstein J. Org. Chem.* **2013**, *9,* 1977-2001; (b) J.-R. Chen, X.-Q. Hu, L.Q. Lu, W.-J. Xiao, *Chem. Soc. Rev.* **2016**, *45,* 2044-2056; For selected reports, see: (c) M. Zhu, N. Zheng, *Synlett* **2011**, 2223-2236; (d) S. Maity, N. Zheng, *Angew. Chem. Int. Ed.* **2012**, *51,* 9562-9566; (e) G. Cecere, C. M. Konig, J. L. Alleva, D. W. C. MacMillan, *J. Am. Chem. Soc.* **2013**, *135,* 11521-11524; (f) H. Kim, T. Kim, D. G. Lee, S. W. Roh, C. Lee, *Chem. Commun.* **2014**, *50,* 9273-9276; (g) L. J. Allen, P. J. Cabrera, M. Lee, M. S. Sanford *J. Am. Chem. Soc.* **2014**, *136,* 5607-5610; (h) Q. Qin, S. Yu, *Org. Lett.* **2014**, *16,* 3504-3507; (i) J.-D. Wang, Y.-X. Liu, D. Xue, C. Wang, J. Xiao, *Synlett* **2014**, 2013-2018; (j) X.-Q. Hu, J.-R. Chen, Q. Wei, J.-L. Liu, Q.-H. Deng, A. M. Beauchemin, W.-J. Xiao, *Angew. Chem. Int. Ed.* **2014**, *53,* 12163-12167; (k) A. J. Musacchio, L Q. Nguyen, G. H. Beard, R. R. Knowles, *J. Am. Chem. Soc.* **2014**, *136,* 12217-12220; (l) T. W. Greulich, C. G. Daniliuc, A. Studer, *Org. Lett.* **2015**, *17,* 254-257; (m) H. Jiang, X. An, K. Tong, T. Zheng, Y. Zhang, S. Yu, *Angew. Chem. Int. Ed.* **2015**, *54,* 4055-4059; (n) G. Pandey, R. Laha, *Angew. Chem. Int. Ed.* **2015**, *54,* 14875-14879; (o) K. Miyazawa, T. Koike, M. Akita, *Chem. Eur. J.* **2015**, *21,* 11677-11680; (p) J. Davies, S. G. Booth, S. Essafi, R. A. W. Dryfe, D. Leonori, *Angew. Chem. Int. Ed.* **2015**, *54,* 14017-14021; (q) G.

Fumagalli, P. T. G. Rabet, S. Boyd, M. F. Greaney, *Angew. Chem. Int. Ed.* **2015**, *54,* 11481-11484; (r) D. C. Miller, R. R. Knowles, *J. Am. Chem. Soc.* **2015**, *137,* 13492-13495; (s) Q. Qin, D. S; Yu, *Org. Lett.* **2015**, *17,* 1894-1897; (t) Q. Qin, D. Ren, S. Yu, *Org. Biomol. Chem.* **2015**, *13,* 10295-10298; For other reactions of active nitrogen species, see: (u) Y. Chen, A. S. Kamlet, J. B. Steinman, D. R. Liu, *Nat. Chem.* **2011**, *3,* 146-153; (v) J. Xuan, X.-D. Xia, T.-T. Zeng, Z.-J. Zeng, J.-R. Chen, L.-Q. Lu, W.-J. Xiao, *Angew. Chem. Int. Ed.* **2014**, *53,* 5653-5656; (w) E. P. Farney, T. P. Yoon, *Angew. Chem. Int. Ed.* **2014**, *53,* 793-797; (x) E. Brachet, T. Ghosh, I. Ghosh, B. König, *Chem. Sci.* **2015**, *6,* 987-992.

10 (a) M. E. Wolff, *Chem. Rev.* **1963**, *63,* 55-64; (b) R. Carrau, R. Hernández, E. Suárez, *J. Chem. Soc., Perkin Tans. 1* **1987***,* 937-943; (c) R. Freire, A. Martín, I. Pérez-Martín, E. Suárez, *Tetrahedron Lett.* **2002**, *43,* 5113-5116; (d) C. G. Francisco, A. J. Herrera, E. Suárez, *J. Org. Chem.* **2003**, *68,* 1012-1017; (e) A. Martín, I. Pérez-Martín, E. Suárez, *Org. Lett.* **2005**, *7,* 2027-2030; (f) C. G. Francisco, A. J. Herrera, Á. Martín, I. Pérez-Martín, E. Suárez, *Tetrahedron Lett.* **2007**, *48,* 6384-6388; (g) H. Lu, Y. Hu, H. Jiang, L. Wojtas, X. Peter Zhang, *Org. Lett.* **2012**, *14,* 5158-5161.

11 (a) H.-H. Liu, Y. Wang, G. Deng, L. Yang, *Adv. Synth. Catal.* **2013**, *355,* 3369-3374; (b) G. B. Boursalian, M.-Y. Ngai, K. N. Hojczyk, T. Ritter, *J. Am. Chem. Soc.* **2013**, *135,* 13278-13281; (c) K. Foo, E. Sella,I. Thomé, M. D. Eastgate, P. S. Baran, *J. Am. Chem. Soc.* **2014**, *136,* 5279-5282; (d) T. Kawakami, K. Murakami, K. Itami, *J. Am. Chem. Soc.* **2015**, *137,* 2460-2463.

12 For recent reports see: (a) Z. Shunjun, K. Liu, C. Li, *J. Org. Chem.* **2011**, *76,* 8100-8106; (b) A. J. Clark, R. P. Filik, G. H. Thomas, J. Sherringham, *Tetrahedron Lett.* **2013**, *54,* 4094-4097; (c) G. Han, Y. Liu, Q. Wang, *Org. Lett.* **2013**, *15,*

5334-5337; (d) H.-C. Xu, J. M. Campbell, K. D. Moeller, *J. Org. Chem.* **2014**, *79,* 379-391; (e) H. Zhang, Y. Song, J. Zhao, J. Zhang, Q. Zhang, *Angew. Chem. Int. Ed.* **2014**, *53,* 11079-11083; (f) J. Chen, W.-Q. Yan, C. M. Lam, C.-C. Zeng, L.-M. Hu, R. D. Little, *Org. Lett.* **2015**, *17,* 986-989; (g) Y. Li, M. Hartmann, C. G. Daniliuc, A. Studer, *Chem. Commun.* **2015**, *51,* 5706-5709; (h) P. Xiong, F. Xu, X.-Y. Qian, Y. Yohannes, J. Song, X. Lu, H.-C. Xu, *Chem. Eur. J.* **2016**, *22,* 4379-4383; (i) L. Zhu, P. Xiog, Z.-Y. Mao, Y.-H. Wang, W. X. Yan, X. Lu, H.-C. Xu, *Angew. Chem. Int. Ed.* **2016**, *55,* 2226-2229.

13 G. Qiu, Y. Kuang, J. Wu, *Adv. Synth. Catal.* **2014**, *356,* 3483-3504.

14 Molecular structure of **7a**, (1*R**,2*S**)-**9an**, (1*R**,2*S**)-**9aq**, **14s**(*trans*), **15u** and (1*R**,2*S**)-**9an** are shown in the Supporting Information. CCDC 1049306, CCDC1052558, CCDC 1052559, CCDC 1052560, CCDC 1049305 and CCDC 1470156 respectively, contain the supplementary crystallographic data, respectively. These data can be obtained free of charge from The Cambridge Crystallographic Data Center via www.ccdc.cam.ac.uk/data request/cif.

15 The photoexcited states of *fac*-[Ir(ppy)$_3$] and [Ir(ppy)$_2$(dtbbpy)]$^+$ are reductants ($E_{1/2}$ = –2.14 V and –1.37 V vs. Cp_2Fe) stronger than the Ru photocatalyst, [Ru(bpy)$_3$]$^{2+}$ ($E_{1/2}$ = –1.22 V vs. Cp_2Fe), see: (a) L. Flamigni, A. Barbieri, C. Sabatini, B. Ventura, F. Barigelletti, *Top. Curr. Chem.* **2007**, *281,* 143-203; (b) K. Kalyanasundaram, *Cood. Chem. Rev.* **1982**, *46,* 159-244; (c) J. D. Slinker, A. A. Gorodetsky, M. S. Lowry, J. Wang, S. Parker, R. Rohl, S. Bernhard, G. G. Malliaras, *J. Am. Chem. Soc.* **2004**, *126,* 2763-2767.

16 S. Kobayashi, K. Manabe, *Acc. Chem. Res.* **2002**, *35,* 209-217.

17 (a) J. D. Elliott, V. M. F. Choi, W. S. Johnson, *J. Org. Chem.* **1983**, *48,* 2294-2295; (b) J. E. Nordlander, M. J. Payne, F. G. Njoroge, M. A. Balk, G. D. Laikos, V. M.

Vishwanath, *J. Org. Chem.* **1984**, *49,* 4107-4111; (c) T. Izumi, K. Fukaya, *Bull. Chem. Soc. Jpn.* **1993**, *66,* 1216-1221; (d) A. Kawamoto, M. Wills, *Tetrahedron Asymmetry* **2000**, *11,* 3257-3261; (e) T. Ohkuma, D. Ishii, H. Takeno, R. Noyori, *J. Am. Chem. Soc.* **2000**, *122,* 6510-6511; (f) S. Kats, S. C. Bergmeier, *Tetrahedron Lett.* **2002**, *43,* 557-559; (g) V. Nesterenko, K. S. Putt, P. J. Hergenrother, *J. Am. Chem. Soc.* **2003**, *125,* 14672-14673; (h) A. Kamal, G. B. R. Khanna, T. Krishnaji, R. Ramu, *Bioorg. Med. Chem. Lett.* **2005**, *15,* 613-615; (i) S. K. Tanielyan, N. Marin, G. Alvez, R. L. Augustine, *Org. Process Rev. Dev.* **2006**, *10,* 893-898; (j) Z. Xu, Y. Li, J. Liu, N. Wu, K. Li, S. Zhu, R. Zhang, Y. Liu *Org. Biomol. Chem.* **2015**, *13,* 7513-7516.

18 (a) J. Guin, R. Fröhlich, A. Studer, *Angew. Chem. Int. Ed.* **2008**, *47,* 779-782; (b) C.-M. Chou, J. Guin, C. Mück-Lichtenfeld, S. Grimme, A. Studer, *Chem. Asian. J.* **2011**, *6,* 1197-1209.

19 (a) A. B. Tamayo, B. D. Alleyne, P. I. Djurovich, S. Lamansky, I. Tsyba, N. N. Ho, R. Bau, M. E. Thompson, *J. Am. Chem. Soc.* **2003**, *125,* 7377-7387. b) H. B. Ross, M. Boldaji, D. P. Rilema, C. B. Blanton and R. P. White, *Inorg, Chem.* **1989**, *28*, 1013-1021. c) J. D. Slinker, A. A. Gorodetsky, M. S. Lowry, J. Wang, S. Parker, R. Rohl, S. Bernhard, G. G. Milliaras, *J. Am. Chem. Soc*. **2004**, *126*, 2763-2767.

20 a) J. N. Cambre, D. Roy, S. R. Gondi, B. S. Sumerlin, *J. Am. Chem. Soc.* **2007**, *129*, 10348-10349. b) Y. Yasu, T. Koike, M. Akita, *Org. Lett.* **2013**, *15*, 2136-2139. c) S. N. Aslam, P. C. Stevenson, S. J. Phythian, N. C. Veitch, D. R. Hall, *Tetrahedeon* **2006**, *62*, 4214-4226.

21 a) C. Li, L. Zhang, *Org. Lett.* **2011**, *13*, 1738-1741. b) M. Itoh, K. Hirano, T. Satoh, M. Miura, *Org. Lett.* **2014**, *16*, 2050-2053. c) E. J. Corey, M. Chaykocsky, *J. Am. Chem. Soc.* **1965**, *87*, 1353-1364. d) P. Brandt, P. Norrby, A. M. Daly, D. G.

Gilheanyl, *Chem. Eur. J.* **2002**, *8*, 4299-4307.

22 a) J. Llaveria, A. Espinoza, G. Negrón, M. I. Matheu, S. Castillón, *Tetrahedron Lett*. **2012**, *53*, 2525-2529. b) S. Gandhi, A. Bisai, B. A. B. Prasad, V. K. Singh, *J. Org. Chem.* **2007**, *72*, 2133-2142. c) S. Fernandez, E. Klemm, *J. Prakt. Chem.* **1998**, *340*, 178-180. d) F. A. Davis, Zhou, G. V. Reddy, *J. Org. Chem.* **1994**, *59*, 3243-3245. e) M. Pineschi, F. Bertolini, R. M. Haak, P. Crotti, F. Macchia, *Chem. Commun*. **2005**, 1426-1428.

23 J. J. Mousseau, J. A. Bull, C. L. Ladd, A. Fortier, D. S. Roman, A. B. Charette, *J. Org. Chem.* **2011**, *76,* 8243-8261.

24 (a) D. Albanese, D. Landini, M. Penso, *Tetrahedron* **1997**, *53,* 4787-4790; (b) F. Dufrasne, J. Néve, *Monatshefte für Chemie* **2005**, *136,* 739-746. (c) R. Kuwano, N. Kameyama, R. Ikeda, *J. Am. Chem. Soc.* **2011**, *133,* 7312-7315; (d) T. Yamada, A. Kondoh, M. Terada, *J. Am. Chem. Soc.* **2015**, *137,* 1048-1051.

25 (a) J. E. Nordlander, M. J. Payne, F. G. Njoroge, M. A. Balk, G. D. Laikos, V. M. Vishwanath, *J. Org. Chem.* **1984**, *49,* 4107-4111; (b) J. H. Schrittwieser, F. Coccia, S. Kara, B. Grischek, W. Kroutil, N. d'Alessandro, F. Hollmann, *Green Chem.* **2013**, *15,* 3318-3331; (c) C. R. Noe, M. Knollmüller, P. Gärtner, W. Fleischhacker, E. Katikarides, *Monatshefte für Chemie* **1995**, *126,* 481-494.

Chapter 4

Direct Aroyloxylation of Arenes with Aroyloxypyridinium Salts by Photoredox Catalysis

ABSTRACT: A simple strategy for generation of aroyloxy radicals by photoredox catalysis has been developed. Aroyloxylpyridinium salts are the key compounds and serve as oxygen-radical precursors by the action of *fac*-[Ir(ppy)$_3$]. The resultant aroyloxy radicals undergo homolytic aromatic substitution of electron-rich arenes to afford aryl benzoate derivatives.

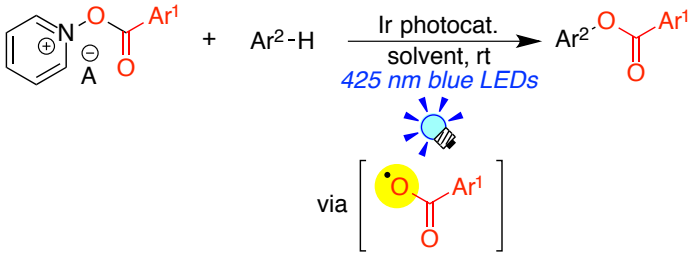

4.1 Introduction

In chapter 3, the author described that effective and regioselective aminohydroxylation of olefins by photoredox catalysis on the basis of generation and control of *N*-centered radicals from *N*-protected aminopyridinium salts and yildes. The result encouraged him to examine the generation of oxygen-centered radicals and to develop the effective method for radical C-O bond formations. In particular, since aromatic compounds with C-O bonds are frequently observed in natural products, drugs, and bioactive compounds (Figure 4.1),[1] development of the method for C(aromatic)-O bond formation is significantly important in the organic synthesis.

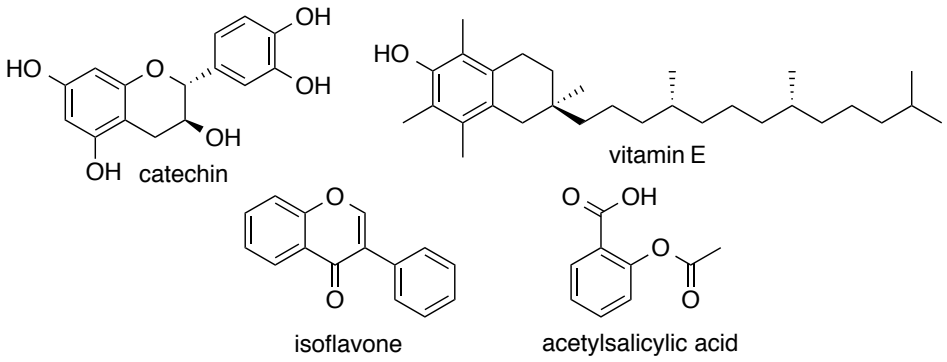

Figure 4.1 Examples of bioactive compounds with aromatic C-O bonds.

Hydroxy radical (•OH), which is generated by Fenton reaction,[2a] has been used for decomposition of organic compounds (Scheme 4.1),[2b] implying that it is too reactive to control the reactivity of •OH.

$$Fe^{II} + H_2O_2 \longrightarrow Fe^{III} + {}^{\bullet}OH + {}^{\ominus}OH$$

$$Fe^{III} + H_2O_2 \longrightarrow Fe^{II} + {}^{\bullet}OOH + {}^{\oplus}H$$

Scheme 4.1 Fenton reaction.

On the other hand, alkoxy radicals have been applied to synthetic methods to some

extent. They are electrophilic and highly reactive intermediates to cause addition to olefin, H-abstraction and β–scission (chapter 1).[3] But again their high reactivity causes limitation of their application. In contrast to those oxygen-centered radical species, the author turned his attention to carboxy radical, especially aromatic carboxy radicals, so-called aroyloxy radicals. carboxy radicals are much more stable tha the hydroxyl and alkoxy radicals due to π-stabilization.

Because of carboxy radical, aroyloxy radicals are more stable than alkyl ones to result in slower decarboxylation (Scheme 4.2 (a)).[4] Alkyl substituted carboxyl radical readily undergo decarboxylation to give the corresponding alkyl radical. Minisci reaction associated with decarboxylation is well-known reaction for homolytic aromatic substitution (Scheme 4.2 (b)).[5] As shown in Scheme 4.2 (c), homolytic aromatic substitution by aroyloxy radical will be discussed in the present chapter.

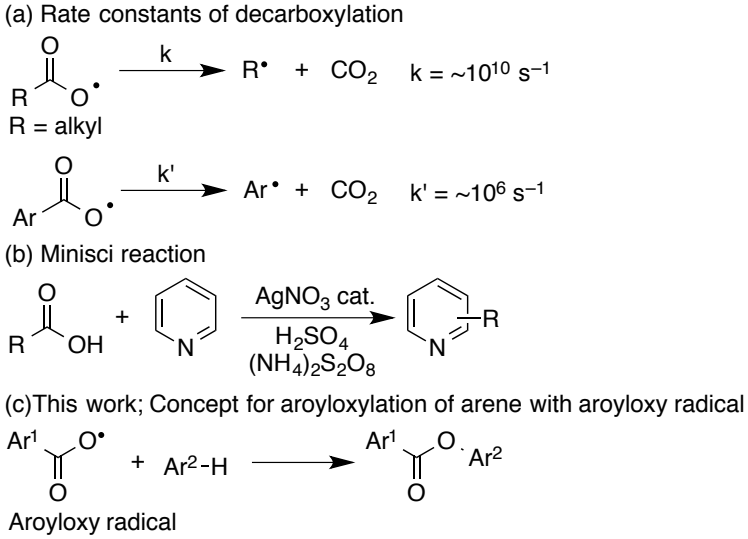

Scheme 4.2 (a) Rate constants of decarboxylation, (b) Minisci reaction, and (c) this work.

Homolytic aromatic substitution with benzoyl peroxide via a benzoyloxy radical has been studied extensively as typically exemplified by the classical report made by Kurz

and Kovanic (Scheme 4.3 (a)).[6a] Recently, Houk and Siegel and co-workers reported that oxidation of arenes with phthaloyl peroxide via the diradical resulted in production of phenol derivatives after hydrolysis. (Scheme 4.3 (b)).[6c]

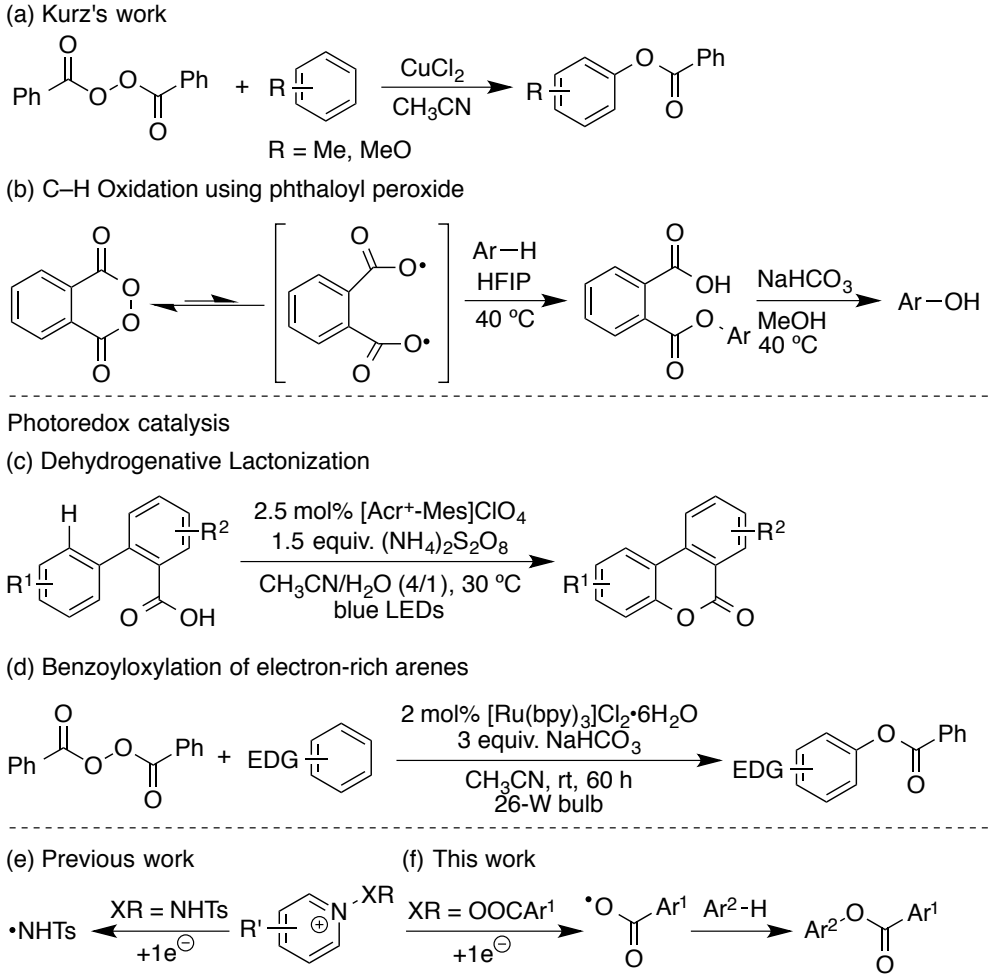

Scheme 4.3 Aroyloxylation of arenes by photoredox catalysis.

Photoredox catalysis[7] induced the generation of aroyloxy radical species. Gonzalez-Gomez and co-workers developed intramolecular lactonization via oxidation of the carboxylic acid by acridinium photocatalyst ([Acr^+-Mes]ClO_4) , which has a highly oxidizing power (($E_{1/2}$ = +1.65 V vs. [Cp_2Fe])),[8] in the presence of an excess amount of co-oxidant, $(NH_4)_2S_2O_8$ (Scheme 4.3 (c)).[6e] Rao and co-workers reported on reduction of benzoyl peroxide by photoredox catalysis (Scheme 4.3 (d)).[6b] However,

since peroxides are potentially explosive, it is dangerous to use a stoichiometric or extra amount of the reagents. As described in Chapter 3, shelf-stable and easy-to-handle *N*-protected aminopyridinium salts serve as nitrogen-centered radical precursors (Scheme 4.3 (e)). This result prompted him to examine analogous aroyloxypyridinium salts as oxygen-radical precursors and application of the resultant radicals (Scheme 4.3 (f)).

4.2 Results and discussion

4.2.1 Synthesis of aroyloxypyridinium salts

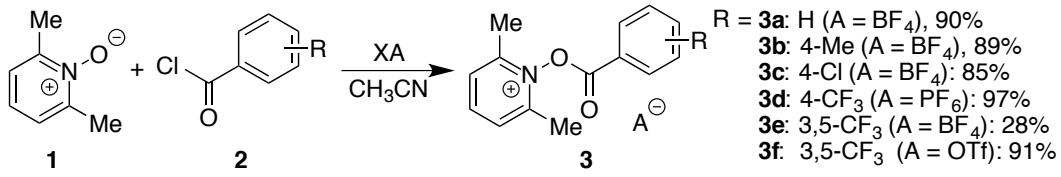

Scheme 4.4 Synthesis of aroyloxypyridinium salts.

First of all, the author designed the aroyloxy radical precursors, which are composed of accessible commercially available pyridine *N*-oxide derivatives, acid chloride (**2**) and counter anion sources. Various aroyloxy-2,6-dimethylpyridinium salts (**3**) were prepared from the reaction of 2,6-dimethylpyridine *N*-oxide **1** with **2**. They are stable and easy to handle. The two methyl groups on the pyridinium moiety are essential to increase the stability of **3** toward moisture. Counter anion plays a key role in control of hygroscopicity and solubility of **3**.

Initially, the author investigated the reaction of styrene with **3a** by photoredox catalysis under the same condition as described in Chapter 3 (Scheme 4.5). As a result, the expected benzoyloxy adduct **A** was obtained in a low yield, and the phenyl adduct **B** was also obtained. The author predicted that the reaction of aroyloxy radical with

olefins was not feasible.

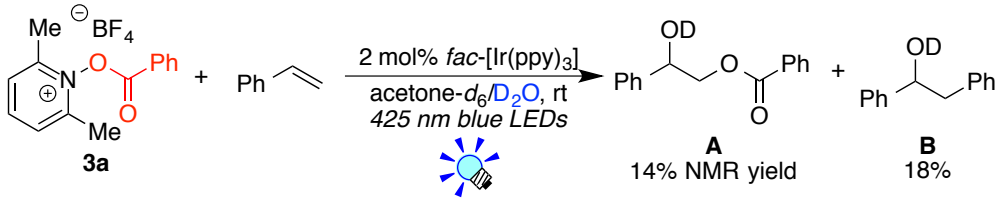

Scheme 4.5 The reaction of syrene with **3a**.

4.2.2 Photocatalytic aroyloxylation of mesitylene[a]

Table 4.1 Optimization of reaction conditions (aroyloxypyridinium salts **3x**).

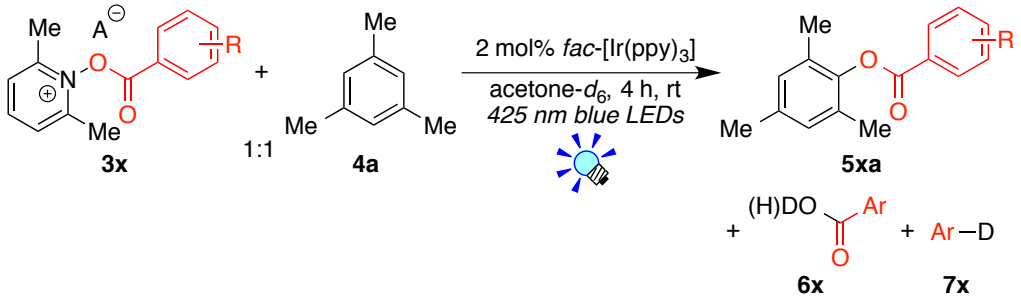

entry	**3x**	yield of **5xa**[b]/%	yield of **6x**[b]/%	yield of **7x**[b]/%
1	**3a** (R = H)	18	27	8
2	**3b** (R = 4-Me)	21	25	6
3	**3c** (R = 4-Cl)	34	27	3
4	**3d** (R = 4-CF_3)	30	16	8
5	**3e** (R = 3,5-CF_3)	69	21	0

[a] Reaction conditions: a reaction mixture of **3x** (0.05 mmol), **4a** (0.05 mmol), **Ir-1** (1.0 μmol) and acetone-d_6 (0.5 mL) was irradiated by 3W blue LEDs (λ = 425 ± 15 nm) for 4 h at room temperature. [b] Yields were determined by ^{1}H NMR spectroscopy using $SiEt_4$ as external standard.

With these reagents in hand, the author commenced the photocatalytic reaction of mesitylene (**4a**) with aroyloxy-2,6-dimethylpyridinium salts **3x** in the presence of *fac*-[Ir(ppy)$_3$] in acetone-d_6 under visible light irradiation with 425 nm blue LEDs (Table 4.1). The reaction with benzoyloxy-2,6-dimethylpyridinium BF_4 (**3a**) afforded

the corresponding the carboxylated product **5aa** in low yield (18%) together with considatable amounts of benzoic acid (**6a**; 27%) and benzene (**7a**; 8%). 4-Substituted benzoyloxy-2,6-dimethylpyridinium salts (**3b-3d**) also afforded the aryl benzoate (**5ba**; 21%, **5ca**; 34%, **5da**; 30%), carboxylic acid (**6b**; 25%, **6c**; 27%, **6d**; 16%) and decarboxylated protonated products (**7b**; 6%, **7c**; 3%, **7d**; 8%) (entry 2-4). To his delight, the reaction with 3,5-bis(trifluoromethyl)benzoyloxy-2,6-dimethylpyridinium BF_4 (**3e**) afforded the corresponding product **5ea** in good yield (69%) (entry 5). Furthermore, decarboxylation products (**7e**) was not observed. The benzoic acids **6** should be formed by H-abstraction of aroyloxy radical from the solvent, and the arene **7** should be formed via decarboxylation of aroyloxy radical followed by H-abstraction from the solvent (Scheme 4.6). It is known that the H-abstraction and decarboxylation processes are dependent on the aryl group and then the substituent effect of the benzoyl moiety was examined.[11] It turns out that, as the substituents on the benzene ring become more electron-withdrawing, the yields of the desired ester products **5** increase. In particular, the 3,5-bis(trifluoromethyl)benzoyl derivative **3** did not follow the decarboxylation process at all but afforded the desired product **5ae**.

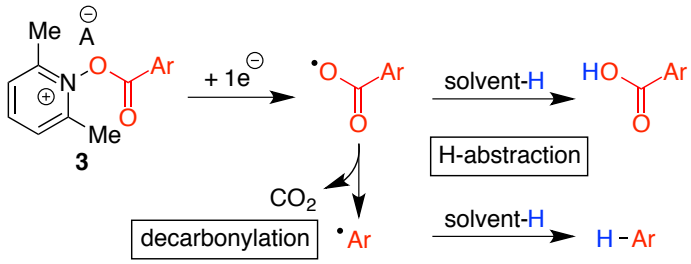

Scheme 4.6 H-Abstraction and decarboxylation of aroyloxy radical.

Table 4.2 Optimization of conditions (Photocatalyst and solvent).

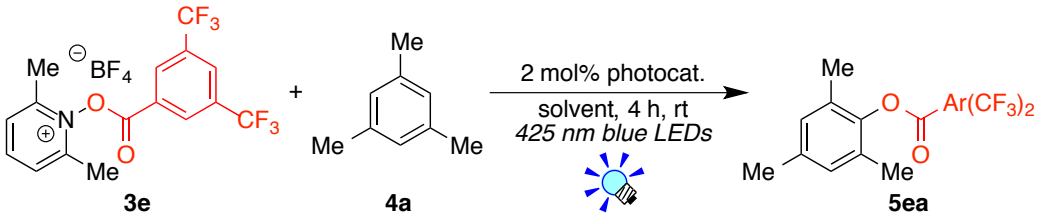

entry	photocatalyst	solvent	yield of **5ea**[b]/%
1	*fac*-[Ir(ppy)$_3$] (**Ir-1**)	acetone-d_6	69
2	[Ru(bpy)$_3$](PF$_6$)$_2$ (**Ru-1**)	acetone-d_6	40
3	[Ir(dF(CF$_3$)ppy)$_2$(bpy)](PF$_6$) (**Ir-3**)	acetone-d_6	<5
4	**Ir-1**	DMSO-d_6	0
5	**Ir-1**	CD$_3$CN	61
6	**Ir-1**	CD$_2$Cl$_2$	57
7[c]	**Ir-1**	CD$_2$Cl$_2$	76
8	–	CD$_2$Cl$_2$	0
9[d]	**Ir-1**	CD$_2$Cl$_2$	0

[a] Reaction conditions: A reaction mixture of **3e** (0.05 mmol), **4a** (0.05 mmol), photocatalyst (1.0 μmol) and solvent (0.5 mL) was irradiated by 3W blue LEDs (λ = 425 ± 15 nm) at room temperature for 4 h. [b] Yields were determined by ^{1}H NMR spectroscopy using SiEt$_4$ as external standard. [c] The ratio of **3e** to **4a** was 1:4. [d] The reaction was conducted in the dark.

Next, the author examined the photoredox catalysts and the reaction solvents (Table 4.2). For the catalyst, *fac*-[Ir(ppy)$_3$] (**Ir-1**) with the strongest reducing power of the photoexcited state ($E_{1/2}$ = –2.14 V vs. [Cp$_2$Fe])[9] turned out to be the best (entry 1-3). For the solvent, DMSO-d_6 solution did not afford **5ea** at all (entry 4), but CD$_3$CN and CD$_2$Cl$_2$ resulted in formation of the desired product **5ea** (entries 5, 6). Finally, an extra amount of **4a** with respect to **3e** in CH$_2$Cl$_2$ provided **5ea** in an excellent yield (76%) (entry 7). Notably, the product **5ea** was not obtained either in the dark and in the absence of the photocatalyst (entries 8, 9).

4.2.3 Scope and limitation of aroyloxylation with 3f

Table 5.3 Scope of the photocatalytic aroyloxylation.[a,b]

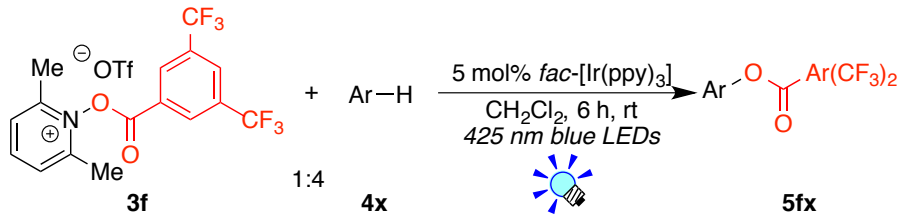

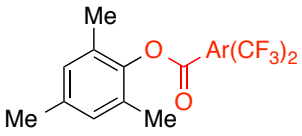

5fa: 72%

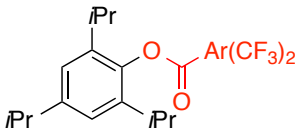

5fb: 57%

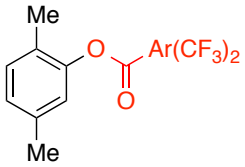

5fc: 51%

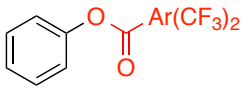

5fd: 30%

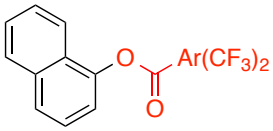

5fe: 63%

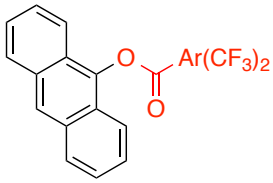

5ff: 37%[c]

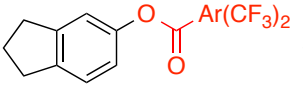

A

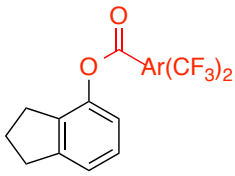

B

5fg: 33%, A:B =1:1[e]

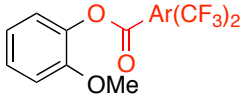

***o*-5fh**

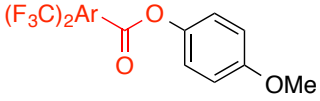

***p*-5fh**

5fh: 68%, *o*:*p* = 3:1[e]

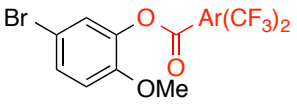

5fi: 39%

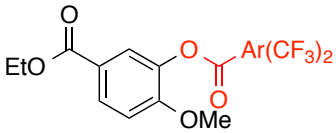

5fj: 40%[d]

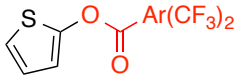

5fk: 28%[f]

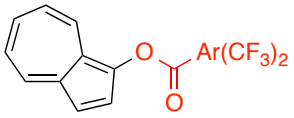

5fl: 22%[g]

Not applicable to

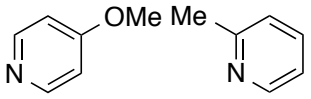

4m **4n**

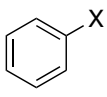

X = NHBoc; **4o**
OH; **4p**
CF_3; **4q**

[a] Reaction conditions: A reaction mixture of **3f** (0.40 mmol), **4** (1.60 mmol), photocatalyst (20.0 μmol) and solvent (4.0 mL) was irradiated by 3W blue LEDs (λ = 425 ± 15 nm) for 8 h at room temperature. [b] Yields of isolated products. [c] 2.0 equiv. of **4f** with respect to **3f** was used. [d] 2.5 equiv. of **4j** with respect to **3f** was used. [e] The ratios of regioisomers were determined by ^{1}H NMR spectra of crude reaction mixtures. [f] Reaction time was 12 h. [g] **3f** (0.480 mmol) and **4l** (0.400 mmol) were used.

Under the optimized conditions, the scope of the present photocatalytic aroyloxylation is summarized in Table 4.3. Mesitylene (**4a**), bulky 1,3,5-tri(isopropyl)benzene (**4b**) and *p*-xylene (**4c**) produced the corresponding products in good yields (**5fa**: 72%, **5fb**: 57%, **5fc**: 51%). The reaction of benzene (**4d**) afforded the product **5fd** in a low yield (30%) but naphthalene (**4e**) afforded **5fe** in a good yield (63%) as a single regioisomer. The reaction of anthracene (**4f**) was regioselective but the yield was low because of the low solubility of anthracene in CH_2Cl_2. Indan (**4g**) afforded the mono-aroyloxylated product as an equimolar mixture of regioisomers (**5fg**: 33%, A:B = 1:1). The reaction of anisole (**4h**), however, was regioselective to give a mixture of *o*- and *p*-isomer **5fh** in a 68% yield (*o*:*p* = 3:1). Furthermore, 4-bromoanisole (**4i**) and ethyl *p*-anisate (**4j**) produced the corresponding product as single regioisomers in 39% and 40% yields, respectively.

In addition, thiophene (**4k**) and azulene (**4l**) could be also applied to the present reaction but in low yields (**5fk**; 28%, **5fl**: 22%) due to other side reactions. The precursors **3** decomposed in pyridine (**4m**, **4n**). The reaction of aniline derivatives (**4o**), phenol (**4p**) and electron-deficient benzene derivatives (**4q**) did not proceed at all.

The reactions of **4d**, **4f**, **4g** and **4j** gave the corresponding carboxylic acids in low yields, indicating that the substitution reaction is competitive with H-abstraction reaction from solvents.

4.2.4 Experiments for analysis of reaction mechanism

Reaction mechanism was studied by CV measurements, Stern-Volmer plots and kinetic isotope experiment.

Reduction potentials of aroyloxy radical precusors (**3a**-**g**) were investigated by CV measurements (Figure 4.2). Irreversible reduction waves were ovserved at –1.39 V (**3a**),

–1.42 V (**3b**), –1.33 V (**3c**), –1.33 (**3d**), and –1.22 V (**3e**), respectively, indicating that these reagents can be reduced by photoexcited ***Ir-1** with the reduction potential of the photoexcited state ($E_{1/2}$ = –2.14 V vs. [Cp_2Fe]). The trend is in accord with the electron-withdrawing nature of the substituents. Reagent **3e** with two electron-withdrawing CF_3 groups can undergo 1e-reduction the most readily. The order is, fortunately, in accord with the order of preventing the decarboxylation process to afford the ester product **5** in yields better than those to the others.

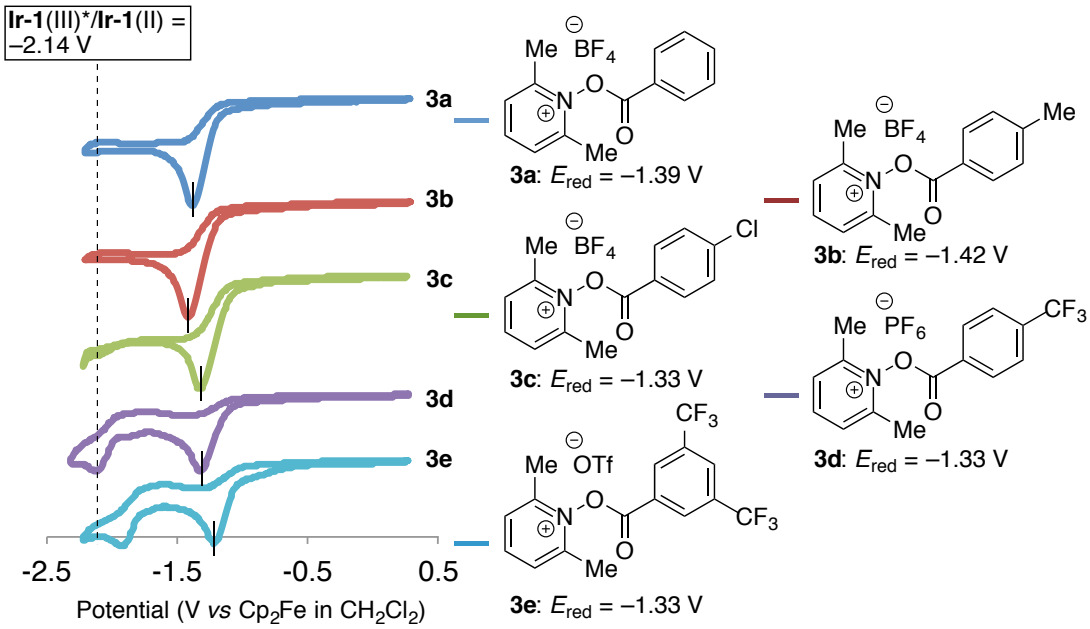

CV conditions: observed as 2 mM acetonitrile solutions; [NBu_4](PF_6) = 0.1 M; Ag/AgCl =electrode; reported with respect to the [$FeCp_2$]/[$FeCp_2$]$^+$ couple.

Figure 4.2 Cyclic voltammograms for **3**.

The Stern-Volmer plots for quenching the photoexcited photocatalyst ***Ir-1** by the action of **3e** and **4a** (Figure 4.3) confirmed that ***Ir-1** was not quenched by **4a** but by **3e**, indicating that electron transfer event occurs between ***Ir-1** and **3e**.

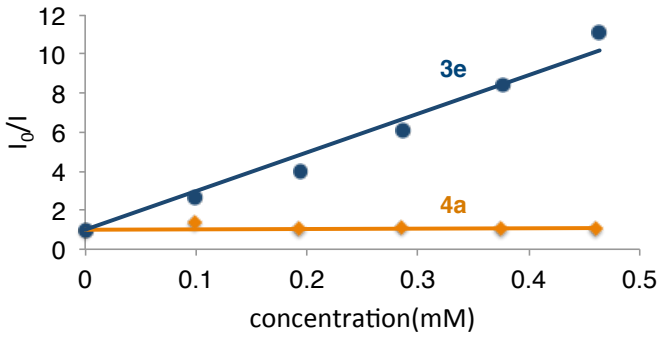

Intensities of the emission at 506 nm were recorded upon excitation of a CH_2Cl_2 solution of **Ir-1** at 363 nm.

Figure 4.3 Stern-Volmer studies of photocatalyst **Ir-1**.

Possible mechanism for the reaction of aroyloxy radical (**A**) with arenes involve H-abstraction from arenes (Scheme 4.7 (a) i) or radical addition to arenes (Scheme 4.6 (a) ii). In order to distinguish the two possibilities, the author conducted the competition experiment of benzene (**4d-H**) and benzene-d_6 to access potential deuterium kinetic isotope effect (Scheme 4.7 (b)). As a result, KIE value is 1.04, indicating that de-hydrogen-atom step is not rate-limiting. The author proposed that radical addition followed by 1e-oxidation and subsequent deprotonation was involved in this reaction. An electron-withdrawing substituent on the aroyloxy groups increases the reactivity of the radical addition as well as the H-abstraction.[10] In this reaction, two trifluoromethyl substituents promoted the radical addition and it is important that the radical addition takes place in prefence to the H-abstraction from the solvent.

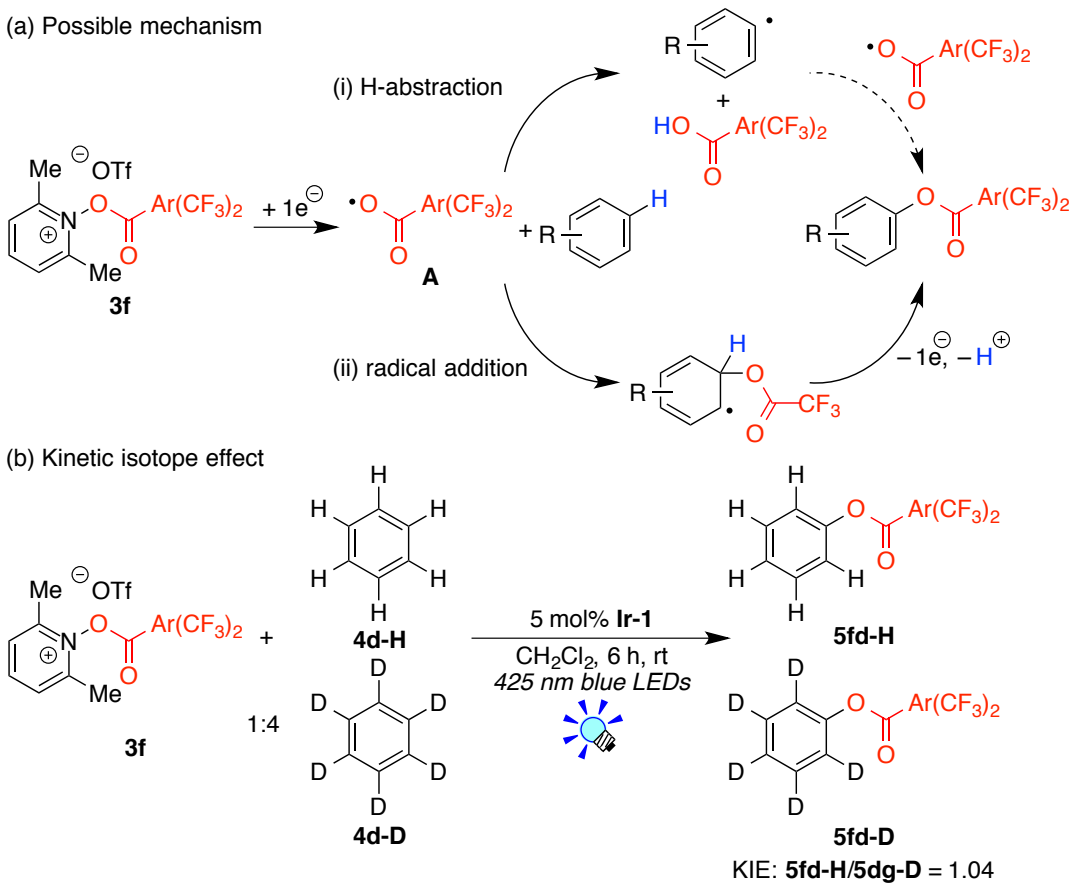

Scheme 4.7 Kinetic isotope effect.

On the basis of the experiments results, a plausible mechanism is shown in Scheme 4.8. Firstly, visible light irradiation to the ground state of Ir catalyst $\boldsymbol{Ir^{III}}$ generates the photoexcited state of Ir species $\boldsymbol{*Ir^{III}}$. The aroyloxy-2.6-dimethylpyridinium salts **3** is reduced by the $\boldsymbol{*Ir^{III}}$ to afford stabilized radical intermediate **3'** and highly oxidizing Ir species $\boldsymbol{Ir^{IV}}$. The radical **3'** fragmentates into aroyloxy radical **A** and 2,6-lutidine. The oxygen-centered radical **A** follows the three reactions: (i) H-abstraction from the solvent gives the carboxylic acid **6**, (ii) decarboxylation of **A** followed by H-abstraction of aryl radical affords the arene **7**, and (iii) radical addition to arene **4**. Route (iii) leads to the radical intermediate **8**, which is oxidized by the strongly oxidizing Ir species $\boldsymbol{Ir^{IV}}$ to afford the carbocationic species **9** and to regenerate the ground state of $\boldsymbol{Ir^{III}}$. Finally,

deprotonation of carbocationic intermediate **9** by 2,6-lutidine produces the oxidation product **5**.

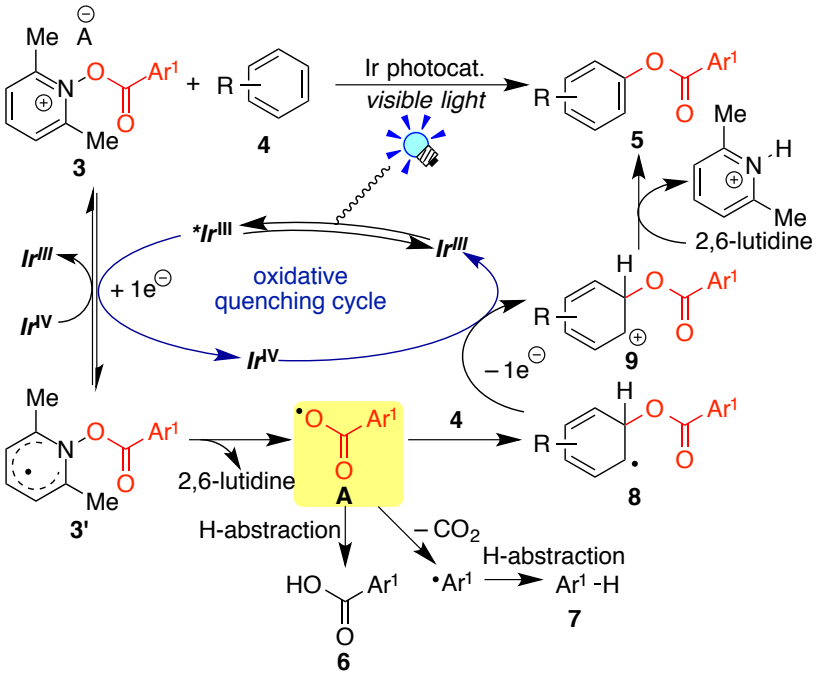

Scheme 4.8 Plausible reaction mechanism.

4.3 Conclusion

The author has developed aroyloxylation of arenes with the well-designed 3,5-bis(trifluoromethyl)benzoyloxy-2,6-dimethylpyridinium salt (**3e** (BF_4) and **3f** (OTf)) by *fac*-[Ir(ppy)$_3$] under visible light irradiation. The salts **3e** and **3f** are easy-to handle and serve as efficient aroyloxy radical precursors. The electron-withdrawing group in the benzoyl moiety of **3** increases the reactivity of the aroyloxy radical to increase the yields of the substituted oxidized products **5**. Furthermore, in the present reaction the aromatic moiety (C(sp^2)-H) is oxidized selectively in preference to the alkyl moiety (C(sp^3)-H).

4.4 Experimental

General

1, **2a**, **2b**, **2c**, **2d**, **2e**,**4b**, **4c**, **4g**, **4h**, **4i**, **4j**, **4l**, **4m**, and **4n** were purchased from TCI. **4a** were purchased from Wako. **4d**, **4e**, and **4f** were purchased from Kanto. **4f**, **4p**, and **4q** were purchased from Aldrich. CH_2Cl_2 was purified through the columns containing alumina and alumina-Cu catalyst and stored N_2 atmosphere. Other conditions were the same as those described in previous chapters

General procedure for the synthesis of aroyloxy-2,6-dimethylpyridinium salts

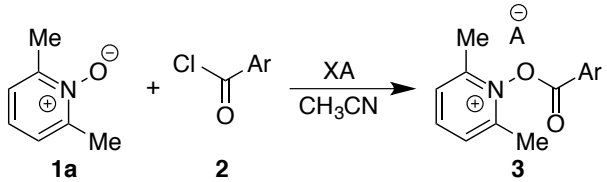

Under N_2, to a mixture of 2,6-dimethylaminopyridine *N*-oxide (**1a**) (1.0 eq.), XA (1-1.2 eq) and dry CH_3CN were added carboxylic acid chloride (2) (1.0 eq). The reaction mixture was stirred for the reaction time at rt. The volatiles were removed under reduced pressure and the residue was extract with CH_2Cl_2 and filtered. The filtrate was concentrated *in vacuo*. The residue was washed with Et_2O and obtained as a white solid.

1-Benzoyloxy-2,6-dimethylpyridinium tetrafluoroborate (3a)

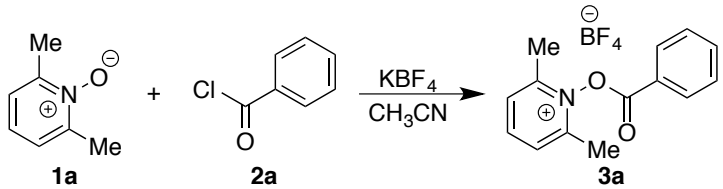

The reaction of **1a** (237.3 mg, 1.93 mmol), potassium tetrafluoroborate (254 mg, 2.02 mmol) and **2a** (324 mg, 2.31 mmol) following the general procedure afforded **3a** (547 mg, 90%, reaction time = 5 h) as a white solid.

^{1}H NMR (400 MHZ, CD_3CN, rt) δ 8.43 (t, ^3J = 8.0 Hz, 1H; C_5NHH_2), 8.29 (dd, ^3J = 8.4 Hz, q, ^4J = 1.2 Hz, 2H; C_5NHH_2), 7.93 (m, 3H; $C_6H_3H_2$), 7.73 (m, 2H). **^{13}C NMR** (125 MHz, CD_3CN, rt) δ 162.4, 155.0, 147.1, 137.9, 132.0, 130.7, 129.3, 123.8, 18.4. **HRMS** (ESI-TOF) calculated for $[C_{14}H_{14}NO_2]^+$ requires 228.1019, found 228.1019.

1-(4-Methylbenzoyloxy)-2.6-dimethylpyridinium tetrafluoroborate (3b)

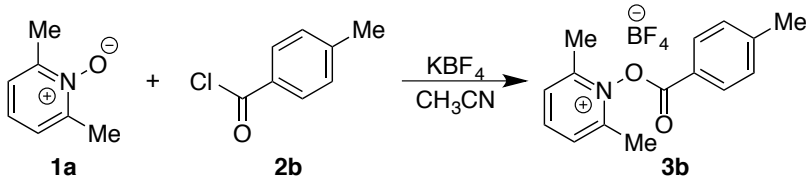

The reaction of **1a** (258 mg, 2.01 mmol), potassium tetrafluoroborate (268 mg, 2.13 mmol) and **2b** (381 mg, 2.46 mmol) following the general procedure afforded **3b** (611 mg, 89%, reaction time = 15 h) as a white solid.

^{1}H NMR (400 MHz, CD_3CN) δ 8.42 (t, ^3J = 8.0 Hz, 1H; C_5NHH_2), 8.18 (d, ^3J = 8.4 Hz, 2H; C_5NHH_2), 7.94 (d, ^3J = 8.0 Hz, 2H; $C_6H_2H_2$), 7.54 (d, ^3J = 8.0 Hz, 2H; $C_6H_2H_2$), 2.71 (s, 6H; $(CH_3)_2$), 2.52 (s, 3H; CH_3). **^{13}C NMR** (125 MHz, CD_3CN, rt) δ 162.3, 155.0, 149.9, 147.0, 132.0, 131.3, 129.2, 120.9, 22.1, 18.4. **HRMS** (ESI-TOF): calculated for $[C_{15}H_{16}NO_2]^+$ requires 242.1176, found 242.1175.

1-(4-Chlorobenzoyloxy)-2,6-dimethylpyridinium tetrafluoroborate (3c)

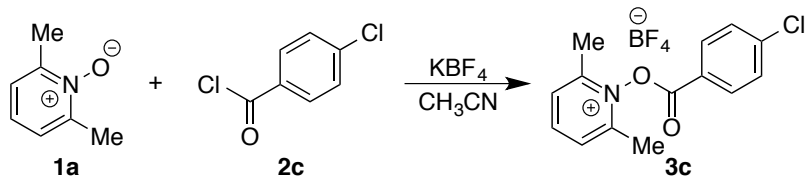

1a **2c** **3c**

The reaction of **1a** (237.8 mg, 1.93 mmol), potassium tetrafluoroborate (254 mg, 2.02 mmol) and **2c** (367 mg, 2.01 mmol) following the general procedure afforded **3c** (547 mg, 90%, reaction time = 16 h) as a white solid.
^{1}H NMR (400 MHZ, CD_3CN, rt) δ 8.43 (t, ^3J = 8.0 Hz, 1H; C_5NHH_2), 8.25 (m, 2H; C_5NHH_2), 7.94 (d, ^3J = 8.0 Hz, 2H; $C_6H_2H_2$), 7.74 (d, ^3J = 8.8 Hz, 2H; $C_6H_2H_2$), 2.71 (s, 6H; $(CH_3)_2$). **^{13}C NMR** (125 MHz, CD_3CN, rt) δ 161.7, 155.0, 147.2, 144.0, 133.7, 130.9, 129.2, 122.6, 18.4. **HRMS** (ESI-TOF) calculated for $[C_{14}H_{13}ClNO_2]^+$ requires 262.0629, found 262.0626.

1-(4-trifluoromethylbenzoyloxy)-2,6-dimethylpyridinium hexafluorophosphate (3d)

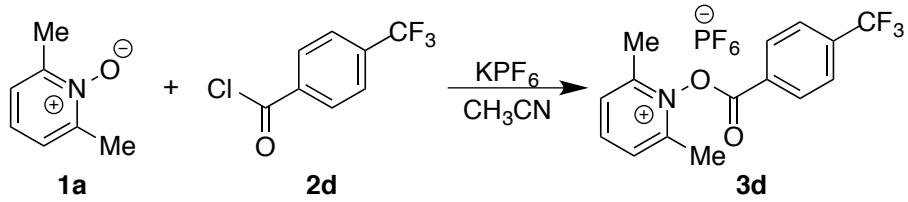

1a **2d** **3d**

The reaction of **1a** (236 mg, 1.91 mmol), potassium hexafluorophosphate (446 mg, mmol) and **2d** (381 mg, 2.14 mmol) following the general procedure afforded **3d** (817 mg, 97%, reaction time = 5 h) as a white solid.
^{1}H NMR (400 MHZ, CD_3CN, rt) δ 8.46 (m, 3H; C_5NH_3), 8.04 (d, ^3J = 8.8 Hz, 2H; $C_6H_2H_2$), 7.96 (d, ^3J = 8.0 Hz, 2H; $C_6H_2H_2$). **^{13}C NMR** (125 MHz, CD_3CN, rt) δ 161.5, 155.0, 147.3, 137.7 (q, ^3J = 32.6 Hz), 132.9, 129.4, 127.7, 127.5 (q, ^4J = 3.9 Hz), 124.4 (q, ^2J = 271 Hz), 18.5. **^{19}F NMR** (376 MHz, $CDCl_3$, rt) δ –64.3. **HRMS** (ESI-TOF) calculated for $[C_{15}H_{13}F_3NO_2]^+$ requires 296.0893, found 296.0893.

1-(3,5-bis(trifluoromethyl)benzoyloxy)-2,6-dimethylpyridinium tetrafluoroborate (3e)

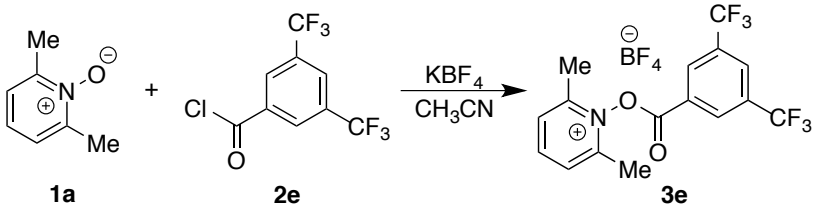

1a **2e** **3e**

The reaction of **1a** (266 mg, 2.016 mmol), potassium tetrafluoroborate (317 mg, 2.52 mmol) and **2e** (381 mg, 2.36 mmol) following the general procedure afforded **3e** (307 mg, 32%, reaction time = 2 h) as a white solid after washed with as small amount of $CHCl_3$.
^{1}H NMR (400 MHZ, CD_3CN, rt) δ 8.79 (s, 2H; $C_6H_2H(CF_3)_2$), 8.54 (s, 1H; $C_6H_2H(CF_3)_2$), 8.47 (t, ^3J = 8.0 Hz, 1H; C_5NHH_2), 7.97 (d, ^3J = 8.0 Hz, 2H; C_5NHH_2), 2.74 (s, 6H; $(CH_3)_2$). **^{13}C NMR** (125 MHz, CD_3CN, rt) δ 160.5, 154.9, 147.6, 133.4 (q, ^3J = 34.4 Hz), 132.7 (q, ^4J = 3.5 Hz), 131.1 (q, ^4J = 3.1 Hz), 129.5, 126.7, 123.7 (q, ^2J = 271 Hz). **^{19}F NMR** (376 MHz, $CDCl_3$, rt) δ –64.3, –154.3**HRMS** (ESI-TOF) calculated for $[C_{16}H_{12}F_6NO_2]^+$ requires 364.0767, found 364.0763.

1-(3,5-bis(trifluoromethyl)benzoyloxy)-2,6-dimethylpyridinium trifluoromethanesulfonate (3f)

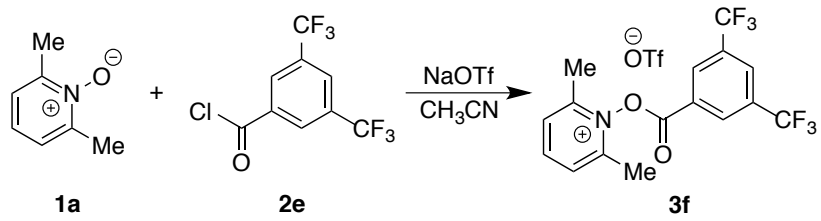

1a **2e** **3f**

The reaction of **1a** (249 mg, 2.02 mmol), sodium trifluoromethanesufonate (691 mg, 2.50 mmol) and **2e** (427 mg, 2.48 mmol) following the general procedure afforded **3f** (944 mg, 91%, reaction time = 3 h) as a white solid.
^{1}H NMR (400 MHZ, CD_3CN, rt) δ 8.79 (s, 2H; $C_6H_2H(CF_3)_2$), 8.54 (s, 1H; $C_6H_2H(CF_3)_2$), 8.47 (t, ^{3}J = 8.0 Hz, 1H; C_5NHH_2), 7.98 (d, ^{3}J = 8.0 Hz, 2H; C_5NHH_2), 2.75 (s, 6H; $(CH_3)_2$). **^{13}C NMR** (125 MHz, CD_3CN, rt) δ 160.5, 155.0, 147.6, 133.4 (q, ^{3}J = 34.4 Hz), 132.7 (q, ^{4}J = 3.1 Hz), 131.1 (q, ^{4}J = 3.1 Hz), 129.5, 126.7, 123.7 (q, ^{2}J = 271 Hz), 121.9 (q, ^{2}J = 366 Hz; CF_3SO_3). **^{19}F NMR** (376 MHz, $CDCl_3$, rt) δ –64.4, –79.8. **HRMS** (ESI-TOF) calculated for $[C_{16}H_{12}F_6NO_2]^+$ requires 364.0767, found 364.0763.

Typical NMR experimental procedure
*Photocatalytic aroyloxylation of mesitylene (**4a**)*

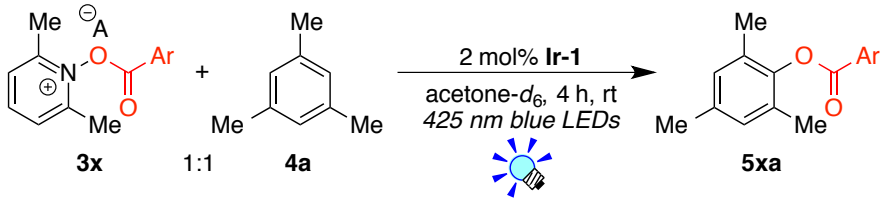

3x 1:1 **4a** **5xa**

Under N_2, to **4a** (50.0 mmol) dissolved in a deuterated acetone (0.50 mL) in an NMR tube, **3x** (50.0 mmol), **Ir-1** (1.00 mmol) and tetraethylsilane (an external standard dissolved CD_3CN in capillary tube) were added. The mixture was degassed by three freeze-pump-thaw cycles. The reaction was carried out at room temperature (water bath) under irradiation of visible light (placed at a distance of 2-3 cm from the blue LED lamp: $h\nu$ = 425 ± 15 nm).

General procedure for the photocatalytic aroyloxylation of arenes with 3f

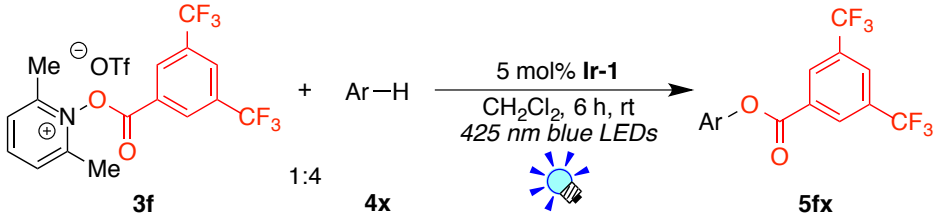

3f 1:4 **4x** **5fx**

Under N_2, to arene (**4x**) (1.60 mmol) dissolved in a dry and dehydrated CH_2Cl_2 (4.0 mL) in a 20 mL-Schlenk tube, **3f** (0.4 mmol) and **Ir-1** (0.02 mmol) were added. The tube was placed at a distance of 2-3 cm from blue LED lamp (hν = 425 ± 15 nm). The resulting mixture was stirred at room temperature (water bath) under visible light irradiation. Then, the reaction mixture was concentrated *in vacuo* to remove volatile compounds. The residue was purified by flash column chromatography on silica gel to give **5fx**. Then the reaction was followed by ^{1}H NMR spectroscopy.

Mesityl 3,5-bis(trifluoromethyl)benzoate (5fa)

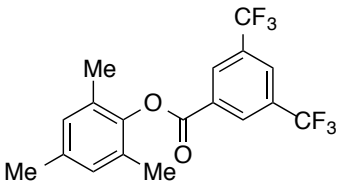

The reaction of **3f** (205.4 mg, 0.400 mmol), mesitylene (**4a**) (191.7 mg, 1.59 mmol), and **Ir-1** (13.2 mg, 20.2 μmol) following the general procedures afforded **5fa** (108.4 mg, 72% yield, reaction time = 6 h) as a white solid after purification with flash column chromatography on silica gel (hexane:EtOAc = 100:1).
^{1}H NMR (400 MHz, $CDCl_3$) δ 8.69 (s, 2H; $C_6H_2H(CF_3)_2$), 8.16 (s, 1H; $C_6H_2H(CF_3)_2$), 6.95 (s, 2H; $C_6H_2(CH_3)_3$), 2.32 (s, 3H; $C_6H_2(CH_3)_2(CH_3)$), 2.16 (s, 6H; $C_6H_2(CH_3)_2(CH_3)$). **^{13}C NMR** (125 MHz, $CDCl_3$, rt) δ 162.1, 145.8, 136.2, 132.7 (q, ^3J = 33.8 Hz), 131.7, 130.3 (q, ^4J = 3.4 Hz), 129.7, 127.1 (seq, ^4J = 3.5 Hz), 123.0 (q, ^2J = 271 Hz), 21.0, 16.4. **^{19}F NMR** (376 MHz, $CDCl_3$, rt) δ –64.3. **HRMS** (ESI-TOF): calculated for $[C_{18}H_{14}O_2+Na]^+$ requires 399.0790, found 399.0789.

2,4,6-Triisopropylphenyl 3,5-bis(trifluoromethyl)benzoate (5fb)

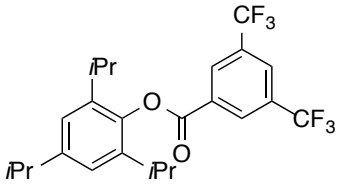

The reaction of **3f** (204.9 mg, 0.399 mmol), 1,3,5-triisopropylbenzen (**4b**) (191.7 mg, 1.59 mmol), and **Ir-1** (13.2 mg, 20.2 μmol) following the general procedures afforded **5fb** (97.4 mg, 63% yield, reaction time = 4 h) as a white solid after purification with flash column chromatography on silica gel (hexane:EtOAc = 10:1).
^{1}H NMR (400 MHz, $CDCl_3$) δ 8.67 (s, 2H; $C_6H_2H(CF_3)_2$), 8.17 (s, 1H; $C_6H_2H(CF_3)_2$), 7.06 (s, 2H; $C_6H_2(CH_3)_3$), 2.93 (seq, ^3J= 7.2 Hz, 1H; $(CH_3)_2CH$), 2.88 (seq, ^3J = 7.2 Hz, 2H; $(CH_3)_2CH$), 1.28 (d, ^3J = 6.8 Hz, 6H; $(CH_3)_2(CH_3)$), 1.21 (d, ^3J = 6.8 Hz, 12H; $(CH_3)_2(CH_3)$). **^{13}C NMR** (125 MHz, $CDCl_3$, rt) δ 163.0, 147.5, 143.4, 139.8, 132.8 (q, ^3J = 34.1 Hz), 131.9, 130.3, 130.3, 127.1 (q, ^4J = 3.3 Hz), 123.0 (q, ^2J = 272 Hz), 34.3, 28.0, 24.3, 24.0, 22.9. **^{19}F NMR** (376 MHz, $CDCl_3$, rt) δ –64.2. **HRMS** (ESI-TOF): calculated for $[C_{24}H_{26}F_6O_2+Na]^+$ requires 483.1729, found 483.1732.

2,5-dimethylphenyl 3,5-bis(trifluoromethyl)benzoate (5fc)

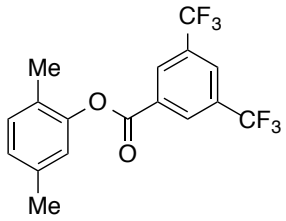

The reaction of **3f** (205.5 mg, 0.400 mmol), *p*-xylene (**4c**) (169.7 mg, 1.60 mmol), and **Ir-1**(13.2 mg, 20.2 μmol) following the general procedures afforded **5fc** (73.4 mg, 51% yield, reaction time = 6 h) as a white solid after purification with flash column chromatography on silica gel (hexane:EtOAc = 10:1).
^{1}H NMR (400 MHz, $CDCl_3$) δ 8.66 (s, 2H; $C_6H_2H(CF_3)_2$), 8.15 (s, 1H; $C_6H_2H(CF_3)_2$), 7.19 (d, ^3J = 7.6 Hz, 1H; C_6HHH), 7.04 (d, ^3J = 7.6 Hz, 1H; C_6HHH), 6.96 (s, 1H; C_6HHH), 2.36 (s, 3H; $C_6H_3(CH_3)(CH_3)$), 2.19 (s, 3H; $C_6H_3(CH_3)(CH_3)$). **^{13}C NMR** (125 MHz, $CDCl_3$, rt) δ 162.5, 149.0, 137.5, 132.7 (q, ^3J = 33.8 Hz), 131.9, 131.3, 130.3 (q, ^4J = 3.1 Hz), 127.7, 127.1 (seq, ^4J = 3.9 Hz), 123.0 (q, ^2J = 272 Hz), 122.2, 21.1, 15.9. **^{19}F NMR** (376 MHz, $CDCl_3$, rt) δ –64.3. **HRMS** (ESI-TOF): calculated for $[C_{17}H_{12}F_6O_2+Na]^+$ requires 385.0634, found 385.0635.

Phenyl 3,5-bis(trifluoromethyl)benzoate (5fd)

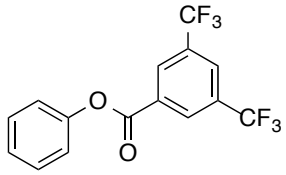

The reaction of **3f** (204.7 mg, 0.399 mmol), benzene (**4d**) (125.3 mg, 1.60 mmol), and **Ir-1** (13.2 mg, 20.2 μmol) following the general procedures afforded **5fd** (27.6 mg, 30% yield, reaction time = 6 h) as a colorless oil after purification with flash column chromatography on silica gel (hexane:EtOAc = 10:1).
^{1}H NMR (400 MHz, $CDCl_3$) δ 8.66 (s, 2H), 8.15 (s, 1H), 7.47 (m, 2H), 7.35 (m, 1H), 7.25 (m, 2H). **^{13}C NMR** (125 MHz, $CDCl_3$, rt) δ 162.7, 150.5, 132.6 (q, ^3J = 34.0 Hz), 130.4 (q, ^4J = 3.3 Hz), 129.9, 127.1 (q, ^4J = 3.5 Hz), 126.7, 123 (q, ^2J = 272 Hz), 121.5. **^{19}F NMR** (376 MHz, $CDCl_3$, rt) δ –64.3. **HRMS** (ESI-TOF): calculated for $[C_{14}H_{18}O_4+Na]^+$ requires 261.1097, found 261.1105.

Naphthalen-1-yl 3,5-bis(trifluoromethyl)benzoate (5fe)

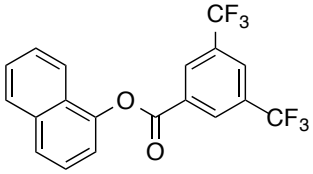

The reaction of **3f** (204.9 mg, 0.399 mmol), naphthalene (**4e**) (205.5 mg, 1.60 mmol), and **Ir-1** (13.2 mg, 20.2 μmol) following the general procedures afforded **5fe** (97.4 mg, 63% yield, reaction time = 6 h) as a white solid after purification with flash column chromatography on silica gel (hexane:EtOAc = 10:1).
^{1}H NMR (400 MHz, $CDCl_3$) δ 8.78 (s, 1H), 8.21 (s, 1H; $C_6H_2H(CF_3)_2$), 7.95 (m, 1H $C_6H_2H(CF_3)_2$), 7.86 (m, 2H; napht-*H*), 7.55 (m, 3H; napht-*H*), 7.39 (m, 1H; napht-*H*). **^{13}C NMR** (125 MHz, $CDCl_3$, rt) δ 162.8, 146.4, 134.9, 132.8 (q, ^3J = 34.1 Hz), 131.8, 130.5 (q, ^4J = 33 Hz), 128.4, 127.3 (seq, ^4J = 3.8 Hz), 127.03, 126.98, 126.9, 126.6, 125.6, 123.0 (q, ^2J = 271 Hz), 120.9, 118.2. **^{19}F NMR** (376 MHz, $CDCl_3$, rt) δ –64.2. **HRMS** (ESI-TOF): calculated for $[C_{19}H_{10}F_6O_2+Na]^+$ requires 407. 0477, found 407.0474.

Anthracen-9-yl 3,5-bis(trifluoromethyl)benzoate (5ff)

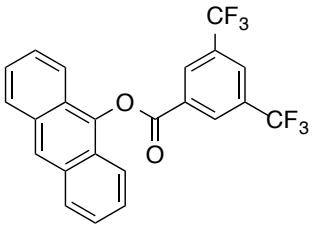

The reaction of **3f** (204.8 mg, 0.399 mmol), anthracene (**4f**) (142.2 mg, 0.798 mmol), and **Ir-1** (13.3 mg, 20.3 μmol) following the general procedures afforded **5ff** (64.9 mg, 37% yield, reaction time = 6 h) as a white solid after purification with flash column chromatography on silica gel (hexane:EtOAc = 1:0-50:1).
^{1}H NMR (400 MHz, $CDCl_3$) δ 8.90 (s, 2H; $C_6H_2H(CF_3)_2$), 8.45 (s, 1H; anth-*H*), 8.26 (s, 1H; $C_6H_2H(CF_3)_2$), 8.09 (m, 2H; anth-*H*), 7.91 (m, 2H; anth-*H*), 7.52(m, 4H; anth-*H*). **^{13}C NMR** (125 MHz, $CDCl_3$, rt), δ 162.9, 141.6, 133.0 (q. ^3J = 33.9 Hz) 132.0, 131.4, 130.6, 128.8, 127.6 (seq, ^4J = 3.6 Hz), 126.9, 125.9, 125.7, 123.9, 123 (q, ^2J = 271 Hz), 121.0. **^{19}F NMR** (376 MHz, $CDCl_3$, rt) δ –64.2. **HRMS** (ESI-TOF): calculated for $[C_{23}H_{12}F_6O_2+Na]^+$ requires 457.0634, found 457.0632.

Indan-5-yl 3,5-bis(trifluoromethyl)benzoate and indan-4-yl 3,5-bis(trifluoromethyl)benzoate (5fh)

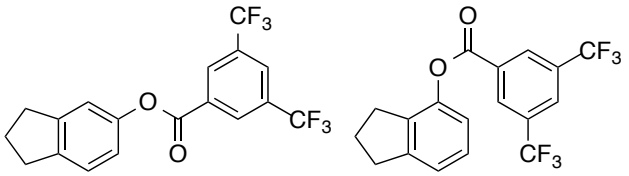

A-5fh **B-5fh**

The reaction of **3f** (205.1 mg, 0.400 mmol), indan (**4h**) (188.5 mg, 1.60 mmol), and **Ir-1** (12.8 mg, 19.5 μmol) following the general procedures afforded **5fh** (48.7 mg, 33% yield, reaction time = 6 h) as a colorlessoil after purification with flash column chromatography on silica gel (hexane:EtOAc = 50:1). Regioisomer ratio (1:1) was determined by ^{1}H NMR analysis of unpurified product mixture. The spectral data of regioisomer were determined with separated products by GPC (CH_3Cl).

A-5fh **^{1}H NMR** (400 MHz, $CDCl_3$) δ 8.64 (s, 2H; C_6H_2H$(CF_3)_2$), 8.14 (s, 1H; $C_6H_2H(CF_3)_2$), 7.29 (m, 1H; C_6HHH), 7.07 (s, 1H; C_6HHH), 6.96 (m,1H;C_6HHH), 2.96 (t, ^3J = 8.0 Hz, 2H; $CH_2CH_2CH_2$), 2.94 (t, ^3J = 8.0 Hz, 2H; $CH_2CH_2CH_2$), 2.14 (tt, ^3J = 7.6 Hz, ^3J = 7.6 Hz, 2H; $CH_2CH_2CH_2$). **^{13}C NMR** (125 MHz, CD_3Cl) δ 136.1, 147.5, 147.0, 136.1, 132.6 (q, ^3J = 34.1 Hz), 132.0, 130.4 (q, ^4J = 3.0 Hz), 127.9, 127.0 (q, ^4J = 3.8 Hz), 123.0 (q, ^2J = 272 Hz), 122.9, 118.8, 33.3, 30.1, 25.2. **^{19}F NMR** (376 MHz, $CDCl_3$, rt) δ –64.3..

B-5fh **^{1}H NMR** (400 MHz, $CDCl_3$) δ 8.65 (s, 2H; C_6H_2H$(CF_3)_2$), 8.14 (s, 1H; $C_6H_2H(CF_3)_2$), 7.22 (d, ^3J = 7.6 Hz, 1H; C_6HHH), 7.20 (t, ^3J = 7.2 Hz, 1H; C_6HHH), 6.98 (d, ^3J = 7.6 Hz, 1H; C_6HHH), 3.01 (t, ^3J = 7.2 Hz, 2H; $CH_2CH_2CH_2$), 2.84 (t, ^3J = 7.2 Hz, 2H; $CH_2CH_2CH_2$), 2.12 (tt, ^3J = 7.2 Hz, ^3J = 7.2 Hz, 2H; $CH_2CH_2CH_2$). **^{13}C NMR** (125 MHz, CD_3Cl) δ 162.1, 149.0, 142.7, 132.5 (q, ^3J = 34.1 Hz), 132.2, 130.4 (q, ^4J = 3.1 Hz), 126.9 (q, ^4J = 3.5 Hz), 125.2 123.0 (q, ^2J = 271 Hz), 119.0, 117.5, 33.2, 32.5, 25.9. **^{19}F NMR** (376 MHz, $CDCl_3$, rt) δ –64.3. **HRMS** (ESI-TOF): calculated for $[C_{18}H_{12}F_6O_2$+Na$]^+$ requires 397.0634, found 397.0633.

2-Methoxyphenyl 3,5-bis(trifluoromethyl)benzoate (5fi)

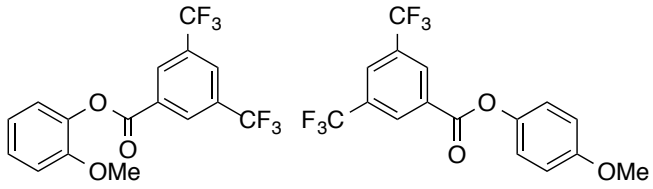

***o*-5fi** ***p*-5fi**

The reaction of **3f** (205.7 mg, 0.401 mmol), anisole (**4i**) (173.3 mg, 1.60 mmol), and **Ir-1** (12.9 mg, 20.0 μmol) following the general procedures afforded **5fi** (99.1 mg, 68% yield, reaction time = 6 h) as a white solid after purification with flash column chromatography on silica gel (hexane:EtOAc = 100:1). Regioisomer ratio (3:1) was determined by ^{1}H NMR analysis of the crude product before chromatography.

***o*-5fi**: **^{1}H NMR** (400 MHz, $CDCl_3$) δ 8.67 (s, 2H; C_6H_2H$(CF_3)_2$), 8.14 (s, 1H; $C_6H_2H(CF_3)_2$), 7.30 (m, 1H; C_6HH$_3$), 7.17 (m, 1H; C_6HH$_3$), 7.03 (m, 2H; C_6H_2H$_2$), 3.837 (s, 3H; OCH_3). **^{13}C NMR** (125 MHz, $CDCl_3$, rt) δ 162.3, 151.1, 139.5, 132.5 (q, ^3J = 34.1 Hz), 131.9, 130.5 (q, ^4J = 3.5 Hz), 127.7, 127.0. (seq, ^4J = 3.5 Hz), 122.7. 123.0 (q, ^2J = 272 Hz), 121.1, 112.7, 56.0. **^{19}F NMR** (376 MHz, $CDCl_3$, rt) δ –64.27.

***p*-5fi**: **^{1}H NMR** (400 MHz, $CDCl_3$) δ 8.65 (s, 2H; C_6H_2H$(CF_3)_2$), 8.14 (s, 1H; $C_6H_2H(CF_3)_2$), 7.16 (m, 2H; $C_6H_2H_2$), 6.97 (m, 2H; $C_6H_2H_2$), 7.03 (m, 2H; $C_6H_2H_2$), 3.843 (s, 3H; OCH_3). **^{13}C NMR** (500 MHz, $CDCl_3$, rt) δ 163.1, 157.9, 143.9, 132.6 (q, ^3J = 34.0 Hz), 132.1, 130.4 (q, ^4J = 3.1 Hz), 127.0 (seq, ^4J = 3.5 Hz), 123.0 (q, ^2J = 271 Hz), 122.3, 114.8, 55.8. **^{19}F NMR** (376 MHz, $CDCl_3$, rt) δ –64.29.

HRMS (ESI-TOF): calculated for $[C_{16}H_{10}F_6O_3$+Na$]^+$ requires 387.0426, found 387.0424.

5-Bromo-2-methoxyphenyl 3,5-bis(trifluoromethyl)benzoate (5fg)

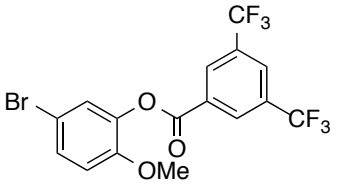

The reaction of **3f** (205.1 mg, 0.400 mmol), 4-bromoanisole (**4g**) (299.9 mg, 1.60 mmol), and **Ir-1** (13.0 mg, 19.9 μmol) following the general procedures afforded **5fg** (68.6 mg, 39% yield, reaction time = 6 h) as a white solid after purification with flash column chromatography on silica gel (hexane:EtOAc = 100:1) and GPC (CH_3Cl).
^{1}H NMR (400 MHz, $CDCl_3$) δ 8.63, (s, 2H; $C_6H_2H(CF_3)_2$), 8.15 (s, 1H; $C_6H_2H(CF_3)_2$), 7.40 (dd, ^3J = 8.8 Hz, ^4J = 2.4 Hz, 1H; C_6HHH), 7.34 (d, ^4J = 2.4 Hz, 1H; C_6HHH), 6.92 (d, ^3J = 8.8 Hz, 1H; C_6HHH), 3.82. **^{13}C NMR** (125 MHz, $CDCl_3$, rt) δ 161.9, 150.6, 139.9, 132.6 (q, ^3J = 34.1 Hz), 131.4, 130.5 (q, ^4J = 3.3 Hz), 130.5, 127.2 (seq, ^4J = 3.5 Hz), 126.0, 122.9 (q, ^2J = 271 Hz), 114.0, 112.3, 56.3. **^{19}F NMR** (376 MHz, $CDCl_3$, rt) δ –64.3. **HRMS** (ESI-TOF): calculated for $[C_{16}H_9BrF_6O_3+Na]^+$ requires 464.9531, found 464.9535.

Ethyl 3-(3,5-bis(trifluoromethyl)benzoyloxy)-4-methoxybenzoate (5fj)

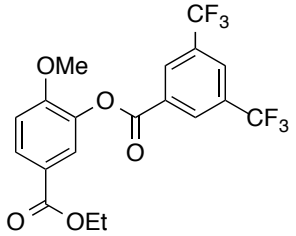

The reaction of **3f** (204.6 mg, 0.399 mmol), ethyl *p*-anisate (**4j**) (174.9 mg, 0.970 mmol), and **Ir-1** (12.9 mg, 19.7 μmol) following the general procedures afforded **5fj** (69.6 mg, 40% yield, reaction time = 6 h) as a white solid after purification with flash column chromatography on silica gel (hexane:EtOAc = 50:1-10:1).
^{1}H NMR (400 MHz, $CDCl_3$) δ 8.65 (s, 2H; $C_6H_2H(CF_3)_2$), 8.15 (s, 1H; $C_6H_2H(CF_3)_2$), 8.03 (dd, ^3J = 8.4 Hz, ^4J = 2.0 Hz, 1H; C_6HHH), 7.87 (d, ^4J = 2.0 Hz, 1H; C_6HHH), 7.06 (d, ^3J = 8.8 Hz, 1H; C_6HHH), 4.37 (q, ^3J = 7.2 Hz, 2H; CH_3CH_2COO), 3.89 (s, 3H; CH_3O), 1.38 (t, ^3J = 7.2 Hz, 3H; CH_3CH_2COO). **^{13}C NMR** (125 MHz, $CDCl_3$, rt) δ 165.6, 162.1, 154.9, 139.0, 132.6 (q, ^3J = 34.0 Hz), 131.5, 130.6, 129.9, 127.2 (q, ^4J = 2.5 Hz), 124.3, 123.6, 123.0 (q, ^2J = 271 Hz), 111.9, 61.2, 56.3, 14.5. **^{19}F NMR** (376 MHz, $CDCl_3$, rt) δ –64.3. **HRMS** (ESI-TOF): calculated for $[C_{14}H_{18}O_4+Na]^+$ requires 261.1097, found 261.1105.

Thiopen-2-yl 3,5-bis(trifluoromethyl)benzoate (5fk)

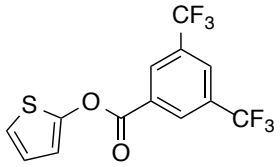

The reaction of **3f** (205.7 mg, 0.401 mmol), thiophene (**4k**) (135.9 mg, 1.60 mmol), and **Ir-1** (12.9 mg, 19.7 μmol) following the general procedures afforded **5fk** (38.4 mg, 28% yield, reaction time = 12 h) as a white solid after purification with flash column chromatography on silica gel (hexane).
^{1}H NMR (400 MHz, acetone-d_6) δ 8.74 (s, 2H; $C_6H_2H(CF_3)_2$), 8.45 (s, 1H; $C_6H_2H(CF_3)_2$), 7.18 (m, 1H; thiophene-*H*), 7.04 (m, 1H; thiophene-*H*), 6.97 (m, 1H; thiophene-*H*). **^{13}C NMR** (125 MHz, $CDCl_3$, rt) δ 161.0, 151.5, 132.8 (q, ^3J = 34.1 Hz), 130.9, 130.4 (q, ^4J = 3.4 Hz), 127.4 (q, ^4J = 3.5 Hz), 123.8, 122.9 (q, ^2J = 272 Hz), 119.0, 114.5. **^{19}F NMR** (376 MHz, $CDCl_3$, rt) δ –64.3. **HRMS** (ESI-TOF): calculated for $[C_{13}H_6F_6O_2+Na]^+$ requires 362.9885, found 362.9881.

Azulen-1-yl 3,5-bis(trifluoromethyl)benzoate (5fl)

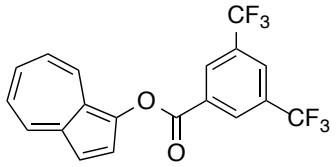

The reaction of **3f** (246.4 mg, 0.480 mmol), azulene (**4l**) (51.2 mg, 0.399 mmol), and **Ir-1** (13.0 mg, 19.9 μmol) following the general procedures afforded **5fl** (34.2 mg, 22% yield, reaction time = 24 h) as a dark green solid after purification with flash column chromatography on silica gel (hexane).
^{1}H NMR (400 MHz, $CDCl_3$) δ 8.77 (s, 2H; $C_6H_2H(CF_3)_2$), 8.33 (d, ^3J = 9.2 Hz, 1H; C_7H_4H), 8.28 (d, ^3J = 9.6 Hz, 1H; C_7H_4H), 8.18 (s, 1H; $C_6H_2H(CF_3)_2$), 7.95 (d, ^3J = 4.4 Hz, 1H; C_5HH), 7.65 (dd, ^3J = 9.6 Hz, ^3J = 9.6 Hz, 1H; C_7H_4H), 7.35 (d, ^3J = 4.4 Hz, 1H; C_5HH), 7.14 (dd, ^3J = 9.6 Hz, ^3J = 9.2 Hz, 2H; C_7H_4H). **^{13}C NMR** (125 MHz, $CDCl_3$, rt) δ 162.6, 139.1, 138.8, 137.1, 136.9, 132.7 (q, ^3J = 34.0 Hz), 132.3, 132.1, 130.4 (q, ^4J = 3.1 Hz), 127.7, 127.0 (q, ^4J = 3.8 Hz), 126.5, 123.4, 123.0 (q, ^2J = 271 Hz), 114.3. **^{19}F NMR** (376 MHz, $CDCl_3$, rt) δ –64.2. **HRMS** (ESI-TOF): calculated for $[C_{14}H_{18}O_4+Na]^+$ requires 261.1097, found 261.1105.

Luminescence quenching experiments
A solution of the Ir catalyst was prepared as to show the absorbance 0.1 exitation wavelength and degassed by three freeze-pump-thaw cycles in a 1 cm quartz cell equipped with an sphere moiety for freeze. The solution of quencher was added to the solution of the Ir catalyst before measurement of emission intensities.

Experiment for kinetic isotope effect
Under N_2, to benzene (**4d**) (62.8 mg, 0.80 mmol) and benzene-d_6 (67.6 mg, 0.80 mmol) dissolved in a dry and dehydrated CH_2Cl_2 (4.0 mL) in a 20 mL-Schlenk tube, **3f** (205.1 mg, 0.40 mmol) and **Ir-1** (13.0 mg, 0.020 mmol) were added. The tube was placed at a distance of 2-3 cm from blue LED lamp (hν = 425 ± 15 nm). The resulting mixture was stirred at room temperature (water bath) under visible light irradiation. Then, the reaction mixture was concentrated *in vacuo*. The KIE was determined by the clude ^{1}H NMR.

4.5 References

1 Z. Rappoport. *The chemistry of Phenols*; Wiley-VCH: Weinheim, 2003.

2 (a) H. J. H. Fenton, *J. Chem. Soc.* **1894**, *65,* 899-910 (b)Y. Gong, C. Yang, H. Ji, C. Chen, W. Ma, J. Zhao, *Chem. Asian. J.* **2016**, DOI; 10.1002/asia.201601299. and references there in.

3 For selected book and review, see: (a) *Radicals in Organic Synthesis,* Vol. 1-4 (Eds: P. Renaud, M. P. Sibi), John Wiley-VCH: Weinheim, Germany, 2001. (b) J. Hartung, *Eur. J. Org. Chem.* **2001**, 619-632; (3) J. Hartung, T. Gottwald, K. Špehar, *Synthesis* **2002**, *11*, 1469-1498. and references there in.

4 (a) H. Togo, "*Free Radical Reaction for Organic synthesis*", MARUZEN, **2015**. (b) D. H. R. Barton, B. Lacher, S. Z. Zard, *Tetrahedron* **1987**, *43,* 4321-4328; (c) J. Chateauneuf, J. Lusztyk, K. U. Ingold, *J. Am. Chem. Soc.* **1988**, *110,* 2886-2893.

5 (a) F. Minisci, R. Bernardi, F. Bertini, R. Galli, M. Perchinummo, *Tetrahedron* **1971**, *27,* 3575-3579; (b) F. Minisci, E. Vismara, F. Fontana, *Heterocycles*, **1989**, *28*, 489-519; (c) M. A. J. Duncton, *Chem. Commun.* **2011**, *2,* 1135-1161.

6 (a) M. E. Kurz, M. Pellegrini, *J. Org. Chem.* **1968**, *33*, 1950-1956; (b) H. Rao, P. Wang, C.-J. Li, *Eur. J. Org. Chem.* **2012**, 6503-6507; (c) C. Yuan, Y. Liang, T. Hernandez, A. Berriochoa, K. N. Houk, D. Siegel, *Nature* **2013**, *499,* 192-196; (d) J. Li, P. Zhang, N.-N. Yao, L.-L. Zhao, J.-J. Wang, Y. K. Shim, *Tetrahedron Lett.* **2014**, *55,* 1086-1089; (e) N. P. Ramirez, I. Bosque, J. C. Conzalez-Gomez, *Org. Lett.* **2015**, *17,* 4550-4553.

7 For selected reviews on photoredox catalysis, see: (a) T. P. Yoon, M. A. Ischay, J. Du, *Nat. Chem.* **2010**, *2,* 527-532; (b) J. M. R. Narayanam, C. R. J. Stephenson, *Chem. Soc. Rev.* **2011**, *40,* 102-113; (c) J. Xuan, W.-J. Xiao, *Angew. Chem. Int. Ed.* **2012**, *51,*6828-6838; (d) C. K. Prier, D. A. Rankic, D. W. C. MacMillan, *Chem. Rev.* **2013**, *113,* 5322-5363; (e) D. P. Hari, B. König, *Angew. Chem. Int. Ed.* **2013**, *52,* 4734-4743; (f) M. Reckenthäler, A. G. Griesbeck, *Adv. Synth. Catal.* **2013**, *355,* 2727-2744; (g) M. N. Hopkinson, B. Sahoo, J.-L. Li, F. Glorius, *Chem. Eur. J.* **2014**, *20,* 3874-3886; (h) T. Koike, M. Akita, *Inorg. Chem. Front.* **2014**, *20,* 3874-3886; (i) K. L. Skubi, T. R. Blum, T. P. Yoon, *Chem. Rev.* **2016**, *116,* 10035-10074; (j) M. H. Shaw, J. Twilton, D. W. C. MacMillan, *J. Org. Chem.* **2016**, *81,* 6898-6926.

8 K. Ohkubo, K. Mizushima, R. Iwata, K. Souma, N. Suzuki, S. Fukuzumi, *Chem. Commun.* **2010**, *46,* 601-603.

9 The photoexcited state of *fac*-[Ir(ppy)$_3$] (**Ir-1**) is reductant ($E_{1/2}$ = –2.14 V vs. Cp_2Fe) stronger than $[Ru(bpy)_3]^{2+}$ (**Ru-1**) and [Ir(dF(CF_3)ppy)(ppy)](PF_6) (**Ir-3**) ($E_{1/2}$ = –1.22 V and –1.41 V), ree: (a) L. Flamigni, A. Barbieri, C. Sabatini, B. Ventura, F. Barigelletti, *Top. Curr. Chem.* **2007**, *281,* 143-203; (b) K. Kalyanasundaram, *Cood. Chem. Rev.* **1982**, *46,* 159-244; (c) D. Hanss, J. C. Freys, G. Bernardinelli, O. S. Wenger, *Eur. J. Inorg. Chem.* **2009**, 4850-4859.

10 J. Chateauneuf, J. Lusztyk, K. U. Ingold, *J. Am. Chem. Soc.* **1988**, *110,* 2886-2893.

Chapter 5

Summary and Outlook

The author has developed new methods for introduction of *O*- and *N*-functionalities to alkenes or arenes via *C*-, *N*-, and *O*-centered radical intermediates generated by photoredox catalysis. Organotrifluoroborates and amino- and carboxy-pyridinium salts undergo 1e-oxidation and 1e-reduction via reductive and oxidative quenching cycles, respectively, to generate the corresponding *C*-, *N*-, and *O*-centered radicals, which undergo hydro-aminomethylation (Chapter 2), hydro-alkoxymethylation (Chapter 2), amionohydroxylation (Chapter 3), and aroyloxylation (Chapter 4).

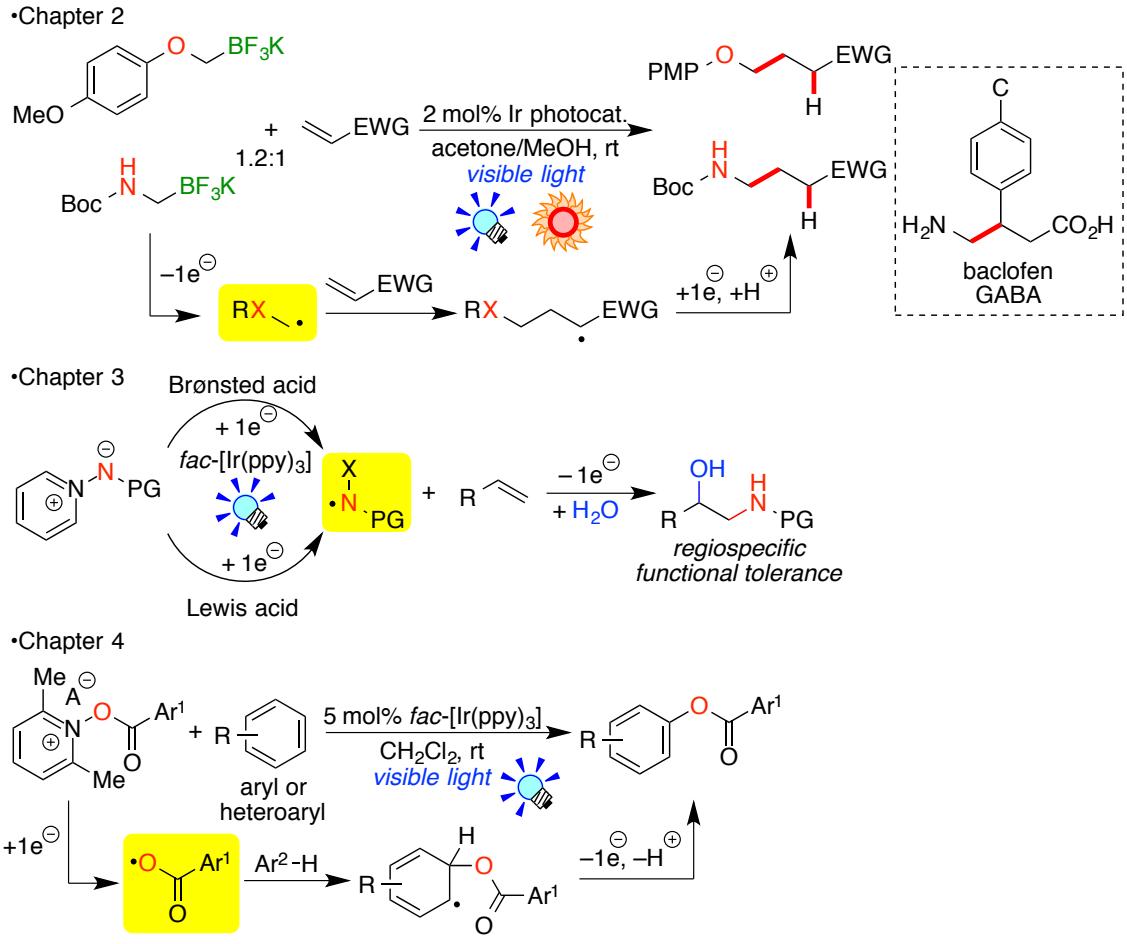

In Chapter 2, hydro-aminomethylation and hydro-alkoxymethylation of electron-deficient olefins with organotrifluoroborates following reductive quenching cycle have been described. In particular, *N*-Boc-aminomethyltrifluoroborate and *p*-methoxyphenoxymethyltrifluoroborate serve as the efficient radical precursors. The aminomethyl and alkoxymethyl radicals are so reactive toward electron-deficient alkenes as to afford the corresponding ethers and primary amines, where the carbon chains of alkenes are elongated by one methylene unit. In addition, the hydro-aminomethylation can be applied to synthesis of GABA (γ-aminobutyric acid) derivatives.

Chapter 3 deals with utilization of aminohydroxylation of olefins with well-designed *N*-protected aminopyridinium salts and the corresponding deprotonated ylides activated by a Lewis acid, $Sc(OTf)_3$. The reactions follow oxidative quenching cycle to afford amidyl radicals. In particular, *N*-Ts protected aminopyridinium BF_4 is the most effective precursor to afford the corresponding aminoalcohols with a wide range of functional groups as single regioisomers. Furthermore, dual Lewis acid/photoredox catalysis enables the use of various *N*-protected iminopyridinium ylides. This method will be welcomed as a new regioselective synthetic method for vicinal aminoalcohol.

In chapter 4, C-H oxidation reaction of arenes via aroyloxy radical ($Ar^1COO^{\bullet}$) generated from aroyloxy-2,6-pyridinium salts has been described. The radicals increase the reactivity by strong electron-withdrawing groups on the aroyl group *i.e.* two trifluoromethyl groups. Furthermore, this aroyloxypyridinium salts are easy-to-handle and non-explosive so that the reaction is a safe oxidation method under mild conditions in contrast to the reaction of peroxides.

In this thesis, radical initiating systems with organoborates and pyridinium scaffold by photoredox catalysis have been developed. The present methodology allows us the chemo- and regio-selective reaction by choice of functionalities on the radical. On the basis of the knowledge from this thesis, the author envisions that enantioselective radical reactions can be developed. Catalytic enantioselective radical reaction is a challenging topic due to highly reactive radical species. To achieve these reactions, the author proposed the combination of thermodynamic and kinetic control of the radical species. For example, the radical coupling reaction of the kinetically stable amidyl radical controlled by the bulky chiral ligand from aminopyridinium salt and thermodynamically stable radical from organoborates to afford chiral amine by photoredox catalysis.

The author believes that further continuous study on photoredox catalysis on the basis of this thesis will open a new strategy for synthesis of fine chemical, agrochemical, drug, bioactive compounds and material.

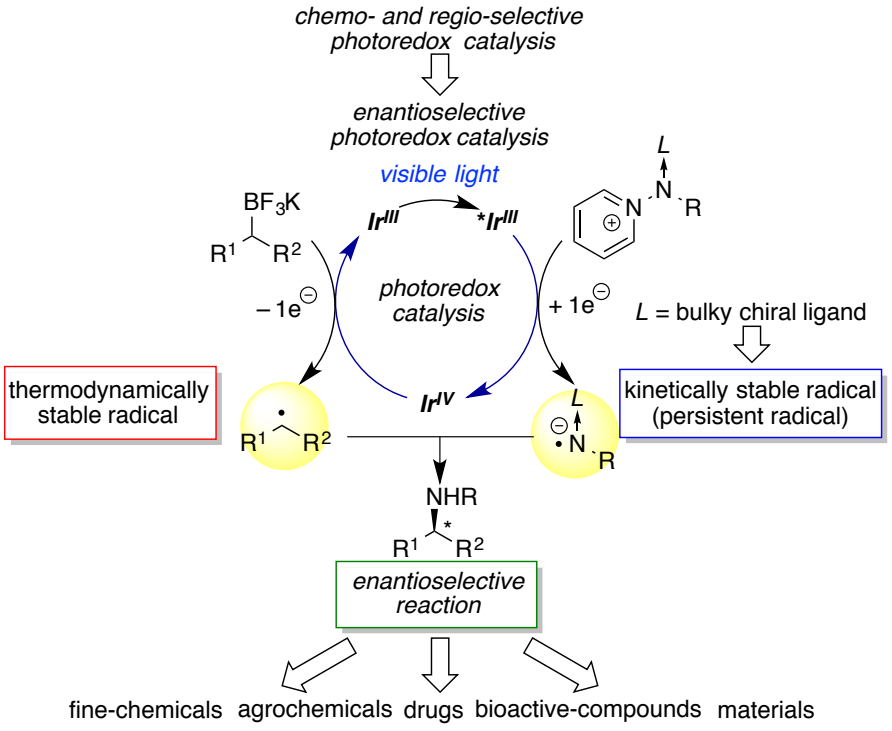

List of Publications

Chapter 2

Visible-light-induced Hydroalkoxymethylation of Electron-deficient Alkenes by Photoredox Catalysis

K. Miyazawa, Y. Yasu, T. Koike, M. Akita, *Chem. Commun.* **2013**, *49*, 7249–7251.

Hydroaminomethylation of Olefins with Aminomethyltrifluoroborate by Photoredox Catalysis

K. Miyazawa, T. Koike, M. Akita, *Adv. Synth. Catal.* **2014**, *356*, 2749–2755.

Chapter 3

Regiospecific Intermolecular Aminohydroxylation of Olefins by Photoredox Catalysis

K. Miyazawa, T. Koike, M. Akita, *Chem. Eur. J.* **2015**, *21*, 11677–11680.

Aminohydroxylation of Olefins with Iminopyridinium Yildes by Dual Ir photocatalysis and $Sc(OTf)_3$ Catalysis

K. Miyazawa, T, Koike, M. Akita, *Tetrahedron* **2016**, *72*, 7813–7820.

Other Publications

1 1,2–アミノアルコール骨格を持つ化合物の製造方法（特許出願）

宮澤和己・小池隆司・穐田宗隆

特願 2014-241563, 2014 年 11 月 28 日（出願人　東京工業大学）

2 Redox-Economical Radical Generation from Organoborates and Carboxylic Acids by Organic Photoredox Catalysis

T. Chinzei, **K. Miyazawa**, Y. Yasu, T. Koike, M. Akita, *RSC Advances*, **2015**, *5*, 21297–21300.

3 Alkyl- and Aryl-Thioalkylation of Olefins with Organotrifluoroborates by Photoredox Catalysis

Y. Li, **K. Miyazawa**, T. Koike, M. Akita, *Org. Chem. Front.* **2015**, *2*, 319–323.

4 Anti-Diastereoselective Synthesis of CF_3-Containing Spirooxazolines and Spirooxazines via Regiospecific Trifluoromethylative Spirocyclization by Photoredox Catalysis

N. Noto, **K. Miyazawa**, T. Koike, M. Akita, *Org. Lett*. **2015**, *17*, 3710–3713.

Acknowledgements

This research work presented in this thesis was carried out under the supervision of Professor Dr. Munetaka Akita at Tokyo Institute of Technology from April 2012 to March 2017.

First of all, the author wishes to express his sincerest gratitude to Professor Dr. Munetaka Akita for his continuous guidance, constructive suggestions and discussions, substantial encouragement, and warm enthusiasm through this study.

Next, the author would like to appreciate to Associate Professor Dr. Michito Yoshizawa and Associate Professor Dr. Akiko Inagaki of Tokyo Metropolitan University for their helpful advice and discussions, critical comments, and encouragement.

The author also wishes to extend his gratitude to Assistant Professor Dr. Takashi Koike for his deepest and sincere gratitude, valuable advices and discussion, critical comments, and encouragement throughout his study.

The author would like to express his thanks to Assistant professor Dr. Yuya Tanaka and Dr. Yusuke Yasu for their helpful advices and discussions, and encouragements.

The author would like to thank Miss HItomi Otomo for kindly supporting his daily work.

The author is grateful to Dr. Kei Murata, Dr. Zhiou Li, Dr. Huifang Li, Dr. Norifumi Kishi, Dr. Kei Kondo, Dr. Keita Hagiwara, Dr. Akira Suzuki, Dr. Yamashina Masahiro, and Dr. Yazaki Kohei for fruitful discussion and comments, and kidly assistance in life of study. The author gratefully thanks to Dr. Ren Tomita, Mr. Tatsuya Chinzei, Mr. Yusuke Arai, Mr. Ando Gaku, Mr. Naoki Noto, Mr. Yusuke Konishi for their active and valuable collaboration. The author also expresses his thanks to present students of Akita-Yoshizawa laboratory.

The author thanks the JSPS (Japan Society for the Promotion of Science) Young Scientist Fellowship for financial support.

Finally, the author wishes to heartily thank his parents, Mr. Akiyoshi Miyazawa and Mrs. Yumiko Miyazawa, and his brothers, Mr. Masato Miyazawa and Mr. Kyohei Miyazawa, for their permanently kind assistance and encouragement.

March 2017

Kazuki Miyazawa